(4)

THE OHIO STATE UNIVERSITY

Performance Analysis of Large Adaptive Sidelobe Canceller Arrays with Reused Elements

J. Ward and R. T. Compton, Jr.

The Ohio State University

ElectroScience Laboratory

Department of Electrical Engineering
Columbus, Ohio 43212

Final Report 719711-1
Contract No. N00014-87-K-2011
June 1989

Naval Research Laboratory
4555 Overlook Avenue, S.W.
Washington, D.C. 20375

NOTICES

When Government drawings, specifications, or other data are used for any purpose other than in connection with a definitely related Government procurement operation, the United States Government thereby incurs no responsibility nor any obligation whatsoever, and the fact that the Government may have formulated, furnished, or in any way supplied the said drawings, specifications, or other data, is not to be regarded by implication or otherwise as in any manner licensing the holder or any other person or corporation, or conveying any rights or permission to manufacture, use, or sell any patented invention that may in any way be related thereto.

50272-101

REPORT DOCUMENTATION PAGE	1. REPORT NO.	2.	3. Recipient's Accession No.
4. Title and Subtitle Performance Analysis of Large Adaptive Sidelobe Canceller Arrays with Reused Elements			5. Report Date May 1989 6.
7. Author(s) J. Ward and R.T. Compton, Jr.			8. Performing Org. Rept. No. 719711-1
9. Performing Organization Name and Address The Ohio State University ElectroScience Laboratory 1320 Kinnear Road Columbus, OH 43212			10. Project/Task/Work Unit No. 11. Contract(C) or Grant(G) No. (C) N00014-87-K-2011 (G)
12. Sponsoring Organization Name and Address Naval Research Laboratory 4555 Overlook Avenue, S.W. Washington, D.C. 20375			13. Report Type/Period Covered Final Report 14.

15. Supplementary Notes

16. Abstract (Limit: 200 words)

This report considers adaptive sidelobe canceller arrays (SLCs) in which the mainbeam and auxiliary signals are obtained from the same set of elements. The SLC with element reuse is different from the conventional SLC in that thermal noise components of the mainbeam and auxiliary signals are correlated. This correlation causes sidelobe degradation when the number of degrees of freedom exceeds the number necessary to cancel a given jammer scenario.

The equations for a general planar array with an arbitrary signal scenario are first formulated. These equations are then used to examine array performance with different auxiliary configurations. Both auxiliaries form from a single array element and auxiliaries form from subarrays of elements are studied. Various auxiliary configurations are investigated to determine how the auxiliaries should be chosen to provide good cancellation of multiple jammers while retaining low sidelobes in the mainbeam.

It is shown that using single-element auxiliaries may result in serious SLL degradation whenever there are extra degrees of freedom. This degradation can be overcome by using subarray auxiliaries that satisfy an orthogonality condition on their patterns. Excellent cancellation and sidelobe level performance can be attained with small subarrays chosen to satisfy this orthogonality condition.

17. Document Analysis a. Descriptors

b. Identifiers/Open-Ended Terms

c. COSATI Field/Group

18. Availability Statement	19. Security Class (This Report)	21. No. of Pages
A. Approved for public release; Distribution is unlimited.	Unclassified	225
	20. Security Class (This Page) Unclassified	22. Price

(See ANSI-Z39.18) *See Instructions on Reverse* OPTIONAL FORM 272 (4-77)
Department of Commerce

Contents

1 Introduction **7**

2 The Planar Array Sidelobe Canceller with Reused Elements **10**
- 2.1 Introduction 10
- 2.2 Problem formulation 10
- 2.3 Signal Models 20
- 2.4 The element pattern 22

3 The Effect of Random Amplitude and Phase Errors on Array Performance **29**
- 3.1 Introduction 29
- 3.2 Derivation of average power pattern 30
- 3.3 Results using pdf of pattern magnitude 34
- 3.4 Integrated Average Sidelobe Level 46

4 SLC Performance Using One Array Element for the Auxiliaries: One Interfering Signal **54**
- 4.1 Introduction 54
- 4.2 A CW jammer 55
- 4.3 A jammer with non-zero bandwidth 69

5 Multiple Single-Element Auxiliary Signals: One or More Jammers **95**
- 5.1 Introduction 95
- 5.2 A single CW jammer 96
- 5.3 A single jammer with non-zero bandwidth 99
- 5.4 Multiple CW jammers 104

6 Auxiliary Signals from Multiple Elements **118**
- 6.1 Introduction 118
- 6.2 Mainbeam-auxiliary orthogonality 119
- 6.3 Steered beam auxiliaries using subarrays of the mainbeam 128
- 6.4 Non-orthogonal steered beam auxiliary signals 142

7 Auxiliary Selection for Planar Sidelobe Cancellers **151**
- 7.1 Introduction 151
- 7.2 Single-element Auxiliaries 152
- 7.3 Auxiliaries meeting the orthogonality condition 163

8 Conclusions **171**

9 References 173

A Adaptive SLC Program Documentation 175

List of Figures

2.1 Planar array geometry 11
2.2 The antenna element and T/R module model. 13
2.3 The power spectral densities of the incident desired and interfering signals and for the element noise signals. 21
2.4 Diagram of a space based radar on an orbiting satellite. 23
2.5 The angular extent of the earth, θ_e, viewed from an orbiting satellite, as a function of the orbit altitude. 24
2.6 Element patterns for different h and different ϵ_r. A:ϵ_r = 2.0 B:ϵ_r = 5.0 C:ϵ_r = 10.0 26
2.7 The mainbeam pattern of a 100 x 1 array with 55 dB Dolph-Chebyshev weighting. 28

3.1 Probability density functions for the amplitude and phase errors present on an element. 35
3.2 Probability that the actual SLL exceeds -48 dB. Amplitude errors ±0.2 dB, Phase error ±3°. 37
3.3 Pr{peak SLL > S dB} vs. S, for ±0.1 dB amplitude error and varying phase errors. A:±0.17578125° B:±0.3515625° C:±0.703125° D:±1.40625° 40
3.4 Comparison between predicted and simulated results, for a 100 element linear array. Amplitude error ±0.1 dB, Phase error ±1.40625° 41
3.5 The increase in Peak SLL vs. the Chebyshev design SLL; Phase errors only. A:±0.3515625° B:±0.703125° C:±1.40625° D:±2.8125° 43
3.6 The increase in Peak SLL vs. the Chebyshev design SLL; Amplitude errors only. 44
3.7 The increase in Peak SLL vs. the Chebyshev design SLL; the amplitude error is ±0.1 dB and the phase error is varied. A:±0.17578125° B:±0.3515625° C:±0.703125° D:±1.40625° 45
3.8 Ensemble of 5 patterns of the 100×1 array, with amplitude error ±0.1 dB, and phase error ±0.1758°. 47
3.9 Regions of interest for the sidelobe integration of a planar array pattern. . . 52
3.10 Typical mainbeam and adapted patterns. The computed ASLL is indicated by the dashed lines. 53

4.1 SINR vs θ_{i1}: SNR=-30 dB, INR=40 dB, B=0. 56
4.2 Output P_d vs θ_{i1}: SNR=-30 dB, INR=40 dB, B=0. 58
4.3 Desired signal improvement ratio vs. θ_{i1}: SNR=-30 dB, INR=40 dB, B=0. 59
4.4 Output P_i vs θ_{i1}: SNR=-30 dB, INR=40 dB, B=0. 60
4.5 Cancellation ratio vs. θ_{i1}: SNR=-30 dB, INR=40 dB, B=0. 62
4.6 Output P_n vs θ_{i1}: SNR=-30 dB, INR=40 dB, B=0. 63
4.7 Noise signal improvement ratio vs. θ_{i1}: SNR=-30 dB, INR=40 dB, B=0. . . 65
4.8 Increase in ASLL vs θ_{i1}: SNR=-30 dB, INR=40 dB, B=0. 66

4.9 Adapted patterns with $\theta_{i1} = 0°$ for different auxiliary element locations: (a) element (50,1) (b) element (25,1) (c) element (12,1) (d) element (1,1) 68
4.10 SINR performance with a single complex weight on element (1,1), INR=60 dB. 70
4.11 The effect of INR on SINR performance: $\theta_{i1} = -45°$, element (1,1). 71
4.12 The equivalent filter seen by a signal arriving from angles (θ, ϕ). 72
4.13 A tapped delay line filter. 74
4.14 SINR performance of a 2-tap TDL on element (1,1). The intertap delay is $38\lambda_0$. INR=60 dB. 78
4.15 SINR performance of a 2-tap TDL on element (1,1). The intertap delay is $38\lambda_0$. INR=90 dB. 79
4.16 Output P_i performance of a 2-tap TDL on element (1,1). The intertap delay is $38\lambda_0$. INR=60 dB; 90 dB 80
4.17 Output P_i performance of a 2-tap delay line on element (1,1). INR=60 dB, B=0.001. 82
4.18 Performance of a TDL on the center element as a function of the intertap delay: (a) SINR; (b) Output P_i ; INR=60 dB, B=0.001 84
4.19 Output P_i comparison of end and center element TDLs. One 60 dB jammer. (a) $\tau = 10\lambda_0$ (b) $\tau = 24.75\lambda_0$ (c) $\tau = 38\lambda_0$ (d) $\tau = 50\lambda_0$ 86
4.20 Symmetric TDL structure, composed of equal positive and negative delay sections. 87
4.21 Output P_i comparison of conventional and symmetric TDL structures on element(50,1). (a) $\tau = 10\lambda_0$ (b) $\tau = 24.75\lambda_0$ (c) $\tau = 38\lambda_0$ (d) $\tau = 50\lambda_0$ 89
4.22 Output P_i comparison of two TDL structures. (a) A 2-tap, one delay=$38\lambda_0$ TDL on element (1,1). (b) A 2-tap, two delays=$-19\lambda_0$, $19\lambda_0$ TDL on (50,1). 90

5.1 Mainbeam and adapted patterns of a SLC with 2 single element auxiliary signals in the presence of a single jammer. 98
5.2 Comparison of a TDL on element (50,1) (C1) with a multiple auxiliary configuration consisting of single complex weights on elements (50,1) and (51,1) (C2). $B = 0.001$. (a) SINR (b) Output P_i 101
5.3 Increase in ASLL comparison of a TDL on element (50,1) (C1) with a multiple auxiliary configuration consisting of single complex weights on elements (50,1) and (51,1) (C2). 102
5.4 Performance of a SLC with two auxiliaries, elements (1,1) and (5,1), in the presence of two 50 dB CW interfering signals. (a) SINR (b) Increase in ASLL 107
5.5 Patterns resulting from a SLC with auxiliary elements (1,1) and (5,1) when the spacing between jammers is close to the spacing between grating lobes in the weighted auxiliary pattern. Two 40 dB CW jammers: $\theta_{i1} = 40°$, $\theta_{i2} = -20.9°$. (a) Weighted auxiliary pattern (b) Adapted pattern 108
5.6 Performance of a SLC with two closely spaced auxiliaries, elements (1,1) and (2,1), with two 40 dB CW jammers incident. $\theta_{i1} = 40°$ (a) SINR (b) Output P_i 110

5.7 Patterns resulting from the SLC with elements (1,1) and (2,1) as the auxiliaries, in the presence of two closely spaced 40 dB CW jammers: $\theta_{i1} = 40°$, $\theta_{i2} = 39°$. (a) Adapted pattern (b) Weighted auxiliary pattern 112
5.8 Increase in ASLL from the SLC using elements (1,1) and (2,1) as auxiliaries. Two 40 dB jammers incident, $\theta_{i1} = 40°$. 113
5.9 Performance of a SLC using an unequally spaced auxiliary array of five auxiliaries: elements (1,1),(2,1),(14,1),(47,1), and (100,1). Two 50 dB CW jammers are incident, with $\theta_{i1} = 40°$. (a) SINR (b) Increase in ASLL. 115

6.1 Comparison between a SLC with two 2-element auxiliary signals satisfying the orthogonality condition (solid line) and a configuration using (50,1) and (51,1) as the two auxiliary elements (dashed line). (a) SINR (b) Increase in Average SLL. 122
6.2 Patterns of auxiliary beams formed from an 8-element subarray, elements (47,1)-(54,1). Each auxiliary satisfies the orthogonality condition between mainbeam and combiner vectors. 131
6.3 Performance with multiple beams formed from the same subarray. A single 40 dB CW jammer is incident. (a) SINR (b) Increase in Average SLL. 132
6.4 Performance with multiple beams formed from the same subarray. Two 40 dB CW jammers are incident, with $\theta_{i1} = 40°$. (a) SINR (b) Increase in Average SLL. 133
6.5 Auxiliary beams resulting from 6 equally spaced 8-element subarrays, each orthogonal to the mainbeam. 135
6.6 Performance of a SLC using 6 equally spaced subarrays for the auxiliaries. Two 40 dB CW jammers, $\theta_{i1} = 40°$.(a) SINR (b) Increase in Average SLL. . 136
6.7 Performance of a SLC using 6 equally spaced subarrays for the auxiliaries. No TDLs. Two 60 dB jammers, $B = 0.001$, $\theta_{i1} = 40°$. (a) SINR (b) Increase in Average SLL. 139
6.8 Performance of a SLC using 6 equally spaced subarrays, with a 2-tap TDL on each auxiliary beam. Two 60 dB jammers, $B = 0.001$, $\theta_{i1} = 40°$. (a) SINR (b) Increase in Average SLL. 141
6.9 Patterns resulting from a single auxiliary using the subarray of elements (38,1)-(62,1). No jammers. (a) Auxiliary pattern, $\theta_a = -41.3°$. (b) Adapted pattern, $\theta_a = -41.3°$. (c) Adapted pattern, $\theta_a = -38.2°$. (d) Adapted pattern, $\theta_a = -35.5°$. 144
6.10 Patterns resulting from a single auxiliary using the full array, elements (1,1)-(100,1). No jammers. (a) Mainbeam pattern (b) Adapted pattern, $\theta_a = -39.8°$. (c) Adapted pattern, $\theta_a = -40.25°$. (d) Adapted pattern, $\theta_a = -40.5°$. 146
6.11 Auxiliary patterns for a SLC configuration using four auxiliaries, each using the full array. 147
6.12 Performance of a SLC with multiple uniformly weighted steered beam auxiliaries. 3 40 dB CW jammers present. $\theta_{i2} = -39.25°$, $\theta_{i3} = -37.75°$ (a) Cancellation Ratio (b) Increase in ASLL 148

6.13 Adapted pattern resulting from 3 jammers within one auxiliary beamwidth. $\theta_{i1} = -40.0°$, $\theta_{i2} = -39.8°$, $\theta_{i3} = -40.2°$ 149

7.1 Mainbeam pattern magnitude resulting from an 80 x 50 array with 50 dB Dolph-Chebyshev weighting. 154
7.2 Adapted pattern resulting from the mainbeam pattern of Figure 7.1 using element (1,1) as the auxiliary element. 156
7.3 Contour plot and pattern cuts of the adapted pattern shown in Figure 7.2. 157
7.4 Mainbeam pattern of an 80 x 50 array with 55 dB Dolph-Chebyshev weighting. The element errors are ±0.2711 dB and ±0.6325°. 158
7.5 Adapted patterns from an SLC with element (40,25) as the auxiliary. A single 40 dB CW jammer is present. (a) $(u_{i1}, v_{i1}) = (-0.5, 0.5)$. (b) $(u_{i1}, v_{i1}) = (0.5, 0.5)$. 160
7.6 Adapted pattern from an SLC with 5 auxiliary elements. Two 40 dB CW jammers, $(u_{i1}, v_{i1}) = (-0.7071, 0.)$ and $(u_{i2}, v_{i2}) = (0., 0.5)$ are incident. . . . 162
7.7 Subarrays used for planar SLC example with steered beam auxiliary signals. 166
7.8 Adapted pattern from an SLC using nine steered beam auxiliaries from equally spaced subarrays. $(u_{i1}, v_{i1}) = (-0.7071, 0.)$ and $(u_{i2}, v_{i2}) = (0., 0.5)$. . 167

1. Introduction

A sidelobe canceller(SLC) array is an adaptive antenna system comprised of a main antenna with a relatively large aperture and one or more auxiliary antennas. An adaptive processor combines the signals received from these antennas so that interfering signals(jammers) that arrive from the sidelobe region of the main antenna are suppressed. In this report we examine the performance of sidelobe canceller arrays where the main antenna is a large phased array and the auxiliary antennas are either single elements or subarrays of this same phased array.

This SLC system is to be used in a space based radar. In addition to standard adaptive array performance measures such as SINR and cancellation ratio, the sidelobe level of the adapted pattern is important in this application. We assume that the main antenna, formed from the full aperture, is a low sidelobe antenna designed to provide interference protection against small to moderate power jamming. Thus the adaptive capability must provide cancellation of high power jamming while retaining the low sidelobe structure of the main antenna.

The performance of conventional SLCs that use separate main and auxiliary antennas is well known.[1,2,3] These arrays perform best when the main antenna has a low design sidelobe level and the auxiliary antennas have patterns with maxima near the interfering signal arrival angles. In our previous work[4], we showed that the major difference between the conventional SLC and the SLC with reused elements is that the noise components of the mainbeam and auxiliary signals are correlated[1].

[1]We are assuming that the only noise source is internally generated thermal noise from the Low Noise Amplifiers(LNAs) or the Transmit/Receive(T/R) modules present on each antenna element.

Depending on how the auxiliary signals are chosen, this noise correlation may or may not affect the cancellation and SLL performance of the array.

In this report we examine the performance of large linear(100×1) and planar(80×50) SLC arrays where the auxiliary signals are formed from antenna elements also used to form the mainbeam signal. We seek to determine how the auxiliaries should be chosen to attain best overall performance, considering SINR, cancellation, bandwidth, multiple jammers, and resultant adapted pattern SLL. Related work has been done by White[5], who specifically considered bandwidth performance, and by Davis and Gleich[6], who considered auxiliary element placement. We first examine numerous canceller configurations and signal scenarios using a 100×1 linear array, starting with a single auxiliary element and a single CW jammer, and progressing to more complicated configurations that used multiple steered beam auxiliary beams in an environment of multiple jamming signals. The results obtained for the linear array are then applied to a planar array SLC using an 80×50 element array.

We show that when the number of adaptive degrees of freedom exceed the number of incident jammers, the array responds to the noise correlation between mainbeam and auxiliary signals. Depending on the auxiliary configuration, this can result in a drastic increase in SLL. In general, this noise correlation is smallest when a small fraction of the total array elements is used for the auxiliaries and when the auxiliary elements are formed from elements at the ends of the array, where the elements have small weights in the mainbeam amplitude taper. However, to handle multiple jammer scenarios without resolution and grating lobe problems requires a configuration consisting of multiple auxiliary elements with more degrees of freedom than the number of jammers. As a result, canceller configurations of

multiple auxiliaries generally have poor sidelobe level performance.

To overcome the SLL degradation evident with multiple auxiliary configurations, we show how the auxiliary signals may be formed from combinations of array elements, or subarrays, so that there is zero noise correlation between the mainbeam and auxiliary signals. Arrays with auxiliary signals formed from subarrays are able to provide sufficient cancellation of multiple jammer scenarios with little, if any increase in SLL for a larger range of jammer scenarios than is possible using just multiple auxiliary elements.

Chapter 2 reviews the mathematical formulation of the adaptive sidelobe canceller array with reused elements, defines several quantities of interest, and describes the element pattern used in the mathematical model. Chapter 3 provides some background material on the effects of random amplitude and phase errors on the mainbeam SLL. We use the results of this chapter to determine the amount of randomness to include in the model for a given configuration. We also define a quantity called Integrated Average Sidelobe Level (ASLL), which will allow us to evaluate the SLL performance of various SLC configurations. In Chapter 4 we start the analysis of linear array SLCs by considering configurations where a single array element is used for the auxiliaries. Chapter 5 describes cases where multiple auxiliary elements are used. Chapter 6 describes results with SLCs using combinations of array elements for each auxiliary signal. Included in this chapter are steered beam auxiliaries using subarrays of the main aperture. In Chapter 7, the results of the previous chapters are applied to planar array SLCs. Finally, Chapter 8 contains our conclusions.

2. The Planar Array Sidelobe Canceller with Reused Elements

2.1 Introduction

In this chapter we review the mathematical formulation of the adaptive sidelobe canceller array. We consider an array in which the signals from small subsets of the array elements are "reused" to form the auxiliary signals for the canceller. We assume a rectangular planar array geometry, of which the linear array canceller is a special case. The auxiliary signals may or may not have tapped delay lines behind them.

We first describe the array geometry and the general element combining techniques. The adaptive processing and array output power calculations are given next. We then describe the signal models used for the desired, interfering, and noise signals present. Finally, we discuss the element pattern used in the model. Much of the next two sections of this chapter is taken from our previous work [4].

2.2 Problem formulation

Consider the planar array of antenna elements shown in Figure 2.1. The array has N_x elements in the x direction and N_y elements in the y direction[1]. The spacing between adjacent elements in both the x and y directions is β wavelengths. We assume that each element is an isolated monopole on an infinite ground plane, and that all elements are identical with element voltage pattern $f(\theta, \phi)$.[2]The angles (θ, ϕ)

[1] $N_y = 1$ for the linear array case.

[2] The effects of mutual coupling between elements will be neglected. Furthermore we assume that the element is broadband enough so that its response is constant over all signal bandwidths of interest. The element pattern will be discussed in a Section 2.4.

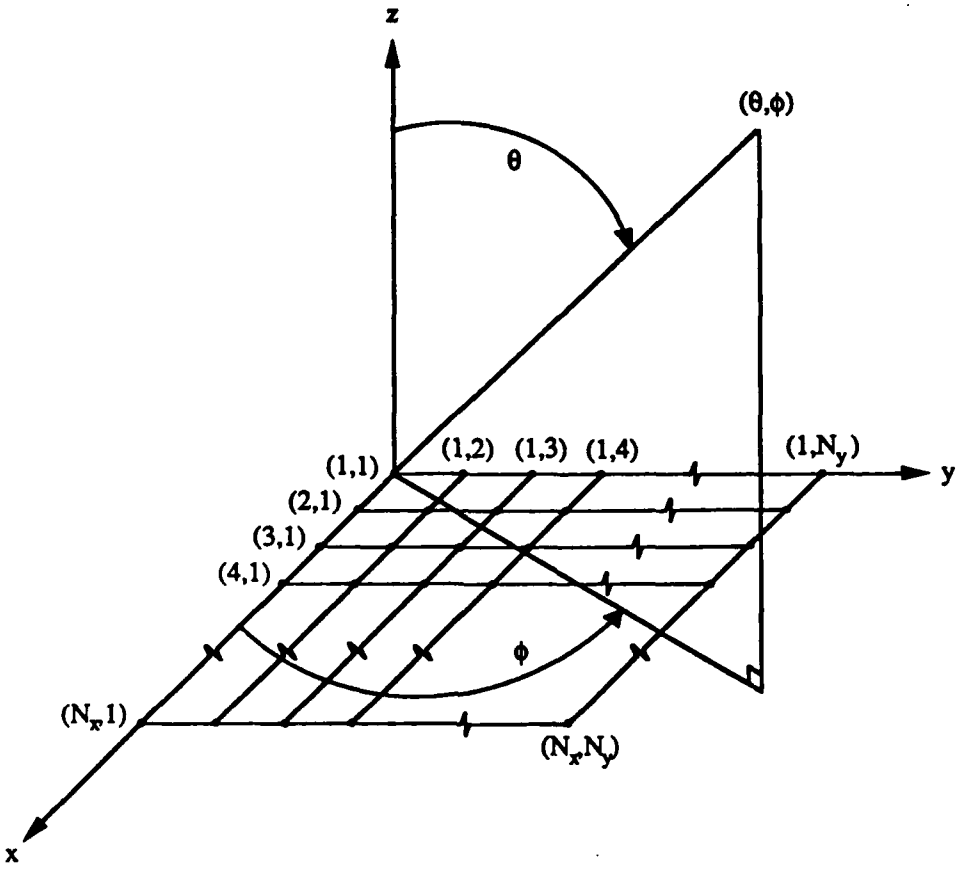

Figure 2.1: Planar array geometry

are defined by the standard spherical coordinate system as shown in Figure 2.1.

We assume that the incident signal scenario consists of a desired signal arriving from angles (θ_d, ϕ_d) and P interfering signals, with arrival angles (θ_{i1}, ϕ_{i1}), ..., (θ_{iP}, ϕ_{iP}). We denote the incident desired signal on element (1,1) of the array as $\tilde{d}(t)$ and the P interfering signals on this element as $\tilde{i}_1(t)$, ..., $\tilde{i}_P(t)$. Then the total received signal on the $(l,m)^{th}$ element in the array, $\tilde{z}_{lm}(t)$, is given by

$$\tilde{z}_{lm}(t) = f(\theta_d, \phi_d)\tilde{d}(t - T^d_{lm}) + \sum_{k=1}^{P} f(\theta_{ik}, \phi_{ik})\tilde{i}_k(t - T^k_{lm}) , \tag{2.1}$$

where T^d_{lm} and T^k_{lm} are the interelement propagation times between element (1,1) and element (l,m) for the desired and k^{th} interfering signals , respectively. We also assume that each element is followed by a transmit/receive (T/R) module with gain g_{lm} and phase shift $e^{jP_{lm}}$. The g_{lm} and P_{lm} will later be modelled as random quantities to incorporate the effects of random errors in the array weighting. In addition, assume T/R module (l,m) adds a thermal noise signal $\tilde{n}_{lm}(t)$ with power σ^2_{lm}. We assume that the element noise signals are all of equal power $\sigma^2_{lm} = \sigma^2$. Hence, the total output signal $\tilde{y}_{lm}(t)$ from the T/R module on element (l,m) is modelled as shown in Figure 2.2 and given by

$$\tilde{y}_{lm}(t) = G_{lm}\tilde{z}_{lm}(t) + \tilde{n}_{lm}(t) , \tag{2.2}$$

where

$$G_{lm} = g_{lm}e^{jP_{lm}} . \tag{2.3}$$

We shall find it convenient to separate $\tilde{y}_{lm}(t)$ into its desired, interfering, and noise signal components as

$$\tilde{y}_{lm}(t) = \tilde{d}_{lm}(t) + \sum_{k=1}^{P} \tilde{i}^k_{lm}(t) + \tilde{n}_{lm}(t) , \tag{2.4}$$

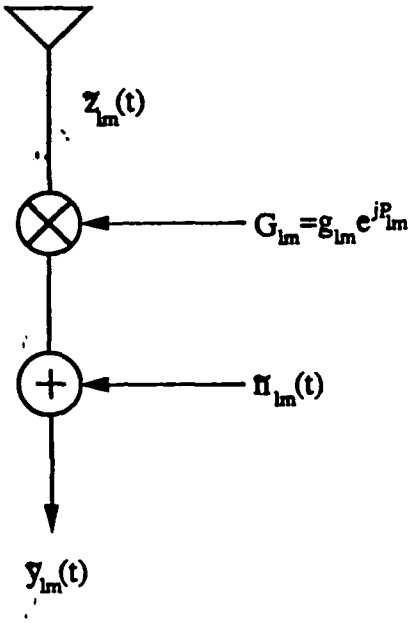

Figure 2.2: The antenna element and T/R module model.

where

$$\tilde{d}_{lm}(t) = G_{lm} f(\theta_d, \phi_d) \tilde{d}(t - T^d_{lm}) \,, \tag{2.5}$$

and

$$\tilde{i}^k_{lm}(t) = G_{lm} f(\theta_{ik}, \phi_{ik}) \tilde{i}_k(t - T^k_{lm}) \,. \tag{2.6}$$

The signals $\tilde{y}_{lm}(t)$ are used to produce both the mainbeam signal and one or more auxiliary signals for the adaptive processor. The mainbeam signal is obtained by combining the signals $\tilde{y}_{lm}(t)$ with an equal delay corporate feed. We assume that each element of the array is weighted during this combination so that the main beam is steered in the desired look direction and so the mainbeam pattern has a desired sidelobe level. If $\tilde{x}_m(t)$ denotes the mainbeam signal and M_{lm} denotes the

mainbeam combiner weight on the $(l,m)^{th}$ element, then

$$\tilde{x}_m(t) = \sum_{l=1}^{N_x} \sum_{m=1}^{N_y} M_{lm} \tilde{y}_{lm}(t) \,. \tag{2.7}$$

The mainbeam combiner weights for a beam steered to the (θ, ϕ) directions are given by

$$M_{lm} = m_{lm} e^{-j\Psi_{lm}} \,, \tag{2.8}$$

where the m_{lm} form the amplitude taper required to achieve a desired mainbeam pattern sidelobe level. In the arrays we consider in this report, we use either a one-dimensional or a separable two-dimensional Dolph-Chebyshev amplitude taper.[7,8] Ψ_{lm}, given by

$$\Psi_{lm} = 2\pi\beta[(l-1)\cos\phi + (m-1)\sin\phi]\sin\theta \,, \tag{2.9}$$

is the phase angle of the signal received on element (l,m) with respect to the signal received on element (1,1) for a plane wave incident from (θ, ϕ).

The auxiliary signals are also weighted sums of the $\tilde{y}_{lm}(t)$ signals. In addition, the auxiliary signals may include delay elements that allow tapped delay line processing. We define the i^{th} auxiliary signal $\tilde{x}_i(t)$ to be

$$\tilde{x}_i(t) = \sum_{l=1}^{N_x} \sum_{m=1}^{N_y} A_{lm}^i \tilde{y}_{lm}(t - \tau^i) \,, \tag{2.10}$$

where A_{lm}^i is the combiner weight on the $(l,m)^{th}$ element for the i^{th} auxiliary signal and τ^i is the delay applied to the i^{th} auxiliary. We suppose there are K auxiliary signals altogether, and X to be a vector containing these signals,

$$X = \left[\tilde{x}_1(t), \;\; \tilde{x}_2(t), \;\; \ldots, \;\; \tilde{x}_K(t) \right]^T \,. \tag{2.11}$$

Each of the K auxiliary signals is adaptively weighted by a complex weight w_i and then summed with the mainbeam signal to produce the array output signal. The optimal auxiliary signal weights are given by[2]

$$W = -\Phi^{-1}V \,, \tag{2.12}$$

where W is the $K \times 1$ vector $[\ w_1,\ w_2,\ \ldots,\ w_K\ ]^T$, Φ is the $K \times K$ covariance matrix of the auxiliary signals,

$$\Phi = E\left[X^* X^T\right] \,, \tag{2.13}$$

and V is the $K \times 1$ vector of cross-correlations between the auxiliary signals and the mainbeam signal,

$$V = E\left[X^* \tilde{x}_m(t)\right] \,, \tag{2.14}$$

which we refer to as the steering vector. We use Eqs. (2.7), (2.10), and (2.11) to write the α^{th} component of the steering vector V as

$$(V)_\alpha = \sum_{i=1}^{N_x}\sum_{j=1}^{N_y}\sum_{l=1}^{N_x}\sum_{m=1}^{N_y}(A_{ij}^\alpha)^* M_{lm} E[\tilde{y}_{ij}^*(t-\tau^\alpha)\tilde{y}_{lm}(t)] \,. \tag{2.15}$$

Similarly, we can write the $\alpha\beta^{th}$ component of the covariance matrix, $\Phi_{\alpha\beta}$, as

$$(\Phi)_{\alpha\beta} = \sum_{i=1}^{N_x}\sum_{j=1}^{N_y}\sum_{l=1}^{N_x}\sum_{m=1}^{N_y}(A_{ij}^\alpha)^* A_{lm}^\beta E[\tilde{y}_{ij}^*(t-\tau^\alpha)\tilde{y}_{lm}(t-\tau^\beta)] \,. \tag{2.16}$$

Once the weight vector is computed, the array output signal $\tilde{s}_o(t)$ is given by

$$\tilde{s}_o(t) = \tilde{x}_m(t) + W^T X \,. \tag{2.17}$$

We split the mainbeam signal, the auxiliary signals, and the array output signal into desired, interfering, and noise signal components by using Eq. (2.4). Then

$$X = X_d + X_i + X_n \,, \tag{2.18}$$

$$\tilde{x}_m(t) = \tilde{x}_m^d(t) + \tilde{x}_m^i(t) + \tilde{x}_m^n(t)\,, \tag{2.19}$$

and

$$\tilde{s}_o(t) = \tilde{s}_o^d(t) + \tilde{s}_o^i(t) + \tilde{s}_o^n(t) \tag{2.20}$$

where the particular signal component is indicated by a d, i, or n subscript or superscript. We assume that the desired, interfering, and noise signals on each element are zero mean, wide-sense stationary random processes. Under the additional assumptions that the desired and interfering signals incident on the array are uncorrelated with each other and with the noise signals at each element, and that the noise signals are uncorrelated from element to element, Φ and V can be decomposed into desired, interfering, and noise components:

$$\Phi = \Phi_d + \Phi_i + \Phi_n \tag{2.21}$$

$$V = V_d + V_i + V_n\,. \tag{2.22}$$

For example, $\Phi_d = E[X_d^* X_d^T]$ and $V_d = E[X_d^* \tilde{x}_m^d(t)]$, where the $\alpha\beta^{th}$ element of Φ_d is

$$(\Phi_d)_{\alpha\beta} = \sum_{i=1}^{N_x}\sum_{j=1}^{N_y}\sum_{l=1}^{N_x}\sum_{m=1}^{N_y}(A_{ij}^{\alpha})^* A_{lm}^{\beta} E[\tilde{d}_{ij}^*(t-\tau^{\alpha})\tilde{d}_{lm}(t-\tau^{\beta})]\,, \tag{2.23}$$

and the α^{th} element of V_d is given by

$$(V_d)_{\alpha} = \sum_{i=1}^{N_x}\sum_{j=1}^{N_y}\sum_{l=1}^{N_x}\sum_{m=1}^{N_y}(A_{ij}^{\alpha})^* M_{lm} E[\tilde{d}_{ij}^*(t-\tau^{\alpha})\tilde{d}_{lm}(t)]\,. \tag{2.24}$$

In order to evaluate Eqs. (2.23) and (2.24) we must evaluate the expectations. We define the autocorrelation function of the incident desired signal to be

$$R_{\tilde{d}}(\tau) = E[\tilde{d}(t)^*\tilde{d}(t+\tau)]\,. \tag{2.25}$$

With this definition and Eq. (2.5), Eqs. (2.23) and (2.24) become

$$(\Phi_d)_{\alpha\beta} = |f(\theta_d,\phi_d)|^2 \sum_{i=1}^{N_x}\sum_{j=1}^{N_y}\sum_{l=1}^{N_x}\sum_{m=1}^{N_y}(A_{ij}^{\alpha}G_{ij})^* A_{lm}^{\beta}G_{lm}R_{\tilde{d}}(T_{ij}^{d}+\tau^{\alpha}-T_{lm}^{d}-\tau^{\beta}) \quad (2.26)$$

$$(V_d)_{\alpha} = |f(\theta_d,\phi_d)|^2 \sum_{i=1}^{N_x}\sum_{j=1}^{N_y}\sum_{l=1}^{N_x}\sum_{m=1}^{N_y}(A_{ij}^{\alpha}G_{ij})^* M_{lm}G_{lm}R_{\tilde{d}}(T_{ij}^{d}+\tau^{\alpha}-T_{lm}^{d})\,. \quad (2.27)$$

In a similar fashion, by defining the interference and noise autocorrelation functions to be

$$R_{\tilde{i}_k}(\tau) = E[\tilde{i}_{ik}(t)^*\tilde{i}_{ik}(t+\tau)]\,, \quad (2.28)$$

$$R_{\tilde{n}}(\tau) = E[\tilde{n}_{ij}(t)^*\tilde{n}_{ij}(t+\tau)]\,, \quad (2.29)$$

the elements of the interfering and noise components of Φ and V can be found as

$$(\Phi_i)_{\alpha\beta} = \sum_{i=1}^{N_x}\sum_{j=1}^{N_y}\sum_{l=1}^{N_x}\sum_{m=1}^{N_y}(A_{ij}^{\alpha}G_{ij})^* A_{lm}^{\beta}G_{lm}\sum_{k=1}^{P}|f(\theta_{ik},\phi_{ik})|^2 R_{\tilde{i}_k}(T_{ij}^{k}+\tau^{\alpha}-T_{lm}^{k}-\tau^{\beta})\,, \quad (2.30)$$

$$(V_i)_{\alpha} = \sum_{i=1}^{N_x}\sum_{j=1}^{N_y}\sum_{l=1}^{N_x}\sum_{m=1}^{N_y}(A_{ij}^{\alpha}G_{ij})^* M_{lm}G_{lm}\sum_{k=1}^{P}|f(\theta_{ik},\phi_{ik})|^2 R_{\tilde{i}_k}(T_{ij}^{k}+\tau^{\alpha}-T_{lm}^{k})\,, \quad (2.31)$$

$$(\Phi_n)_{\alpha\beta} = \sum_{i=1}^{N_x}\sum_{j=1}^{N_y}(A_{ij}^{\alpha})^* A_{ij}^{\beta}R_{\tilde{n}}(\tau^{\alpha}-\tau^{\beta})\,, \quad (2.32)$$

$$(V_n)_{\alpha} = \sum_{i=1}^{N_x}\sum_{j=1}^{N_y}(A_{ij}^{\alpha})^* M_{ij}R_{\tilde{n}}(\tau^{\alpha})\,. \quad (2.33)$$

Once Φ, V, and then the weight vector are computed from Eqs. (2.12)- (2.14), the output desired, interfering, and noise signal powers can be found from

$$P_d = \frac{1}{2}E\left\{|\tilde{s}_o^d(t)|^2\right\} = P_{d0} + \frac{1}{2}W^H\Phi_d W + Re\{W^H V_d\} \quad (2.34)$$

$$P_i = \frac{1}{2}E\left\{|\tilde{s}_o^i(t)|^2\right\} = P_{i0} + \frac{1}{2}W^H\Phi_i W + Re\{W^H V_i\} \quad (2.35)$$

$$P_n = \frac{1}{2}E\left\{|\tilde{s}_o^n(t)|^2\right\} = P_{n0} + \frac{1}{2}W^H\Phi_n W + Re\{W^H V_n\}, \quad (2.36)$$

where P_{d0}, P_{i0}, and P_{n0} are the desired, interference, and noise powers present in the mainbeam signal. The superscript H denotes complex conjugate transpose. The mainbeam signal powers are given by

$$P_{d0} = \frac{1}{2}E[|\tilde{x}^d_m(t)|^2] \tag{2.37}$$
$$= \frac{1}{2}|f(\theta_d,\phi_d)|^2 \sum_{i=1}^{N_x}\sum_{j=1}^{N_y}\sum_{l=1}^{N_x}\sum_{m=1}^{N_y}(M_{ij}G_{ij})^* M_{lm}G_{lm}R_{\tilde{d}}(T^d_{ij}-T^d_{lm}) ,$$

$$P_{i0} = \frac{1}{2}E[|\tilde{x}^i_m(t)|^2] \tag{2.38}$$
$$= \frac{1}{2}\sum_{i=1}^{N_x}\sum_{j=1}^{N_y}\sum_{l=1}^{N_x}\sum_{m=1}^{N_y}(M_{ij}G_{ij})^* M_{lm}G_{lm}\sum_{k=1}^{P}|f(\theta_{ik},\phi_{ik})|^2 R_{\tilde{i}k}(T^k_{ij}-T^k_{lm}) ,$$

and

$$P_{n0} = \frac{1}{2}E[|\tilde{x}^n_m(t)|^2] = \frac{1}{2}R_{\tilde{n}}(0)\sum_{i=1}^{N_x}\sum_{j=1}^{N_y}|M_{ij}|^2 . \tag{2.39}$$

From the mainbeam and output signal powers, several adaptive array performance measures may be computed. First, the output-signal-to-interference-plus-noise ratio(SINR) is

$$SINR = \frac{P_d}{P_i + P_n}. \tag{2.40}$$

Second, we define the cancellation ratio CR as the ratio of (1) the interference power in the mainbeam output, to (2) the output interference power after adaptation:

$$CR = \frac{P_{i0}}{P_i} . \tag{2.41}$$

Finally, we define the ratios R_d and R_n to be

$$R_d = \frac{P_d}{P_{d0}}, \tag{2.42}$$

and

$$R_n = \frac{P_n}{P_{n0}}. \tag{2.43}$$

R_d and R_n will be called the desired signal and noise signal improvement ratios.

In addition to the above performance measures, we may also be interested in the various array antenna patterns pertaining to a given configuration and/or signal scenario. We define the patterns of interest here for future reference. The pattern of an array antenna is a single frequency concept and our definitions are valid at the center frequency ω_d of the signal bandwidth.

The mainbeam pattern $F_M(\theta,\phi)$ is defined to be

$$F_M(\theta,\phi) = f(\theta,\phi)\sum_{l=1}^{N_x}\sum_{m=1}^{N_y} M_{lm} e^{j2\pi\beta[(l-1)\cos\phi+(m-1)\sin\phi]\sin\theta}\,. \tag{2.44}$$

Similarly, we define the pattern of the α^{th} auxiliary to be

$$F_\alpha(\theta,\phi) = f(\theta,\phi)\sum_{l=1}^{N_x}\sum_{m=1}^{N_y} A_{lm}^{\alpha} e^{j2\pi\beta[(l-1)\cos\phi+(m-1)\sin\phi]\sin\theta}\,. \tag{2.45}$$

Once the weights are computed, we may be interested in the weighted auxiliary pattern and the adapted pattern. The weighted auxiliary pattern, $F_X(\theta,\phi)$ is defined to be

$$F_X(\theta,\phi) = \sum_{\alpha=1}^{K} w_\alpha e^{-j\omega_d\tau^\alpha} F_\alpha(\theta,\phi)\,, \tag{2.46}$$

where the w_α are the weights, the τ^α are the delays on the auxiliary signals, and the $F_\alpha(\theta,\phi)$ are the individual auxiliary patterns defined above. Finally, the adapted pattern is defined as the sum of the mainbeam and weighted auxiliary patterns,

$$F_A(\theta,\phi) = F_M(\theta,\phi) + F_X(\theta,\phi)\,. \tag{2.47}$$

2.3 Signal Models

We assume that the incident desired and interfering signals have the rectangular power spectral densities shown in Figure 2.3(a) and (b). We also assume that the noise signal on each element has the power spectral density shown in Figure 2.3(c). We assume that these signals all have the center frequency ω_d. We define the desired signal relative bandwidth to be

$$B_d = \frac{\Delta\omega_d}{\omega_d} \ . \tag{2.48}$$

Similarly, we define the relative bandwidth of the k^{th} interfering signal by

$$B_{ik} = \frac{\Delta\omega_{ik}}{\omega_d} \ . \tag{2.49}$$

We shall assume that the noise relative bandwidth is equal to the desired signal relative bandwidth.

The autocorrelation functions (ACFs) for the incident desired and k^{th} interfering signals, and for the element noise signals are given by the inverse Fourier transforms of the signal spectra shown in Fig. 2.3. These ACFs are given by

$$R_d(\tau) = p_d \text{sinc}\left(\frac{\Delta\omega_d\tau}{2}\right) e^{j\omega_d\tau} \ , \tag{2.50}$$

$$R_{ik}(\tau) = p_{ik} \text{sinc}\left(\frac{\Delta\omega_{ik}\tau}{2}\right) e^{j\omega_d\tau} \ , \tag{2.51}$$

$$R_n(\tau) = \sigma^2 \text{sinc}\left(\frac{\Delta\omega_d\tau}{2}\right) e^{j\omega_d\tau} \ , \tag{2.52}$$

where p_d and p_{ik} are the powers of the incident desired and k^{th} interfering signals as would be received on an isotropic element, and σ^2 is the power of the noise signal added by the T/R module at each element.

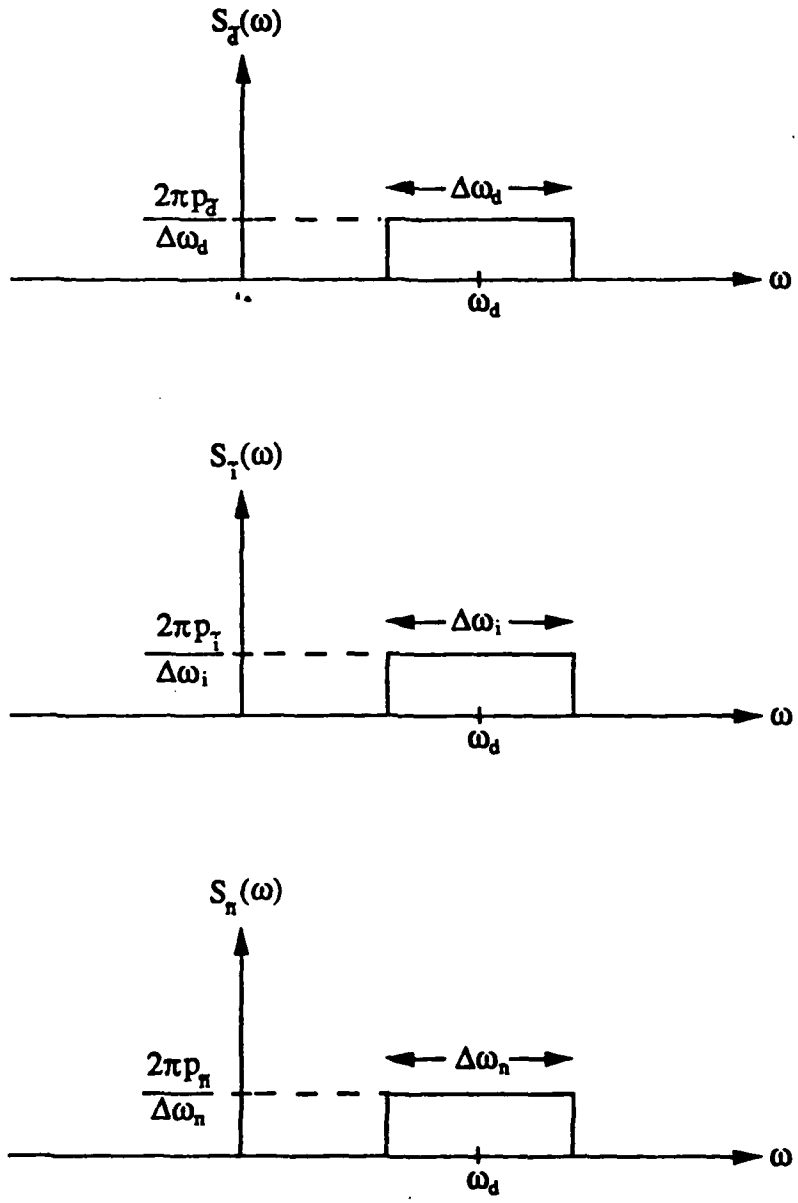

Figure 2.3: The power spectral densities of the incident desired and interfering signals and for the element noise signals.

Once the incident signal powers are specified, the ACFs above are used to compute Φ, V, and the array weights. We define the desired-signal-to-noise ratio (SNR) as

$$SNR = 10\log\left(\frac{p_d}{\sigma^2}\right) . \tag{2.53}$$

Similarly, we define the interference-to-noise ratio of the k^{th} interfering signal to be

$$INR_k = 10\log\left(\frac{p_{ik}}{\sigma^2}\right) . \tag{2.54}$$

The SNR and INRs relate the signal powers received on an isotropic element. We find that a convenient normalization is to set $\sigma^2 = 1$, so that the input signal powers are obtained, from Eqs. (2.53) and (2.54), by specifying the SNR and the INR for each interfering signal. Then if we express the output signal powers, given by Eqs. (2.34)- (2.39), in dB, we mean dB relative to the noise power on an isotropic element.

2.4 The element pattern

The received signal at a particular element in the array depends not only on the incident signal environment but also on the radiation pattern of the element itself. In this section we shall briefly describe the element pattern used in the mathematical model of the adaptive array.

We assume the adaptive array is to be used to provide jamming protection to a space based radar, as shown in Figure 2.4. This radar is to be mounted on a satellite in a low altitude earth orbit. The altitude h_s of the satellite in this orbit will be in the range from 600 to 1000 nautical miles(nmi). The array will be oriented so

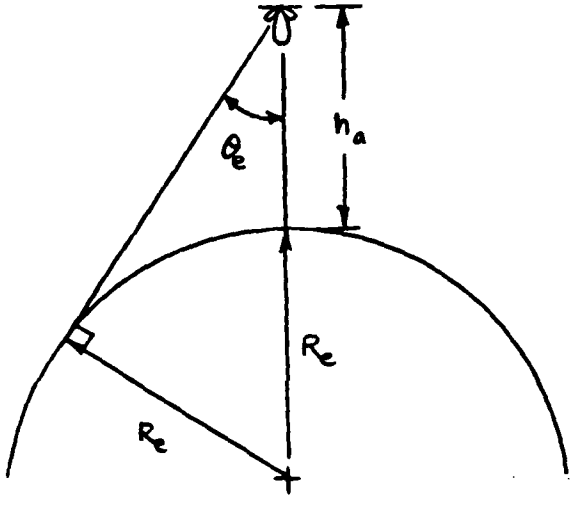

Figure 2.4: Diagram of a space based radar on an orbiting satellite.

its broadside direction points straight down toward the center of the earth. It is assumed that the array will only receive signals from the surface of the earth.

From a given altitude h_a, the edge of the earth subtends an angle of $2\theta_e$ at the satellite, as shown in Figure 2.4. θ_e varies with the altitude of the satellite, according to

$$\theta_e = \sin^{-1}\left(\frac{R_e}{R_e + h_a}\right) , \tag{2.55}$$

where $R_e = 6367.65$ km is the radius of the earth. Figure 2.5 shows θ_e as a function of the altitude, over the range 600 to 1000 nmi. We assume that no potential targets nor any jammers originate from outside the earth's extent. The element pattern should have good coverage out to θ_e. Thus one requirement on the element pattern

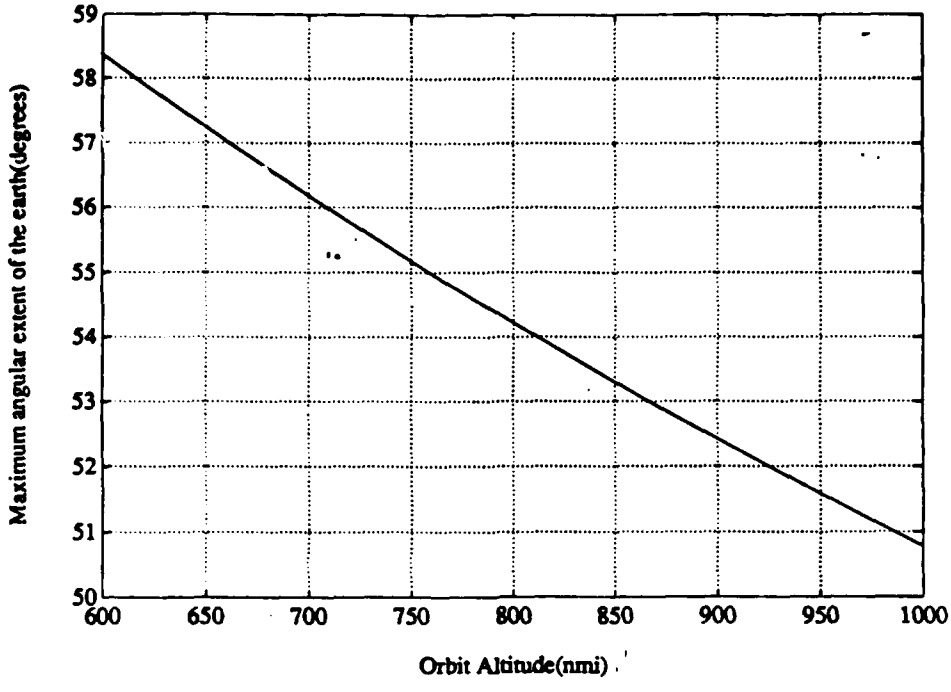

Figure 2.5: The angular extent of the earth, θ_e, viewed from an orbiting satellite, as a function of the orbit altitude.

should be that it has a maximum near θ_e and a null at endfire. A second application requirement should be that the element also have a null at broadside to suppress the strong clutter return due to specular reflection. We also require that there be no other nulls in the element pattern.

A vertical monopole above a perfectly conducting infinite ground plane will have a pattern null at broadside, and will radiate with maximum directivity at endfire, i.e. along the ground plane. The angle of maximum radiation can be reduced from $\theta = 90°$(endfire) to a value $\theta < 90°$ by adding a dielectric layer over the ground plane. For this study, we will assume for the element a monopole overa

thick dielectric sheet, and model its radiation pattern $f(\theta, \phi)$ by [9]

$$f(\theta,\phi) = \left|\frac{1}{\sin\theta}\left[e^{jk_0h\cos\theta} - j\cos\theta\sin k_0h - \cos k_0h + R_g(\theta)\left(e^{-jk_0h\cos\theta} + j\cos\theta\sin k_0h - \cos k_0h\right)\right]\right| , \quad (2.56)$$

where k_0 is the free space propagation constant, h is the height of the monopole, and

$$R_g(\theta) = \frac{\epsilon_r\cos\theta - \sqrt{\epsilon_r - \sin^2\theta}}{\epsilon_r\cos\theta + \sqrt{\epsilon_r - \sin^2\theta}} , \quad (2.57)$$

with ϵ_r the relative permittivity of the dielectric half-space. This result is obtained from image theory by integrating the fields of an infinitesimal vertical dipole over the finite length h. R_g is the Fresnel reflection coefficient for an electric field polarized parallel to the plane of incidence. The pattern of the vertical monopole is only dependent on the angle θ because the monopole itself is symmetric with respect to the azimuth angle ϕ.

In the pattern function of Eq. (2.56) there are two parameters to specify: the physical length h of the monopole and the relative permittivity ϵ_r of the dielectric half-space. Figures 2.6 (a)-(d) show the normalized patterns obtained for $\epsilon_r = 2., 5., 10.$ and for different monopole lengths up to one wavelength. For reference, the dashed curve in these plots is the element pattern function of an ideal infinitesimal monopole on a perfect ground plane (a $\sin\theta$ pattern).

The patterns of the $0.25\lambda_0$ monopoles are very similar, each providing a slightly stronger response than the ideal monopole for angles $|\theta| \lesssim -70°$. The $0.5\lambda_0$ monopole has a more directive pattern, with a peak which moves closer to endfire as the relative permittivity is increased. For small values of ϵ_r the peak is near $\theta = \pm 70°$, which is greater than the angular extent of the earth. For this reason the

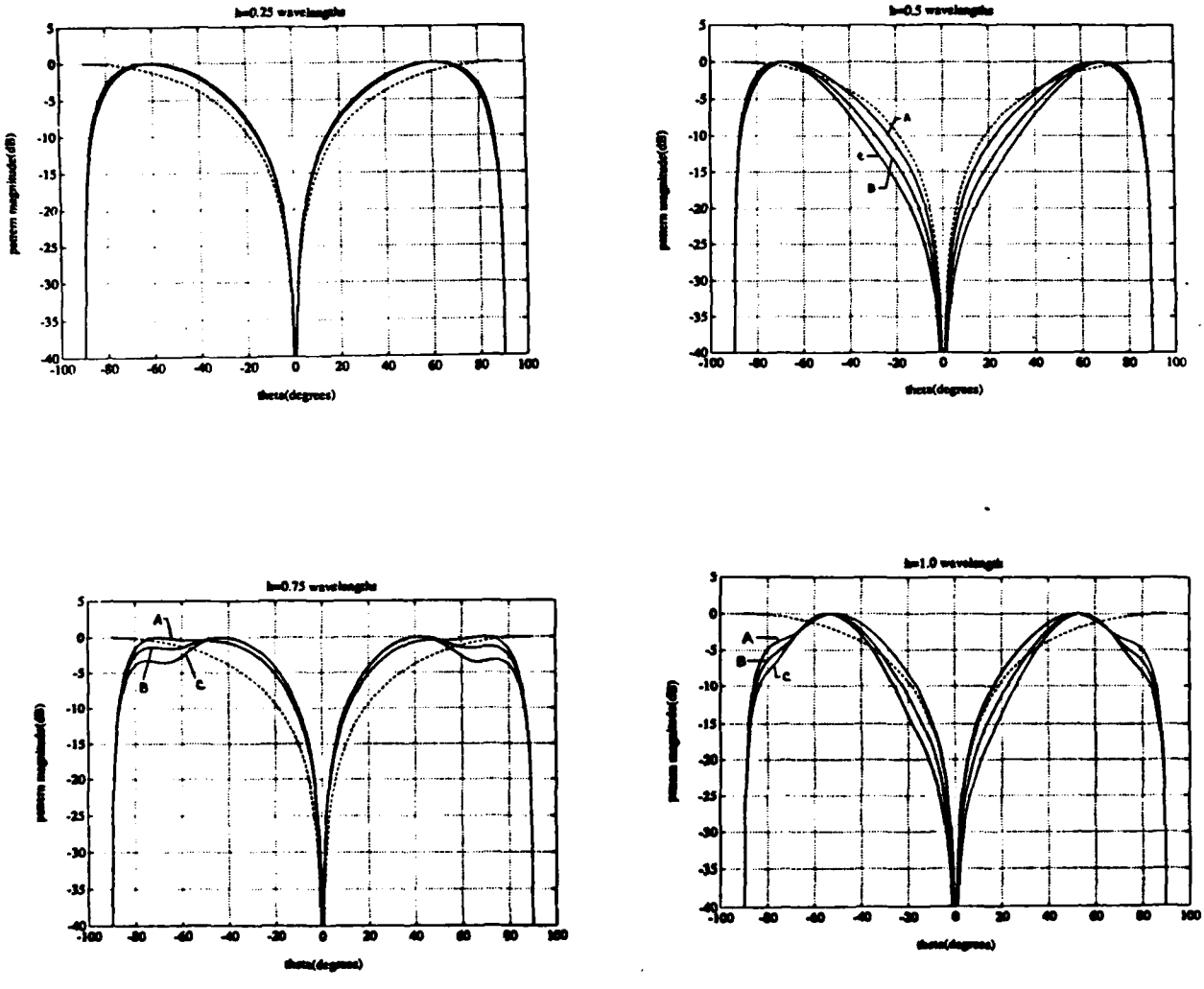

Figure 2.6: Element patterns for different h and different ϵ_r. A:$\epsilon_r = 2.0$ B:$\epsilon_r = 5.0$ C:$\epsilon_r = 10.0$

$0.5\lambda_0$ monopole would not be a good element choice. Similar behavior is observed for the $1\lambda_0$ monopole. The patterns for the $h = 0.75\lambda_0$ are different in that they are nearly flat for a wider angular region than the other lengths. The $\epsilon_r = 5.$ pattern crosses the ideal pattern at about $\theta = \pm 59°$, which is nearly equal to the angular extent of the earth when the satellite is at its maximum orbit. This pattern has a stronger response than the ideal monopole for angles within the earth's extent, and because of the null at endfire, a smaller response for angles $|\theta| > \theta_e$. For these reasons we shall use the $h = 0.75\lambda_0$ monopole above an $\epsilon_r = 5$ dielectric half-space in the mathematical model.

There are, of course, other factors that will affect the patterns of the elements, such as the mutual coupling between monopoles, the finite thickness of the dielectric layer, and the finite size of the ground plane. However, these matters are beyond the scope of the present study. In this study, we shall use the element pattern in Eq. (2.56), with $\epsilon_r = 5$ and $h = 0.75\lambda_0$ for all the calculations of sidelobe canceller performance in this report.

Figure 2.7 shows an example of a mainbeam pattern formed with this element pattern, for a 100×1 array. Figure 2.7. This pattern was obtained by applying a 55 dB Dolph-Chebyshev amplitude taper to the elements. The main lobe was steered to $\theta_d = 30°$ from broadside.

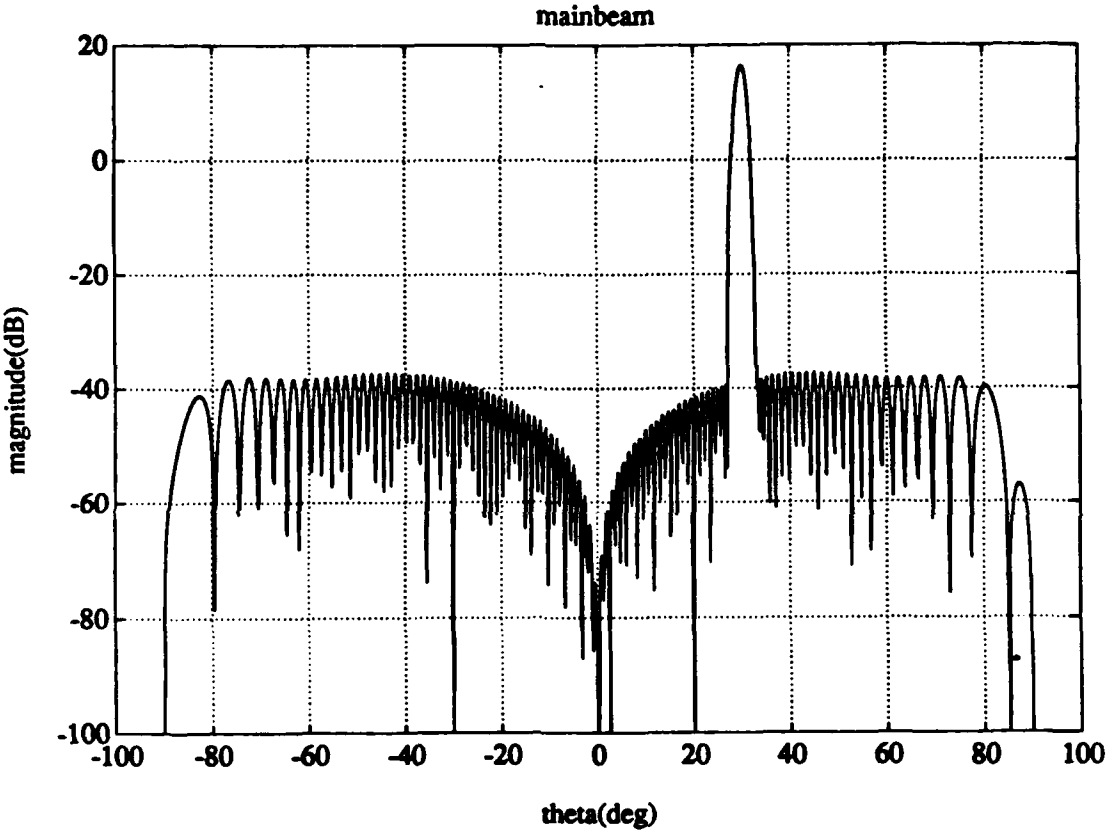

Figure 2.7: The mainbeam pattern of a 100×1 array with 55 dB Dolph-Chebyshev weighting.

3. The Effect of Random Amplitude and Phase Errors on Array Performance

3.1 Introduction

The Dolph-Chebyshev method for calculating the amplitude taper for an array antenna allows one to create a pattern that will have a specified peak sidelobe level. Theoretically, antennas with arbitrarily low sidelobes are possible. In practice, however, several factors limit the accuracy with which the theoretical Dolph-Chebyshev amplitude taper can be achieved. Examples of such factors are slight amplitude and phase mismatches in the T/R modules present at each array element and quantization errors from digital phase shifters used at each array element to steer the mainbeam. The accuracy to which the ideal element weights can be set determines the sidelobe level achieved in practice, and thus it is important to know the effect of random amplitude and phase errors on the array performance, especially on the sidelobe level.

Many authors have considered the effects of random errors on phased array performance.[10,11,12] Our purpose in this chapter is to apply these results to a planar array of monopoles above a ground plane. First we derive the expression for the ensemble average,(or expected) power pattern of the array with errors. This derivation is similar to that given by Ruze[10]. Then we use the Rician probability distribution of the array pattern magnitude (in the sidelobe region) to calculate results for various levels of amplitude and phase errors. These results are in the form of probabilities that a specified sidelobe level is not exceeded as a function of the variances of the amplitude and phase errors and as a function of angle. We then

use these results to calculate peak sidelobe probabilities and show examples which illustrate the effects of errors on the peak sidelobe level(SLL) expected for various error scenarios, design SLLs and array sizes.

Our main goal in this section is to determine the degradation in peak sidelobe level expected for typical values of amplitude and phase errors. Once the degradation can be predicted, we can then determine the proper design sidelobe level so that the actual performance in the presence of errors meets the desired sidelobe level requirement.

Ultimately, our goal is not only to determine the effects of random errors on the mainbeam performance, but also to determine their effects on the performance of the adaptive array system in which the array is used.

3.2 Derivation of average power pattern

Consider again the planar array geometry shown in Figure 2.1. The voltage pattern of the mainbeam of this array was defined in Eq. (2.44) to be

$$F(\theta,\phi) = f(\theta,\phi)\sum_{l=1}^{N_x}\sum_{m=1}^{N_y} M_{lm}e^{j2\pi\beta[(l-1)\cos\phi+(m-1)\sin\phi]\sin\theta} \tag{3.1}$$

where $f(\theta,\phi)$ is the element pattern, and the rest of Eq. (3.1) is the array factor. The main beam combiner weights, M_{lm}, for a beam steered to the (θ_d,ϕ_d) directions were given in Eq. (2.8) as

$$M_{lm} = m_{lm}e^{-j\Psi^d_{lm}}, \tag{3.2}$$

where the m_{lm} form the Dolph-Chebyshev amplitude taper applied to achieve a specified sidelobe performance and

$$\Psi^d_{lm} = 2\pi\beta[(l-1)\cos\phi_d + (m-1)\sin\phi_d]\sin\theta_d \tag{3.3}$$

is the phase factor required to steer the beam in the (θ_d, ϕ_d) directions. Thus the ideal, or error-free voltage pattern is given by

$$F_0(\theta,\phi) = f(\theta,\phi)\sum_{l=1}^{N_x}\sum_{m=1}^{N_y} m_{lm} e^{j(\Psi_{lm}-\Psi_{lm}^d)} . \tag{3.4}$$

(Hereafter, pattern quantities with a 0 subscript will refer to the case where the $m_{lm} and \Psi_{lm}^d$ are not random.) To model the effects of random amplitude and phase errors, we replace the m_{lm} in Eq. (3.4) with

$$m'_{lm} = m_{lm}(1+\delta_{lm})e^{j\phi_{lm}} \tag{3.5}$$

where δ_{lm} and ϕ_{lm} are the random amplitude and phase errors, respectively, at the $(i,j)^{th}$ element.[1]

The actual voltage pattern, which includes the effects of errors, can be written as

$$F(\theta,\phi) = f(\theta,\phi)\sum_{l=1}^{N_x}\sum_{m=1}^{N_y} m_{lm}(1+\delta_{lm})e^{j\phi_{lm}}e^{j[(l-1)\mu+(m-1)\nu]} \tag{3.6}$$

where

$$\mu = 2\pi\beta(\cos\phi\sin\theta - \cos\phi_0\sin\theta_0) \tag{3.7}$$

and

$$\nu = 2\pi\beta(\sin\phi\sin\theta - \sin\phi_0\sin\theta_0) \tag{3.8}$$

The power pattern is then

$$P(\theta,\phi) = |F(\theta,\phi)|^2 \tag{3.9}$$

Normalizing to the beam maximum gives the normalized power pattern $P_n(\theta,\phi)$:

$$P_n(\theta,\phi) = \frac{P(\theta,\phi)}{|F(\theta_d,\phi_d)|^2} \tag{3.10}$$

[1]In the model of Chapter 2, we let $G_{lm} = (1+\delta_{lm})\exp(j\phi_{lm})$ to incorporate random amplitude and phase errors.

The expected value, or ensemble average, of the power pattern, denoted by $P_a(\theta,\phi)$, is

$$P_a(\theta,\phi) = E\{P(\theta,\phi)\} \tag{3.11}$$

where the E denotes expectation. It will be assumed that the amplitude errors are independent and identically distributed from element to element, that the phase errors are also independent and identically distributed, that the amplitude errors δ_{lm} are independent of the phase errors ϕ_{lm}, and that both the δ_{lm} and the ϕ_{lm} are zero mean random variables. Then the expected power pattern is

$$\begin{aligned} P_a(\theta,\phi) &= |f(\theta,\phi)|^2 \sum_{m=1}^{N_x}\sum_{n=1}^{N_y}\sum_{r=1}^{N_x}\sum_{s=1}^{N_y} A_{mn}A_{rs}E\{(1+\delta_{mn})(1+\delta_{rs})\} \times \\ &\quad E\{e^{j(\phi_{mn}-\phi_{rs})}\}e^{j[(m-r)\mu-(n-s)\nu]} \end{aligned} \tag{3.12}$$

To simplify this expression we must consider two types of terms: those for which $m \neq r$ or $n \neq s$ and those for which $m = r$ and $n = s$. For the first type,

$$E\{(1+\delta_{mn})(1+\delta_{rs})\} = 1 \tag{3.13}$$

and

$$E\{e^{j(\phi_{mn}-\phi_{rs})}\} = |\Phi(1)|^2 \tag{3.14}$$

where $\Phi(1) = \int p_\phi(\phi)e^{j\phi}d\phi$ is the characteristic function of the phase error. For the second type we find

$$E\{(1+\delta_{mn})(1+\delta_{rs})\} = 1+\sigma_\delta^2 \tag{3.15}$$

where σ_δ^2 is the variance of the amplitude error. Also

$$E\{e^{j(\phi_{mn}-\phi_{rs})}\} = 1 \tag{3.16}$$

We combine the results from Eqs. (3.13)- (3.16) to get

$$P_a(\theta,\phi) = |f(\theta,\phi)|^2 \left\{ |\Phi(1)|^2 \sum\sum_{m\neq r}\sum\sum_{n\neq s} A_{mn}A_{rs}e^{j[(m-r)\mu+(n-s)\nu]} + \sum_m\sum_n A_{mn}^2(1+\sigma_\delta^2) \right\} \quad (3.17)$$

Adding and subtracting the $m = r$ and $n = s$ terms in Eq. (3.17) yields

$$P_a(\theta,\phi) = |\Phi(1)|^2 P_0(\theta,\phi) + (1+\sigma_\delta^2 - |\Phi(1)|^2)|f(\theta,\phi)|^2 \sum_{m=1}^{N_x}\sum_{n=1}^{N_y} A_{mn}^2 \quad (3.18)$$

Finally, we can normalize this equation to the beam maximum to get

$$P_{an}(\theta,\phi) = |\Phi(1)|^2 P_{n0}(\theta,\phi) + (1+\sigma_\delta^2 - |\Phi(1)|^2)\frac{|f(\theta,\phi)|^2 \sum_{m=1}^{N_x}\sum_{n=1}^{N_y} A_{mn}^2}{|f(\theta_d,\phi_d)|^2 (\sum_{m=1}^{N_x}\sum_{n=1}^{N_y} A_{mn})^2} \quad (3.19)$$

where $P_{n0}(\theta,\phi)$ is the normalized error-free pattern. This is essentially the expression developed by Ruze.[10]

The first term of Eq. (3.19) is the error-free normalized pattern multiplied by a constant which depends only on the phase error. The second term is a contribution due to both the amplitude and phase errors. Aside from the angular dependence of the element factor, it may be seen that the effect of the random errors can be seen to add(on the average) a constant bias, or 'statistically omnidirectional'[10] sidelobe level to the error-free pattern. We can also see from the form of this term that for a given error level(for fixed σ_δ^2 and $|\Phi(1)|^2$) the effect of the errors will be smaller for larger arrays. The reason for this behavior is that the denominator of the second term increases faster than the numerator, by a factor approximately equal to the total number of elements in the array. This fact will be evident in the results to follow.

3.3 Results using pdf of pattern magnitude

In order to discuss the peak sidelobe level, we need to know the probability distribution at a point in the sidelobe region. It can be shown[10] that the magnitude $R = |F_n(\theta, \phi)|$ of the normalized pattern has a Rician distribution in the sidelobe region. Its probability density function is

$$p(R) = \frac{R}{\gamma^2} e^{-(\frac{R^2+a^2}{2\gamma^2})} I_0(\frac{Ra}{\gamma^2}) \tag{3.20}$$

where

$$a^2 = |\Phi(1)|^2 P_{n0}(\theta, \phi) \tag{3.21}$$

$$\gamma^2 = \frac{(1 + \sigma_\delta^2 - |\Phi(1)|^2)|f(\theta, \phi)|^2 \sum_{m=1}^{N_x} \sum_{n=1}^{N_y} A_{mn}^2}{2|f(\theta_0, \phi_0)|^2 (\sum_{m=1}^{N_x} \sum_{n=1}^{N_y} A_{mn})^2} \tag{3.22}$$

and I_0 is the modified Bessel function of zeroth order. We can now find the probability, at a point in the sidelobe region, that a specified sidelobe level is or is not exceeded. The probability that the pattern magnitude at (θ, ϕ) exceeds a specified level S with respect to the beam maximum is given by

$$Pr\{R > S\} = \int_S^\infty \frac{R}{\gamma^2} e^{-(\frac{R^2+a^2}{2\gamma^2})} I_0(\frac{Ra}{\gamma^2}) dR = Q(\frac{a}{\gamma}, \frac{S}{\gamma}) \,, \tag{3.23}$$

where $Q(\alpha, \beta)$ denotes Marcum's Q function[13,14]. Because both R and γ^2 are a function of angular position in the sidelobe pattern, the probability that a certain level is exceeded will also be a function of angle. $\Pr\{R > S\}$ will be much higher for points at the peak of a sidelobe than for points near nulls in the error-free pattern.

As an illustration, consider a 100x1 linear array of monopoles, with a 55 dB Dolph-Chebyshev amplitude taper and a mainbeam steered to 30.0 degrees off broadside. The ideal pattern was shown in Figure 2.7. The peak sidelobe occurs at the element pattern maximum at angles of $\theta = \pm 43.75°$, and is -53.64 dB

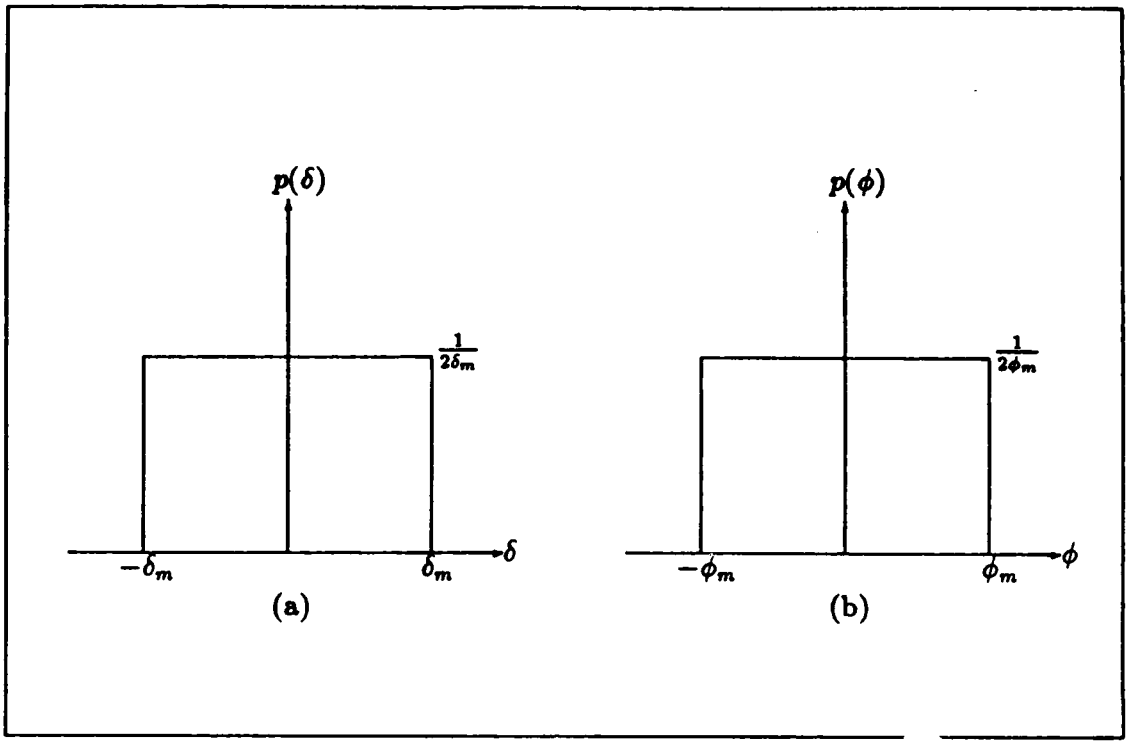

Figure 3.1: Probability density functions for the amplitude and phase errors present on an element.

with respect to the beam maximum.(The magnitude squared of the element pattern at the mainbeam steering angle accounts for the difference between the peak SLL and the -55 dB design SLL.) In the plots that follow, we have assumed that both the amplitude error and the phase error(δ_{lm}, ϕ_{lm}) are uniformly distributed random variables with probability density functions as shown in Figure 3.1. δ_m is the maximum expected amplitude error and ϕ_m is the maximum expected phase error. The uniform distribution of the phase error models the case where the phase is primarily due to quantization by a digital phase shifter present at each array element.

Figure 3.2 shows a typical result with random amplitudes and phases. It shows

the probability that the magnitude of the actual array pattern(with errors) is greater than -48 dB relative to the mainbeam(a 7 dB increase in peak SLL), as a function of θ, for $-90° \leq \theta \leq 20°$ in the sidelobe region. The maximum amplitude and phase errors are assumed to be 0.2 dB and $\pm 3°$, respectively. As noted earlier, the probability that the pattern magnitude exceeds a given level is very dependent on θ. The envelope of the curve of Figure 3.2 follows the magnitude of the element pattern. The oscillatory behavior reflects the sidelobe structure of the ideal(nonrandom) pattern. The probability that a given level is exceeded is higher at peaks of the ideal pattern than for points near the nulls of the ideal pattern.

One must be careful in interpreting these results because they are in terms of the sidelobe level at a point in the sidelobe region, and not a general statement about the peak sidelobe of the whole pattern. To generalize to the peak sidelobe level of the entire pattern, we need to evaluate Eq. (3.23) at N independent angles in the sidelobe region. Then the probability P_t that the peak sidelobe of the pattern exceeds a specified level S is

$$P_t = 1 - \prod_{i=1}^{N}(1 - P_i) \tag{3.24}$$

where the P_i are given by Eq. (3.23) evaluated at the i^{th} sample point of the sidelobe pattern. However, the problem here is to determine both the number of independent angles N and the locations of the independent sample points. It has been shown [15] that for a linear, uniformly illuminated array of isotropic elements, N is given by

$$N = D(1 + |u_0|) \tag{3.25}$$

where $u_0 = \sin\theta_0$, θ_0 is the direction to which the mainbeam is scanned, and D is

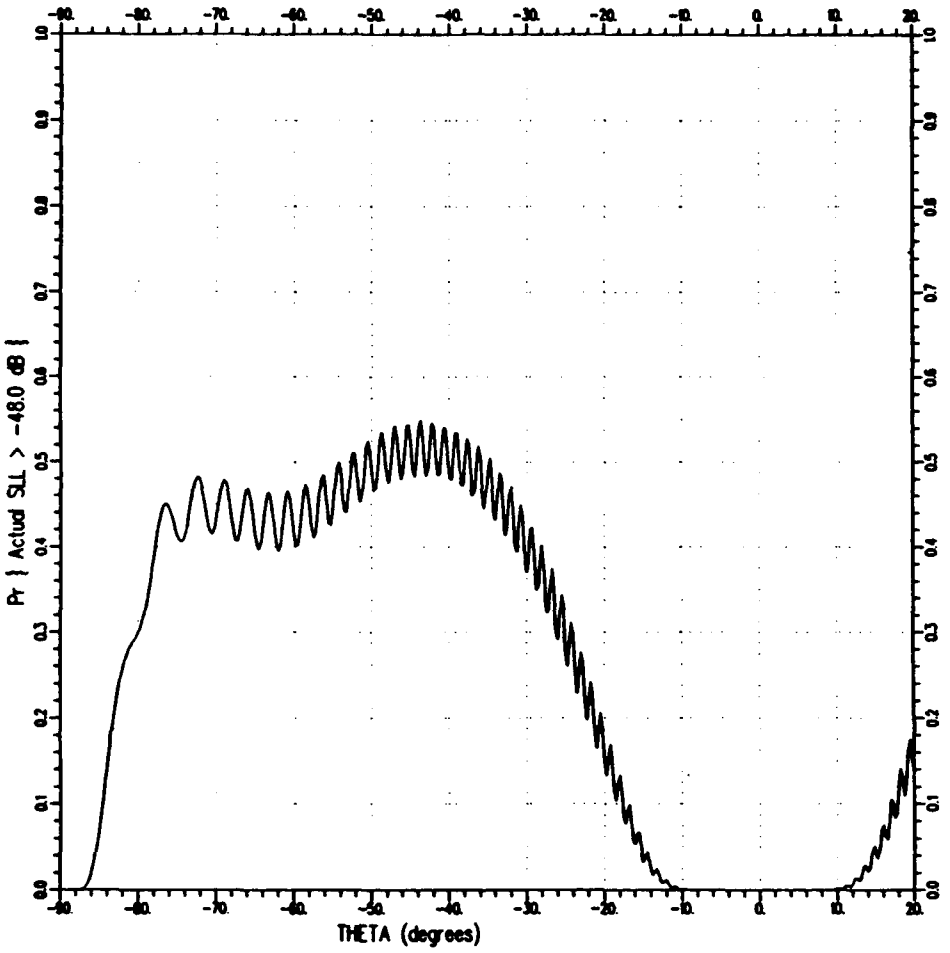

Figure 3.2: Probability that the actual SLL exceeds -48 dB. Amplitude errors ±0.2 dB, Phase error ±3°.

the length of the array in wavelengths. This result can be arrived at by counting the total number of sidelobes present in the visible region or by actually computing the autocorrelation function of the sidelobe pattern to determine the spacing between independent points. Extending this result to the general case is complicated by several factors. First, non-uniform (e.g.Dolph-Chebyshev) weighting causes the sidelobes to be of unequal width. Thus it is not clear at what angular spacing to sample the sidelobe pattern to obtain statistically independent points. Second, the presence of the element pattern also affects the peak sidelobe level. Its effect is to reduce the number of points which contribute significantly to the peak sidelobe probability in Eq. (3.24). The probability is 1 that samples near the nulls of the element pattern will be less than the design SLL.

Our approach will be to assume that it is most likely that the actual peak sidelobe will be near a peak of the ideal sidelobe pattern. Thus, to estimate peak sidelobe probabilities, we sample the sidelobe pattern at points corresponding to sidelobe peaks in the no-error pattern. These points can be found from Dolph-Chebyshev array theory. The probability that a specified level is exceeded will be computed at each of these points and then used in Eq. (3.24) to give the probability that the peak sidelobe exceeds the specified level. The element factor will be taken into consideration by neglecting the contribution of points corresponding to angles where the magnitude of the normalized element pattern is less than -10 dB. If necessary, this element pattern cutoff may be adjusted to include more samples to improve the estimate of the peak sidelobe probabilities.

We shall next compute peak sidelobe probabilities using the above assumptions. We compare these results with similar results obtained from simulations. In the

simulations, probabilities are calculated from ensembles of 1000 actual patterns, for which the sidelobe region is scanned to find the level of the peak sidelobe. Different random errors are generated for each pattern, selected from distributions whose maximum values are specified.

Figure 3.3 shows the theoretical results for a 100×1 array with ±0.1 dB amplitude errors and different phase error levels. We plot the probabilities, calculated from Eq. (3.24) with the approximations described above, that the peak SLL will exceed S dB, as a function of S. The design SLL is 55 dB. The phase errors present correspond to different levels of phase shifter quantization, varying from 7 bits for curve D, to 10 bits, or a maximum phase error of 0.1758 degrees, for curve A. We are interested in the SLL for which Pr{peak SLL> S} is small, for we want to know the SLL which will not be exceeded with high probability by the array with errors. As an example from curve A, we can say that for the errors given, the peak SLL will be less than -48.0 dB with a probability of 0.92. Conversely, we can specify a peak SLL and interpolate to find the probability that this level is or is not exceeded(i.e. find the confidence level).

As a test of the assumptions made, we show in Figure 3.4 a comparison between the predicted results and a simulation, for the case of curve D of Figure 3.3. In the simulation, probabilities are computed from an ensemble of 1000 sample patterns. Each pattern in the ensemble was computed using a different set of computer generated amplitude and phase errors with the given distributions. The probabilities were computed by searching each pattern for the peak SLL and counting the number of patterns out of the 1000 in which this peak exceeded the level S dB, as S was varied. The excellent agreement between predicted and simulated values verifies

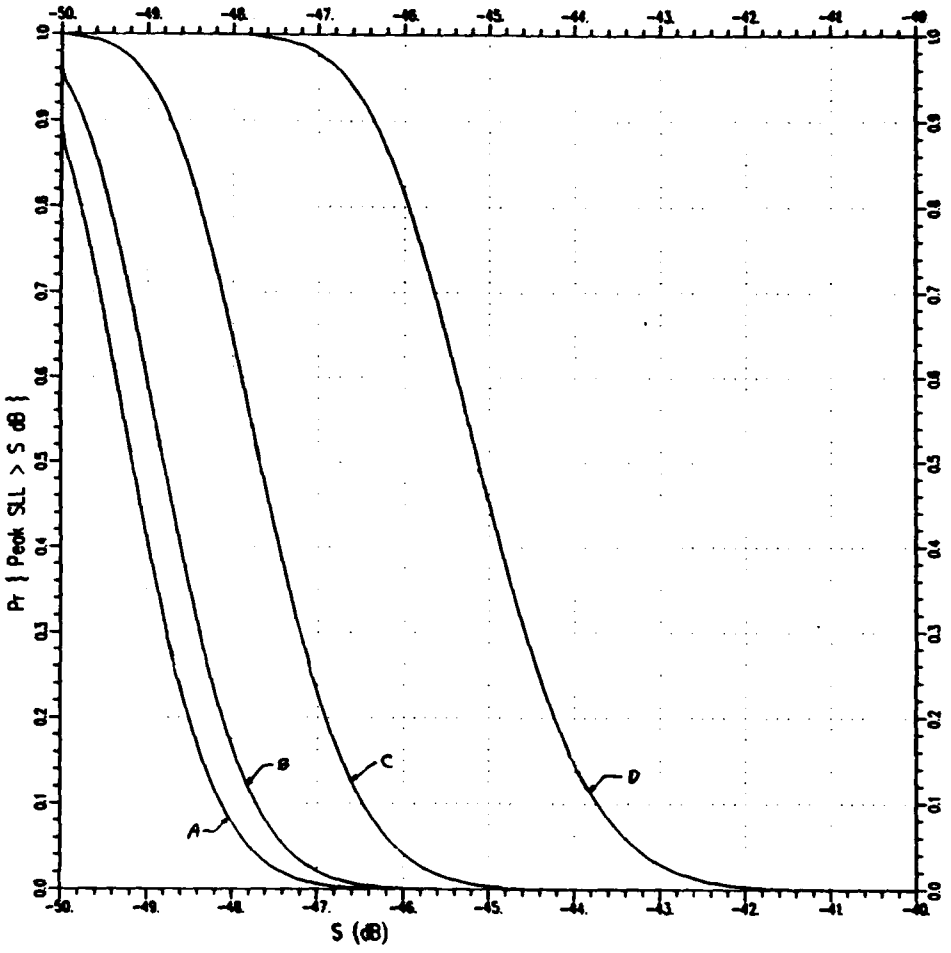

Figure 3.3: Pr{peak SLL > S dB} vs. S, for ± 0.1 dB amplitude error and varying phase errors. A:$\pm 0.17578125°$ B:$\pm 0.3515625°$ C:$\pm 0.703125°$ D:$\pm 1.40625°$

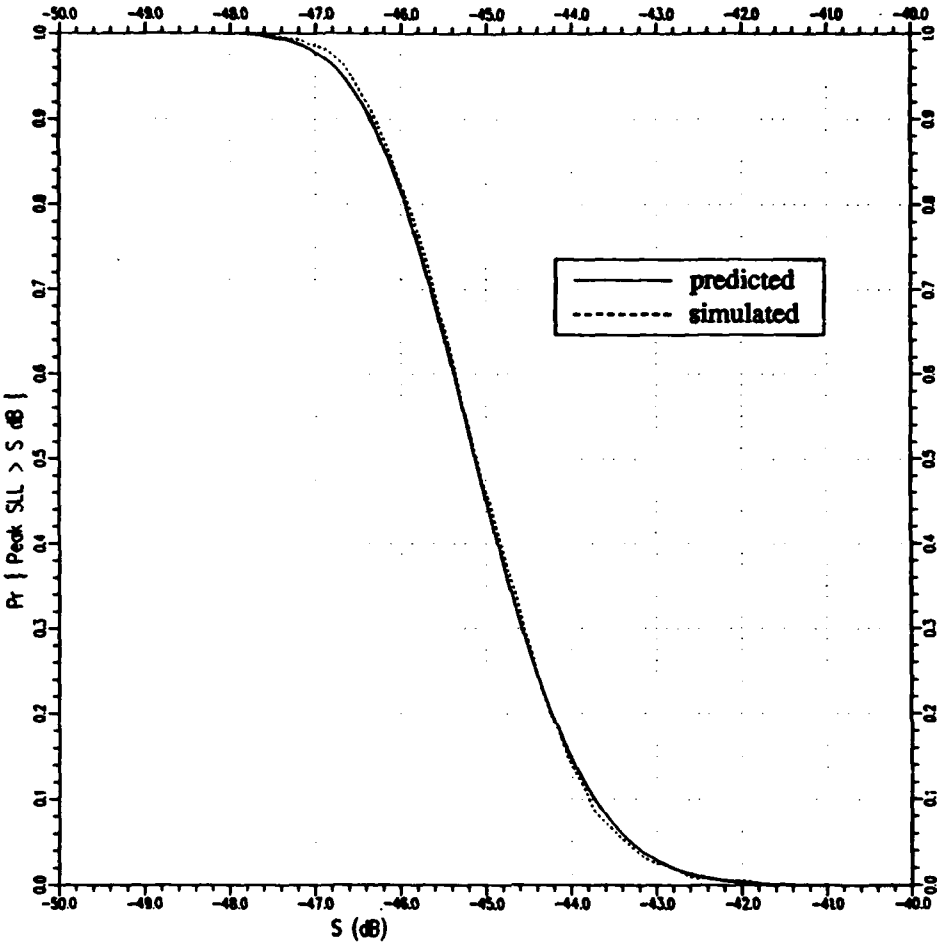

Figure 3.4: Comparison between predicted and simulated results, for a 100 element linear array. Amplitude error ±0.1 dB, Phase error ±1.40625°

that the method used in selecting sample points at which to evaluate Eq. (3.24) is indeed valid, and that the approximations used lead to useful results.

A more meaningful representation of peak SLL data is shown in Figure 3.5. Here we have combined the results from a number of different 100 element linear arrays, with their design SLL varying from -55 dB to -40 dB. We plot the increase in peak SLL, defined as the peak SLL with errors minus the peak SLL of the ideal pattern, vs the design SLL. In this figure only phase errors are present on each array element. This plot can be used to determine the design level needed to overcome the given error levels and achieve a desired peak SLL performance. The confidence level on the peak SLL is 0.95. Note that the increase in peak SLL becomes larger as we lower the design SLL. In other words, an array designed for low sidelobes will be more sensitive to random errors. By designing for a 55 dB SLL and keeping the phase errors within $\pm 0.703125°$, or 8 bits of phase quantization, the actual pattern will have a peak SLL no higher than about -49 dB.

Figure 3.6 shows a similar curve where it is assumed that there are only amplitude errors and no phase error in the element weights. In the absence of phase errors, we need to design for 55 dB sidelobes and keep the amplitude tolerances to within ± 0.1 dB to achieve an actual SLL of about -50 dB.

Figure 3.7 shows the case when both amplitude and phase errors are present. The amplitude error is fixed at$\pm$ 0.1 dB and the maximum phase error is varied. With amplitude errors, we now need to keep the phase error within $\pm 0.1758°$, or 10 bits of phase quantization, to keep the actual SLL 50 dB with a 55 dB design.

Figure 3.8 shows five such patterns, each using a different set of random weights with amplitude error ± 0.1 dB and phase error $\pm 0.1758°$, superimposed on one

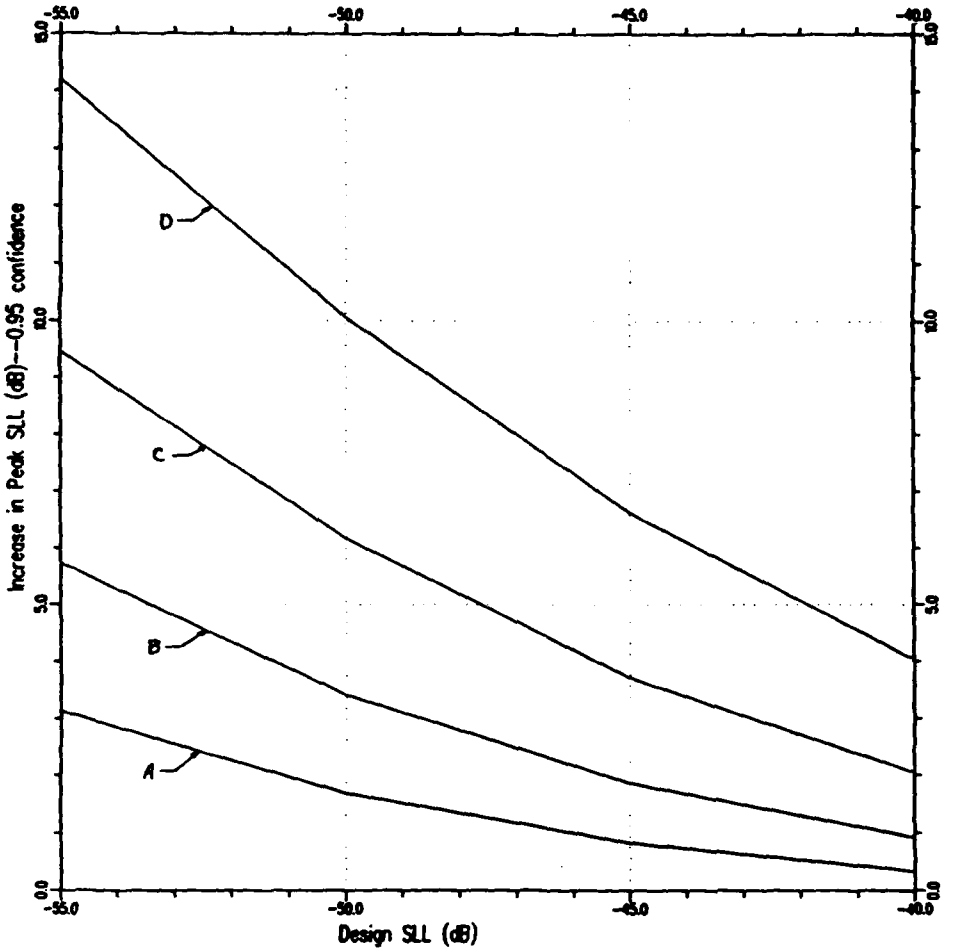

Figure 3.5: The increase in Peak SLL vs. the Chebyshev design SLL; Phase errors only. A:±0.3515625° B:±0.703125° C:±1.40625° D:±2.8125°

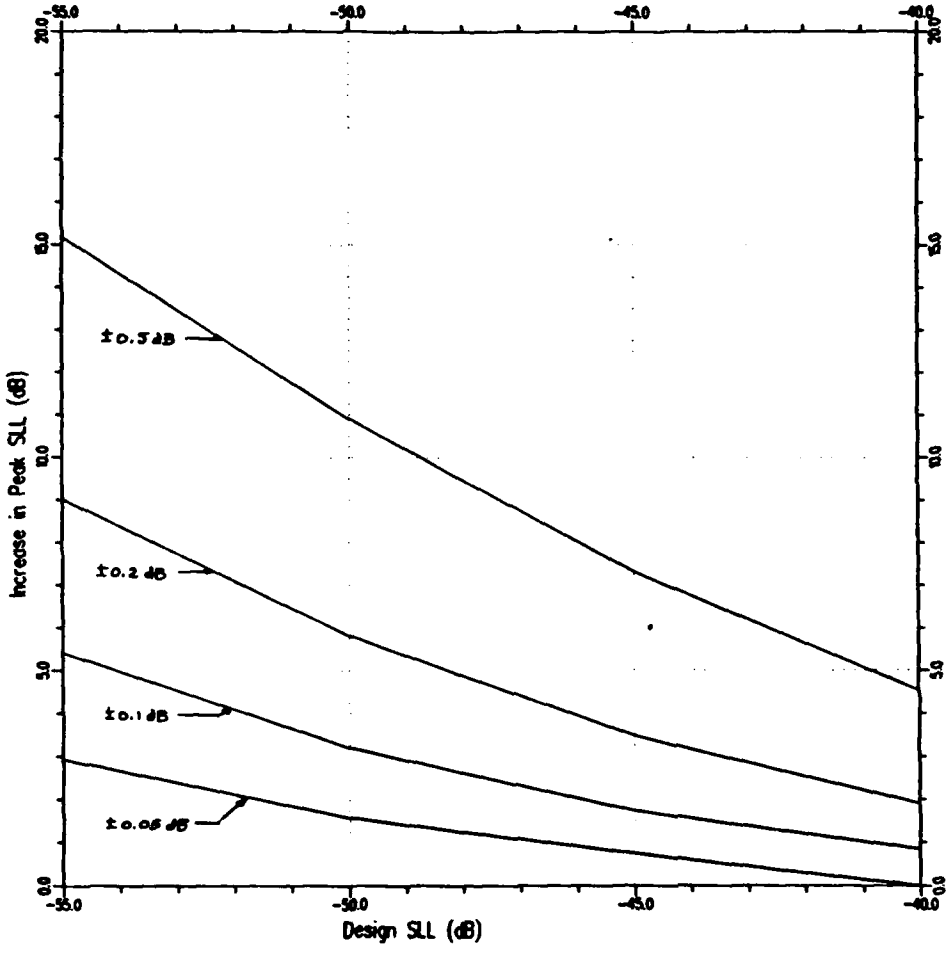

Figure 3.6: The increase in Peak SLL vs. the Chebyshev design SLL; Amplitude errors only.

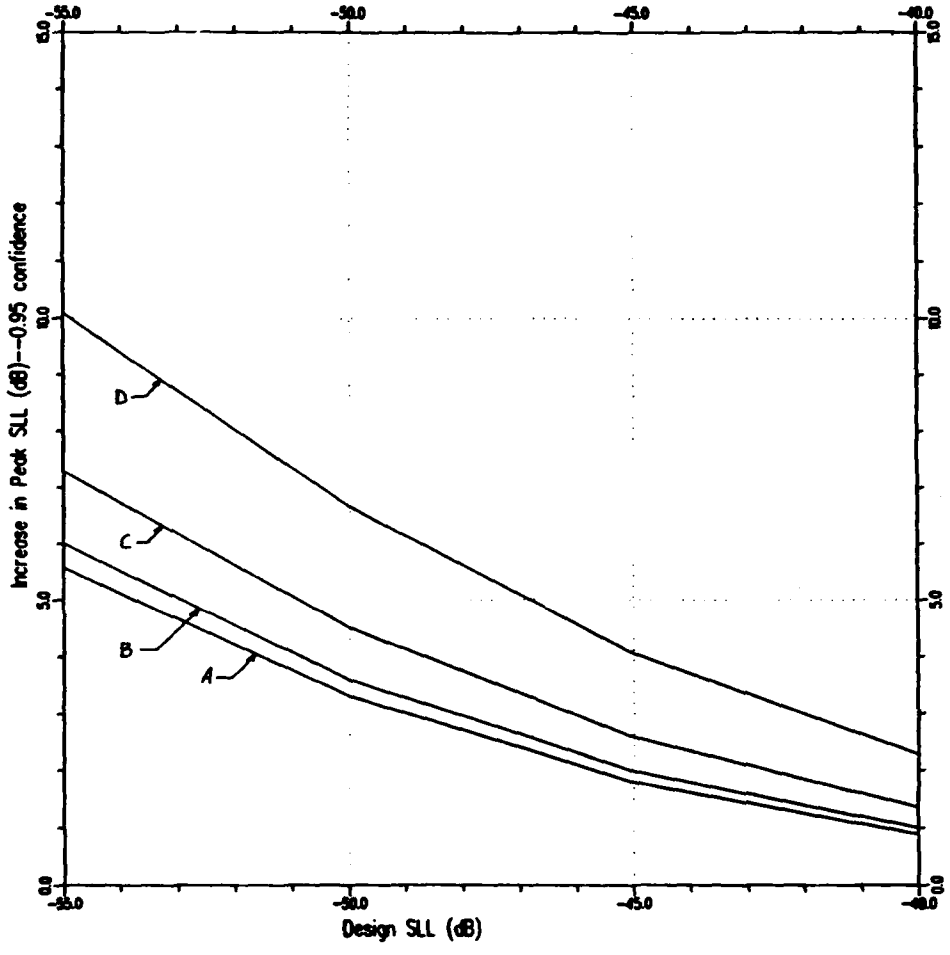

Figure 3.7: The increase in Peak SLL vs. the Chebyshev design SLL; the amplitude error is ±0.1 dB and the phase error is varied. A:±0.17578125° B:±0.3515625° C:±0.703125° D:±1.40625°

graph. The patterns are normalized to the array factor maximum, and we see that the peak SLL is 50 dB or less, as predicted. These error levels provide the desired 50 dB SLL, and will be used for most of the linear array sidelobe canceller configurations to be examined in the following chapters.

3.4 Integrated Average Sidelobe Level

The previous section discussed how randomness affects the sidelobe level of an array. A single array of this type is to be used to form the mainbeam of the adaptive array system. In the total array, however, it is not the mainbeam SLL but the SLL of the adapted pattern that is of concern. The adapted pattern, defined in Eq. (2.47), can be written as

$$F_A(\theta,\phi) = F_M(\theta,\phi) + \sum_{\alpha=1}^{K} w_\alpha e^{-j\omega_d \tau^\alpha} F_\alpha(\theta,\phi)\,, \tag{3.26}$$

where $F_M(\theta,\phi)$ and $F_\alpha(\theta,\phi)$ are the mainbeam and α^{th} auxiliary voltage patterns, and the other variables are as defined in Chapter 2.

The adapted pattern will be affected not only by the randomness in the mainbeam pattern, but also by the adaptive weights and the choices of auxiliary patterns.(The same randomness is present in the auxiliary patterns as in the mainbeam pattern, since both are formed from elements of the same array.) The weights themselves depend on the mainbeam and auxiliary patterns, and also on the power levels, bandwidths, and arrival angles of the incoming desired and interfering signals, and the noise signals present on each array element. In order to determine how the signal scenario and the auxiliary selection affects the SLL of the adaptive system, it will be helpful to define a quantity that can be used to characterize the sidelobe

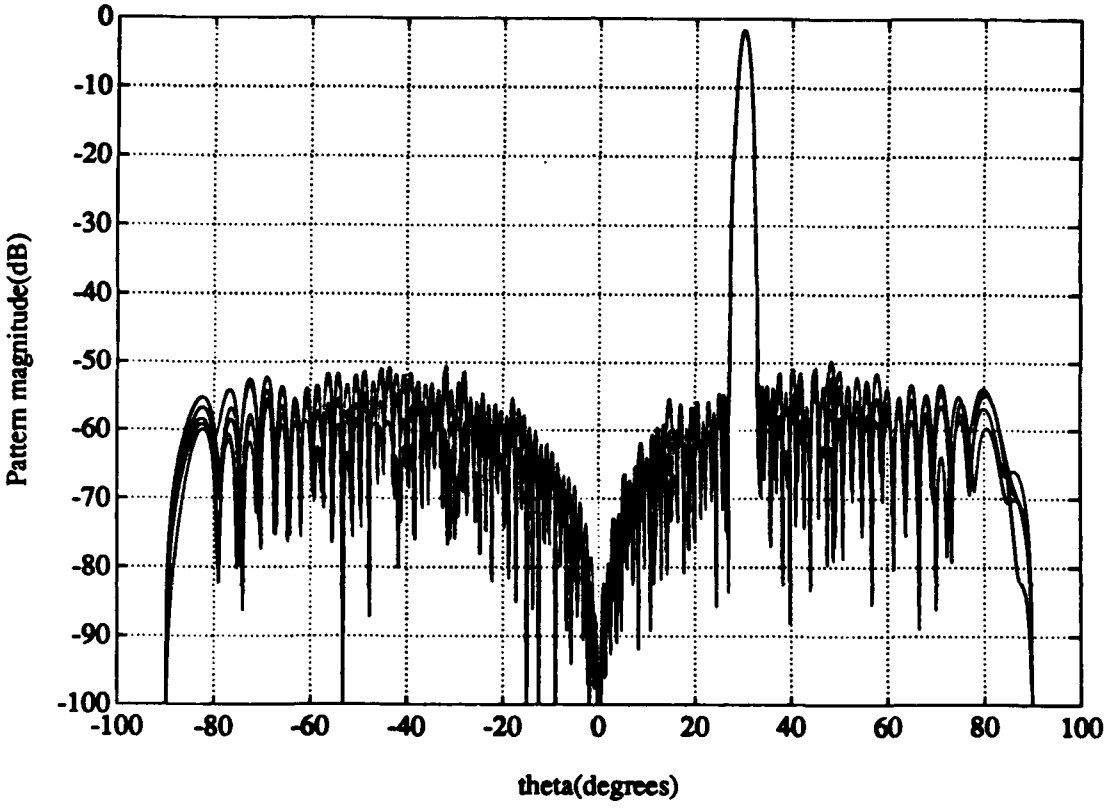

Figure 3.8: Ensemble of 5 patterns of the 100×1 array, with amplitude error ±0.1 dB, and phase error ±0.1758°.

level of the adapted pattern. For this purpose, we define the integrated average SLL(or ASLL), of the adapted power pattern $P_A(\theta,\phi) = |F_A(\theta,\phi)|^2$ as

$$I_A = \int_{\Omega_{SL}} P_A(\theta,\phi)d\Omega \,, \tag{3.27}$$

where $d\Omega = \sin\theta d\theta d\phi$ is a differential element of solid angle, and Ω_{SL} is a specified sidelobe region, consisting of some specified region of visible space and excluding the region covered by the main lobe. We define a similar quantity for the mainbeam power pattern,

$$I_M = \int_{\Omega_{SL}} P_M(\theta,\phi)d\Omega \,, \tag{3.28}$$

where $P_M(\theta,\phi) = |F_M(\theta,\phi)|^2$, and then compute the difference

$$I_{SL} = I_A - I_M \,, \tag{3.29}$$

which indicates the change in ASLL due to adaptation. I_{SL} is a useful quantity mainly because, as shown below, it can be computed fairly easily as a function of the various interference parameters. Such computations allow the sidelobe level performances of arrays with different auxiliary configurations to be compared without the need to examine adapted patterns for every possible signal and interference scenario.

The integral I_A can be evaluated as follows. First, we expand the adapted power pattern by means of Eq. (3.26) as

$$\begin{aligned} P_A(\theta,\phi) &= |F_A(\theta,\phi)|^2 = F_A(\theta,\phi)F_A^*(\theta,\phi) \\ &= |F_M(\theta,\phi)|^2 + \sum_{i=1}^{K} w_i e^{-j\omega_d\tau^i} F_i(\theta,\phi)F_M^*(\theta,\phi) + \\ &\quad \sum_{i=1}^{K} w_i^* e^{j\omega_d\tau^i} F_i^*(\theta,\phi)F_M(\theta,\phi) + \sum_{i=1}^{K}\sum_{j=1}^{K} w_i w_j^* e^{-j\omega_d(\tau^i-\tau^j)} F_i(\theta,\phi)F_j^*(\theta,\phi) \end{aligned}$$

$$= |F_M(\theta,\phi)|^2 + 2Re\{\sum_{i=1}^{K} w_i e^{-j\omega_d \tau^i} F_i(\theta,\phi) F_M^*(\theta,\phi)\} + \sum_{i=1}^{K}\sum_{j=1}^{K} w_i w_j^* e^{-j\omega_d(\tau^i-\tau^j)} F_i(\theta,\phi) F_j^*(\theta,\phi)\,. \quad (3.30)$$

We see that the adapted power pattern consists of the mainbeam power pattern plus sums of mainbeam-auxiliary cross products and auxiliary-auxiliary cross products multiplied by the array weights. As the interference scenario changes, only the weights change in this expression. The mainbeam and auxiliary patterns are independent of the interference and signal scenario[2]. For a given scenario, the computed weights are constant and independent of θ and ϕ. Thus Eq. (3.27) can be written as

$$I_A = I_M + 2Re\{\sum_{i=1}^{K} w_i e^{-j\omega_d \tau^i} \int_{\Omega_{SL}} F_i(\theta,\phi) F_M^*(\theta,\phi) d\Omega\} + \sum_{i=1}^{K}\sum_{j=1}^{K} w_i w_j^* e^{-j\omega_d(\tau^i-\tau^j)} \int_{\Omega_{SL}} F_i(\theta,\phi) F_j^*(\theta,\phi) d\Omega. \quad (3.31)$$

Therefore, I_A can be evaluated by first computing the integrals in Eq. (3.31) of the mainbeam power pattern and the cross product terms over the sidelobe region. I_A is then obtained by combining these integrals with the weights computed for a particular signal scenario. In this manner, the integrations need be done only once, and the ASLL can be obtained as a function of any signal scenario parameter, such as INR or θ_d, very easily. By taking advantage of Hermitian symmetry in the auxiliary-auxiliary cross products, a total of $N_{int} = 1 + 2K + K(K-1)/2$ integrals must be computed for a canceller with K auxiliaries.

To compute the ASLL for a given scenario according to Eq. (3.31), we must

[2]The desired signal arrival angle is assumed to be the same as the angle to which the mainbeam is scanned. Thus the mainbeam pattern will change as the desired signal arrival angle is varied.

define the sidelobe region of integration Ω_{SL}. We first define Ω_T as the angular region of space where the pattern responses are of interest. This region may or may not be the entire visible half-space. For example, if the array is to be used in a satellite mounted space-based radar, look angles exceeding the angular extent of the earth as viewed from the satellite are not of concern. Once Ω_T is defined, the sidelobe region Ω_{SL} is then taken to be

$$\Omega_{SL} = \Omega_T - \Omega_M \ , \tag{3.32}$$

where Ω_M is the region covered by the main lobe of the mainbeam.

To permit a simple definition of Ω_M we find it convenient to transform the variables of integration in Eq. (3.31) from (θ, ϕ) to the rectangular variables (u, v) according to

$$u = \sin\theta\cos\phi \ , \ v = \sin\theta\sin\phi \ . \tag{3.33}$$

Equation (3.33) is a one-to-one transformation between angles in the visible half-space $0° \leq \theta \leq 90°, 0° \leq \phi \leq 360°$ and points on or inside the unit circle of the uv plane. This transformation of variables can also be viewed as the projection of a point on a unit radius hemisphere centered at the origin, representing a given (θ, ϕ), to the uv plane. Given a point on or inside the unit circle in the uv plane, we use the inverse transformation,

$$\theta = \sin^{-1}(\sqrt{u^2 + v^2}) \ , \ \phi = \tan^{-1}\frac{v}{u} \ , \tag{3.34}$$

to get the corresponding angles (θ, ϕ).

For a linear array, the patterns are 2-dimensional, depending only on the variable u. The visible region is $-90° \leq \theta \leq 90°$ which transforms to $-1 \leq u \leq 1$. If we

specify an angle θ_{max} as the maximum angle from broadside at which the pattern response is of concern, then Ω_T is the region $-u_{max} \leq u \leq u_{max}$, where $u_{max} = \sin\theta_{max}$. The mainbeam region is defined to be the interval $[u_1, u_2]$, where u_1 and u_2 are the locations of the first nulls on each side of the main lobe of the ideal mainbeam pattern. The quantity $u_2 - u_1$ is the null-to-null beam width(in u) of the ideal mainbeam pattern. The sidelobe region is then

$$\Omega_{SL} = [-u_{max}, u_1] \cup [u_2, u_{max}] . \tag{3.35}$$

Each integration in Eq. (3.31) must be performed over each of the two intervals comprising Ω_{SL}.

The corresponding regions in the planar array case are shown in Figure 3.9. Specifying θ_{max} defines Ω_T as the region $\sqrt{u^2 + v^2} \leq \sin\theta_{max}$. The mainbeam region Ω_M is defined as the rectangular region with lower left corner (u_1, v_1) and upper right corner (u_2, v_2), where the intervals $[u_1, u_2]$ and $[v_1, v_2]$ define the main lobe of the ideal mainbeam pattern and the null-to-null beamwidths in the u and v dimensions. They are determined from the Dolph-Chebyshev tapers on the array in the x and y directions, respectively. The sidelobe region Ω_{SL} is the shaded region in the figure. In the planar case each integration in Eq. (3.31) is performed over both Ω_T and Ω_M and the results subtracted to get I_A.

An example of the ASLL computation is given in Figure 3.10, which shows the mainbeam in (a) and the adapted pattern in (b) for a 100×1 array with a jammer incident at $-45°$. The mainbeam ASLL I_M is -40.7 dBi. (Because the ASLL is an integrated average, it is necessarily lower than the peak SLL, and should not to be interpreted as such.) The adapted pattern shows the deep null in the interference

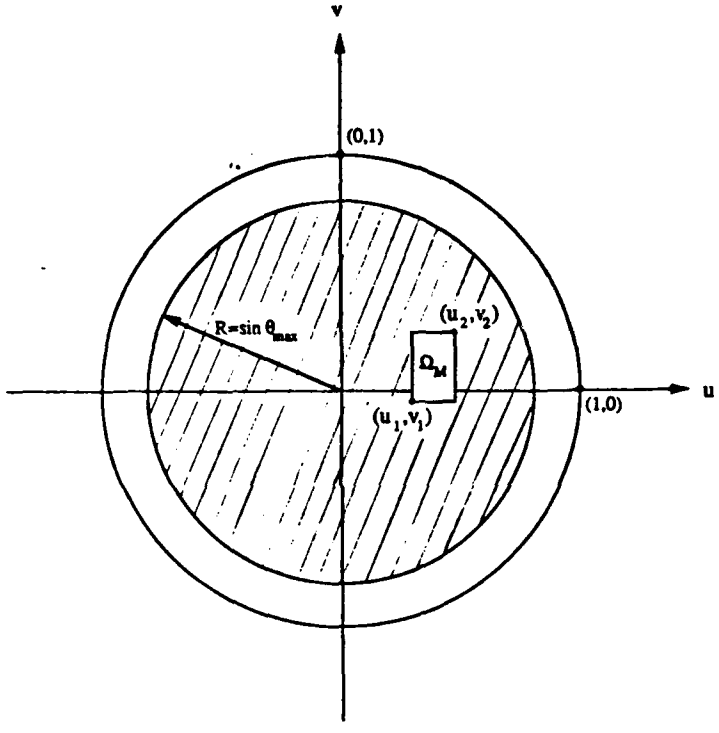

Figure 3.9: Regions of interest for the sidelobe integration of a planar array pattern.

direction, and shows that the sidelobes are up slightly. The ASLL of the adapted pattern is -37.95 dBi, which is an increase of 2.75 dB over the mainbeam. This number also corresponds well with the observed increase in peak SLL in this case.

The performance measure I_{SL}, as described above will be used to characterize adapted pattern SLL performance of the various signal scenarios and auxiliary configurations to be examined in the subsequent chapters.

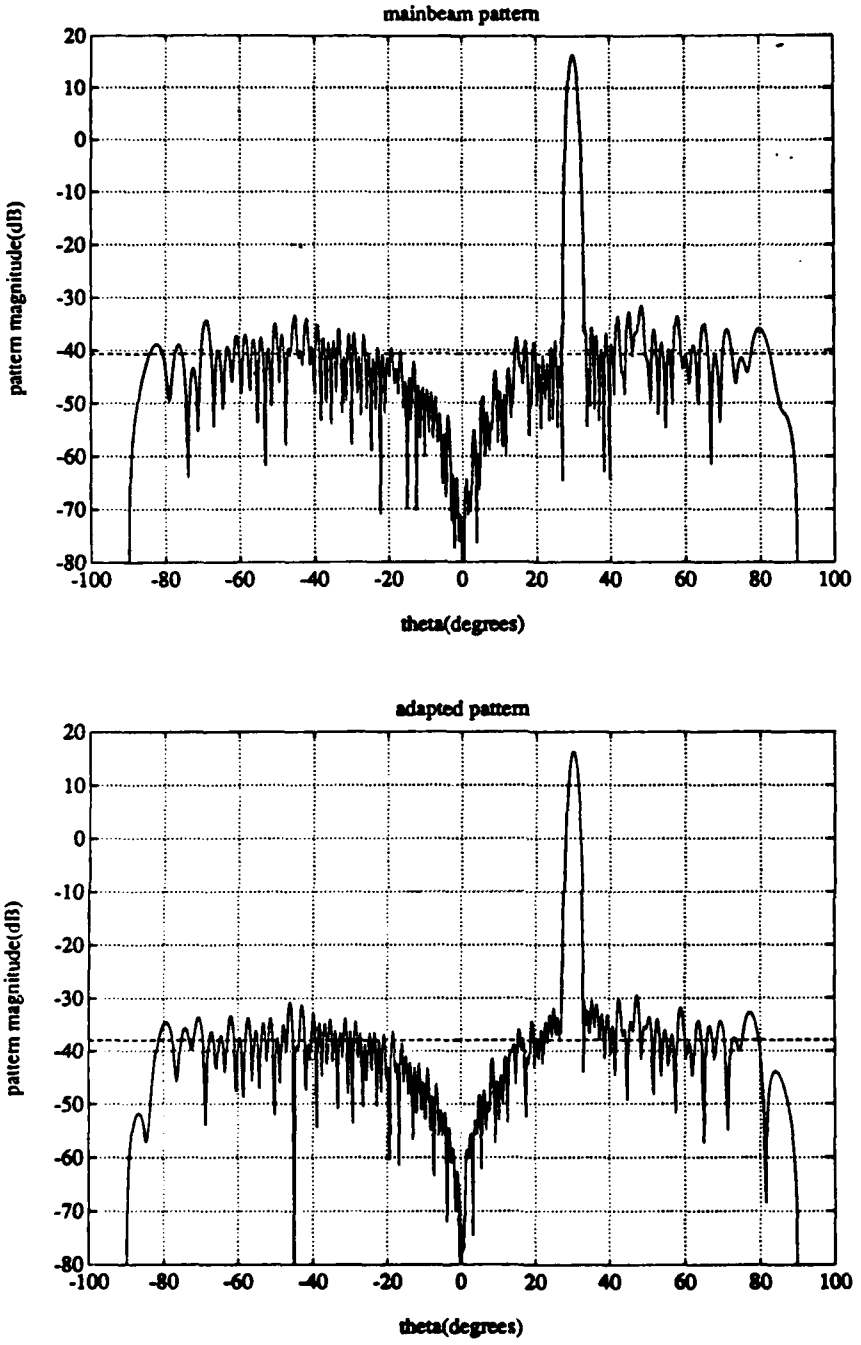

Figure 3.10: Typical mainbeam and adapted patterns. The computed ASLL is indicated by the dashed lines.

4. SLC Performance Using One Array Element for the Auxiliaries: One Interfering Signal

4.1 Introduction

In this chapter we begin our investigation of SLC performance by considering a large linear array, specifically a 100×1 element array. For a linear array the pattern depends on only one angular variable θ. We assume that this array is formed with a 55 dB Dolph-Chebyshev taper and steered to the desired signal arrival angle, which we fix at $\theta_d = 30°$. Random amplitude and phase error levels of ± 0.1 dB and $\pm 0.1°$ on each element result in a mainbeam pattern with peak SLL of about 50 dB with respect to the beam maximum. The mainbeam pattern of this array was shown in Figure 3.10.

In this chapter we assume the array has a single auxiliary formed from the output of one array element. The sidelobe canceller then has one spatial degree of freedom. We examine the performance of the array when there is one jammer as a function of the location of the auxiliary within the array. We do this for a CW jammer first, in which case only a single complex weight is needed on the auxiliary element. Then we consider a jammer with non-zero bandwidth, when a tapped delay line may be necessary behind the auxiliary to obtain satisfactory nulling. We examine performance as a function of the number of taps and the delay between taps, for different auxiliary element locations.

4.2 A CW jammer

With a CW jammer, a single complex weight on the auxiliary signal is sufficient to cancel the jammer. However, the location of the element used for the auxiliary signal affects the SLC performance. We shall consider two extremes: an element at the end of the array (elements (1,1) or (100,1)) and an element near the center of the array(elements (50,1) or (51,1)). We shall show that *for a single CW interfering signal, the SINR, cancellation ratio, and sidelobe levels are best for an end element auxiliary.*

Figures 4.1- 4.8 compare the performance of an end element auxiliary to that of a center element auxiliary as a function of the interfering signal arrival angle (θ_{i1}). In these curves, the CW jammer has an INR per element (as defined in Eq. (2.53)) of 40 dB. This value results in an INR of about 0 dB at the mainbeam output when the jammer arrival angle is at the peak of a sidelobe in the mainbeam pattern. The desired signal arrives from $\theta_d = 30°$ and has an SNR per element of -30 dB, which results in an SNR at the mainbeam output of -13 dB.

Figure 4.1 shows the output SINR from the array. Note that the curves for the (1,1) and (50,1) auxiliaries are identical for θ_{i1} outside the mainbeam, and nearly identical within the mainbeam. As the jammer moves into the mainlobe, both curves show severe SINR degradation. This degradation occurs not only because, as θ_{i1} approaches θ_d, the jammer null reduces the output desired signal power, but also because the large auxiliary weight necessary to cancel a jammer in the mainlobe causes an increase in output noise power. The curves for the two auxiliary locations differ only in the mainbeam direction, where the end element shows slightly better resolution than the center element. Although the difference between the two curves

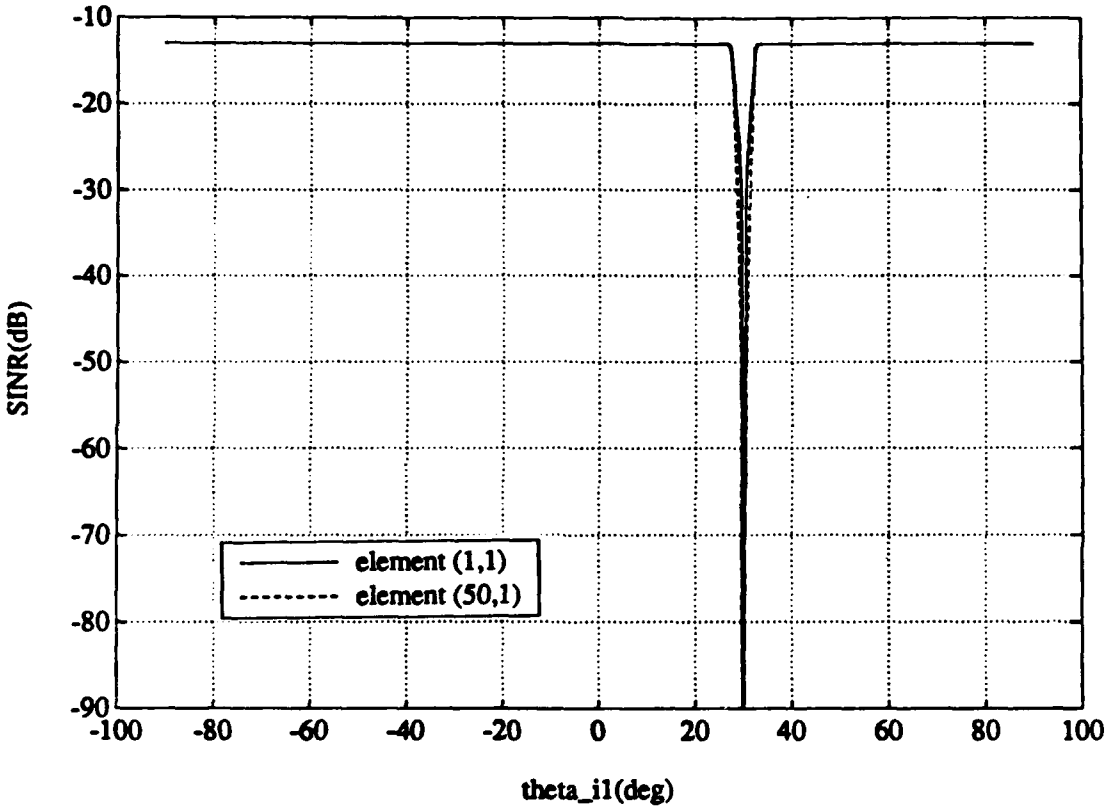

Figure 4.1: SINR vs θ_{i1}: SNR=-30 dB, INR=40 dB, B=0.

is small, it will be instructive to examine the behavior of P_d, P_i, and P_n with the two different auxiliaries.

Figure 4.2 shows the output desired signal powers for the two auxiliaries. P_d is plotted in dB relative to the noise power per element. The figure shows that the output desired signal power is unaffected by the auxiliary location except when the jammer is in the mainbeam region. For the end element auxiliary, there is a slight rise in P_d and then a very sharp drop as θ_{i1} is scanned through the mainbeam. For the center element auxiliary, there is no rise but a broader null. This small difference occurs because the phase difference between the jammer signals in the mainbeam and in the auxiliary varies much more rapidly for an end element auxiliary than for a center element auxiliary auxiliary.

The desired signal improvement ratio R_d is plotted in Figure 4.3. Because the desired signal power in the mainbeam signal is constant with respect to the jammer arrival angle, the curves of R_d are just the P_d curves normalized to P_{d0}. In this case, R_d does not provide any additional information.

Now consider the output interference power, shown in Figure 4.4.(P_i is plotted in dB relative to the noise power on a single element). For all $\theta_i 1$ outside the mainbeam, the end element auxiliary results in a smaller output interference power than a center element auxiliary. The difference between the two curves is as much as 20 dB. However, the jammer is sufficiently suppressed in both cases so that this difference in P_i has a negligible effect on the output SINR. The reason that P_i varies with auxiliary location is that, in maximizing SINR, the array responds not only to the jammer, but also to the desired signal and noise. For this example, the desired signal-to-noise ratio of -30 dB is too small for the disired signal to affect the

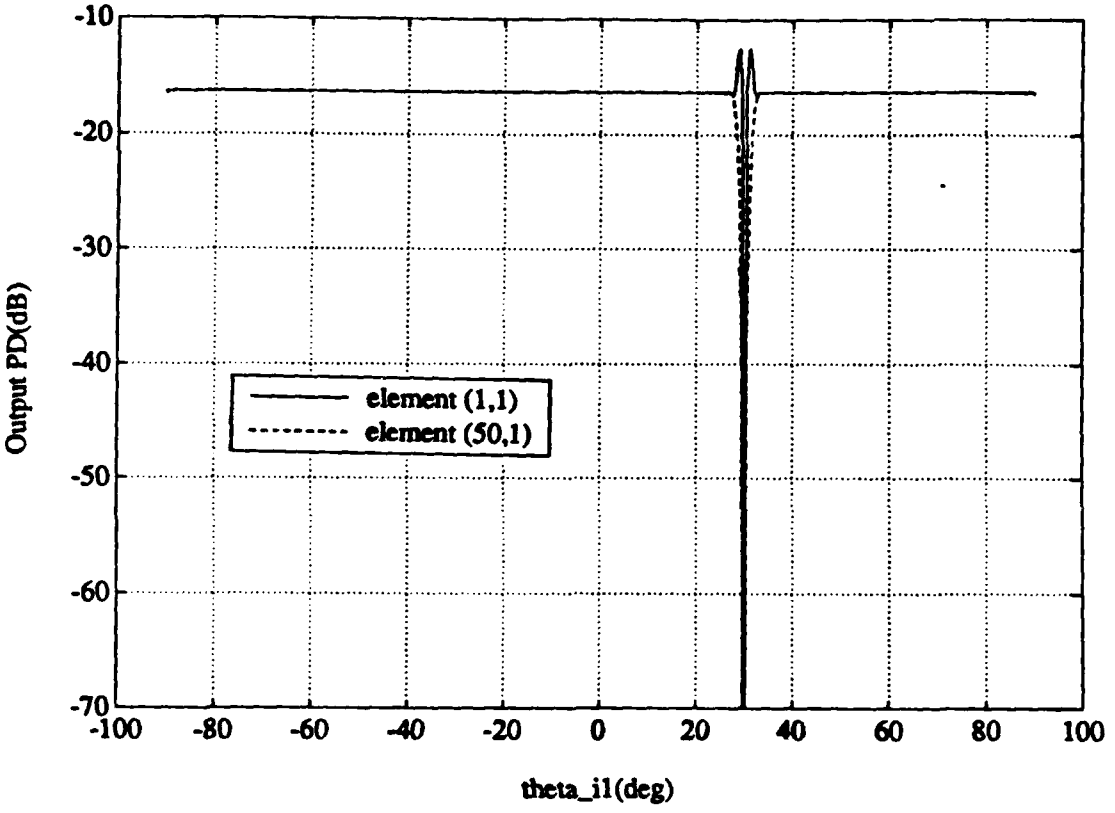

Figure 4.2: Output P_d vs θ_{i1}: SNR=-30 dB, INR=40 dB, B=0.

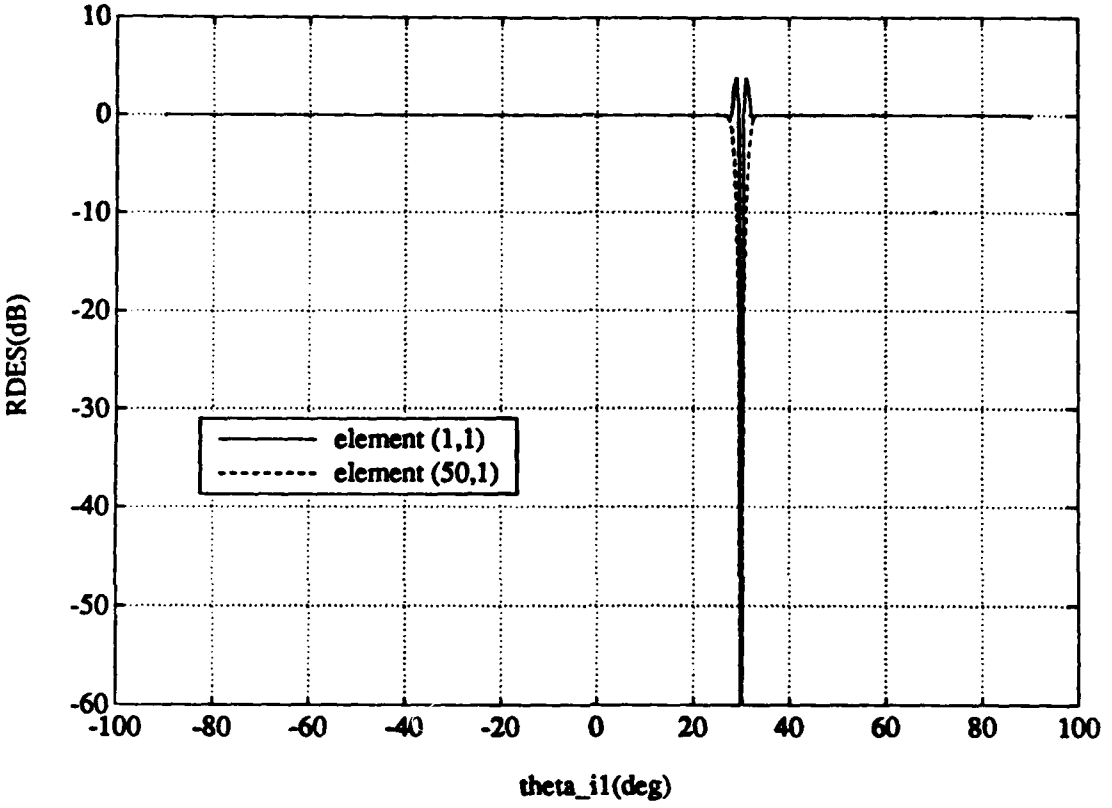

Figure 4.3: Desired signal improvement ratio vs. θ_{i1}: SNR=-30 dB, INR=40 dB, B=0.

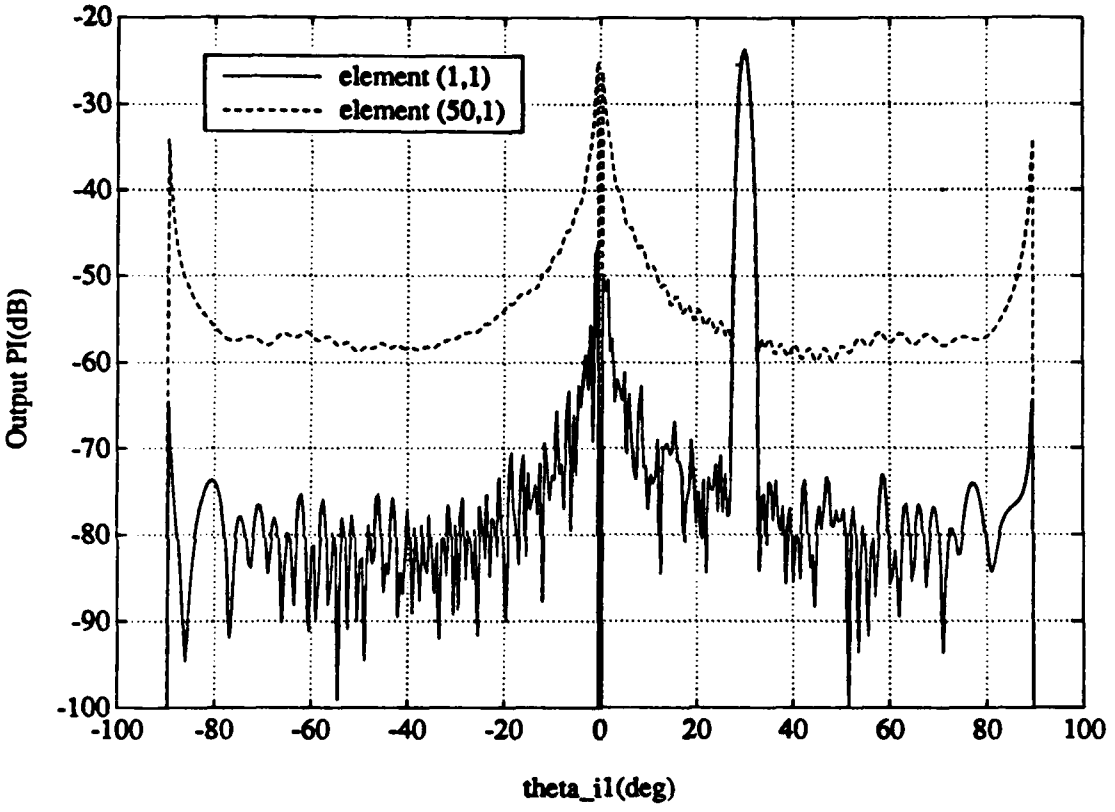

Figure 4.4: Output P_i vs θ_{i1}: SNR=-30 dB, INR=40 dB, B=0.

weights. However, the noise does have an effect, because the noise on the auxiliary is correlated with the noise in the mainbeam.(The auxiliary is formed from an element also used in the mainbeam.) Because the end elements have much smaller weights in the mainbeam combiner (i.e. at the edge of the Chebyshev amplitude taper) than the center elements, the noise correlation between the auxiliary and the mainbeam is smaller for an end element. Therefore the weight on an end element auxiliary is influenced less by the noise; it responds more to the interference and provides a deeper null on the jammer. The center element auxiliary compromises the jammer null in order to keep the output noise power down and maximize the output SINR.

Figure 4.5, which shows the cancellation ratio, also indicates the superior P_i performance of the end element auxiliary. The end element auxiliary provides at least 20 dB better cancellation for all jammer angles of arrival outside of the mainbeam.

Figure 4.6 shows the output noise power, also plotted in dB relative to the element noise signal power, as a function of θ_{i1}, for the two choices of the auxiliary signal. The two curves are indistinguishable for all θ_{i1}; the output noise power is the same for either choice of auxiliary signal. This result occurs because the adaptive weight magnitudes for the two auxiliaries differ only slightly. Although a slight difference in the adaptive weight magnitude may significantly affect the jammer null depth and thus the output jammer power, it has little effect on the output noise power. To see this, recall that the output noise power is a weighted sum of the noise powers from all 100 array elements. Thus a small change in the total weight on one of the array elements has little effect on the output noise power of the whole array. Also, for a single element auxiliary, the noise added by the auxiliary to the output is significant compared to the mainbeam noise power only when the

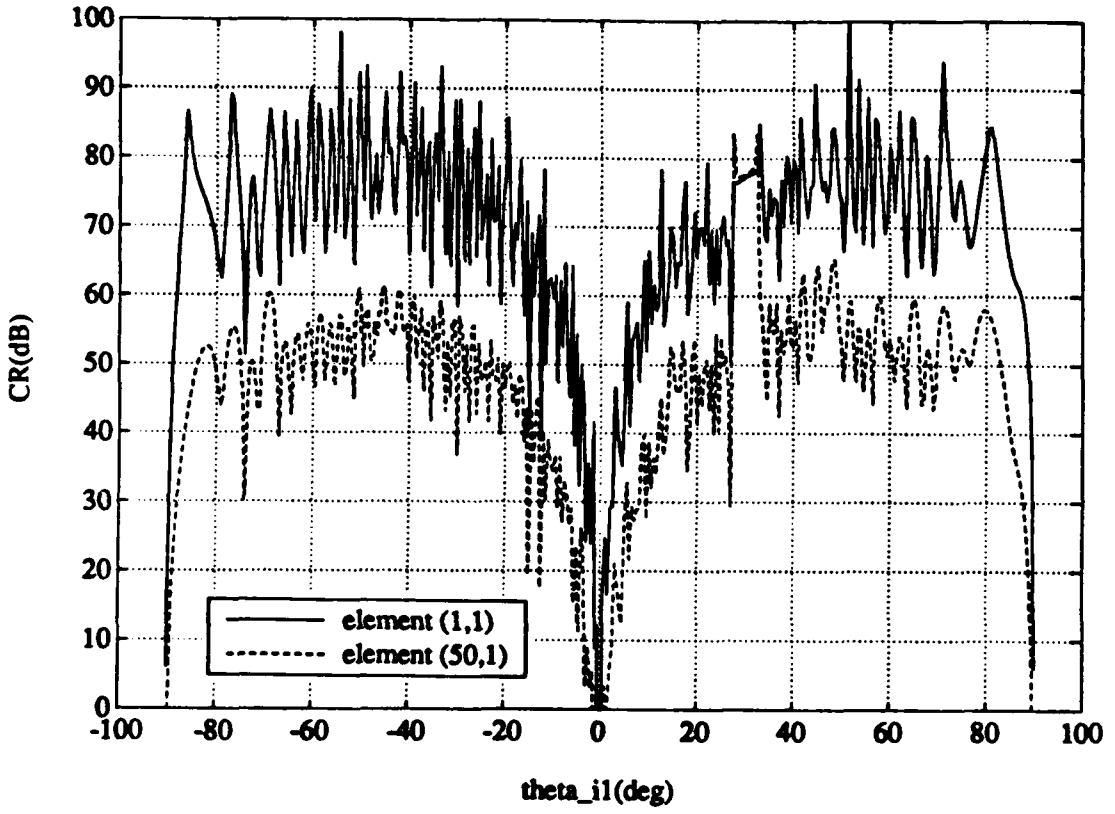

Figure 4.5: Cancellation ratio vs. θ_{i1}: SNR=-30 dB, INR=40 dB, B=0.

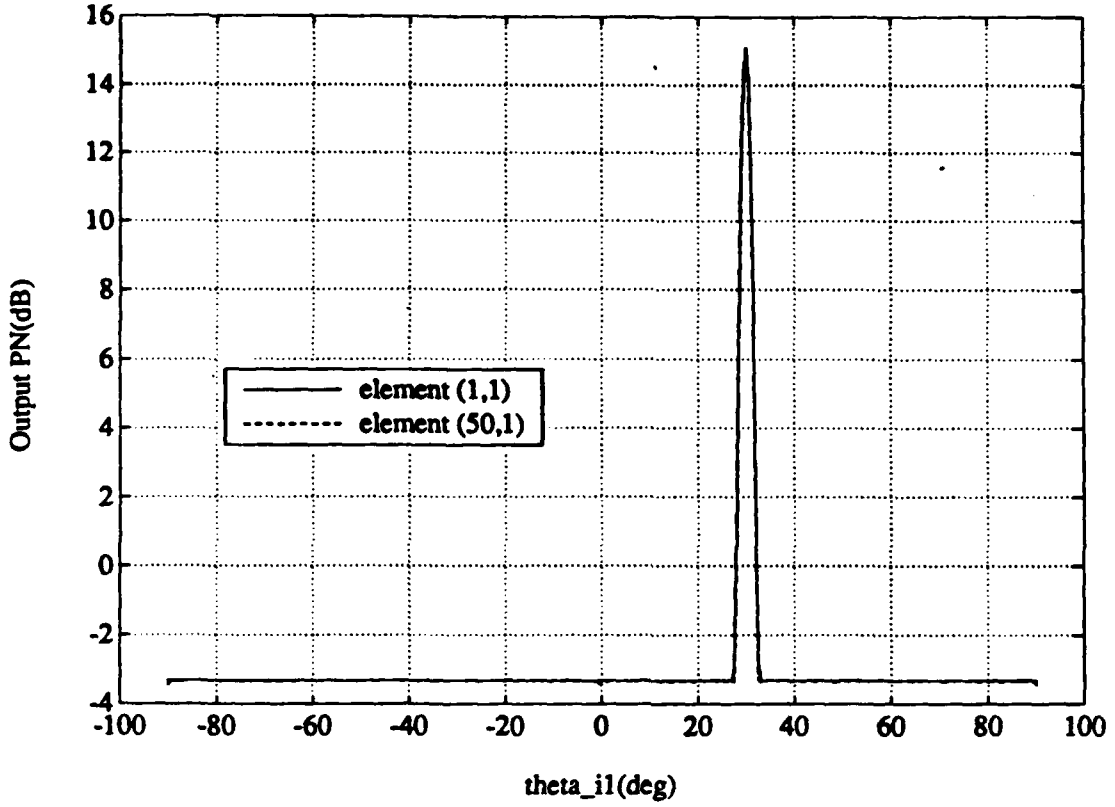

Figure 4.6: Output P_n vs θ_{i1}: SNR=-30 dB, INR=40 dB, B=0.

weight magnitude is large, i.e. when a jammer arrives in the mainbeam. Figure 4.7 shows the noise signal improvement ratio $R_n = P_n/P_{n0}$ for this array. This figure is just an alternate way of displaying the same information as that in Figure 4.6.

Next we examine the ASLL of the adapted pattern. We define the *increase* in ASLL to be the difference in ASLL between the adapted pattern and the mainbeam pattern. Figure 4.8 shows the increase in ASLL resulting from end and center element auxiliary signals. The sidelobe region for this calculation is taken to be the entire visible space excluding the null-to-null beamwidth of the mainbeam pattern. The large increase in ASLL for θ_{i1} near θ_d is again due to the large weight magnitudes necessary to null a jammer in the mainbeam. For most other angles, both auxiliaries perform similarly and result in an increase in ASLL of 0 to 6 dB. A typical adapted pattern, with element (1,1) as the auxiliary and $\theta_{i1} = -45°$, was shown in Figure 3.10. The increase in ASLL for this case was 2.75 dB. Comparison of the mainbeam and adapted patterns of Figure 3.10 shows that the peak SLL increase is 2 to 3 dB also.

However, there is an interesting difference between the end and center element auxiliaries, as may be seen in Figure 4.8. For angles $\theta_{i1} = 0°, \pm 90°$ the center element auxiliary yields an increase in ASLL of more than 20 dB. These sharp increases do not occur for the end element auxiliary. The reason for this difference is that the angles $\theta_{i1} = 0°, \pm 90°$ correspond to nulls in the element pattern (see section 2.4). At these angles the array is essentially adapting with no interfering signals present. Therefore, the sidelobe canceller, which attempts to optimize SINR, is free to minimize the noise power at the array output by setting the weight on the auxiliary signal equal to the opposite of the mainbeam combiner weight on that element. The

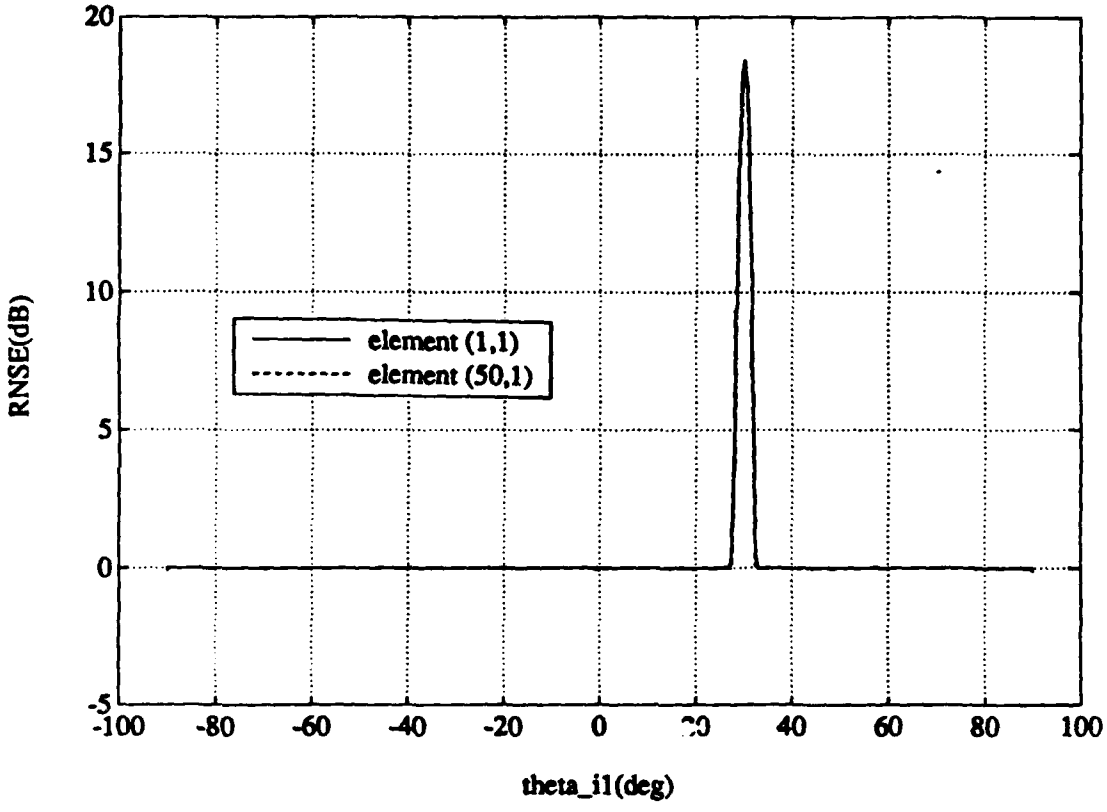

Figure 4.7: Noise signal improvement ratio vs. θ_{i1}: SNR=-30 dB, INR=40 dB, B=0.

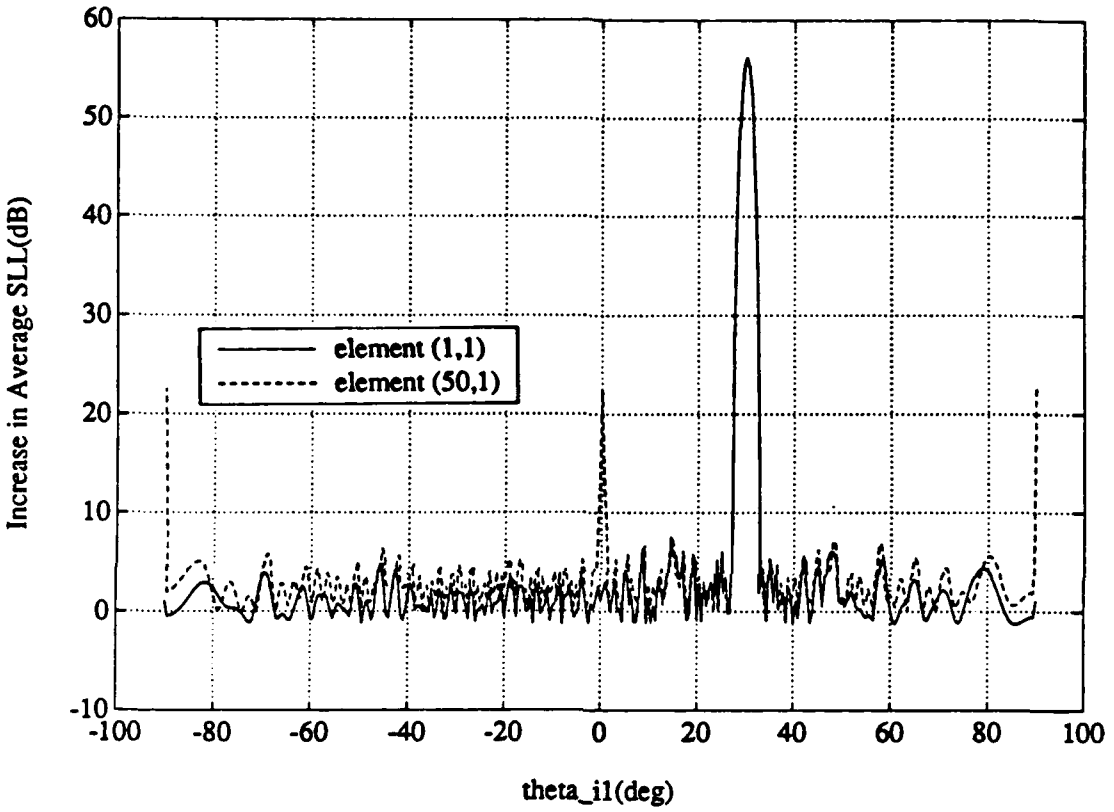

Figure 4.8: Increase in ASLL vs θ_{i1}: SNR=-30 dB, INR=40 dB, B=0.

adapted pattern is then the mainbeam pattern with the auxiliary element removed. The resulting SLL depends on which element is removed. Because the center element has a much higher Dolph-Chebyshev weight than the end element, the output SLL changes much more if the center element is missing than if the end element is missing. A Chebyshev taper with the center element missing is severely distorted; it yields a pattern with sidelobes much higher than the design SLL. Figure 4.9 illustrates the situation. It shows the adapted pattern when $\theta_{i1} = 0°$, for four sidelobe cancellers, each using an auxiliary element in a different part of the array. As the auxiliary element moves closer to the center of the array, the SLL of the adapted pattern becomes worse.

From these results, we conclude that, in the presence of a single CW jammer, an auxiliary using an end element performs best in every respect. First, the end element auxiliary yields significantly smaller output P_i (and thus better CR) than a center element auxiliary. Second, P_d is higher for the end element when θ_{i1} is in the main lobe. Hence, the jammer can be slightly closer to the desired signal with an end element auxiliary before the array begins to null the desired signal as well as the jammer, so the spatial resolution is improved. Third, the output noise power is essentially independent of the location of the auxiliary. Finally, an end element auxiliary has better adapted SLL performance than a center element. If the jammer is in a null of the element pattern or if the array is adapting with no interference present, a center element auxiliary results in a large (20 dB) increase in sidelobe level.

In the next section, we consider how these results are affected by jammer bandwidth.

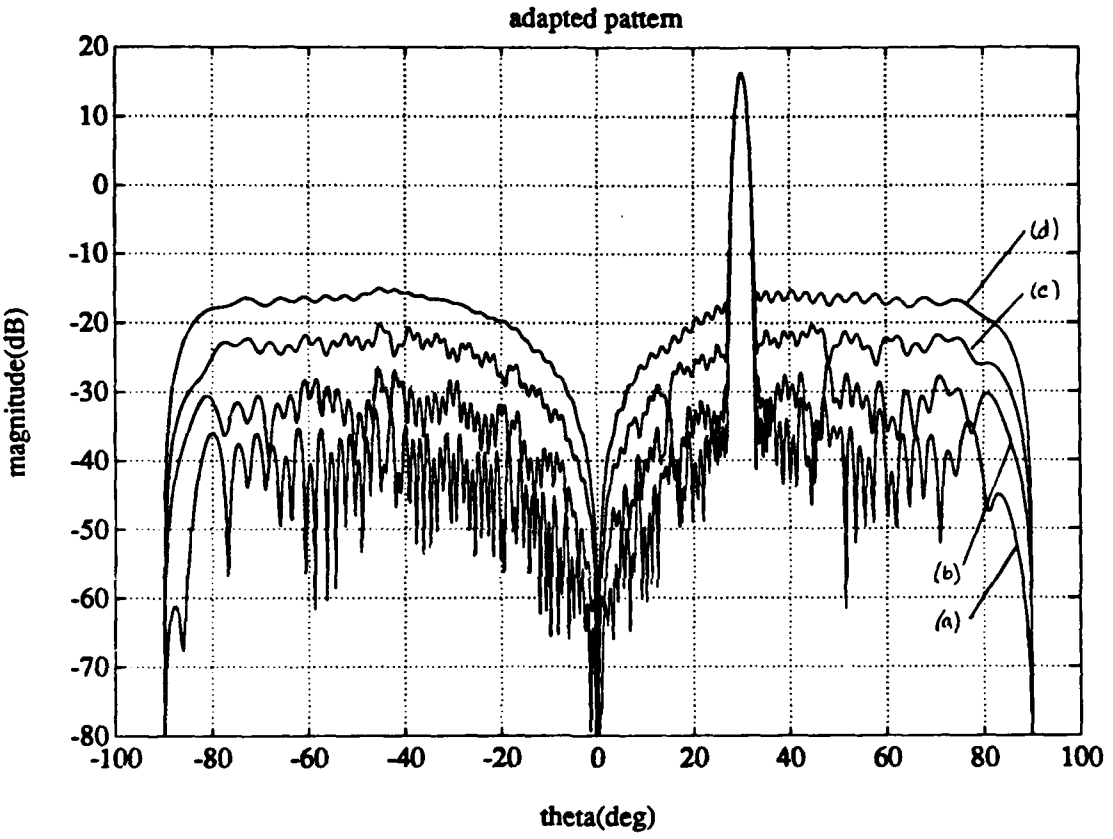

Figure 4.9: Adapted patterns with $\theta_{i1} = 0°$ for different auxiliary element locations: (a) element (50,1) (b) element (25,1) (c) element (12,1) (d) element (1,1)

4.3 A jammer with non-zero bandwidth

In general, jammer bandwidth degrades the performance of the adaptive array. Figure 4.10 shows an example. The output SINR obtained from a SLC using element (1,1) as the auxiliary is plotted for several jammer bandwidths, as the jammer arrival angle is scanned.(In these curves the desired signal, interfering signal, and noise signal bandwidths are all equal, although it is primarily the interference bandwidth that causes the performance degradation[2].) The jammer INR is 60 dB per element. Outside of the mainbeam, the $B = 0.001$ curve shows a small (0 to 3 dB) degradation from the CW case. For the $B = 0.01$ jammer, the degradation is much worse, varying from 0 to 18 dB below that of the CW jammer.

Performance degrades not only with jammer bandwidth but also with jammer power. For a given bandwidth, the SINR worsens as the received interference power increases. To see the effect of jammer power, Figure 4.11 shows the performance for a fixed jammer arrival angle, $\theta_{i1} = -45°$, as a function of the INR per element. For the CW case, the SINR is constant with INR, but for non-zero bandwidth, the SINR drops as the INR is increased. The degradation for $B = 0.001$ becomes evident for INR$\geq$45 dB, and for $B = 0.01$, the degradation begins at INR$\geq$30 dB and is more severe. Note that for $B = 0.001$ and INR$\leq$45 dB, the SINR performance is as good as the CW case.

Bandwidth degradation occurs because the interfering signal sees different transfer functions in the main channel and the auxiliary channel. Figure 4.12 shows the equivalent filter seen by an incident signal arriving from the angles (θ, ϕ). $F_M(\omega, \theta, \phi)$ represents the frequency response of the mainbeam seen by a signal

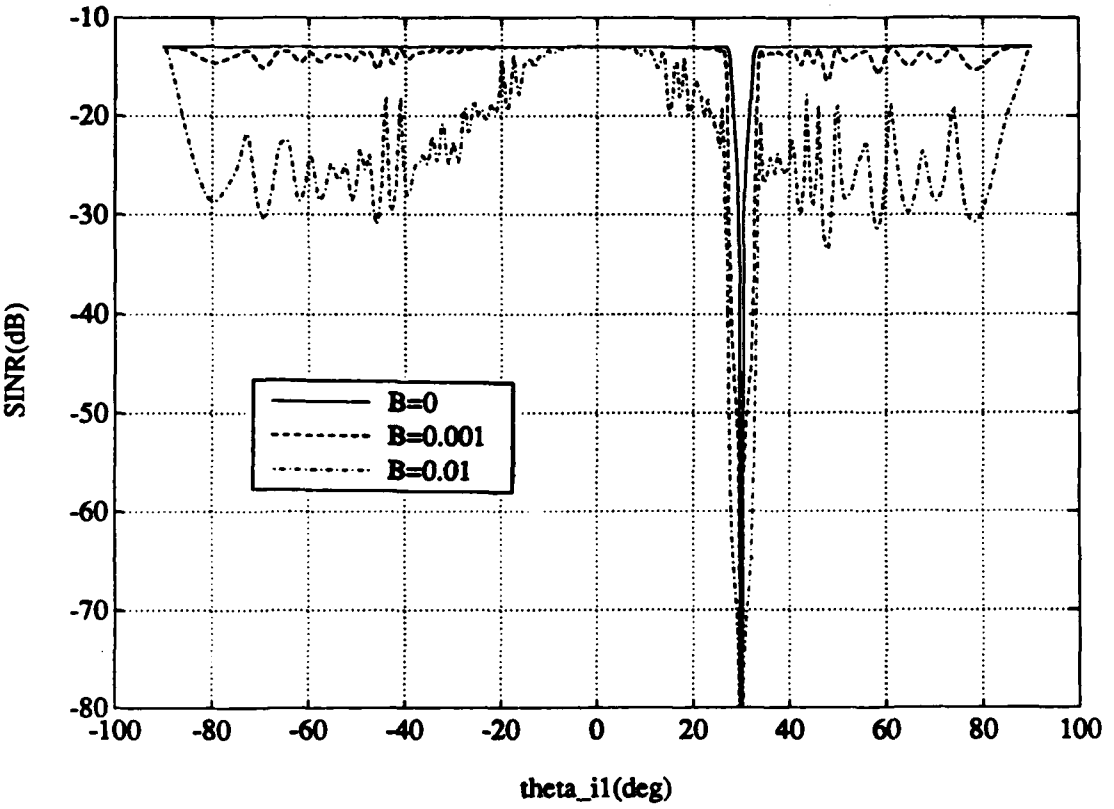

Figure 4.10: SINR performance with a single complex weight on element (1,1), INR=60 dB.

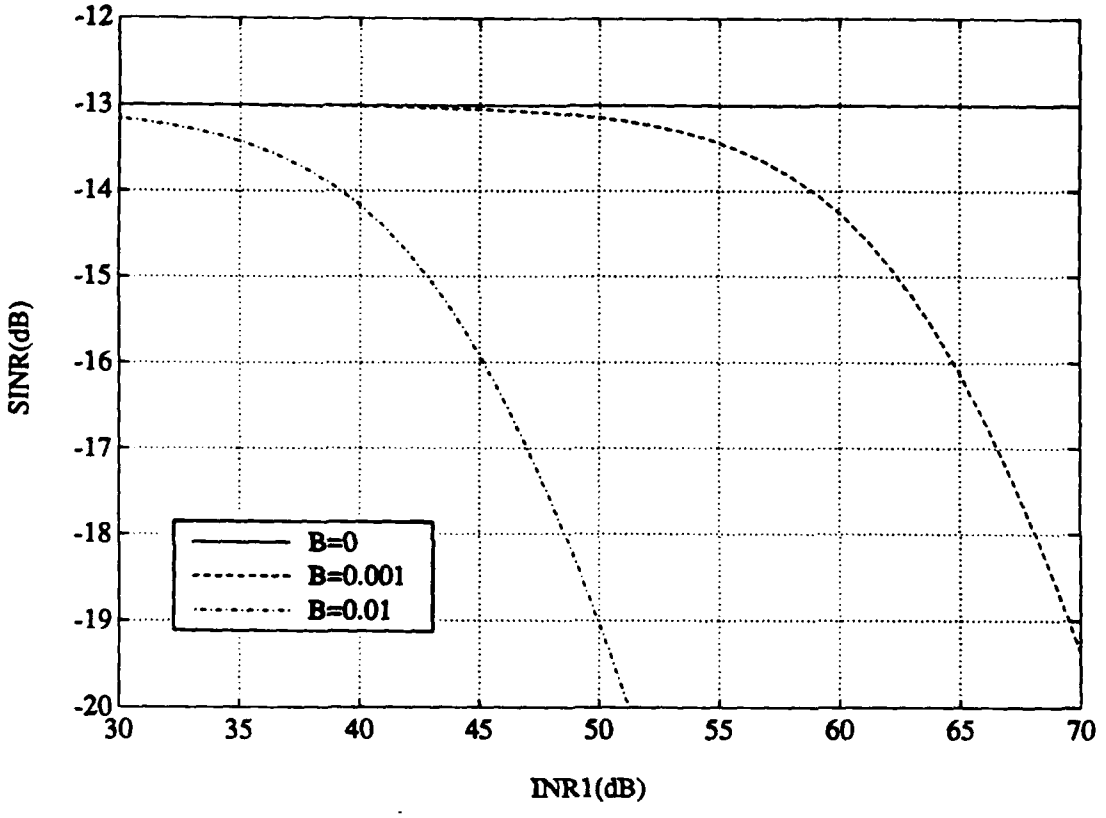

Figure 4.11: The effect of INR on SINR performance: $\theta_{i1} = -45°$, element (1,1).

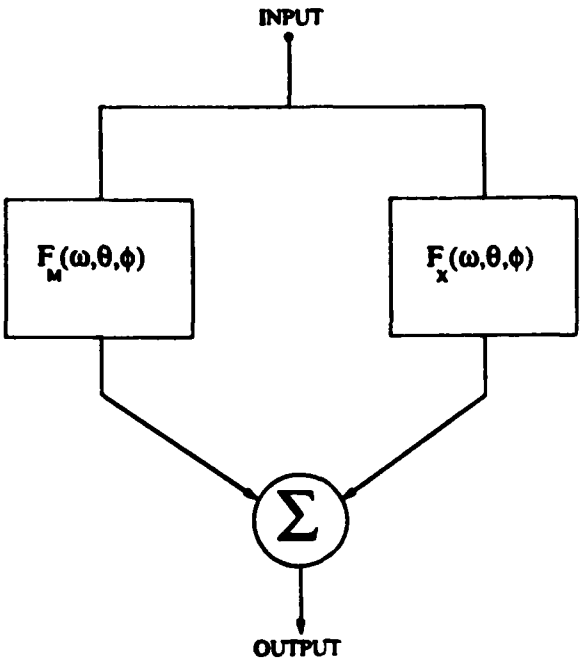

Figure 4.12: The equivalent filter seen by a signal arriving from angles (θ, ϕ).

arriving from angles (θ, ϕ),

$$F_M(\omega, \theta, \phi) = f(\theta, \phi) \sum_{l=1}^{N_x} \sum_{m=1}^{N_y} M_{lm} e^{j\omega \frac{d}{c}[(l-1)\cos\phi + (m-1)\sin\phi]\sin\theta}, \qquad (4.1)$$

where $f(\theta, \phi)$ is the element pattern, M_{lm} is the mainbeam combiner weight defined in Eq. (2.8), d is the interelement spacing and c is the propagation velocity.(We assume the radiating elements themselves are broadband enough that their frequency response is constant over all signal bandwidths of interest[1].) $F_X(\omega, \theta, \phi)$ represents the frequency response of the weighted auxiliary array as seen by a signal arriving

[1]Without this assumption, the autocorrelation function of a received signal(desired or interfering) at the element output would depend not only on the ACF of the incident signal but also on the frequency response of the element in the direction of the incident signal.

from (θ, ϕ). It is given by

$$F_X(\omega, \theta, \phi) = \sum_{i=1}^{K} w_i e^{j\omega\tau^i} \left\{ f(\theta, \phi) \sum_{l=1}^{N_x} \sum_{m=1}^{N_y} A_{lm}^i e^{j\omega \frac{d}{c}[(l-1)\cos\phi + (m-1)\sin\phi]\sin\theta} \right\}, \quad (4.2)$$

where the A_{lm}^i are the auxiliary combiner weights, w_i is the auxiliary signal weight, and τ^i is the delay (for TDL processing) associated with the i^{th} auxiliary signal. The adapted pattern frequency response, $F_A(\omega, \theta, \phi)$, in the (θ, ϕ) direction is the sum of the mainbeam and weighted auxiliary frequency responses. For a TDL on a single element, element (p, q), Eq. (4.2) can be simplified to

$$F_X(\omega, \theta, \phi) = e^{j\omega \frac{d}{c}[(p-1)\cos\phi + (q-1)\sin\phi]\sin\theta} \sum_{i=1}^{K} w_i A_{pq}^i e^{j\omega\tau^i}, \quad (4.3)$$

which consists of just the frequency response of the tapped delay line filter along with a linear phase factor due to the separation between the auxiliary element and the mainbeam phase center.

To cancel a wideband interfering signal arriving from angles (θ_{i1}, ϕ_{i1}) perfectly, the auxiliary weights must be chosen so that the equality

$$F_A(\omega, \theta_{i1}, \phi_{i1}) = F_M(\omega, \theta_{i1}, \phi_{i1}) + F_X(\omega, \theta_{i1}, \phi_{i1}) = 0 \quad (4.4)$$

is satisfied over the whole signal bandwidth($\omega_d - \frac{\Delta\omega_d}{2} \leq \omega \leq \omega_d + \frac{\Delta\omega_d}{2}$). In other words, the weighted auxiliary must provide a magnitude response equal to the magnitude response of the mainbeam and a phase response 180° out of phase with that of the mainbeam. The degree of cancellation is determined by how closely Eq. (4.4) is satisfied at the jammer arrival angles. For a single auxiliary using element (p, q) with a single complex weight, $F_X(\omega, \theta, \phi)$ is

$$F_X(\omega, \theta, \phi) = w_1 A_{pq}^1 e^{j\omega T_{eq}}, \quad (4.5)$$

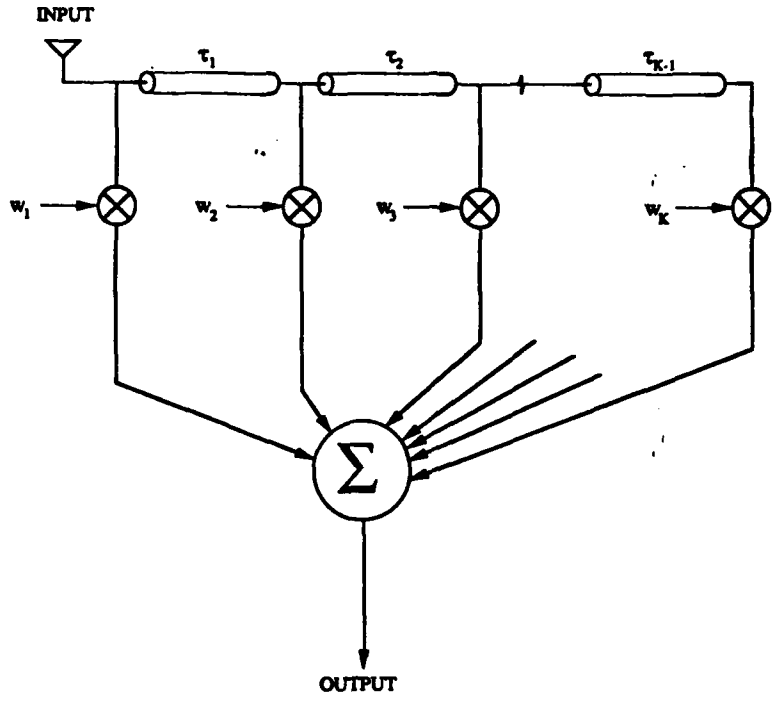

Figure 4.13: A tapped delay line filter.

where

$$T_{eq} = \frac{d}{c}\left[(p-1)\cos\phi + (q-1)\sin\phi\right]\sin\theta - \tau^1 \,. \tag{4.6}$$

For this case, the magnitude $|F_X(\omega,\theta,\phi)|$ is a constant independent of frequency, and the SLC is unable to cancel a jammer except at a single frequency within its bandwidth.

There are two ways to improve the bandwidth performance of the array. One can either use more auxiliaries, or one can add a tapped delay line behind the auxiliary element. Actually, either of these choices can be thought of as a tapped delay line filter, as shown in Figure 4.13. If a TDL is used behind a single element, the input comes from a single element and the τ^i represent the delays between

taps. If multiple elements are used, each tap in Figure 4.13 represents an input from a different element of the array, and the τ^i represent the propagation delays between signals received at the different auxiliaries. The effective intertap delays in a configuration of multiple auxiliary elements depend on the auxiliary element locations and the jammer arrival angles. With an explicit TDL on a single element, the intertap delays are independent of both the element location and the signal environment.

A SLC configuration consisting of multiple auxiliary elements will have more than one spatial degree of freedom and thus will perform better in a multiple jammer environment than a configuration with only a tapped delay line on a single element. However, the wideband null produced by a multiple auxiliary configuration is also spatially broad, while the wideband null produced by a TDL on a single element is spatially narrow[18].

Here we shall consider the performance of a tapped delay line on a single element in response to a single jammer[2]. To use tapped delay line processing on a single element, we must choose the number of taps, the amount of delay between taps, and the location of the element with the tapped delay line weighting.

The number of taps and the intertap delay required are determined by both the bandwidth and the power (INR) of the incident jamming signal. In effect, the TDL provides a finite Fourier series approximation to the mainbeam frequency response in the jammer direction.[16] The jammer bandwidth determines the maximum intertap delay. For a given intertap delay, the number of taps equals the number of terms in this finite series approximation, and thus determines how well the the auxiliary

[2]We consider configurations of multiple auxiliary elements in the next chapter

frequency response will match the mainbeam frequency response.

For a sufficiently strong jammer, the optimal SINR weights are those which cancel the jammer (as opposed to cancelling the noise). These weights result in a weighted auxiliary frequency response that is the best approximation to the mainbeam frequency response, subject to the subject to constraints imposed by the number of taps and the intertap delays. Further increases in INR do not change the weights, which remain at the values that provide best jammer cancellation. Since the weights do not change, the adapted frequency response also remains constant with this increase in INR. Thus, the output jammer power increases by an amount equal to the increase in input jammer power[3]. If the INR is continually increased, eventually the output jammer power will become large enough to cause SINR degradation. At this point the auxiliary array approximation to the mainbeam response is not sufficient and more taps are needed. Some results that illustrate these points are presented next.

Let us consider what happens if we use a two-tap (one delay) TDL on the auxiliary element. To model a 2-tap delay line behind the auxiliary, we use two auxiliary signals, one for each tap in the TDL. Let $\tilde{x}_1(t)$ be the auxiliary signal obtained by tapping off the element signal directly, and let $\tilde{x}_2(t) = \tilde{x}_1(t-\tau)$ be the auxiliary signal at the tap following the intertap delay τ. A given time delay τ will be specified in terms of its equivalent spatial delay in wavelengths. For example, a delay of λ_0 means an intertap time delay $\tau = \lambda_0/c = 1/f_0$. We will examine how the performance is affected by both the location of the auxiliary element within the array and by the intertap delay. We will compare the array performance with the

[3]This behavior is in direct contrast with that of a CW signal and a single complex weight on the auxiliary element. In this case the output P_i *decreases* as the input INR increases.

TDL on the end element and the center element of the array. We assume that the fractional bandwidth is $B = 0.001$.

Figure 4.14 shows the output SINR resulting from a two-tap TDL on element (1,1). The intertap delay is $38\lambda_0$. The INR is 60 dB. Comparison with Figure 4.10 shows that the TDL has fully overcome the bandwidth degradation. The SINR with the TDL is the same as that with a single complex weight and a CW jammer.

Figure 4.15 shows the SINR performance for an end element TDL when the jammer input INR is increased to 90 dB. (The resultant INR at the mainbeam output is about 50 dB.) In this case the SINR is as good as for the CW case when $\theta_{i1} < 0°$, but it is degraded for most $\theta_{i1} > 0°$. The reason is that for $\theta_{i1} < 0°$, the jammer arrives first at element (1,1) of the array. The intertap delay then tends to compensate for the propagation delay (and the resulting decorrelation) between the auxiliary element and the mainbeam phase center. The interference in the mainbeam signal is more correlated with the jammer component of auxiliary signal $\tilde{x}_2(t)$ than with the jammer in $\tilde{x}_1(t)$. On the other hand, for $\theta_{i1} > 0°$ the jammer strikes the end of the array opposite to the auxiliary element first. The intertap delay then adds to the total time delay between the jammer signal in the mainbeam and in auxiliary $\tilde{x}_2(t)$. Auxiliary signal $\tilde{x}_2(t)$ in this case is less correlated with the mainbeam signal than when $\theta_{i1} < 0°$. Therefore the TDL on element (1,1) yields better SINR performance when $\theta_{i1} < 0°$.

Figure 4.16 shows the output interference power P_i for the 90 dB jammer and the 60 dB jammer. Note that P_i for the 90 dB jammer is almost exactly 30 dB larger than for the 60 dB jammer, for all arrival angles except those near the element pattern nulls. The increase in P_i with INR shows that, for θ_{i1} not near an element

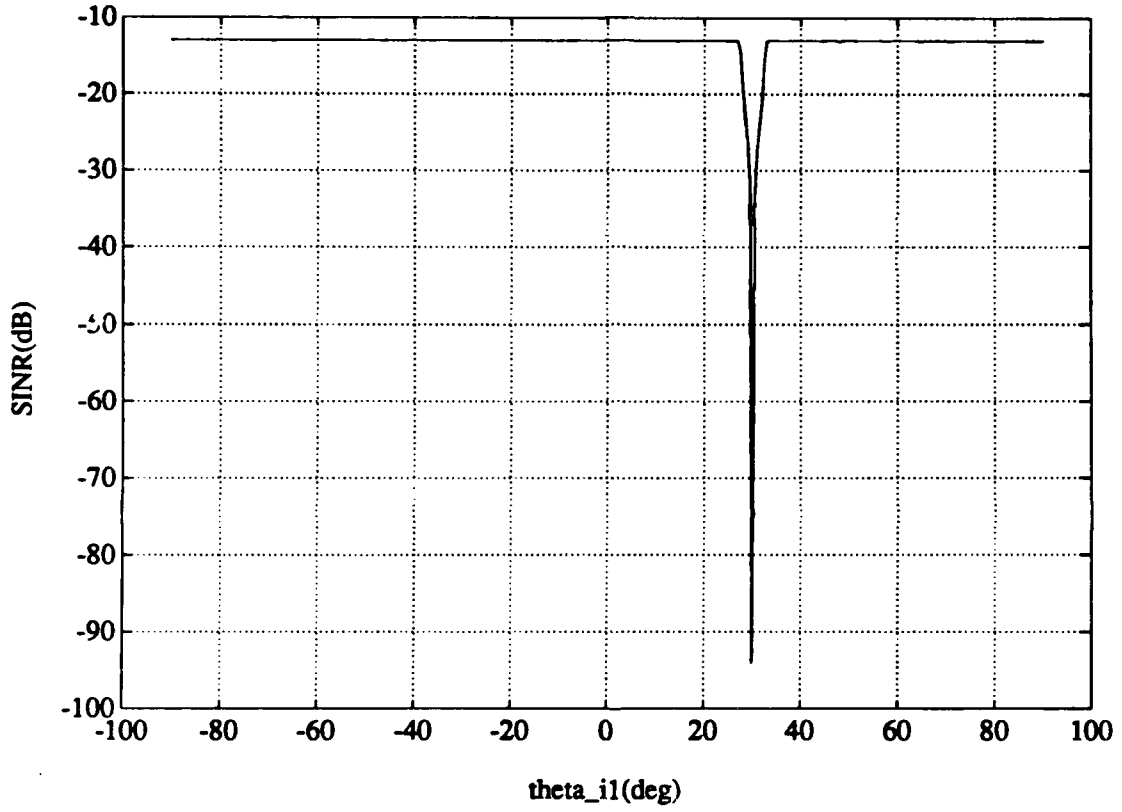

Figure 4.14: SINR performance of a 2-tap TDL on element (1,1). The intertap delay is $38\lambda_0$. INR=60 dB.

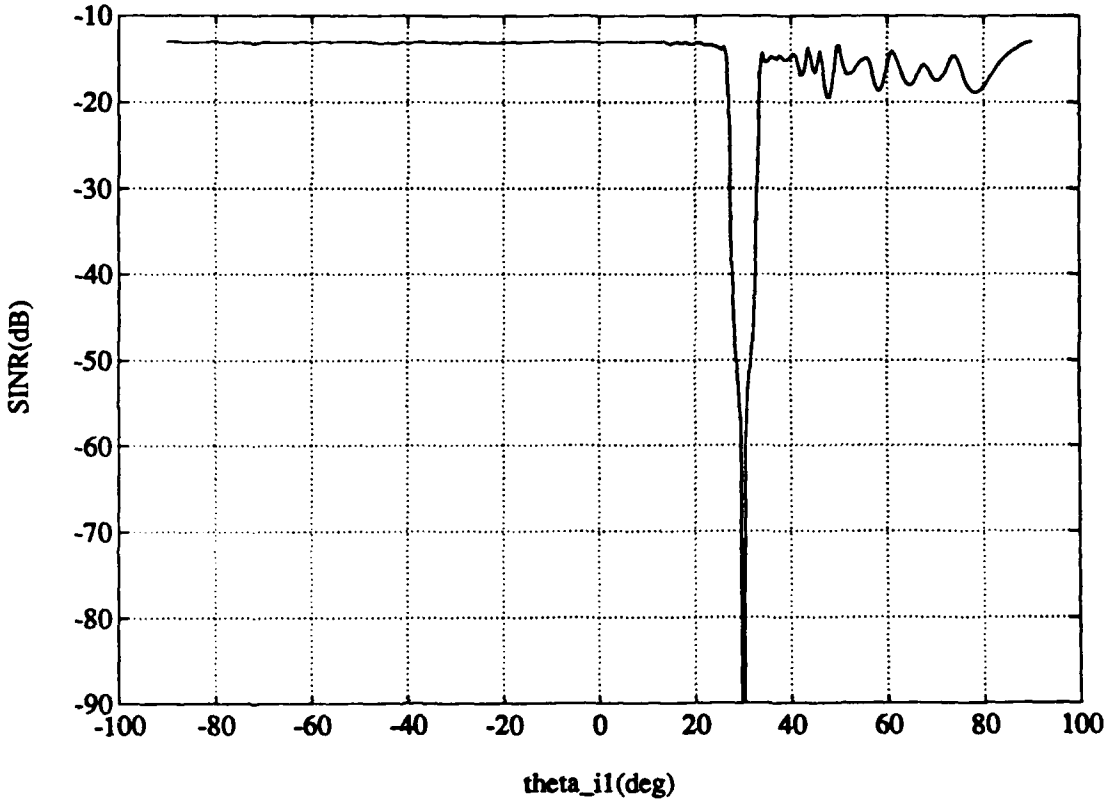

Figure 4.15: SINR performance of a 2-tap TDL on element (1,1). The intertap delay is $38\lambda_0$. INR=90 dB.

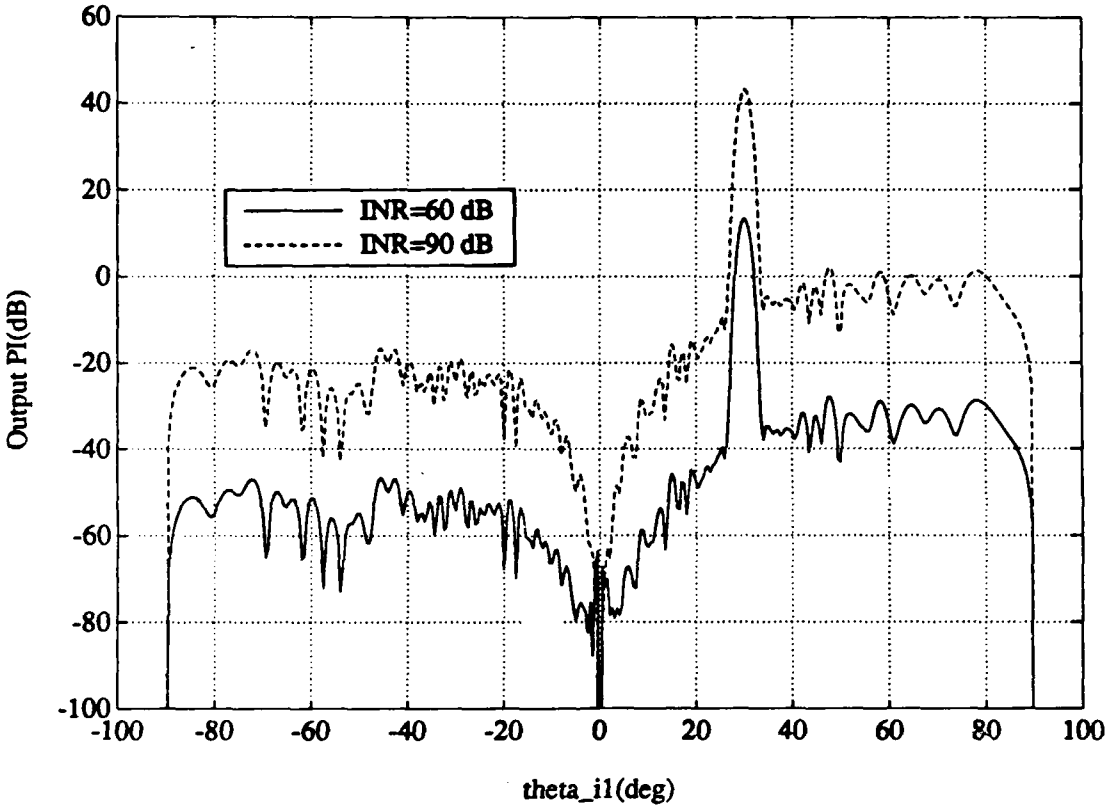

Figure 4.16: Output P_i performance of a 2-tap TDL on element (1,1). The intertap delay is $38\lambda_0$. INR=60 dB; 90 dB

pattern null, the tap weights have already reached their optimum values when the INR is 60 dB, giving a weighted auxiliary frequency response that is the best possible approximation to the mainbeam frequency response (in the jammer direction). Further increases in INR do not change the weights, and the weighted auxiliary and adapted frequency responses remain the same as for 60 dB INR. Therefore the output jammer power increases with the input jammer power. For both curves, the SLC is providing better cancellation for $\theta_{i1} < 0°$ than for $\theta_{i1} > 0°$.

Let us now examine how the intertap delay τ affects the performance of the two-tap end element TDL. Figure 4.17 shows the output interference power for different intertap delays: $10\lambda_0$, $24.75\lambda_0$, $50\lambda_0$, and $250\lambda_0$. Performance as a function of the delay can be divided in to two regions: $\theta_{i1} > 0°$ and $\theta_{i1} < 0°$. For $\theta_{i1} > 0°$ the output P_i increases monotonically as the intertap delay is increased. Thus cancellation performance is degraded as the intertap delay is increased. The reason for this degradation is that for all $\theta_{i1} > 0°$ increasing the intertap delay adds to the decorrelation between the interference in auxiliary signal $\tilde{x}_2(t)$ and the interference in the mainbeam signal.

Output P_i behavior is quite different for $\theta_{i1} < 0°$. For each of the delays, $10\lambda_0$, $24.75\lambda_0$, and $50\lambda_0$, the output P_i is smallest for a different range of θ_{i1}. A particular intertap delay provides smallest output P_i for those jammer arrival angles for which the end-to-end propagation delay of the jammer across the array is equal to the intertap delay. For example, the $24.75\lambda_0$ delay has the smallest P_i for $\theta_{i1} \sim -30°$, when the jammer transit time across the array is $99(\lambda_0/2)\sin 30° = 24.75\lambda_0$. In this case, the intertap delay is matched to a jammer arrival angle of $\theta_{i1} = -30°$. The reason for this behavior is that when the delay on the end element TDL is matched

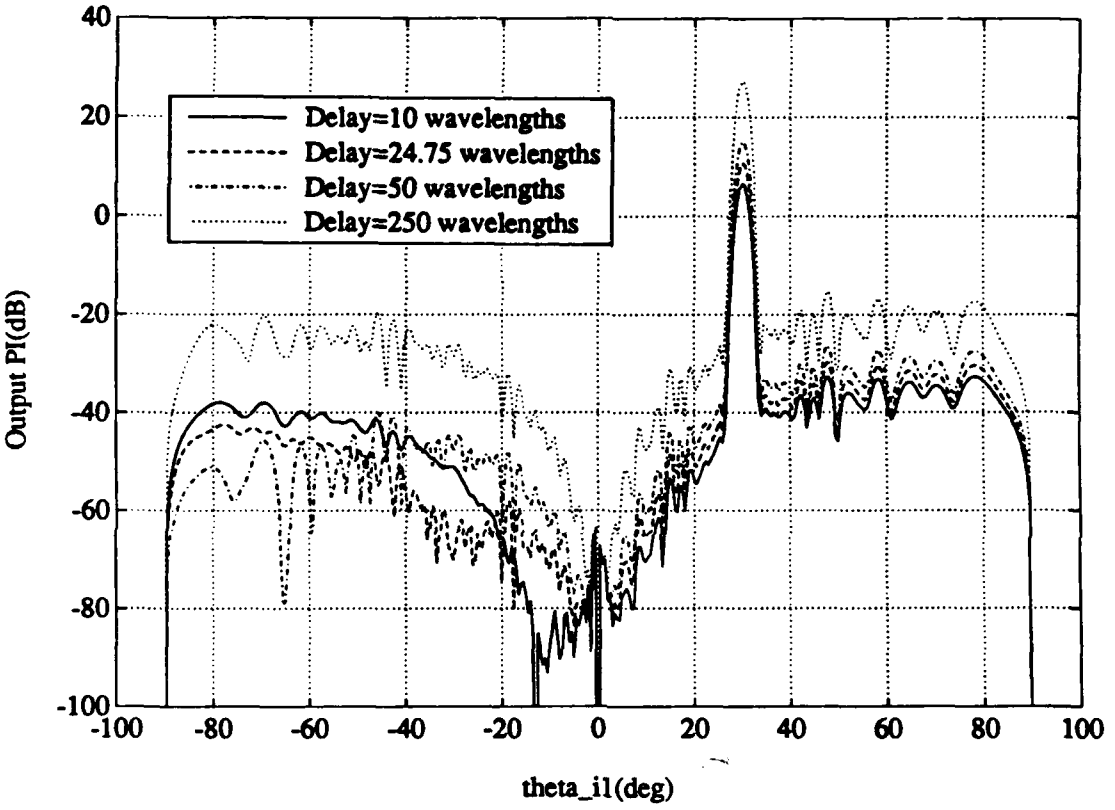

Figure 4.17: Output P_i performance of a 2-tap delay line on element (1,1). INR=60 dB, B=0.001.

to the jammer transit time across the array, the interference components of both auxiliary signals $\tilde{x}_1(t)$ and $\tilde{x}_2(t)$ are equally well correlated with the interference in the mainbeam signal. For delays larger than the maximum transit time across the array (which occurs when the jammer is at $\theta_{i1} = \pm 90°$), there is more decorrelation between the interference in $\tilde{x}_2(t)$ and the mainbeam than between $\tilde{x}_1(t)$ and the mainbeam, regardless of the jammer arrival angle. Therefore the end element TDL performance will degrade monotonically for *all* jammer arrival angles as the intertap delay is increased beyond $49.5\lambda_0$. At a delay of $250\lambda_0$, we see that performance has degraded by between 10 and 20 dB for all θ_{i1}. Increasing the delay even further results in auxiliary signal $\tilde{x}_2(t)$ becoming more and more decorrelated with the mainbeam signal, to the point where the weight on the $\tilde{x}_2(t)$ tap is negligible in magnitude compared with the weight on the $\tilde{x}_1(t)$ tap, and the TDL essentially performs as a single complex weight.

Let us now consider a two-tap TDL on the center element (50,1). Since the auxiliary element is very close to the mainbeam phase center, the performance as a function of jammer arrival angle will not be influenced as much by the intertap delay as it was with an end element auxiliary. Figure 4.18 shows the output jammer power of the center element TDL for intertap delays varying from $10\lambda_0$ to $250\lambda_0$. The jammer INR is 60 dB. We see that output P_i increases monotonically, for both $\theta_{i1} < 0°$ and $\theta_{i1} > 0°$, as the intertap delay is increased. Because the auxiliary element is at the mainbeam phase center, the intertap delay simply decorrelates the auxiliary signal $\tilde{x}_2(t)$ from the mainbeam signal. Hence, as τ is increased the interference cancellation and SINR both become worse. For intertap delays less than $10\lambda_0$, P_i is not noticeably affected by the intertap delay. As the delay is increased

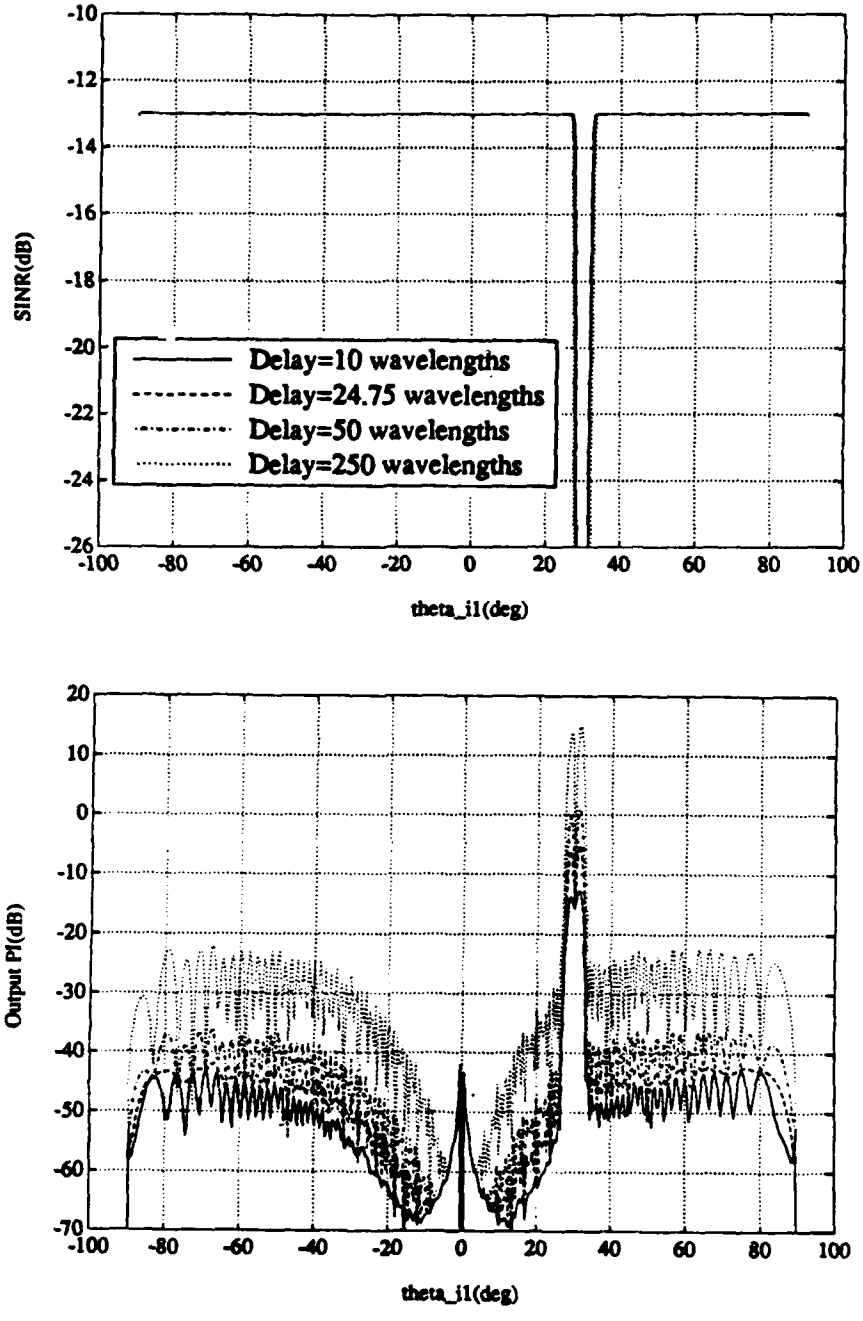

Figure 4.18: Performance of a TDL on the center element as a function of the intertap delay: (a) SINR; (b) Output P_i ; INR=60 dB, B=0.001 .

from $10\lambda_0$ to $50\lambda_0$, the output P_i increases by about 10 dB. For delays in the range $10\lambda_0$ to $50\lambda_0$, the change in output P_i affects the output SINR *only for very* high power jammers (INR$\geq$90 dB).

Figure 4.19 combines the results of Figures 4.18 and 4.17 so that the performance of end and center element auxiliaries with the same TDL structure may be compared. When $\theta_{i1} > 0°$, the center element TDL yields smaller output interference power than the end element TDL, for all intertap delays. Thus the center element provides better cancellation for $\theta_{i1} > 0°$. However, if the intertap delay of the end element TDL is 'matched' to the jammer arrival angle, the end element TDL provides superior performance, by as much as 15-20 dB. This knowledge will only be useful if the jammer arrival angle is known a-priori, so that we can choose the correct end of the array on which to put the TDL. We also see from Figure 4.19 that when θ_{i1} is near an element pattern null the output P_i from the center element TDL is higher than that of the end element TDL, regardless of the intertap delay. This behavior was also observed in the case of a CW jammer, and is caused by the array responding to the mainbeam-auxiliary noise correlation, which is larger for the center element than for the end element auxiliary.

We have observed that for the end element TDL that cancellation is best when the jammer arrival angle and the intertap delay are related such that both auxiliary signals are equally well correlated with the mainbeam signal. With an auxiliary element at the center of the array and a TDL structure composed of physical delay elements, the interference in the mainbeam signal is always less correlated with auxiliary signal $\tilde{x}_2(t)$ than with $\tilde{x}_1(t)$. However, if a digital array implementation where the element signals are first sampled and stored prior to digital weight com-

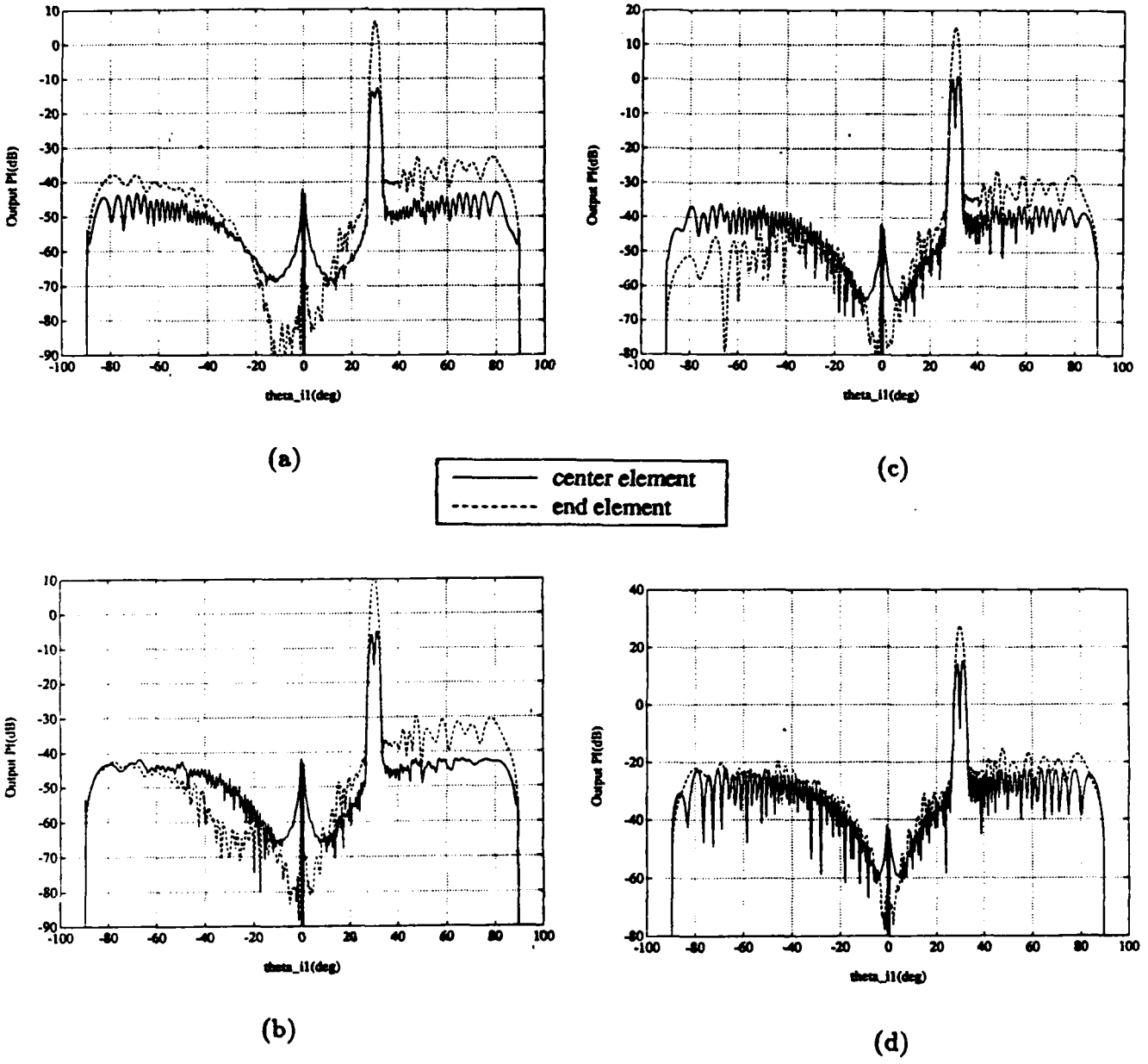

Figure 4.19: Output P_i comparison of end and center element TDLs. One 60 dB jammer. (a) $\tau = 10\lambda_0$ (b) $\tau = 24.75\lambda_0$ (c) $\tau = 38\lambda_0$ (d) $\tau = 50\lambda_0$

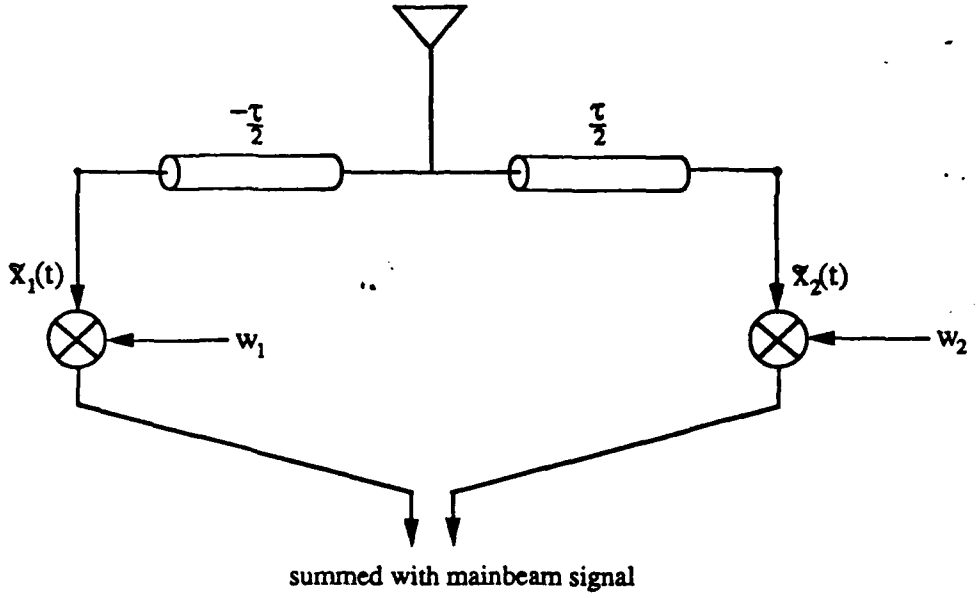

Figure 4.20: Symmetric TDL structure, composed of equal positive and negative delay sections.

putation, it is possible that both positive and negative delays may be implemented in a TDL. Consider the two-tap, two-delay TDL structure that uses equal positive and negative delay sections, as shown in Figure 4.20. We call this TDL structure a symmetric TDL to distinguish it from the conventional two-tap, one delay TDL. A two-tap symmetric TDL on an element at the mainbeam phase center will produce auxiliary signals $\tilde{x}_1(t)$ and $\tilde{x}_2(t)$ that are equally well correlated with the mainbeam signal for all jammer arrival angles. Let us compare the performance of the symmetric TDL with both the center and end element TDLs described previously.

Figure 4.21 compares the output P_i resulting from a symmetric TDL on the center element with that of a conventional TDL on the center element, for different

intertap delays. The delays of the symmetric TDL are $\pm\tau/2$, where τ is the length of the single delay of the conventional TDL. Thus the delay between the two auxiliary signals of each TDL is the same. Results are shown for $\tau = 10\lambda_0$, $24.75\lambda_0$, $38\lambda_0$, and $50\lambda_0$. For each value of τ the symmetric TDL results in a lower output P_i for most jammer arrival angles, and therefore also provides better cancellation. For a center element auxiliary we also see improved performance when both auxiliary signals are equally well correlated with the mainbeam signal.

Figure 4.22 compares the output P_i from a symmetric TDL on the center element with a conventional 2-tap TDL on element (1,1), for $\tau = 38\lambda_0$. A jammer with input INR of 60 dB is assumed. For $\theta_{i1} < 0°$, the two cases yield nearly identical results. However, because the symmetric TDL looks the same to a jammer arriving from a given angle on either side of broadside, the symmetric TDL provides the same output P_i performance for $\theta_{i1} > 0°$ as for $\theta_{i1} < 0°$. Thus the symmetric TDL results in a much smaller output P_i for $\theta_{i1} > 0°$ than the TDL on element (1,1). For this reason, the symmetric TDL structure on the center element of the array is also a better choice than a TDL on the end element. Best performance for most jammer arrival angles is achieved by choosing a delay τ which is matched to a jammer arrival angle somewhere in the middle of the sidelobe region, not too close to either of the element pattern nulls.

Another consideration in selecting the delay between taps is the resulting weight magnitude. In [16], Compton showed that for a two element fully adaptive array, the magnitudes of the individual tap weights increase without bound as the intertap delay was decreased below a quarter-wave delay. Similar behavior occurs in our sidelobe canceller configuration. Since our fractional bandwidth of $B = 0.001$ is

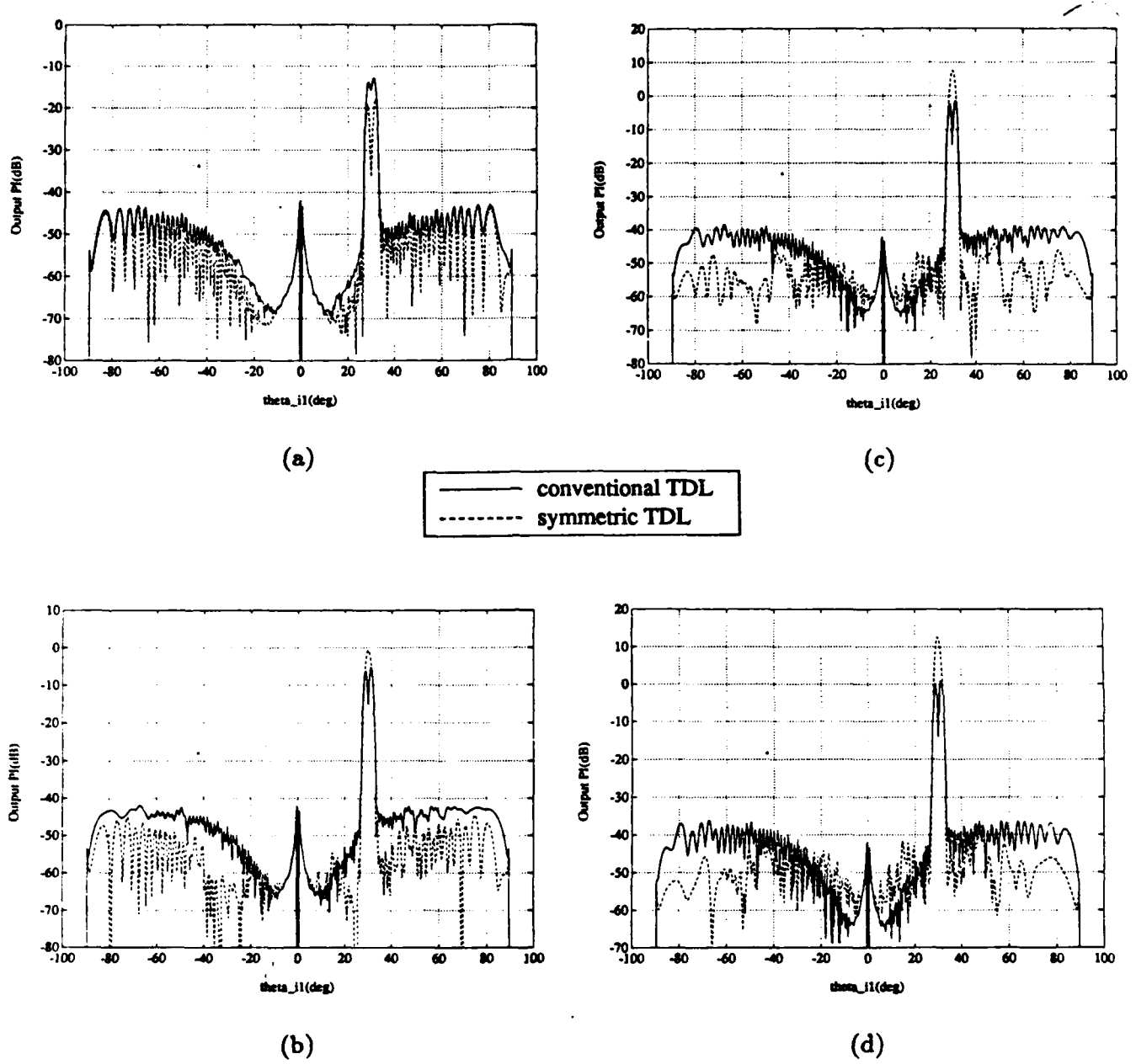

Figure 4.21: Output P_i comparison of conventional and symmetric TDL structures on element(50,1). (a) $\tau = 10\lambda_0$ (b) $\tau = 24.75\lambda_0$ (c) $\tau = 38\lambda_0$ (d) $\tau = 50\lambda_0$

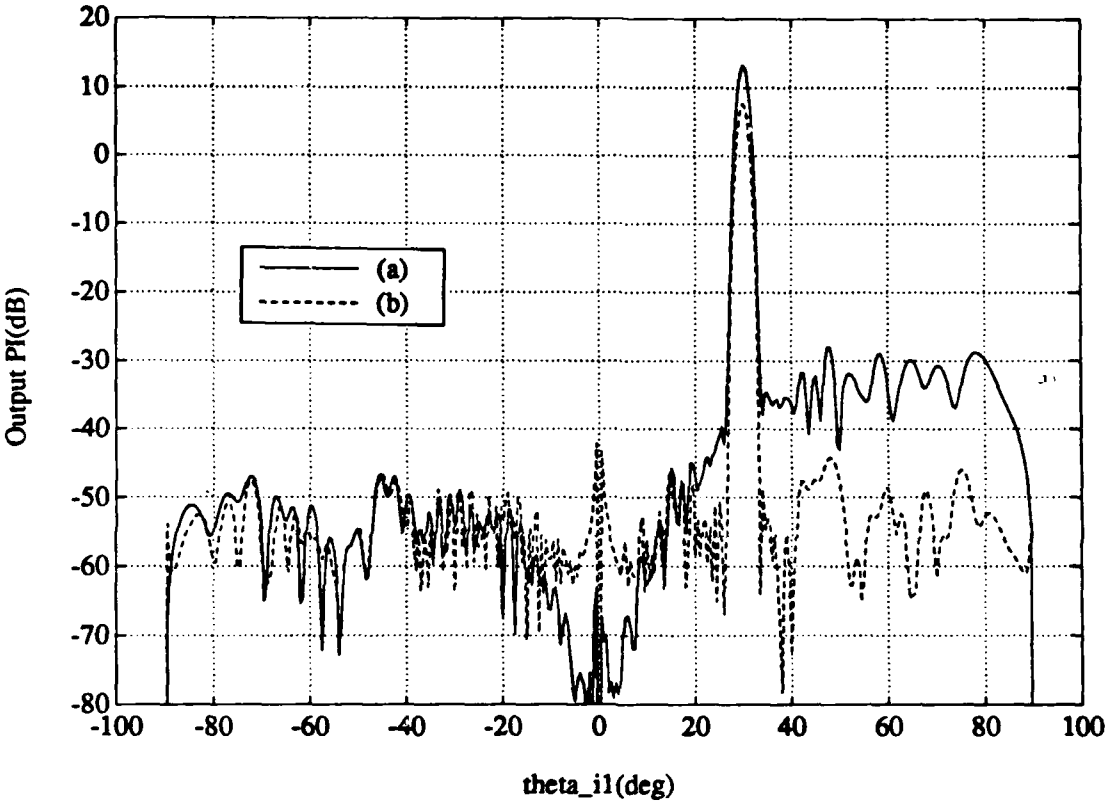

Figure 4.22: Output P_i comparison of two TDL structures. (a) A 2-tap, one delay=$38\lambda_0$ TDL on element (1,1). (b) A 2-tap, two delays=$-19\lambda_0$, $19\lambda_0$ TDL on (50,1).

much smaller than the $B = 0.2$ used in [16], the increase in weight magnitude is observable for larger delays. In our case, the weight magnitudes resulting from a $\lambda_0/4$ delay are on the order of 100 times those resulting from a $24.75\lambda_0$ intertap delay. Although large, these weights are phased such that the magnitude of the vector sum $w_1 + w_2 e^{-j\omega\tau}$ is much smaller than the individual tap weight magnitudes, as it must be to match the mainbeam magnitude response. The reason for the increase in weight magnitudes as the intertap delay decreases is that the covariance matrix becomes nearly singular.[16]

Large weight magnitudes are undesirable not only because they may be unachievable in a hardware implementation, but also because large weight magnitudes usually occur when the software used to calculate these weights is more susceptible to round-off errors. Round-off error problems usually occur at high INR. For these reasons, very small intertap delays should be avoided. Our results indicate that delays of $10\lambda_0$ or greater provide tap weight magnitudes on the same order as a that of a single complex weight in the presence of a CW jammer.

The weight magnitudes are also a major determining factor in the sidelobe level of the adapted pattern. A tapped delay line provides a frequency dependent weight on the auxiliary element. However, the array pattern is a single frequency quantity defined at the center frequency of the signal bandwidth. Therefore it is not the individual tap weight magnitudes but rather the magnitude of the TDL frequency response at the center frequency, $|w_1 + w_2 e^{-j\omega_d\tau}|$, which affects the adapted pattern. As explained above, this resultant magnitude remains small even for very small intertap delays. Assuming the jammer is cancelled, the magnitude and phase of the TDL response at the center frequency are nearly identical to those of the single

complex weight canceling a CW jammer. Therefore the presence of a the tapped delay line has no additional effects on the output pattern SLL. As in the case of a single complex weight, a TDL on the center element will result in a large increase in SLL if the system adapts with no jamming present or when the jammer arrives in a null of the element pattern.

The intertap delay necessary for sufficient cancellation is also important in a digital adaptive array implementation. (e.g. using the SMI algorithm [17]) The intertap delay determines the rate at which the element signals need to be sampled for tapped delay line processing. In a pulsed radar, the absolute signal bandwidth is approximately

$$\Delta f = \frac{1}{\tau_p}, \tag{4.7}$$

where τ_p is the pulse duration. Nyquist rate sampling then corresponds to a sampling interval T_N of

$$T_N = \frac{\tau_p}{2} = \frac{1}{2B}\frac{\lambda_0}{c}, \tag{4.8}$$

where B is the fractional bandwidth and c is the velocity of propagation. This sampling interval is equivalent to a spatial delay of $\frac{1}{2B}\lambda_0$, which is $500\lambda_0$ for our assumed signal bandwidth. Our results have shown that intertap delays half this large do not give very satisfactory adaptive array tapped delay line performance, and that performance for larger intertap delays is worse. Therefore, a sampling rate much higher than the Nyquist rate will be necessary for satisfactory sidelobe canceller performance.

We now summarize the results presented in this section, for signals of fractional bandwidth $B = 0.001$. With a single complex weight on the auxiliary, degradation with respect to the zero bandwidth case is first evident at an INR of about 40 dB.

For higher INRs, tapped delay lines behind an element may be used to overcome the bandwidth degradation. Delay lines with 2 taps were sufficient to provide good cancellation over the whole signal bandwidth for an input INR up to at least 90 dB. We examined performance of conventional TDLs with two taps and a single delay, and of a symmetric TDL structure in which there are two delay sections of equal magnitude, with one positive and one negative.

Examination of performance for different auxiliary element locations and intertap delays led to the following conclusions. First, intertap delays on the order of the jammer propagation delay across the array, when the jammer arrival angle is not too close to broadside, result in good cancellation performance and tap weight magnitudes which are not excessively large. Increasing the intertap delay beyond the maximum jammer propagation delay degrades performance for both end and center element tapped delay lines. With regards to element location, the symmetric TDL on a center element provides the best cancellation performance, considering all possible jammer arrival angles. However, the symmetric TDL can only be implemented in a digital adaptive array implementation where negative delay sections are feasible. In the idealistic case when the jammer arrival angle is known, a conventional TDL on an end element with the intertap delay matched to the jammer transit time across the array will provide best cancellation. Otherwise, a conventional TDL on the center element provides better cancellation than the end element TDL for most jammer arrival angles.

The only disadvantage to using a center element TDL, conventional or symmetric, is the possibility of SLL degradation when no jamming is incident. As explained in Section 4.2, SLL degradation occurs because of the noise correlation

between mainbeam and auxiliary signas that results from element reuse. With a CW jammer, there is no interference decorrelation due to bandwidth, and it is the noise correlation that limits the jammer cancellation. Thus we found best CW cancellation for an end element auxiliary where the noise correlation with the mainbeam is smallest. For non-zero bandwidth jammers, cancellation is affected more by the decorrelation due to bandwidth than by the thermal noise correlation. As a result we found better cancellation performance for most jammer arrival angles when a center element TDL is used. In Chapter 6 we show how the mainbeam auxiliary noise correlation can be eliminated, resulting in the elimination of SLL degradation when no jammers are present and the elimination of CW cancellation dependence on auxiliary element location.

Performance was also shown for signals of fractional bandwidths $B = 0.01$. In this case, performance degradation is evidenced at much lower INRs. The observations made in the $B = 0.001$ case with regard to element location and the intertap delay also apply to this higher bandwidth. It was found that at least a 3 tap delay line is needed on the center element to provide equivalent CW performance for INR=60 dB, while at least 5 taps are needed for INR=90 dB.

5. Multiple Single-Element Auxiliary Signals: One or More Jammers

5.1 Introduction

In the previous chapter, we examined SLC performance when only a single auxiliary element was used. For a single CW jammer, we needed only a single complex weight on the auxiliary. For a jammer with non-zero bandwidth, a tapped delay line was used on the auxiliary. To cancel more than one jammer, however, requires the combined auxiliary signals to match the mainbeam response at more than one arrival angle. In this case the array must have more than one auxiliary signal. In this chapter we consider array performance with multiple auxiliaries, but we restrict the discussion to the case where each auxiliary signal is formed from a single element. The use of multiple auxiliary elements not only allows the array to cancel multiple jammers, but it also affects performance against a single jammer.

We first consider the case where there is a single CW jammer. We show that in an array with multiple auxiliaries the unused spatial degrees of freedom react to thermal noise, which may result in high adapted pattern sidelobe level. We then consider performance of multiple auxiliary configurations against a single jammer of non-zero bandwidth. Although a multiple auxiliary configuration appears as a tapped delay line filter to an incident signal, cancellation and ASLL performance depends on the effective intertap delays more than when a TDL is used on a single auxiliary element. Also, when different auxiliaries are close together or when the jammer arrival angle is near broadside, the performance of a multiple auxiliary configuration is poorer than that of the TDL configurations examined in the last chapter.

Finally we consider performance in an environment of multiple CW jammers. We examine how the spacing between auxiliary elements affects the SINR and ASLL performance. We show that closely spaced auxiliary elements are unable to provide cancellation of closely spaced jammers, while widely separated auxiliaries are unable to cancel jammers whose separation is equal to the spacing between grating lobes in the weighted auxiliary array. We show that one can provide sufficient cancellation for all combinations of jammer arrival angles with an unequally spaced array of auxiliary elements, where the number of auxiliaries is greater than the number of interfering signals. However these extra degrees of freedom also result in an increase in adapted pattern SLL. We have found no configuration of single-element auxiliaries which provided both excellent cancellation of multiple jammers *and* good ASLL performance.

5.2 A single CW jammer

Since a single CW jammer can be completely cancelled with a single complex weight on one auxiliary element, a canceller configuration with multiple auxiliaries has more than the necessary degrees of freedom. Because the auxiliary signals are formed from single elements that are also shared with the mainbeam, the array responds not only to the jammer but also to the noise correlation between the mainbeam and the auxiliaries. We noted in the last chapter how this correlation affects array behavior in a canceller with one auxiliary element when no interference is present(or when the jammer is received in a null of the element pattern). In this case the array adapts anyway, and it maximizes output SINR by minimizing the thermal noise power at the array output. As a result, the adaptive weight on the

auxiliary signal is non-zero, even though no jammers are present. Although the change in output noise power is minimal, the effect on the output sidelobe level can be drastic, especially for auxiliary elements chosen from the center of the array.

Similar problems occur with multiple auxiliaries whenever there are extra degrees of freedom not being used to cancel jammers. The array weights then adapt not only to cancel jammers but also to minimize the noise at the output. With fewer jammers than degrees of freedom, the weight magnitudes become large and the adapted sidelobe pattern is dominated by the weighted auxiliary patterns. Thus the adaptive capability destroys the original low sidelobe mainbeam design. We illustrate this behavior with an example.

Figure 5.1 shows the mainbeam and adapted patterns of a sidelobe canceller using two auxiliary signals when there is one CW jammer. One auxiliary is formed from element (50,1) and the other from element (51,1). A single 40 dB per element CW jammer is incident from $\theta_{i1} = -45°$. It may be seen that the adapted pattern sidelobes are at least 20 dB above those of the mainbeam. Comparison with the adapted pattern of Figure 3.10 resulting from a single auxiliary signal shows the degradation caused by the addition of a second auxiliary element.

The degradation illustrated above can be lessened by forming the auxiliary signals from elements at the ends of the array. End elements have smaller weights in the mainbeam combiner so the signal from an element has smaller noise correlation with the mainbeam signal. The auxiliary signal weights are therefore smaller in magnitude and have less impact on the adapted pattern. In the next chapter we show how this problem can be completely eliminated by forming the auxiliary signals from combinations of elements so that the noise correlation between the

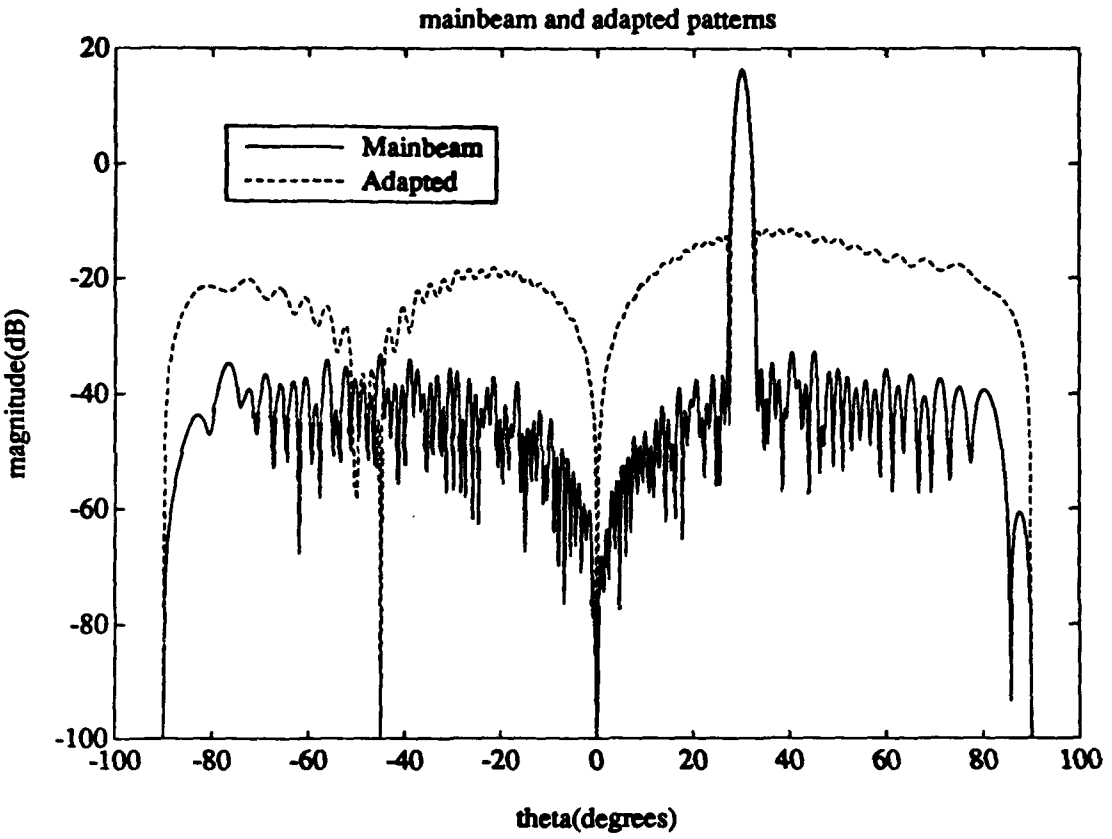

Figure 5.1: Mainbeam and adapted patterns of a SLC with 2 single element auxiliary signals in the presence of a single jammer.

auxiliary signals and the mainbeam signal is zero.

5.3 A single jammer with non-zero bandwidth

A complex weight on one auxiliary element allows cancellation of one jammer at a single frequency. A tapped delay line on the auxiliary element allows a non-zero bandwidth jammer to be cancelled over its whole bandwidth, as discussed in the last chapter. However, a configuration of multiple auxiliary elements also appears to an incident jammer as a tapped delay line filter. The delay line taps are the individual auxiliary element signals, and the intertap delays are the interelement propagation delays experienced by an incident signal. These propagation delays depend on the signal arrival angles.

In [5], White has compared the performance of sidelobe cancellers consisting of multiple auxiliary elements with configurations where a TDL is used on a single auxiliary. He states that, in most cases, both configurations perform equally well against a single wideband jammer. This is true because the interelement propagation delays of a multiple auxiliary configuration are equivalent to the intertap delays of a TDL configuration. In fact, if the auxiliary elements of the multiple auxiliary configuration are chosen so that the interelement propagation delays are the same as the intertap delays of the TDL configuration, both configurations are identical as far as the jammer is concerned. Then the same weights will be required to null the jammer in each case. However, although the two configurations appear identical to directional signals, their responses to the thermal noise signals present in the array are much different. This difference can cause the cancellation and SLL performance of a multiple auxiliary configuration to be much worse than that of a TDL on a

single auxiliary in the presence of a single jammer. We illustrate this problem with an example.

Let configuration $C1$ be a two-tap TDL on element (50,1) with a single intertap delay of $\lambda_0/4$. Let configuration $C2$ consist of two auxiliaries, elements (50,1) and (51,1) with a single complex weight on each. We compare the performance of these two configurations in the presence of a single 60 dB jammer with fractional bandwidth $B = 0.001$. To a directional signal arriving from θ_{i1}, configuration $C2$ appears as a two-tap delay line with equivalent intertap delay of $\frac{\lambda_0}{2}\sin\theta_{i1}$. For most arrival angles this delay is of the same order of magnitude as the intertap delay of $C1$. (They are equal for $\theta_{i1} = -30°$.) Figures 5.2 and 5.3 show the SINR, output P_i, and ASLL resulting from these two configurations. We see that the TDL on the single auxiliary element provides much smaller output P_i and thus better cancellation and better output SINR than the multiple auxiliary configuration. The increase in ASLL is also much smaller for configuration $C1$. In this case the TDL on a single auxiliary is a better choice. The reasons for these differences are given below.

Because both configurations $C1$ and $C2$ appear nearly identical to the jammer, approximately the same weight values are required to suppress the jammer in both cases. The intertap delay($C1$), or the spacing between auxiliary elements($C2$), is small enough so that the weights required to cancel the jammer are large in magnitude. With a tapped delay line on a single auxiliary element, the noise signal on that element sees the same TDL filter transfer function as the jammer. As explained in Section 4.3, the magnitude of this transfer function matches the mainbeam frequency response in the jammer direction, and is small in magnitude. (The jammer

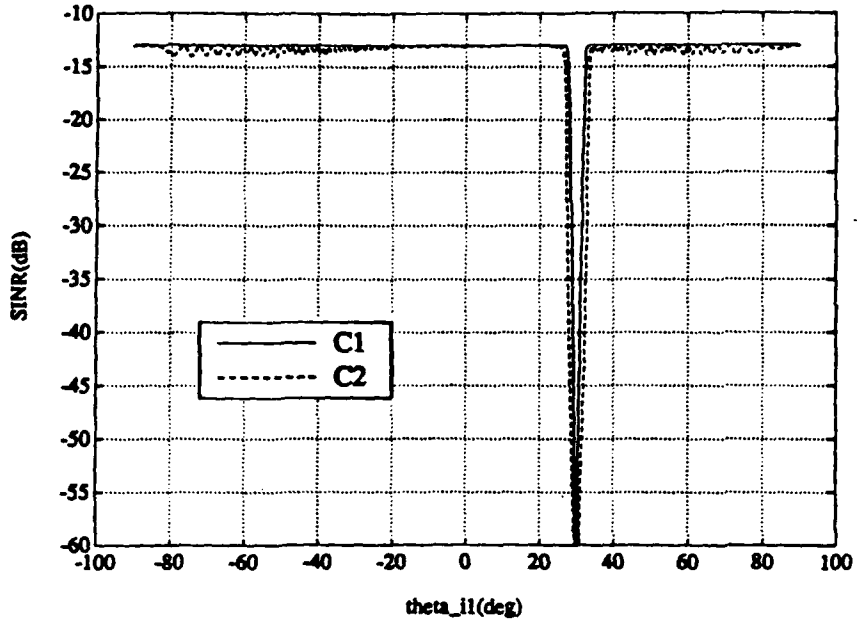

(a)

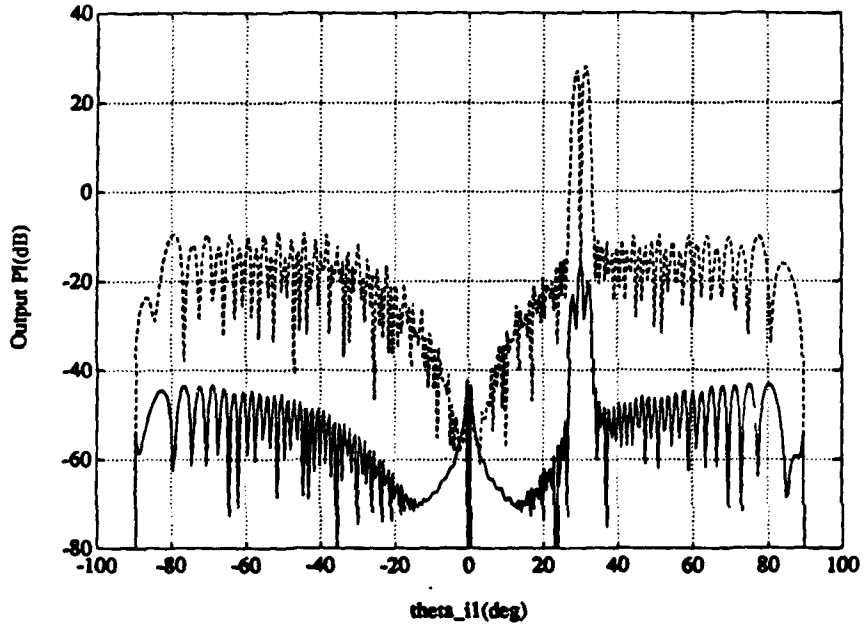

(b)

Figure 5.2: Comparison of a TDL on element (50,1) (C1) with a multiple auxiliary configuration consisting of single complex weights on elements (50,1) and (51,1) (C2). $B = 0.001$. (a) SINR (b) Output P_i

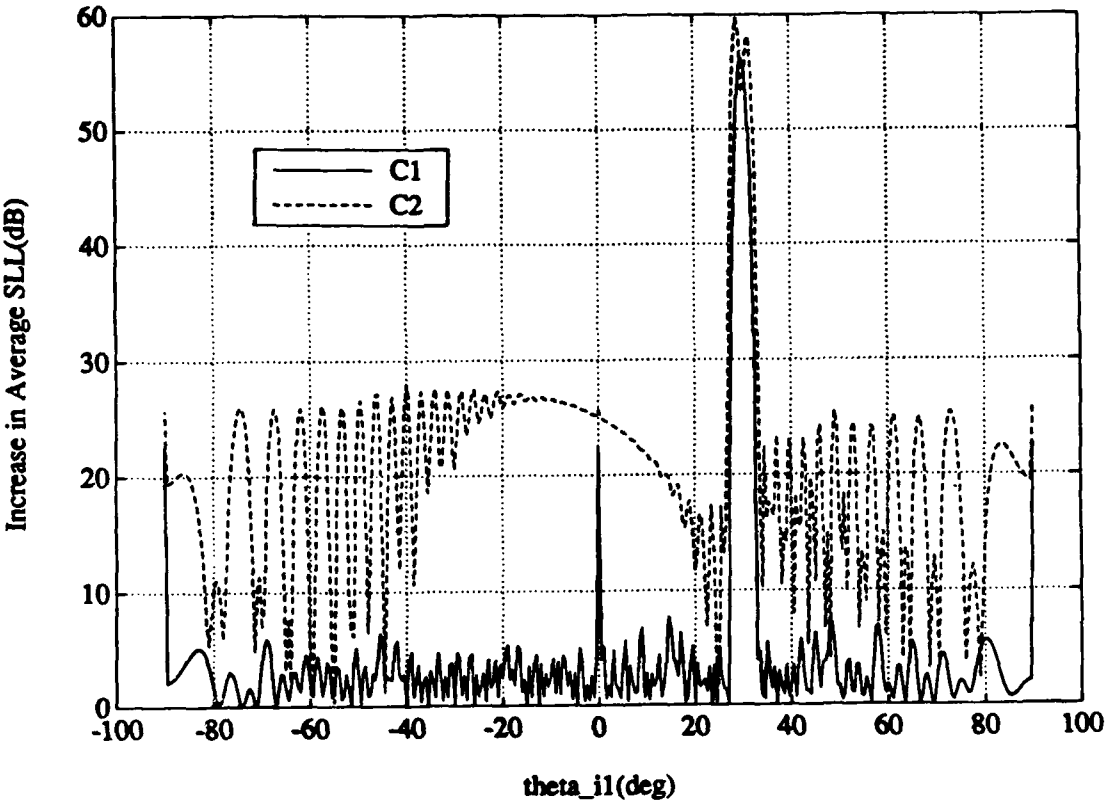

Figure 5.3: Increase in ASLL comparison of a TDL on element (50,1) (C1) with a multiple auxiliary configuration consisting of single complex weights on elements (50,1) and (51,1) (C2).

is in the sidelobe region.) Therefore, the noise added by the weighted auxiliary for $C1$ is insignificant even though the individual tap weights may be large, and the optimal SINR weights are those that cancel the jammer. For configuration $C2$, the delay between taps is the spatial delay between auxiliary elements experienced by the interfering signal. The noise signals on the auxiliary elements do not see the same TDL filter transfer function as the jammer. Instead, each auxiliary adds a noise power proportional to the square of its weight magnitude. In this case, the large weights which cancel the jammer also result in a large increase in output noise power, so that the jammer cancellation is compromised to optimize SINR. Thus the weights of configuration $C2$ settle at values different than those required to cancel the jammer. Likewise, the adapted pattern ASLL depends on the individual weight magnitudes for configuration $C2$, while it only depends on the magnitude of the TDL transfer function for configuration $C1$. (See Section 4.3.) Therefore, large weight magnitudes cause more SLL degradation for a multiple auxiliary configuration than for a configuration with a TDL on a single auxiliary element.

We explained in the TDL results of the last chapter how, as the intertap delay increases, the weight magnitudes required to cancel a jammer decrease. Since the individual weight magnitudes depend on the intertap delay, how a given multiple auxiliary configuration compares with a TDL on a single auxiliary depends on the size of the intertap delay. We noted above that if this delay is small, then the performance of the multiple auxiliary configuration is much worse than that of the TDL on a single auxiliary. Small intertap delays result when the auxiliary elements are closely spaced in the array, or when auxiliaries are widely spaced and the jammer arrival angle is near broadside. When the auxiliaries are chosen such

that the intertap delay is on the order of several wavelengths, the performance of the multiple auxiliary configuration is essentially identical to that of the equivalent configuration consisting of a TDL on a single auxiliary element. A multiple auxiliary configuration with two widely separated auxiliary elements is thus a better choice to combat a single broadband jammer than a multiple auxiliary configuration with two adjacent auxiliary elements.

5.4 Multiple CW jammers

Consider now a scenario with multiple CW jammers. Suppose the auxiliary signals are taken directly from the outputs of selected elements. (There are no TDLs.) To cancel multiple jammers, the weighted auxiliary pattern must exactly match the mainbeam pattern at each jammer arrival angle. The actual cancellation depends on how closely the weighted auxiliary pattern matches the mainbeam pattern at these angles. The behavior of the weighted auxiliary array pattern at other angles will determine the sidelobe level of the adapted pattern.

A sidelobe canceller consisting of a mainbeam and N auxiliary signals has N degrees of freedom and, in most cases, can cancel N narrowband jammers. A difficulty occurs when the auxiliary elements are too closely spaced within the array. Then the array has trouble cancelling jammers closely spaced in angle. This problem is basically a limitation in the resolution of the auxiliary array. It can be overcome by increasing the size of the auxiliary array, either by adding more auxiliary elements or by increasing the spacing between auxiliary elements. Another difficulty occurs when the auxiliary elements are widely spaced. Then the weighted auxiliary pattern repeats itself (has grating lobes) in visible space. In this case, the sidelobe canceller

is unable to cancel combinations of jammers where the angular separation between any two jammers is equal to a multiple of the spacing between grating lobes. To allow sufficient cancellation of closely spaced jammers without severe grating lobe problems, we can use an unequally spaced array of elements as auxiliaries. The end to end separation between elements of the auxiliary array should be chosen large enough to resolve closely spaced jammers. The unequal spacing between auxiliary elements produces a pattern that is not periodic, and one can choose auxiliaries so there are no combinations of jammer arrival angles that render the adaptive array helpless. However, although an unequally spaced array provides cancellation of closely spaced jammers and does not have grating lobe problems, the resulting SLL of the adapted pattern is usually much higher than the sidelobe level of the mainbeam pattern. Unfortunately, we have found no configurations that provided sufficient cancellation as well as good SLL performance for all combinations of jammer arrival angles. We examine these issues in more detail in the examples below.

Consider a sidelobe canceller with 2 auxiliary signals. The auxiliary signals are formed from elements (1,1) and (5,1) in the array and are separated by 2λ. In general, we can write the auxiliary array pattern for a configuration of multiple auxiliary elements as

$$F_X(\theta,\phi) = f((\theta,\phi))A_X((\theta,\phi)) \,, \tag{5.1}$$

where we define

$$A_X(\theta,\phi) = \sum_{i=1}^{K} w_i e^{j\pi[(p_i-1)\cos\phi+(q_i-1)\sin\phi]\sin\theta} \tag{5.2}$$

to be the auxiliary array factor and (p_i, q_i) is the location of the i^{th} auxiliary element.

In this example,

$$AF_X(\theta) = w_1 + w_2 e^{j4\pi \sin\theta} . \qquad (5.3)$$

Note that the auxiliary array factor is periodic in the variable $u = \sin\theta$ with period $u_p = 0.5$. The SINR and increase in ASLL resulting from two 50 dB per element CW jammers is shown in Figure 5.4(a) and (b). The arrival angle of one jammer is fixed at $\theta_{i1} = 40°$. The SINR is plotted versus θ_{i2}, which is scanned across visible space. There are narrow regions of SINR degradation around $\theta_{i2} = 8.2°, -20.9°$, and $-59.0°$. The jammer separations(in sine space) for these values of θ_{i2} are multiples of the period of the auxiliary array factor, and satisfy

$$\sin\theta_{i2} = \sin\theta_{i1} + 0.5n \qquad (5.4)$$

for some integer n. At these θ_{i2} the auxiliary array factor (both magnitude and phase) will be equal to its value at θ_{i1}. Usually, the mainbeam response is different in the two directions, so cancellation of both jammers is impossible.

Although the SINR degradation is only evident over very narrow angular regions, the effects on the ASLL performance of the adapted pattern are evident over larger ranges of jammer arrival angle. Figure 5.4(b) shows the ASLL vs. θ_{i2}. When θ_{i2} approaches the values where Eq. (5.4) is satisfied, the weights become large in magnitude (because the covariance matrix becomes nearly singular). As noted before, large weights cause the weighted auxiliary array patterns to swamp out the mainbeam sidelobes. The actual weighted auxiliary pattern and the adapted pattern resulting for $\theta_{i2} = -20.9°$ are given in Figure 5.5. In this case, not only are the low sidelobes of the mainbeam destroyed, but neither jammer is significantly nulled. (CR=[illegible] in this case.)

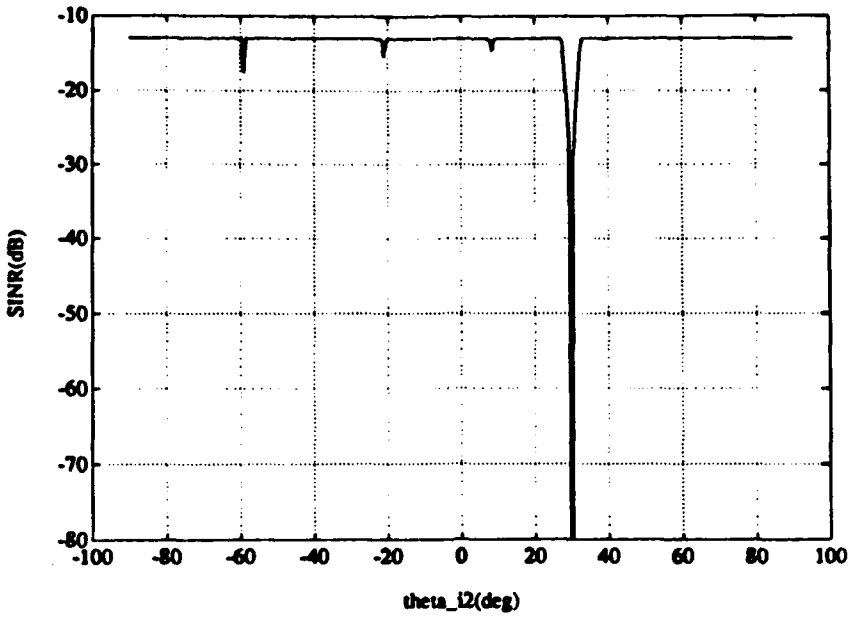

(a)

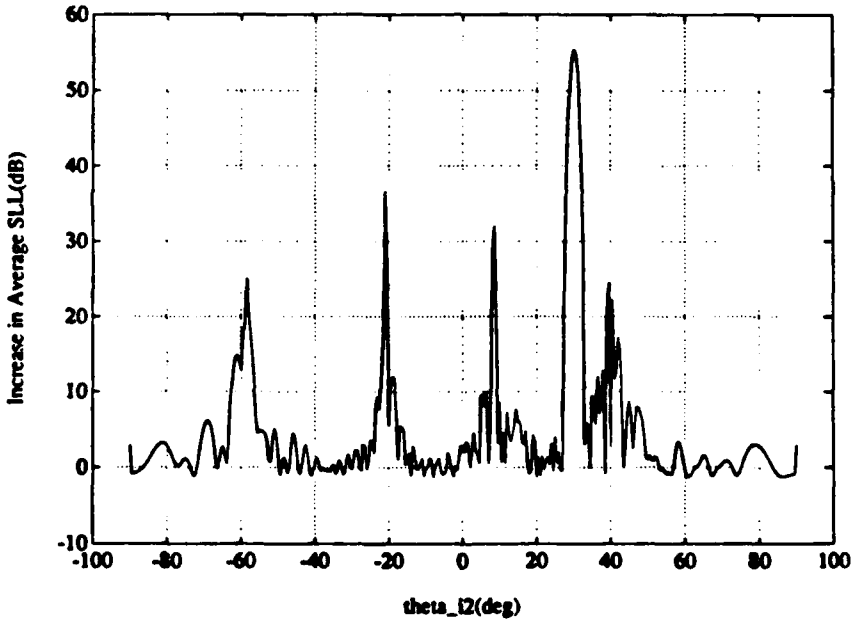

(b)

Figure 5.4: Performance of a SLC with two auxiliaries, elements (1,1) and (5,1), in the presence of two 50 dB CW interfering signals. (a) SINR (b) Increase in ASLL

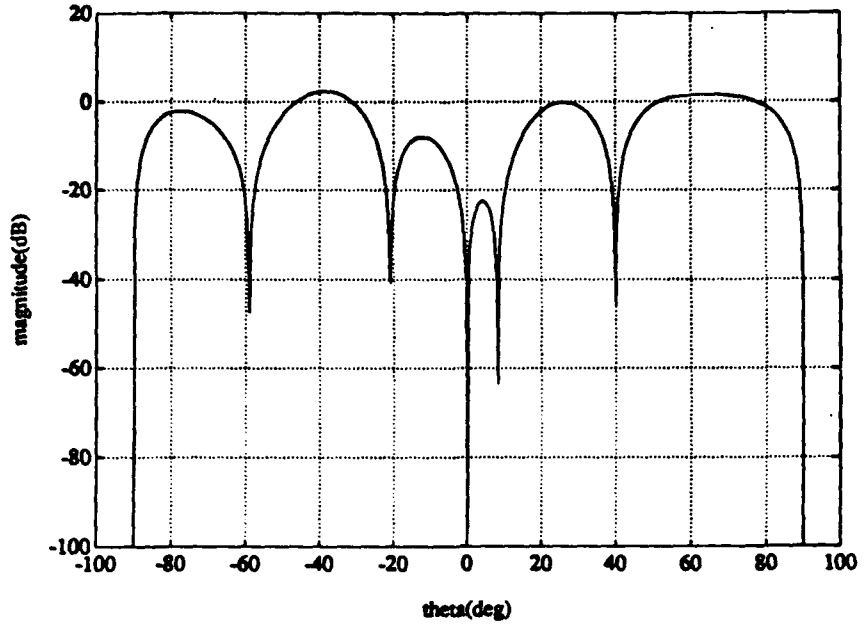

(a)

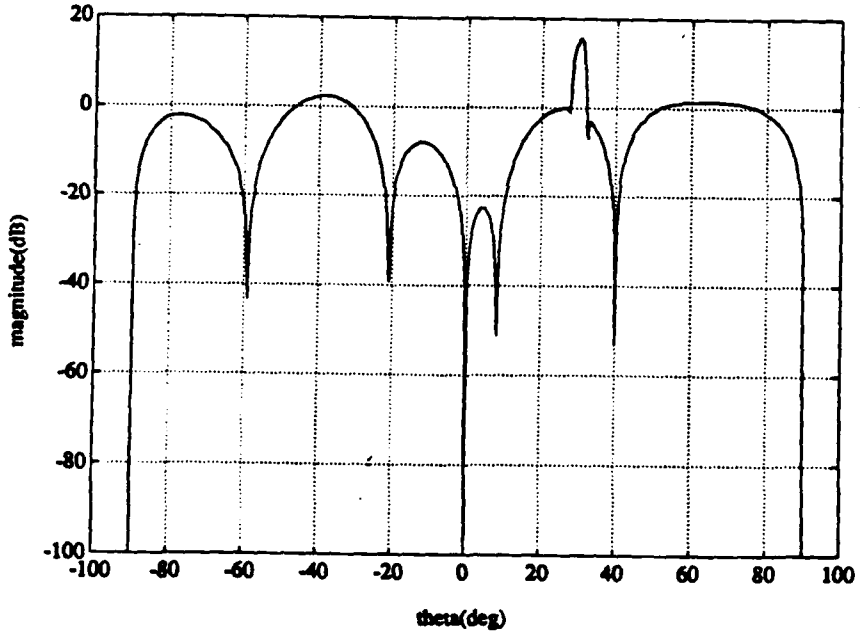

(b)

Figure 5.5: Patterns resulting from a SLC with auxiliary elements (1,1) and (5,1) when the spacing between jammers is close to the spacing between grating lobes in the weighted auxiliary pattern. Two 40 dB CW jammers: $\theta_{i1} = 40°$, $\theta_{i2} = -20.9°$. (a) Weighted auxiliary pattern (b) Adapted pattern

If the jammer arrival angles were known, one could choose the auxiliary elements so that none of the grating lobes would fall near the jammers. But jammer angles are usually not known a-priori, of course, so we instead seek canceller configurations that perform best considering all combinations of arrival angles.

There are two ways to ensure that grating lobes will not be present. One way is to choose auxiliary signals from adjacent elements (separated by $\frac{\lambda_0}{2}$). If only two auxiliary elements are to be used, choosing them as adjacent elements of the array is the only way to completely avoid grating lobes. If more than two auxiliaries are required, spacing them nonuniformly within the array produces an auxiliary array pattern that will not repeat in the visible region. Let us first illustrate the resolution problems inherent in an auxiliary configuration with adjacent elements and then consider an example of an unequally spaced auxiliary array.

Consider first a canceller using elements (1,1) and (2,1) as the auxiliaries. Again assume two 50 dB CW jammers are incident, one whose location is fixed at $\theta_{i1} = 40°$ and another whose location is varied. Figure 5.6 shows the resulting SINR and output P_i. In addition to the usual drop in SINR for θ_{i2} in the main lobe, some SINR degradation is also evident around $\theta_{i2} = 40°$, where the two jammer arrival angles are nearly the same. The output P_i curve shows the reason for the SINR degradation. When the two jammer arrival angles are close, the output interference power increases sharply. When they are identical, essentially only one jammer is present and interference power drops to a very low level.

We can see why these curves behave this way by examining the patterns involved. For perfect cancellation, the weighted auxiliary array must match the mainbeam response perfectly at the two angles θ_{i1} and θ_{i2}. To do this for closely spaced jammers

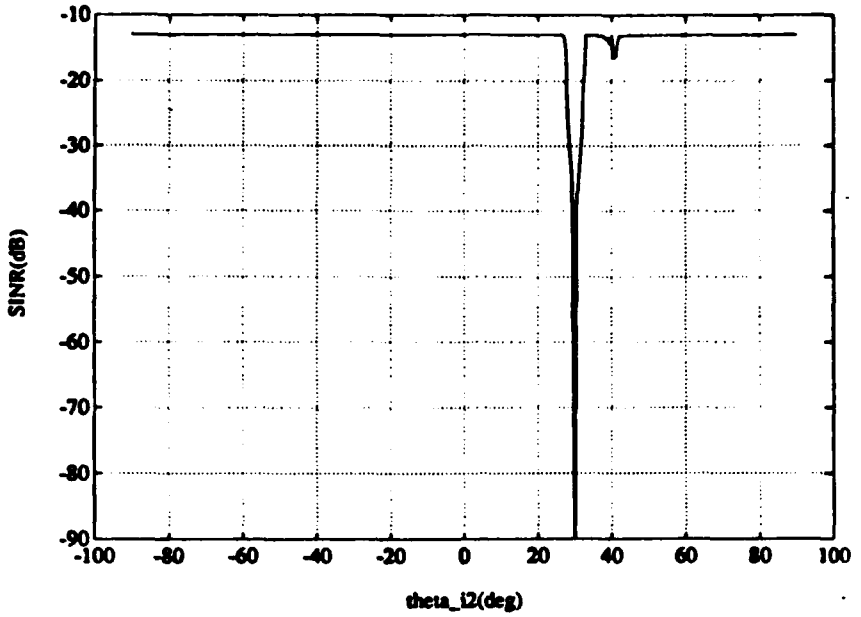

(a)

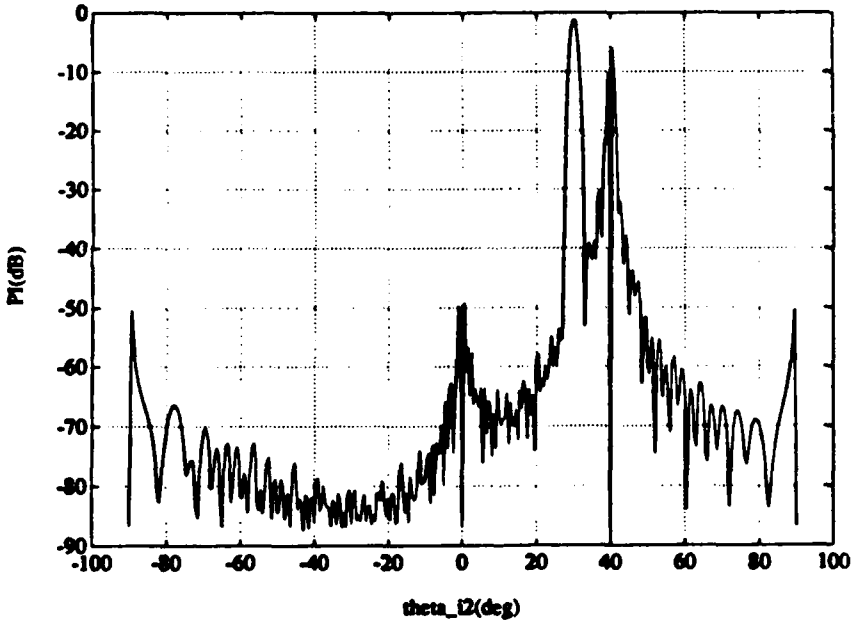

(b)

Figure 5.6: Performance of a SLC with two closely spaced auxiliaries, elements (1,1) and (2,1), with two 40 dB CW jammers incident. $\theta_{i1} = 40°$ (a) SINR (b) Output P_i

requires a high rate of change in the auxiliary array pattern. In this example the auxiliary array consists of two elements separated by one-half wavelength. The rate of change of this pattern is not nearly fast enough to match the mainbeam response near the maximum of the auxiliary pattern. What happens instead is that the two element auxiliary array uses its single degree of freedom to point a null (a high rate of change) near the two jammers. We show this behavior in the pattern plots of Figure 5.7 for jammers at $\theta_{i1} = 40°$ and $\theta_{i2} = 39°$. Both the level and the slope of the weighted auxiliary pattern nearly match that of the mainbeam sidelobe at $\theta = 40°$. The fact that the auxiliary pattern matches the mainbeam response where the auxiliary pattern has a null causes the resultant weight magnitudes to be high. The adapted pattern is then dominated by the shape of the weighted auxiliary array.

While the resolution problems in this instance result in only a few dB degradation in SINR over a small angular region, the effect on adapted pattern ASLL is again much worse. Figure 5.8 shows the increase in ASLL as θ_{i2} is scanned. An increase of at least 10 dB is evident for all θ_{i2} within 20° of θ_{i1}, again due to the increase in weight magnitude.

To provide better performance against closely spaced jammers, the resolution of the auxiliary array must be increased. We have seen that simply increasing the distance between auxiliary elements, while it definitely improves the resolution, results in an inability to cancel jammers at particular combinations of arrival angles. To increase the auxiliary array size without introducing grating lobes requires the addition of more degrees of freedom (i.e., more auxiliary elements). Using more adjacent elements does little to improve the resolution unless a large number of auxiliaries are added. Therefore, we next consider a configuration using a number

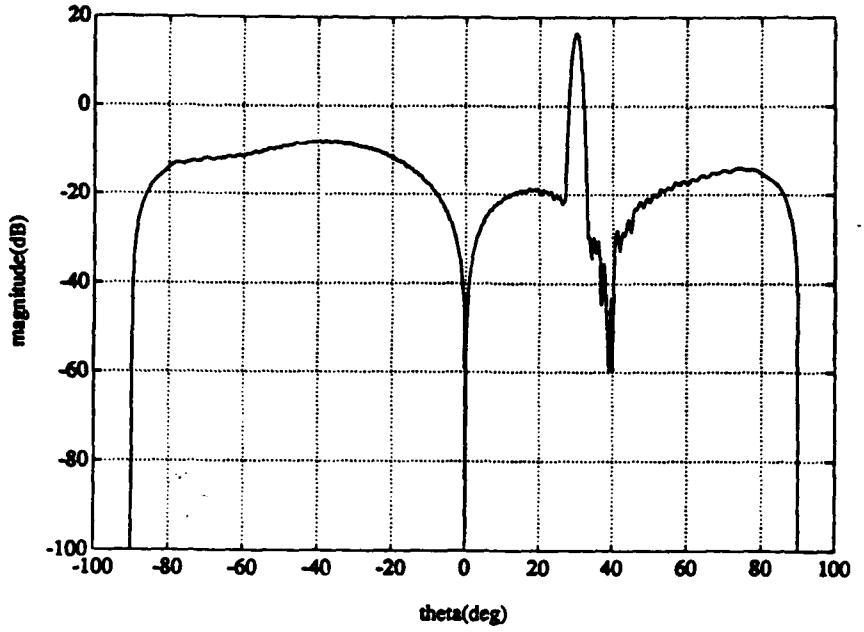

(a)

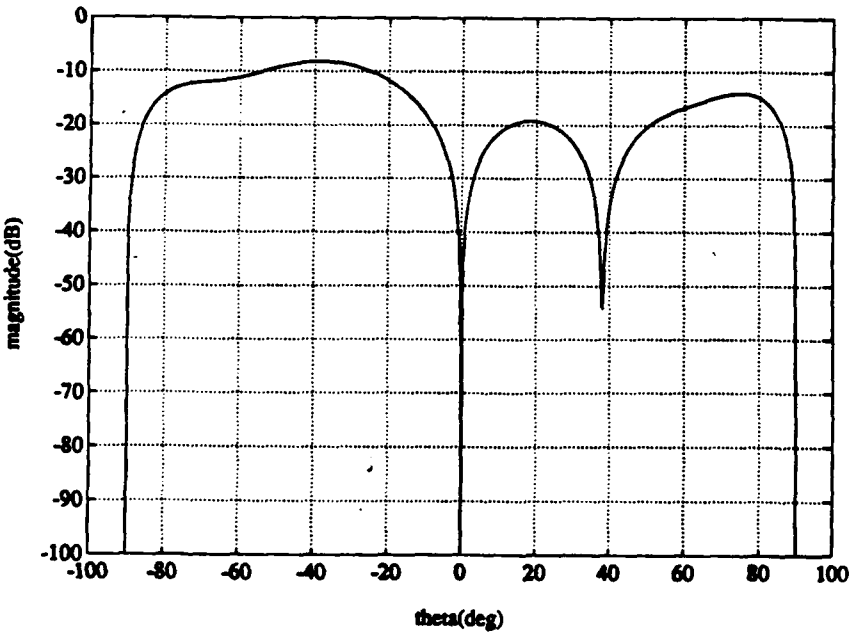

(b)

Figure 5.7: Patterns resulting from the SLC with elements (1,1) and (2,1) as the auxiliaries, in the presence of two closely spaced 40 dB CW jammers: $\theta_{i1} = 40°$, $\theta_{i2} = 39°$. (a) Adapted pattern (b) Weighted auxiliary pattern

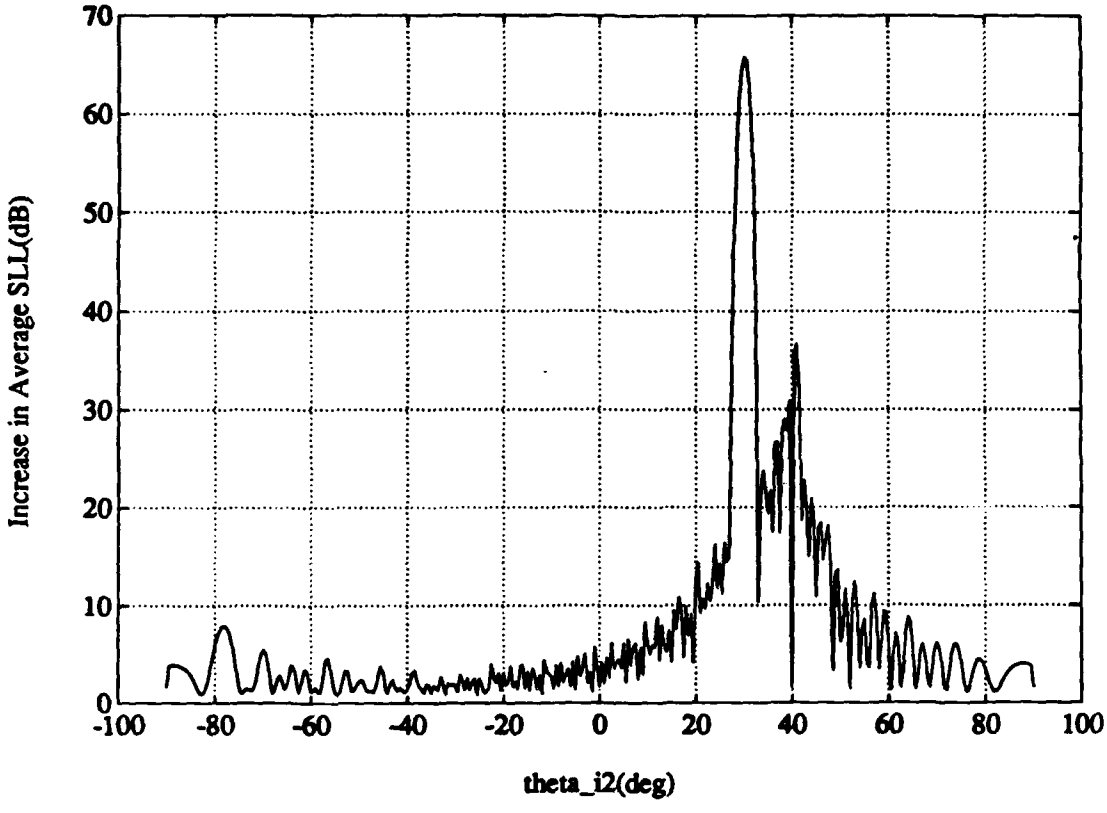

Figure 5.8: Increase in ASLL from the SLC using elements (1,1) and (2,1) as auxiliaries. Two 40 dB jammers incident, $\theta_{i1} = 40°$.

of unequally spaced auxiliary elements.

Consider a sidelobe canceller with five auxiliaries, using elements (1,1), (2,1), (14,1), (47,1), and (100,1) of the array. Although the pattern of such an auxiliary array is not periodic, it will exhibit some grating lobe behavior because individual pairs of auxiliary elements are separated by distances larger than $\lambda_0/2$. In general, unequally spaced arrays least susceptible to grating lobe problems are those where each two element subset of auxiliary elements produces a pattern with a different period, and where none of the auxiliary element pairs result in patterns with periods which are integer multiples of the period resulting from some other auxiliary element pair. The pair of auxiliary elements that contributes most to the auxiliary array pattern in a specific instance depends on the weight magnitudes.

Figure 5.9(a) shows the SINR resulting from the above array as a function of θ_{i2}. There are two 40 dB CW jammers, one whose location is fixed at $\theta_{i1} = 40°$, and a second whose arrival angle is varied. The weighted auxiliary array is able to match the mainbeam response at both jammer angles of arrival, even when the jammers are close together. The SINR shows no noticeable degradation for $\theta_{i2} \sim \theta_{i1}$.

Although the SINR obtained using this unequally spaced array of auxiliaries is excellent, the adapted pattern sidelobe level is not. Figure 5.9(b) shows the increase in ASLL (relative to the mainbeam ASLL) for this same auxiliary configuration. The adapted pattern ASLL is at least 15 dB than the mainbeam ASLL for all θ_{i2} in the sidelobe region. When two adjacent auxiliaries were used, such large degradation occured only when the two jammers were close together. The reason for this SLL degradation is again the noise correlation due to element reuse. In this example we are adapting on five auxiliaries to suppress two CW jammers. Thus

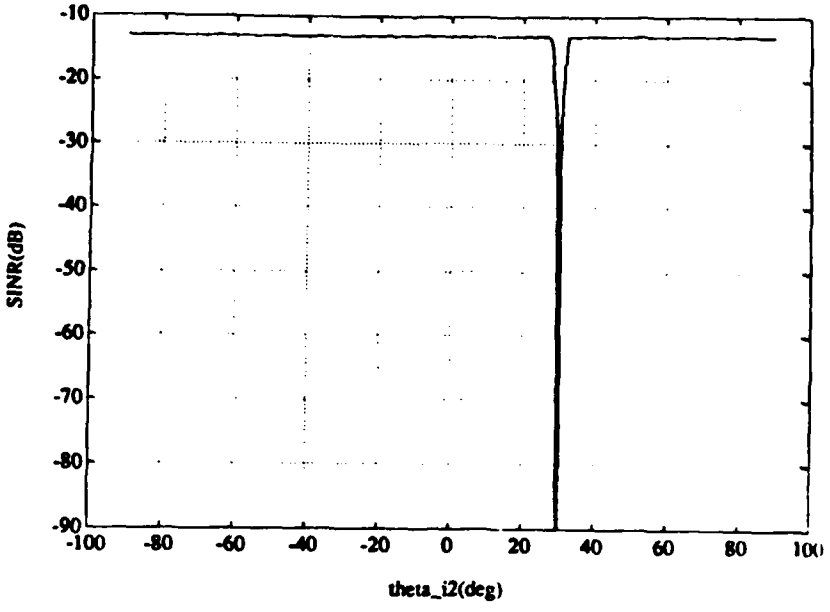

(a)

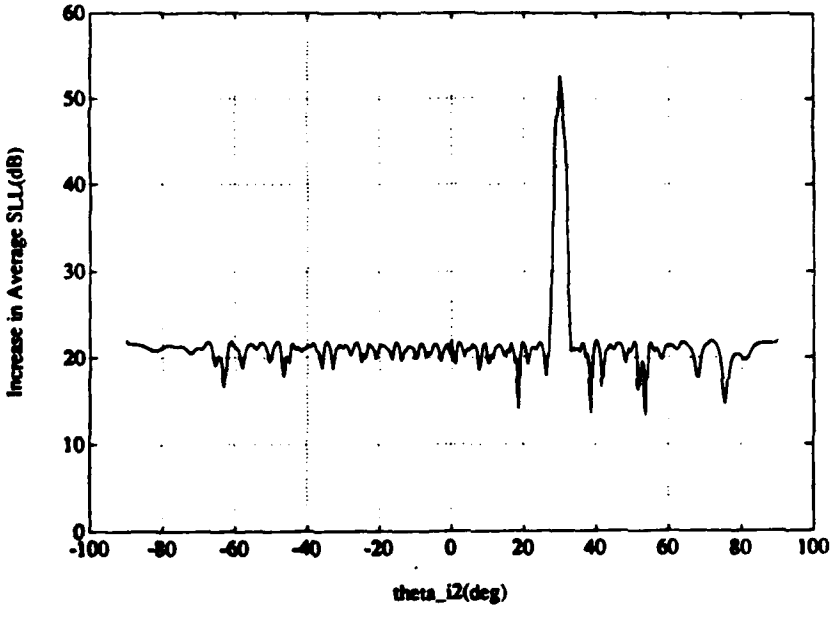

(b)

Figure 5.9: Performance of a SLC using an unequally spaced auxiliary array of five auxiliaries: elements (1,1),(2,1),(14,1),(47,1), and (100,1). Two 50 dB CW jammers are incident, with $\theta_{i1} = 40°$. (a) SINR (b) Increase in ASLL.

there are three unused degrees of freedom, which allow the array to minimize output P_n as well as cancel the jammers. This behavior has been described before both for a single auxiliary and no interference, and for a single jammer and two auxiliaries. To understand this behavior when there are several extra degrees of freedom, we examine the weighted auxiliary pattern. If there is no jamming present, output P_n is minimized by the auxiliary element weights taking values equal to the negatives of the corresponding mainbeam combiner weights. The weighted auxiliary pattern that minimizes output P_n therefore also has a *maximum* in the desired signal direction. Since only a small fraction of the total number of array elements are used for auxiliaries and the auxiliary weights are determined by the mainbeam combiner weights, the sidelobes and grating lobes of the weighted auxiliary pattern will be higher than the mainbeam SLL. Thus the adapted pattern in the sidelobe region will be dominated by the weighted auxiliary pattern. When jammers are present and the array has several extra degrees of freedom, the weighted auxiliary pattern matches the mainbeam response at the jammer directions while also retaining the characteristics of the pattern which minimizes output P_n. As a result, the jammers are nulled and the output noise power is slightly reduced, but the adapted pattern SLL is seriously degraded. For N CW jammers, adding more auxiliaries(more than N) only serves to improve cancellation performance when either auxiliary array resolution or grating lobes are a limiting factor. The cancellation is improved at the expense of the adapted pattern SLL. Other configurations using unequally spaced auxiliary arrays were also examined, and they yielded essentially the same results.

In this chapter we have examined sidelobe canceller configurations using multiple auxiliary elements. Two main conclusions have become evident. First, the perfor-

mance of a multiple auxiliary configuration against non-zero bandwidth jammers depends on the delays between auxiliary element signals as seen by the jammers. If these delays are small such that large weight magnitudes are required to suppress the jammers, optimum SINR is achieved by compromising the jammer cancellation. The adapted pattern SLL is also degraded by the large weight magnitudes. However, the performance of a TDL on a single auxiliary does not depend on the individual weight magnitudes. The cancellation and SLL performance of a TDL on a single auxiliary is better than that of a multiple auxiliary configuration when the delays are small. Second, large SLL degradation occurs whenever the number of auxiliaries exceeds the number necessary to cancel the jammers. This SLL degradation occurs even though jammer cancellation may be excellent. This behavior occurs because the unused degrees of freedom respond to the correlation between the thermal noise in the auxiliary signals and the mainbeam signal. Extra degrees of freedom are, however, needed to cancel multiple jammers over a range of angles while avoiding grating lobe and resolution problems. Thus to provide sufficient cancellation performance while at the same time retaining the mainbeam SLL, the noise correlation between mainbeam and auxiliary signals must be reduced.

6. Auxiliary Signals from Multiple Elements

6.1 Introduction

Up to this point we have considered only sidelobe canceller configurations where the auxiliary signals are formed from single elements. Such configurations are able to cancel single and multiple jammers, but are not always able to do so while retaining the low sidelobe structure of the mainbeam. In this chapter we consider auxiliary signals formed from combinations of array elements. We shall show that simple combinations of elements which satisfy an orthogonality condition between the mainbeam and auxiliary combiner vectors can be used to overcome the SLL degradation evident when there are more degrees of freedom than necessary. We shall also consider cases where the orthogonality condition is satisfied by auxiliaries formed from subarrays with directional beams. (For this purpose, we use subarrays of adjacent elements, so the individual auxiliary patterns will be free of grating lobes.) Directional beams pointed in the directions of interfering signals result in smaller adaptive weights, and have less of an effect on the adapted pattern away from the interference directions.

We shall first discuss the idea of orthogonality between mainbeam and auxiliary combiners. Then we show how both simple combinations of elements and directional auxiliary beams can be formed that satisfy this condition, and we give some examples. The configurations that perform best with respect to both SINR and ASLL in an environment of multiple CW jammers are those that use directive auxiliary beams formed from different subarrays. We then examine the performance of these configurations with non-zero bandwidth jammers. We show that tapped

delay lines on the individual auxiliary beam signals are necessary to maintain the same performance as with CW jammers. Without tapped delay lines, the pattern differences between different auxiliaries result in large weight magnitudes and the ASLL degrades.

6.2 Mainbeam-auxiliary orthogonality

Because the auxiliary signals and the mainbeam signal are formed from the same element signals, the noise components of the mainbeam and auxiliary signals are correlated. In the absence of interfering signals, the SLC with single element auxiliaries responds to this noise correlation by setting the adaptive weight on each auxiliary to the negative of the corresponding mainbeam combiner weight, so that output thermal noise is minimized. The adapted pattern then does not retain the low sidelobes of the mainbeam pattern. When interfering signals are present and the SLC has more degrees of freedom than necessary to cancel the jammers, the extra degrees of freedom are used to minimize output P_n. The auxiliary weights are chosen to match both the jammer and noise components of the mainbeam signal. Large weight magnitudes are required to match the noise component, and the result is that the adapted pattern is dominated by the shape of the weighted auxiliary array pattern.

Eliminating the mainbeam-auxiliary noise correlation makes the array respond solely to the incident signals (and not to thermal noise). In [4], it was shown that the noise component of the mainbeam-auxiliary correlation vector V, will be zero

if we impose the following condition on the auxiliary combiner weights:

$$\sum_{i=1}^{N_x}\sum_{j=1}^{N_y}(A_{ij}^{\alpha})^{*}M_{ij}=0. \tag{6.1}$$

(See Equation (2.33).) The $M_{i,j}$ are the mainbeam combiner weights (the Chebyshev amplitude taper plus the beam steering), and the $A_{i,j}^{\alpha}$ are the auxiliary combiner weights for the α^{th} auxiliary signal. Equation (6.1) may be written in vector form by defining

$$\mathbf{A}^{\alpha}=\begin{bmatrix} A_{1,1}^{\alpha} \\ \vdots \\ A_{N_x,1}^{\alpha} \\ A_{1,2}^{\alpha} \\ \vdots \\ A_{N_x,2}^{\alpha} \\ \vdots \\ A_{1,N_y}^{\alpha} \\ \vdots \\ A_{N_x,N_y}^{\alpha} \end{bmatrix}, \quad \mathbf{M}=\begin{bmatrix} M_{1,1} \\ \vdots \\ M_{N_x,1} \\ M_{1,2} \\ \vdots \\ M_{N_x,2} \\ \vdots \\ M_{1,N_y} \\ \vdots \\ M_{N_x,N_y} \end{bmatrix}. \tag{6.2}$$

Then Eq. (6.1) is then an orthogonality condition between the vectors $\mathbf{A}^{\alpha}$ and M,

$$(\mathbf{A}^{\alpha})^{H}\mathbf{M}=0 \quad . \tag{6.3}$$

If Eq. (6.3) is satisfied by all the auxiliaries, the weights will be zero in the absence of any incident signals and the quiescent pattern will be undisturbed.

For auxiliary signals formed from a single element, the $A_{i,j}^{\alpha}$ are non-zero for only one (i,j) pair. Obviously the orthogonality condition cannot be satisfied in this case. To meet Eq. (6.3) we must form each auxiliary signal from two or more

elements. As an example, consider a sidelobe canceller with two auxiliary signals, one formed from elements (49,1) and (50,1), and the other from elements (51,1) and (52,1) of the 100×1 array. The mainbeam combiner weights on these elements are

$$M_{49,1} = 0.159989595 \ , \ M_{50,1} = -j0.160354361 \tag{6.4}$$

$$M_{51,1} = -0.160354361 \ , \ M_{52,1} = +j0.159989595 \ . \tag{6.5}$$

The orthogonality condition can be satisfied by choosing the auxiliary combiner weights as

$$A^1_{49,1} = 1.0 \ , \ A^1_{50,1} = j\frac{|M_{49,1}|}{|M_{50,1}|} \tag{6.6}$$

$$A^2_{51,1} = \frac{|M_{49,1}|}{|M_{50,1}|} \ , \ A^2_{52,1} = j \ , \tag{6.7}$$

and all the other $A^\alpha_{i,j}$ $(\alpha = 1,2)$ to be zero.

Let us call this auxiliary configuration $C1$. Let us compare the performance of $C1$ with that of the configuration used in Figure 5.1 (elements (50,1) and (51,1) used as the two auxiliaries), which we refer to as $C2$. A single CW jammer with input INR of 40 dB is incident, and its arrival angle is varied. The resulting SINR and ASLL increase are plotted in Figure 6.1. The SINR curves are flat for both $C1$ and $C2$ for θ_{j1} outside of the main lobe, indicating that both configurations suppress a sidelobe jammer with a negligible difference in the thermal noise power at the output. However, $C1$ and $C2$ do not have the same ASLL performance. $C1$, whose auxiliary signals meet the orthogonality condition, results in nearly 20 dB better ASLL than $C2$ for jammer arrival angles away from the main lobe. In addition, because the noise correlation between the mainbeam signal and the auxiliaries of $C2$ is zero, the auxiliaries of $C2$ respond solely to the jamming and provide better

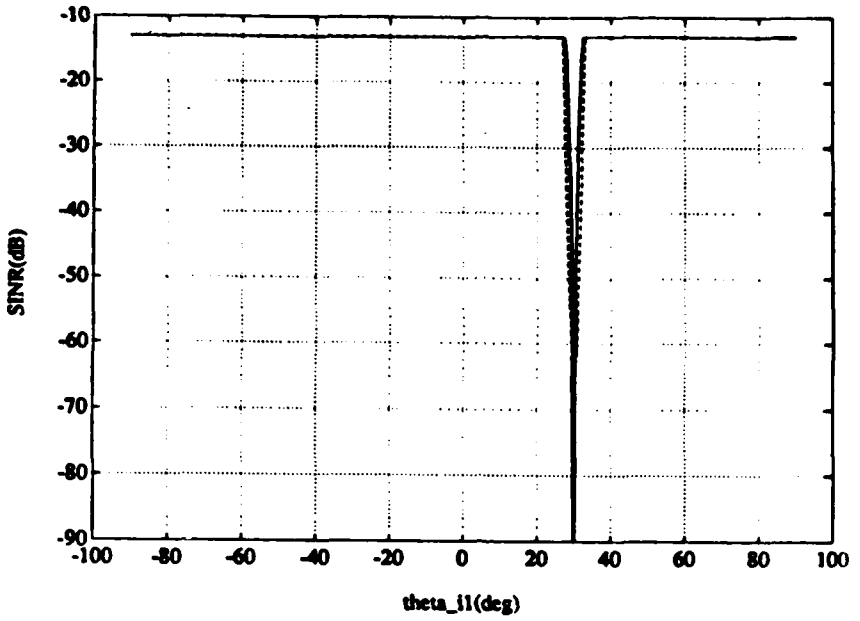

(a)

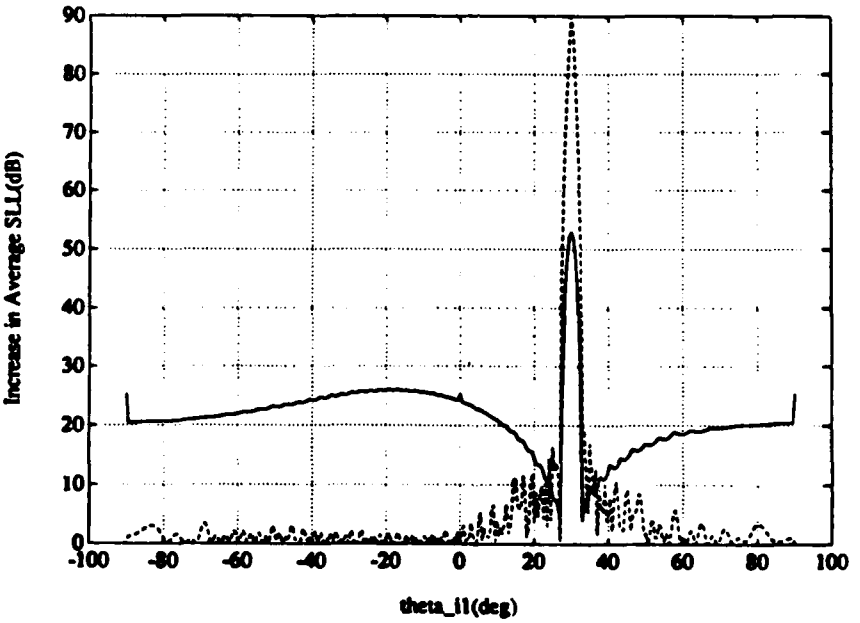

(b)

Figure 6.1: Comparison between a SLC with two 2-element auxiliary signals satisfying the orthogonality condition (solid line) and a configuration using (50,1) and (51,1) as the two auxiliary elements (dashed line). (a) SINR (b) Increase in Average SLL.

cancellation than the single element auxiliaries of $C1$.

Figure 6.1 also shows that the ASLL for $C1$ rises as the jammer angle approaches the desired signal arrival angle. When the jammer is in the main lobe, the ASLL is much higher for $C1$ than for $C2$. This behavior occurs because the patterns of the two element auxiliaries of $C1$ have nulls near the desired signal direction. Thus when the jammer is close to the main lobe, it is also on a skirt of the null of the auxiliary pattern. The weight magnitudes required to null a jammer in the main lobe are much larger for $C1$ and cause the increased degradation in ASLL. For this same reason configuration $C1$ is unable to provide much cancellation when the jammer is in the main lobe. Because the auxiliaries of $C1$ are formed from only two elements, the skirts of their pattern null are fairly wide and performance is affected over a fairly wide range of angles centered at the desired signal arrival angle. By using more than two elements for each auxiliary, we can improve the performance for arrival angles near the mainlobe of the mainbeam.

Suppose we use a subarray of N adjacent elements, beginning with element $(L,1)$, to form an auxiliary signal. All but N entries in the $\mathbf{A}^a$ vector of Eq. (6.2) are zero, and the orthogonality condition reduces to an N-dimensional inner product. We define the auxiliary and mainbeam *subarray* combiner vectors to be

$$\mathbf{A}_s^a = [A_{L,1}^a,\ A_{L+1,1}^a,\ \ldots,\ A_{L+N-1,1}^a]^T \tag{6.8}$$

and

$$\mathbf{M}_s = [M_{L,1},\ M_{L+1,1},\ \ldots,\ M_{L+N-1,1}]^T\ . \tag{6.9}$$

Then Eq. (6.3) becomes

$$(\mathbf{A}_s^a)^H \mathbf{M}_s = \mathbf{M}_s{}^H \mathbf{A}_s^a = 0\ . \tag{6.10}$$

Since $\mathbf{A}_s^\alpha$ and $\mathbf{M}_s$ are members of an N-dimensional complex vector space, there exists $N-1$ mutually orthogonal $\mathbf{A}_s^\alpha$ which are orthogonal to $\mathbf{M}_s$. To discuss how the $\mathbf{A}_s^\alpha$ should be chosen we first discuss the concept of orthogonal directions of arrival.

Define the direction vector $\mathbf{X}_d$ to be the vector of signals received on an $N \times 1$ linear array(or subarray) of isotropic elements, when a single narrowband signal of unit amplitude is incident from direction θ_d.

$$\mathbf{X}_d = [1,\ e^{j\pi \sin\theta_d},\ e^{j2\pi \sin\theta_d},\ \ldots,\ e^{j(N-1)\pi \sin\theta_d}]^T\ . \tag{6.11}$$

$\mathbf{X}_d$ is an N-dimensional vector parameterized by the angle θ_d. For half-wavelength interelement spacing and θ_d in the visible region ($-90° \leq \theta_d \leq 90°$), there is a one-to-one correspondence between angles θ_d and vectors $\mathbf{X}_d$. A uniformly weighted combiner vector $\mathbf{M}_s = \mathbf{X}_d^*$ on these elements would produce a beam steered to the θ_d direction. We define the directions orthogonal to θ_d to be the angles θ_α that produce direction vectors $\mathbf{X}_\alpha$ orthogonal to $\mathbf{X}_d$, satisfying

$$\mathbf{X}_d^H \mathbf{X}_\alpha = 0\ , \tag{6.12}$$

where

$$\mathbf{X}_\alpha = [1,\ e^{j\pi \sin\theta_\alpha},\ e^{j2\pi \sin\theta_\alpha},\ \ldots,\ e^{j(N-1)\pi \sin\theta_\alpha}]^T\ . \tag{6.13}$$

Using $\mathbf{M}_s = \mathbf{X}_d^*$, we can write Eq. (6.12) as

$$\mathbf{M}_s{}^T \mathbf{X}_\alpha = 0\ , \tag{6.14}$$

which says that the directions orthogonal to θ_d are those where the uniformly weighted pattern steered to θ_d has nulls.

We can find the θ_α from Eq. (6.12), which is equivalent to

$$\sum_{m=1}^{N} e^{j(m-1)u} = 0 \,, \tag{6.15}$$

where $u = \pi(\sin\theta_\alpha - \sin\theta_d)$. This equation simplifies to

$$\frac{\sin(\frac{N}{2}u)}{\sin\frac{u}{2}} = 0 \,, \tag{6.16}$$

which has solutions $u = \frac{2}{N}k_\alpha\pi$, for integers $k_\alpha \neq 0$. The orthogonal directions are then given by

$$\sin\theta_\alpha = \frac{2}{N}k_\alpha + \sin\theta_d \,, \tag{6.17}$$

where

$$-\frac{N}{2}(1+\sin\theta_d) \leq k_\alpha \leq \frac{N}{2}(1-\sin\theta_d) \tag{6.18}$$

and $\alpha = 1, \ldots, N-1$. Because we have assumed subarrays of adjacent elements (no grating lobes), there will be $N-1$ distinct non-zero integers satisfying Eq. (6.18), and thus $N-1$ orthogonal directions resulting from Eq. (6.17), corresponding to $N-1$ mutually orthogonal direction vectors also orthogonal to $\mathbf{X}_d$.

If the mainbeam were formed using a uniform aperture taper and steered to θ_d, a particular ($\alpha = j$) auxiliary subarray combiner vector $\mathbf{A}_s^j = \mathbf{X_j}^*$ on an N element subarray will be orthogonal to the mainbeam combiner. This auxiliary beam will have a pattern maximum in the θ_j direction and pattern nulls in the desired signal direction and in the other orthogonal directions θ_α for $\alpha \neq j$. Auxiliary patterns with nulls in the desired signal direction are desirable because the canceller is then unaffected by the presence of the desired signal, and the weighted auxiliaries will not affect the gain in the desired signal direction(the mainbeam gain). Because these auxiliary beams also satisfy Eq. (6.3), the noise signals in the mainbeam and

in the auxiliaries are uncorrelated. The adaptive array in this case will respond solely to the interfering signals.

Our interest, however, is in a mainbeam with a non-uniform amplitude taper, steered to a known direction θ_d. An N element subarray of a non-uniformly weighted mainbeam, beginning with element $(L,1)$, has a subarray combiner vector of the form

$$\mathbf{M}_s = e^{-j\pi(L-1)\sin\theta_d}[m_{L,1},\ m_{L+1,1}e^{-j\pi\sin\theta_d},\ \ldots,\ m_{L+N-1,1}e^{-j\pi(N-1)\sin\theta_d}]^T \quad (6.19)$$

where the $m_{L+i,1}$ are the Dolph-Chebyshev weights required for a broadside array. The $m_{L+i,1}$ are real and positive. In this case we can also satisfy the mainbeam-auxiliary orthogonality condition by steering the auxiliary beams to the directions θ_α, given in Eq. (6.17), orthogonal to the mainbeam direction. Let the auxiliary subarray combiner vectors be specified as

$$\mathbf{A}_s^\alpha = [a_{L,1}^\alpha,\ a_{L+1,1}^\alpha e^{-j\pi\sin\theta_\alpha},\ \ldots,\ a_{L+N-1,1}^\alpha e^{-j\pi(N-1)\sin\theta_\alpha}]^T\ . \quad (6.20)$$

The inner product $\mathbf{M}_s{}^H\mathbf{A}_s^\alpha$ is then given by

$$\mathbf{M}_s{}^H\mathbf{A}_s^\alpha = e^{j\pi(L-1)\sin\theta_d}\sum_{k=L}^{L+N-1} m_{k,1}a_{k,1}^\alpha e^{j\pi(k-L)(\sin\theta_d-\sin\theta_\alpha)}\ . \quad (6.21)$$

Eq. (6.3) is satisfied if the $a_{k,1}^\alpha$ are chosen such that

$$a_{k,1}^\alpha = \frac{\kappa}{m_{k,1}}\ ,\ k = L, L+1, \ldots, L+N-1\ , \quad (6.22)$$

where κ is an arbitrary constant and $\alpha = 1, \ldots, N-1$. Note that the size N of the subarray determines the number of orthogonal directions and thus the number of auxiliaries one can use, assuming the auxiliaries will be chosen to satisfy Eq. (6.3) according to Eqs. (6.20) and (6.22) above.

Because of the nonuniform mainbeam amplitude taper, the amplitude distribution on an auxiliary beam formed according to Eq. (6.22) is also nonuniform. (For small subarrays at the center of the array where the mainbeam Chebyshev taper is nearly uniform, the auxiliary amplitude distribution will also be nearly uniform.) The nonuniform amplitude taper on an auxiliary beam has several implications. First, a given auxiliary, although orthogonal to the mainbeam combiner, does not have a perfect pattern null in the desired signal direction (as in the uniform case) but rather a pattern minimum. Second, if we use the same subarray to form $N-1$ auxiliaries, we obtain a set of auxiliary beams where each beam has the same nonuniform amplitude taper and each beam is steered to a different orthogonal direction. (Eq. (6.17)) These auxiliaries, while orthogonal to the mainbeam combiner, are no longer mutually orthogonal. As a result, a particular auxiliary beam has its pattern maximum in the orthogonal direction to which it was steered, but no longer has perfect nulls in the θ_d direction nor in the other orthogonal directions.

In general, the $N-1$ $\{\mathbf{A}_s^a\}$ are linearly independent and thus span the $N-1$ dimensional subspace orthogonal to $\mathbf{M}_s$. Therefore, any linear combination of the $\{\mathbf{A}_s^a\}$ will produce an auxiliary subarray combiner that is orthogonal to the mainbeam combiner. However, there are reasons why the $\mathbf{A}_s^a$ themselves should be chosen. First, they produce auxiliary beams with known patterns. Forming $N-1$ auxiliary beams from a subarray using the complete set of the $\{\mathbf{A}_s^a\}$ results in a set of overlapping auxiliary beams which cover all of visible space except for angles near the mainbeam scan angle. At least one auxiliary beam will have its maximum near a given jammer arrival angle anywhere outside of the mainbeam region. This property generally results in good sidelobe canceller performance because the weight

magnitudes are small.

Second, the orthogonal directions (Eq. (6.17)) depend on the direction to which the mainbeam is steered(θ_d). In practice, this direction will change as the radar searches some specified region of space. A fixed auxiliary combiner that is orthogonal to the mainbeam combiner at one value of θ_d will not be orthogonal to the mainbeam for other scan angles. As a result, the adapted pattern ASLL will increase at mainbeam scan angles where mainbeam-auxiliary orthogonality is not satisfied. To maintain orthogonality for a range of mainbeam scan angles requires the ability to reconfigure the auxiliary subarray combiners. With the auxiliary signals formed from the $\mathbf{A}_s^a$ of Eq. (6.20), this reconfiguration only involves recomputing the directions orthogonal to θ_d and adjusting the phase factors of $\mathbf{A}_s^a$ accordingly. The magnitudes of the individual auxiliary combiner components remain fixed. An arbitrary auxiliary combiner orthogonal to the mainbeam for one scan angle will need to have both the magnitude and phase factors reconfigured for every mainbeam scan angle.

6.3 Steered beam auxiliaries using subarrays of the mainbeam

In this section we consider SLC configurations using auxiliary beams steered to directions orthogonal to the mainbeam direction. We consider only auxiliary signals formed from subarrays of adjacent elements to ensure that there are no grating lobes in the individual auxiliary patterns. The auxiliary combiner weights are chosen as in Eq. (6.22) to meet the mainbeam-auxiliary orthogonality condition of Eq. (6.3). Note that this condition prevents the weight magnitudes from increasing because of thermal noise correlation between the mainbeam and auxiliary signals, but the

weight magnitudes may also become large if the auxiliary pattern has a response in the jammer direction smaller than that of the mainbeam. By using a system of multiple auxiliary beams overlapping most of visible space we assure that at least one auxiliary has a maximum in a given jammer direction (outside of the mainbeam region). We will not examine cases for every possible subarray size. Our interest is in providing the auxiliary beams with enough directivity so that the resulting adaptive weight magnitudes are small for all jammer angles of arrival.

The selection of subarrays to form these multiple beams involves many of the same trade-offs encountered when selecting locations for single-element auxiliary signals. For example, forming multiple beams from the same subarray makes it difficult to cancel closely spaced jammers. Such a configuration also has problems with non-zero bandwidth jammers. When the auxiliary beams are all formed from the same subarray, they all have the same phase center. In this case, there is no time delay between signals received at the different auxiliaries, and the auxiliary array is unable to cancel a non-zero bandwidth jammer except at a single frequency within its bandwidth.

As an example, consider a SLC using a subarray that consists of the eight center elements, elements (47,1) through (54,1), of the array. This subarray is used to form six auxiliary beams, each orthogonal to the mainbeam combiner. The orthogonal directions are computed from Eq. (6.17) with $N = 8$ and $\theta_d = 30°$, and the auxiliary combiner weights for each beam are obtained from Eqs. (6.20) and (6.22). The resulting auxiliaries are steered to the orthogonal directions given in Table 6.1, and the individual auxiliary patterns are shown in Figure 6.2. Because the subarray is small and at the center of the array, where the mainbeam combiner weights

Auxiliary	Beam steering angle
1	90.°
2	48.5903779°
3	14.4775122°
4	-14.4775122°
5	-30.°
6	-48.5903779°

Table 6.1: Auxiliary beams for the example of Figures 6.2-6.4

are nearly uniform in magnitude, the auxiliary combiner weights resulting from Eq. (6.22) are also approximately uniform in magnitude. Therefore, each auxiliary beam of Fig. 6.2 has a deep null in the desired signal direction and also deep nulls in the other orthogonal directions. This configuration is approximately the same as a Butler matrix beamformer[19] on the center 8 elements, with beams steered to directions orthogonal to the desired signal direction used as the auxiliaries.

The performance of this canceller in the presence of a single 40 dB CW jammer is shown in Figure 6.3. As expected, the SINR is maintained high for all jammer angles of arrival outside of the main lobe. In this region, the directive auxiliary beams result in weights which have little effect on the adapted pattern SLL. The increase over the mainbeam ASLL is less than 5 dB. Because Eq. (6.3) is satisfied by all the auxiliaries, the 5 unused degrees of freedom do not disturb the adapted pattern.

Results from a two jammer scenario are shown in Figure 6.4. We fix the location

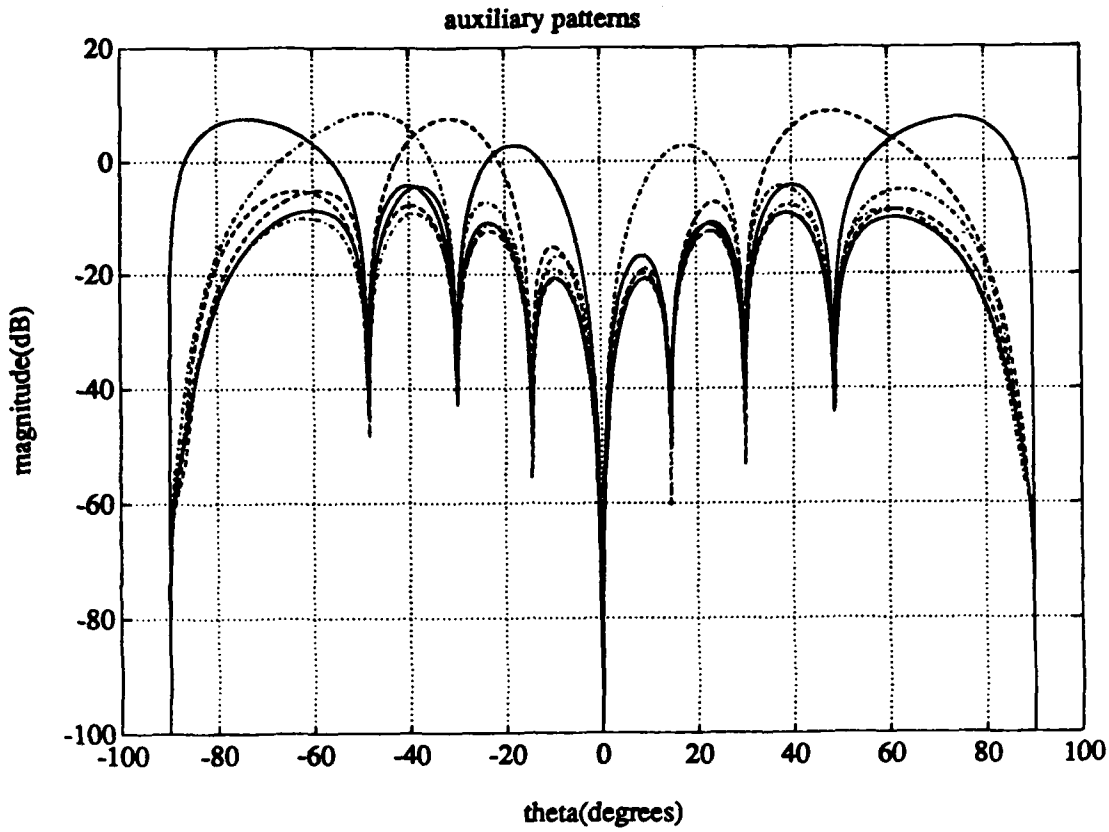

Figure 6.2: Patterns of auxiliary beams formed from an 8-element subarray, elements (47,1)-(54,1). Each auxiliary satisfies the orthogonality condition between mainbeam and combiner vectors.

of one jammer at $\theta_{i1} = 40°$ and vary θ_{i2}. For θ_{i1} near θ_{i2}, we note a large increase in ASLL after adaptation. Because all the auxiliary beams are formed from the same subarray, the auxiliary array resolution is determined by the auxiliary beam width. For jammers spaced more closely than the auxiliary beam width, large weights are required to cancel both jammers. The same problem was discussed relative to single-element auxiliary signals in Chapter 5. As with single-element auxiliary signals, the output P_i increases and cancellation ratio decreases for closely spaced jammers.

Another problem with auxiliaries that use the same subarray, or with auxiliaries using different but overlapping subarrays, is that elements shared between auxiliaries cause the noise components of different auxiliary signals to be correlated. It

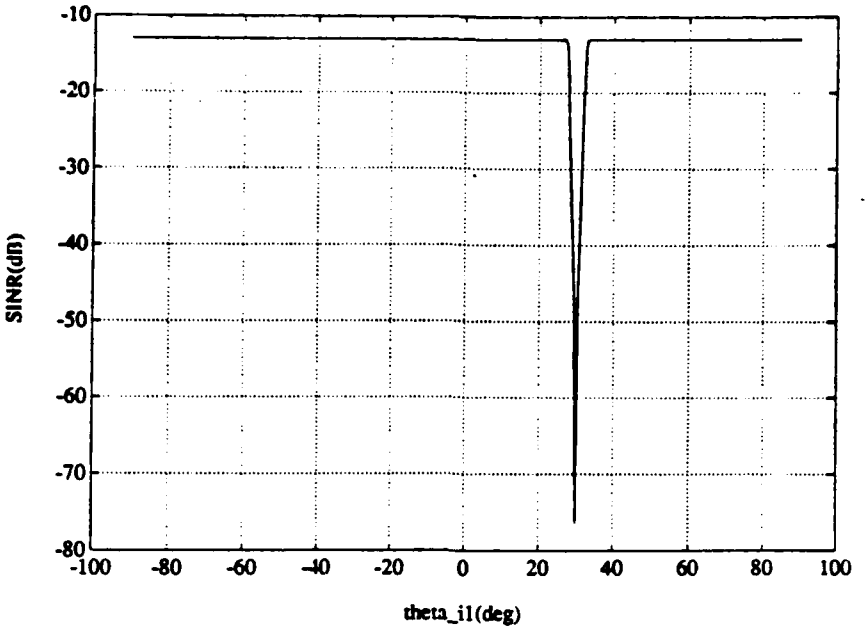

(a)

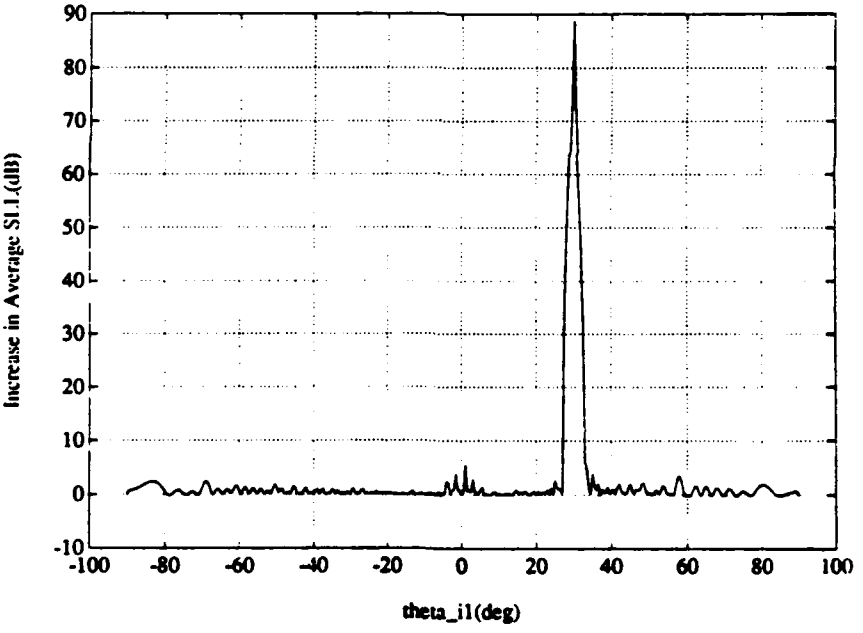

(b)

Figure 6.3: Performance with multiple beams formed from the same subarray. A single 40 dB CW jammer is incident. (a) SINR (b) Increase in Average SLL.

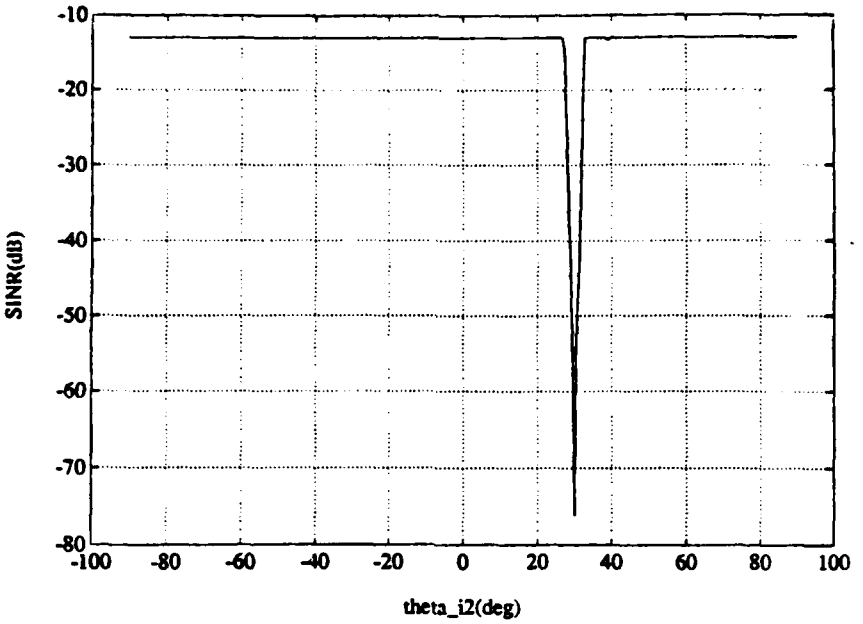

(a)

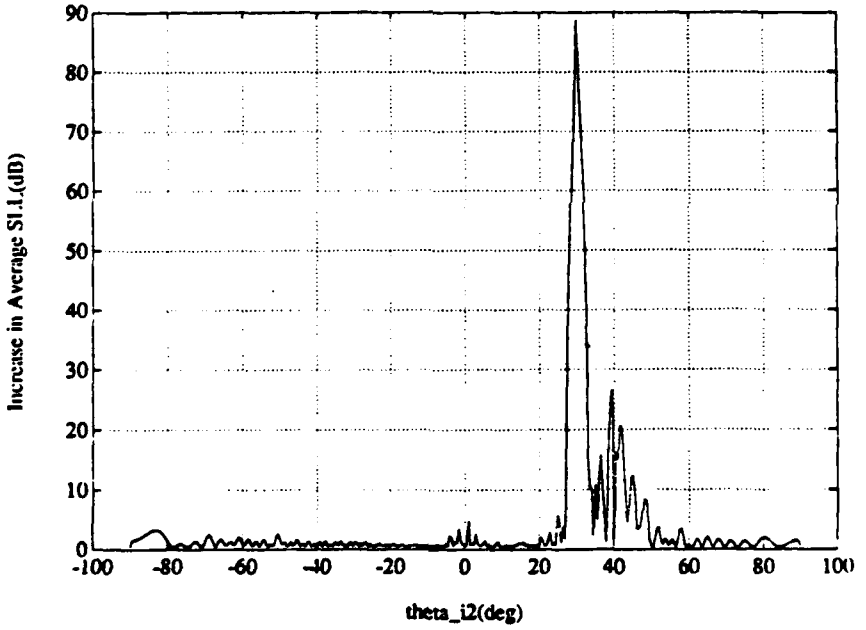

(b)

Figure 6.4: Performance with multiple beams formed from the same subarray. Two 40 dB CW jammers are incident, with $\theta_{i1} = 40°$. (a) SINR (b) Increase in Average SLL.

was shown in [4] that noise correlation between auxiliaries can be eliminated if the auxiliary combiners are mutually orthogonal, in the same sense as Eq.e:orthog.v, which if satisfied eliminates the noise correlation between the mainbeam and the auxiliaries. However, because overlapping the subarrays used for different auxiliaries does little to improve the resolution of the auxiliary array, we shall not consider SLC configurations that use overlapping subarrays. From now on, we shall only consider cases where each auxiliary is formed from a different, non-overlapping subarray.

Using different non-overlapping subarrays for each auxiliary necessarily implies that the phase centers of different subarrays be separated by more than $\lambda_0/2$. However, the wide spacing between subarrays does not result in serious grating lobe problems because the individual auxiliary patterns are all different. Now consider a canceller, again with six auxiliaries, where to overcome resolution problems the subarrays for different auxiliaries are equally spaced across the full aperture. As in the last example, each subarray consists of eight elements and each auxiliary beam is steered to a different direction orthogonal to the mainbeam. The auxiliary combiner weights for each auxiliary are obtained from Eq. (6.22). Table 6.2 lists the subarrays used. The phase centers of the adjacent subarrays are separated by $9\lambda_0$. Because the subarrays are not at the center of the array, the auxiliary combiners orthogonal to the mainbeam are nonuniform in magnitude. Thus the auxiliary patterns, shown in Figure 6.5, for this configuration do not all have sharp nulls in the desired signal direction of $\theta_d = 30°$ or in the other orthogonal directions.

The performance of this SLC when two 40 dB CW jammers are incident is given in Figure 6.6. Again we fix $\theta_{i1} = 40°$ and scan θ_{i2} across visible space. The resolution of the auxiliary array has been improved by using different subarrays

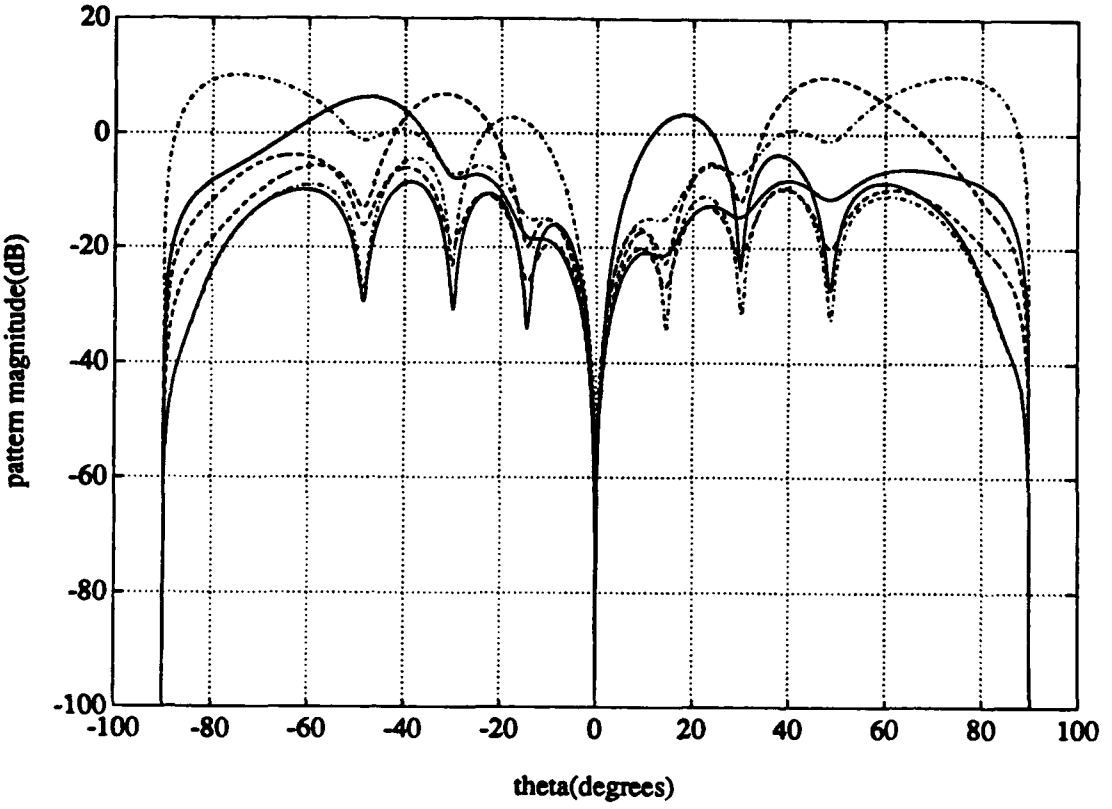

Figure 6.5: Auxiliary beams resulting from 6 equally spaced 8-element subarrays, each orthogonal to the mainbeam.

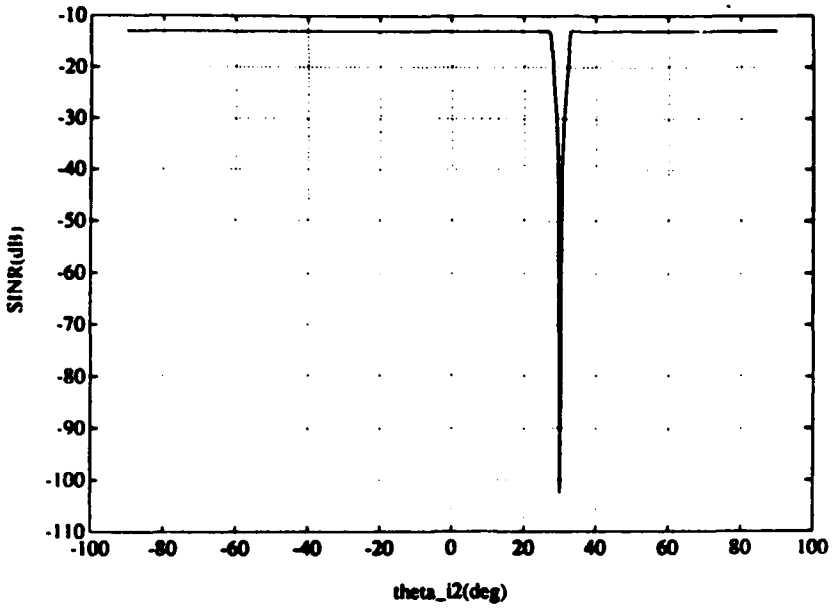

(a)

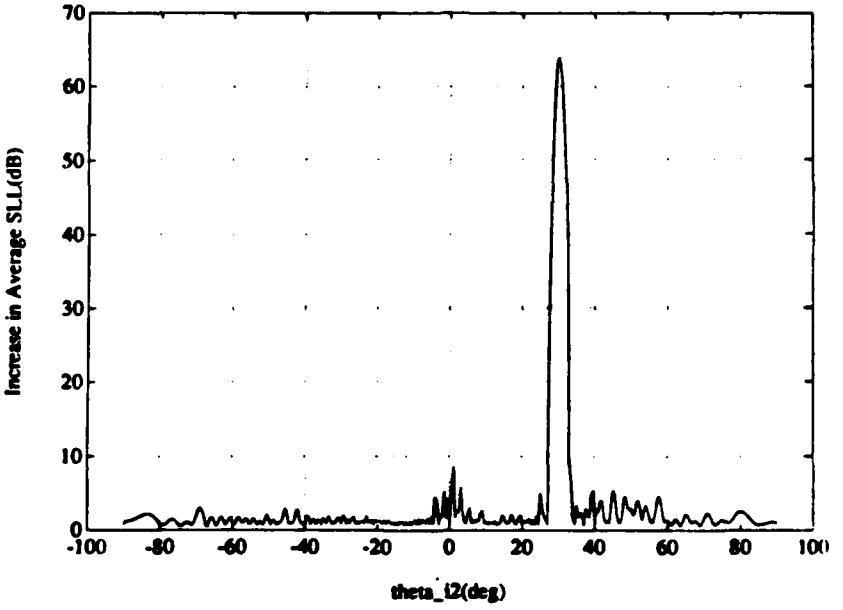

(b)

Figure 6.6: Performance of a SLC using 6 equally spaced subarrays for the auxiliaries. Two 40 dB CW jammers, $\theta_{i1} = 40°$.(a) SINR (b) Increase in Average SLL.

Auxiliary	Subarray	Beam steering angle
1	(2,1)-(9,1)	-48.5903779°
2	(20,1)-(27,1)	-14.4775122°
3	(38,1)-(45,1)	-30.°
4	(56,1)-(63,1)	14.4775122°
5	(74,1)-(81,1)	48.5903779°
6	(92,1)-(99,1)	90.°

Table 6.2: Subarrays used for example of Figures 6.5-6.8

for each auxiliary beam. As a result, closely spaced jammers are effectively nulled with weights of relatively small magnitude. The SINR curve shows no degradation except when θ_{i2} is in the main lobe, indicating that both jammers are significantly suppressed without a significant change in thermal noise power. The increase in ASLL due to adaptation is also well behaved. In the region where $\theta_{i1} \sim \theta_{i2}$, the increase in ASLL is less than 6 dB. This performance is much better than that obtained earlier by using either the same subarray for multiple auxiliary beams or unequally spaced arrays of single-element auxiliaries (Chapter 5).

We now examine the performance of this configuration against jammers of non-zero bandwidth. As with multiple single-element auxiliaries, a jammer sees an effective tapped delay line whose intertap delays are the jammer propagation delays between the phase centers of the different auxiliary subarrays. For multiple single-element auxiliaries, each tap on this effective TDL has the same response at a given angle of arrival (the element pattern). But when each auxiliary is formed

from a different subarray and steered to a different direction, the situation is more complicated. In this case each tap on the effective TDL has a different directional pattern. The adaptive weight magnitudes are then determined by two factors: the intertap delays and the unequal auxiliary patterns at the jammer arrival angles. (A jammer near the maximum of one of the auxiliary beams is near the minima of the other auxiliary patterns.) We have seen in Chapters 4 and 5 that the weights become large when the intertap delays are small. Unequal auxiliary patterns at the taps of a TDL force the weights to overcome the pattern differences at the jammer arrival angles, which may cause high sidelobes in the adapted pattern at angles corresponding to the auxiliary beam maxima.

Figure 6.7 shows the performance of the same SLC as in Figure 6.6 when two 60 dB jammers with fractional bandwidth $B = 0.001$ are incident. One arrival angle is fixed at $\theta_{i1} = 40°$ and the other (θ_{i2}) is scanned. The SINR, shown in Figure 6.7(a), is maintained at the level corresponding to CW jammers for all θ_{i2} outside the mainbeam. The tapped delay line formed by the different subarrays allows this configuration to cancel a jammer over a non-zero bandwidth. Other tests with this same configuration but not presented here show that SINR degradation due to bandwidth is first evident at an INR of 80 dB. Although the SINR performance is excellent, the adapted pattern SLL shows degradation when the INR=60 dB. The increase in ASLL, shown in Figure 6.7(b), is 5 dB to 15 dB higher than that obtained in Figure 6.6 for CW signals. Since the subarray spacing is $9\lambda_0$, the intertap delays are not small enough to cause exceptionally large weights. The ASLL degradation is mostly due to the weights having to overcome the auxiliary pattern differences as described above.

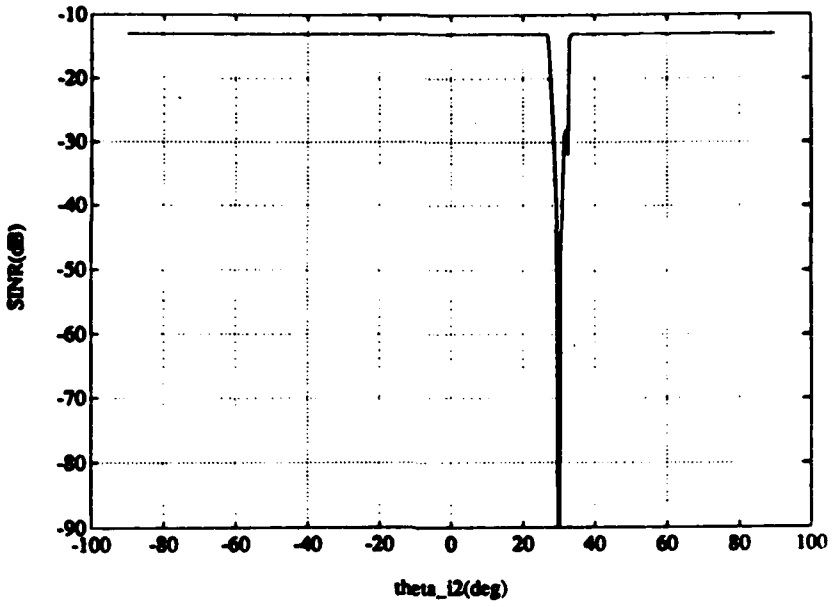

(a)

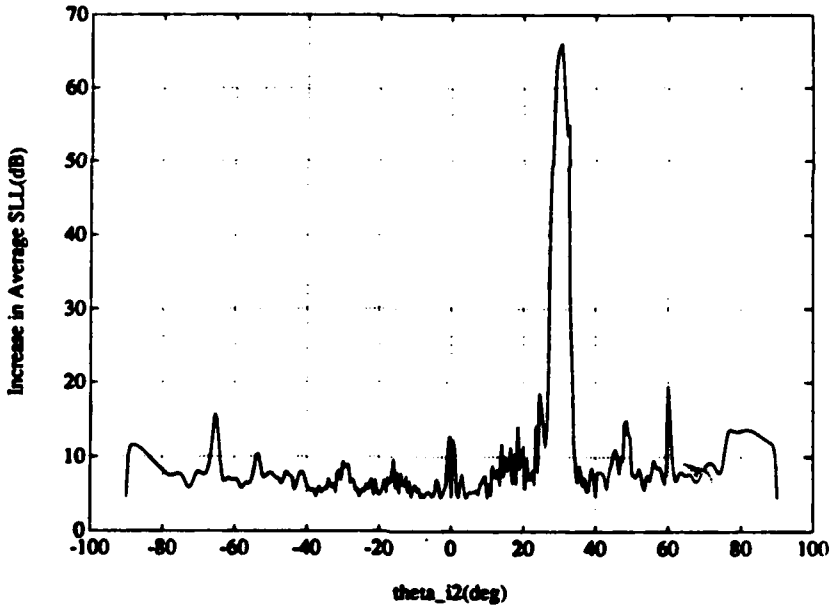

(b)

Figure 6.7: Performance of a SLC using 6 equally spaced subarrays for the auxiliaries. No TDLs. Two 60 dB jammers, $B = 0.001$, $\theta_{i1} = 40°$. (a) SINR (b) Increase in Average SLL.

The primary use of steered beam auxiliaries from equally spaced subarrays is to provide the extra degrees of freedom and resolution necessary to cancel multiple CW jammers and maintain good adapted pattern SLL performance. However, we see that this capability is somewhat reduced when these degrees of freedom are used to combat non-zero bandwidth. By providing a tapped delay line on the output of each auxiliary beam we can handle the non-zero bandwidth without using the spatial degrees of freedom. Therefore we expect a canceller with tapped delay line processing on each auxiliary to provide good ASLL performance even for jammers of non-zero bandwidth.

Now consider a configuration using the same subarrays and the same auxiliary beams as the examples of Figs. 6.6 and 6.7, but with a 2-tap TDL on the output of each beam. The intertap delay for each TDL is $24.75\lambda_0$. Figures 6.8(a) and (b) show both the SINR and ASLL performance against two 60 dB jammers with fractional bandwidth $B = 0.001$. The SINR is maintained constant for all θ_{i2} outside of the mainbeam. We can also see that the adapted pattern SLL behavior is also much better than without the tapped delay lines. Except for a slightly larger increase around $\theta_{i2} = 0°$, the ASLL behavior is identical to the CW case of Figure 6.6. Further tests with this configuration show that no SINR degradation is evident for INRs up to 90 dB. This configuration provides both adequate cancellation and excellent ASLL performance for multiple jammers of non-zero bandwidth.

Although we have only shown results for one configuration of equally spaced subarrays, many others have been examined. While there were no grating lobe problems in our example using 8-element subarrays, some grating lobe problems are present for smaller subarrays separated by larger distances within the array. Then

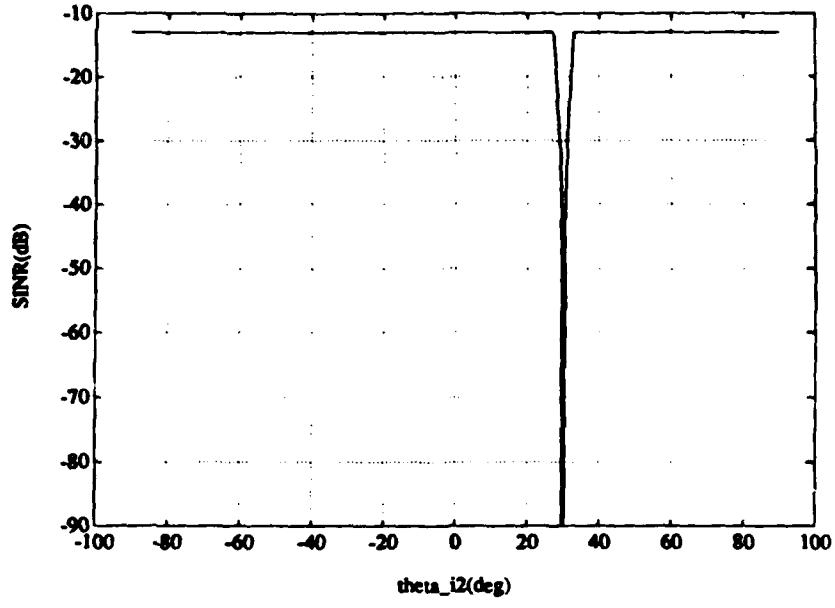

(a)

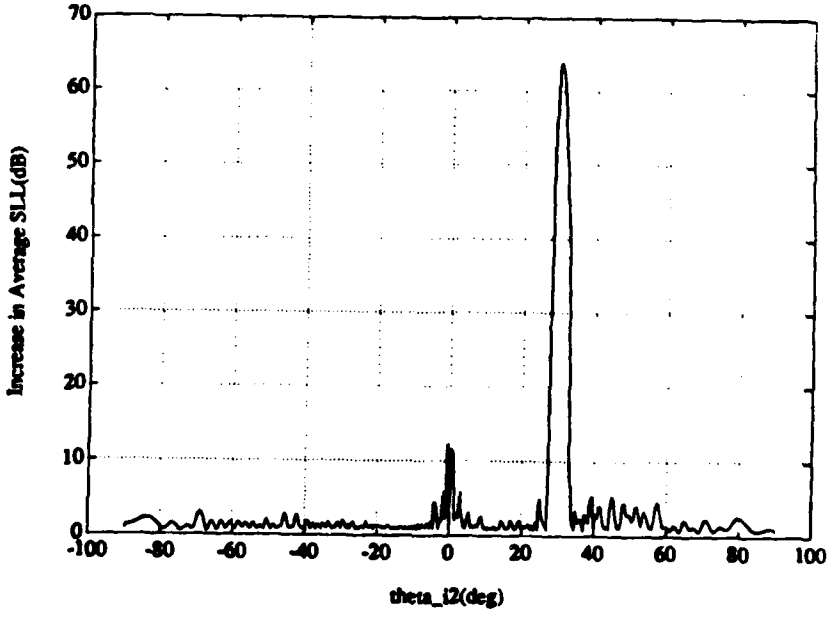

(b)

Figure 6.8: Performance of a SLC using 6 equally spaced subarrays, with a 2-tap TDL on each auxiliary beam. Two 60 dB jammers, $B = 0.001$, $\theta_{i1} = 40°$. (a) SINR (b) Increase in Average SLL.

the angular spacing between grating lobes is small, and the individual auxiliary beamwidths are larger, meaning that the auxiliary patterns have angular regions where they are nearly constant over the grating lobe spacing. Thus grating lobes will be avoided as long as the subarray size is not exceptionally small relative to the separation between subarrays.

We also examined configurations where the different subarrays were unequally spaced across the array. For configurations without TDLs on the auxiliary beam outputs, the performance (both SINR and ASLL) against non-zero bandwidth jammers was significantly worse for unequally spaced subarrays than for the equally spaced subarray case shown in Figure 6.7. This difference was most likely caused by the smaller intertap delays encountered between some of the subarrays of the unequally spaced configuration. With identical TDLs on the auxiliary beam outputs, both equally spaced and unequally spaced subarrays perform similarly.

6.4 Non-orthogonal steered beam auxiliary signals

Up to this point we have examined numerous auxiliary configurations consisting of elements that satisfy the orthogonality condition of Eq. (6.3). It was noted that to maintain good SLL performance, the auxiliaries would have to be reconfigured as the mainbeam is scanned. Since this reconfiguration may be impractical, we consider in this section some typical examples with uniformly weighted steered beam auxiliaries. Such auxiliaries are not orthogonal to the mainbeam in the sense of Eq. (6.3), and may result in SLL degradation. As with single element auxiliaries, this SLL degradation results when the number of degrees of freedom exceeds that necessary to cancel the jammers. However, with uniformly weighted steered beam auxiliaries,

SLL degradation in these cases is localized to the region of the pattern where the auxiliary beam has its pattern maximum. Thus the degradation is somewhat less severe than with single element auxiliaries, where the SLL degradation was present over the whole sidelobe region. We show that the degradation using uniformly weighted steered beam auxiliaries depends on the auxiliary beam scan angle, and decreases as the size of the auxiliary subarray is increased. We also consider some typical multiple auxiliary and multiple jammer scenarios.

First consider a SLC with one auxiliary signal. Let the auxiliary subarray consist of the center 25 elements, elements (38,1)-(62,1), of the array. The auxiliary combiner vector is chosen to be a uniformly weighted beam steered to the θ_a direction. Thus,

$$\mathbf{A}_s = [1,\ e^{j\pi \sin\theta_a},\ e^{j2\pi \sin\theta_a},\ \ldots,\ e^{j24\pi \sin\theta_a}]^T\ . \tag{6.23}$$

Figure 6.9(a) shows the auxiliary pattern for $\theta_a = -41.3°$. Figures 6.9(b)-(d) show the adapted patterns when no jammers are present as the auxiliary scan angle is varied from $\theta_a = -41.3°$ to $\theta_a = -38.2°$ and $\theta_a = -35.5°$. Figures 6.9(b) and (d) show severe SLL degradation especially around θ_a, while there is essentially zero degradation in Figure 6.9(c) where $\theta_a = -38.2°$. The reason for this behavior is that $\theta_a = -38.2°$ is one of the orthogonal directions (see Section 6.2) for a 25 element subarray, and thus the auxiliary combiner vector given by Eq. (6.23) is *nearly* orthogonal to the mainbeam combiner. In general the quiescent SLL degradation is seen to be very dependent on the auxiliary beam scan angle.

Let us now examine similar patterns for a canceller with a single auxiliary beam using the full array, elements (1,1)-(100,1). Again let there be no jammers present. Figure 6.10 shows the mainbeam pattern and adapted patterns resulting for several

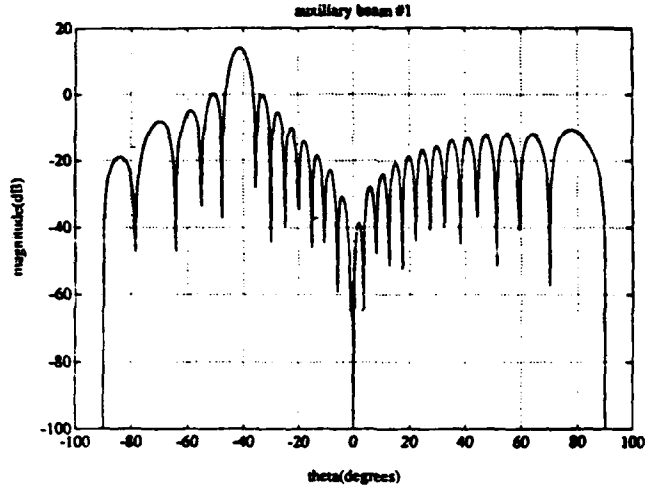

(a)

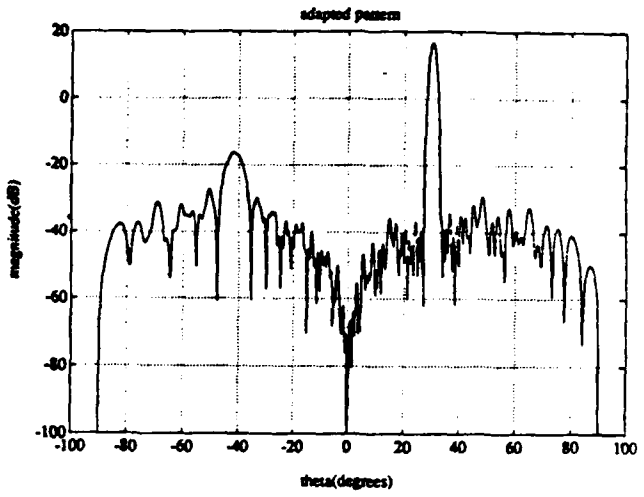

(b)

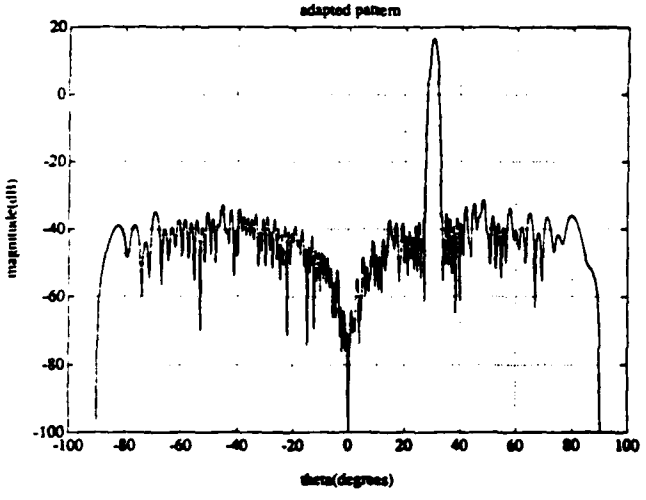

(c)

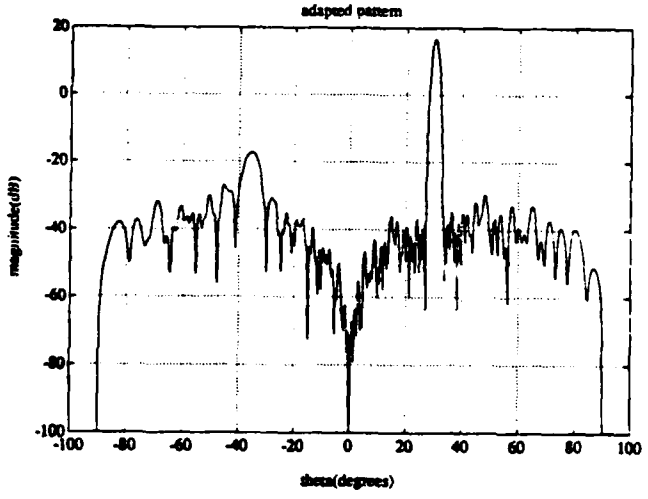

(d)

Figure 6.9: Patterns resulting from a single auxiliary using the subarray of elements (38,1)-(62,1). No jammers. (a) Auxiliary pattern, $\theta_a = -41.3°$. (b) Adapted pattern, $\theta_a = -41.3°$. (c) Adapted pattern, $\theta_a = -38.2°$. (d) Adapted pattern, $\theta_a = -35.5°$.

different auxiliary beam scan angles. In this case the quiescent sidelobe degradation is negligible for each pattern of Figure 6.10. In general it was found that the quiescent SLL degradation decreases as the size of the auxiliary subarray increases. For subarrays of 50 elements or less, this degradation may be significant and depends on the direction to which the auxiliary beam is steered. The same results hold for SLL degradation due to element reuse resulting from a system of steered beam auxiliaries when there are extra degrees of freedom.

Consider now a multiple auxiliary configuration consisting of four auxiliary beams, each using the full array. We choose their patterns to overlap a specific angular region as shown in Figure 6.11, to combat a cluster of jammers in this region. First we examine performance of this system with three 40 dB CW jammers incident. The arrival angles of two of the jammers are fixed at $\theta_{i2} = -39.25°$ and $\theta_{i2} = -37.75°$. The arrival angle of the third jammer is scanned across the sidelobe region where the auxiliary beams are steered. Figure 6.12 shows both the cancellation ratio and the increase in ASLL as a function of θ_{i1}. Note that the CR is nearly flat across the region covered by the overlapping auxiliary beams, and then rises and falls as θ_{i1} moves through the peaks and nulls of the auxiliary beam sidelobes. The ASLL increase is essentially zero for θ_{i1} within the auxiliary beam maxima, but is quite large when the jammer is at positions where the auxiliary sidelobe pattern has nulls. In this case the weights are very large.

As a final example consider the case where several jammers arrive within an auxiliary beamwidth of this same 4-auxiliary beam configuration. Fix $\theta_{i1} = -40.0°$, $\theta_{i2} = -39.8°$, and $\theta_{i3} = -40.2°$. The adapted pattern is shown in Figure 6.13. Although the jammers are cancelled, there is a region of high sidelobes in the

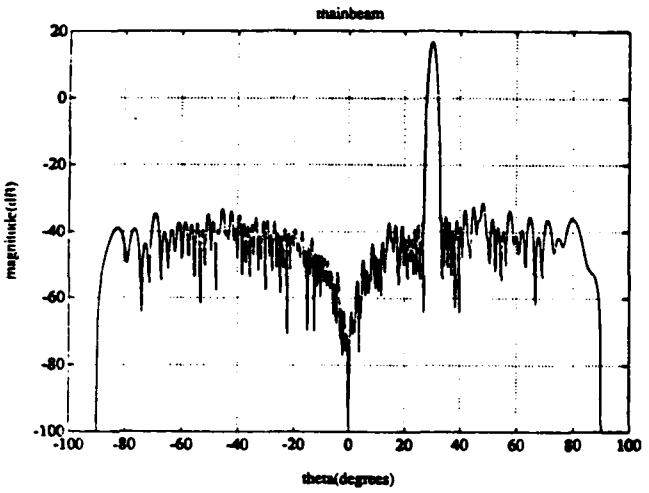

(a)

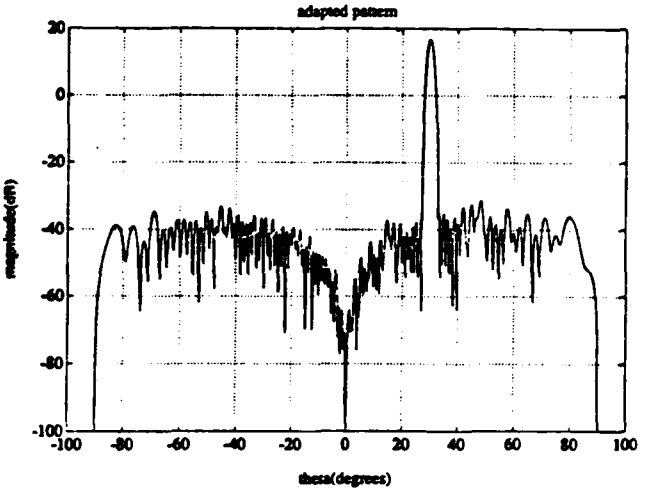

(b)

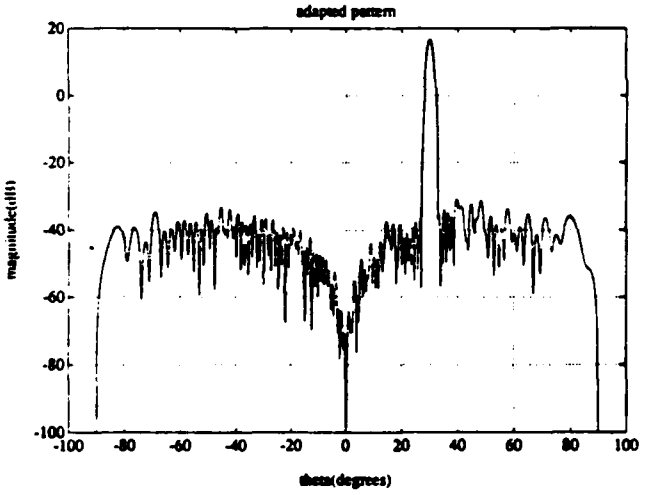

(c)

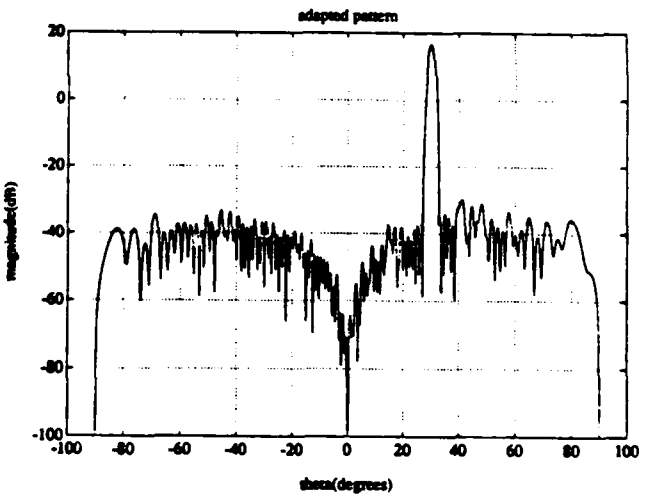

(d)

Figure 6.10: Patterns resulting from a single auxiliary using the full array, elements (1,1)-(100,1). No jammers. (a) Mainbeam pattern (b) Adapted pattern, $\theta_s = -39.8°$. (c) Adapted pattern, $\theta_s = -40.25°$. (d) Adapted pattern, $\theta_s = -40.5°$.

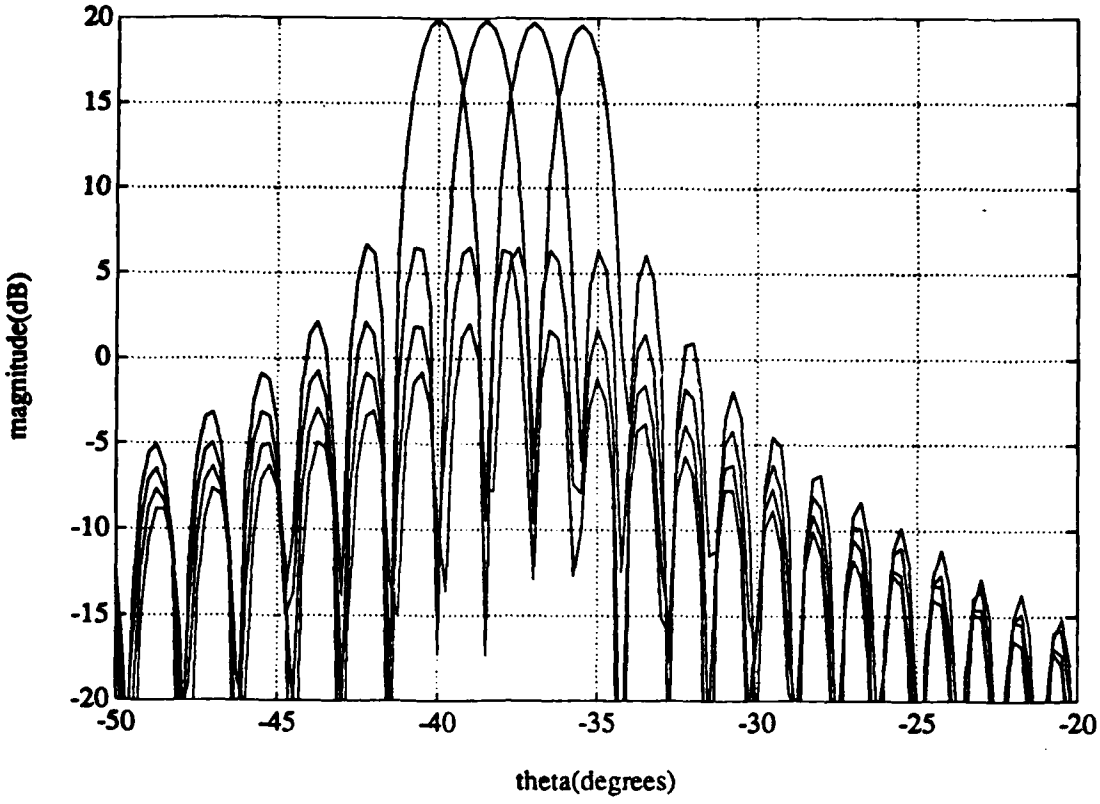

Figure 6.11: Auxiliary patterns for a SLC configuration using four auxiliaries, each using the full array.

adapted pattern where the auxiliary beam maxima are located. Because the jammers are all located in the main lobe of the same auxiliary beam, the other beams whose pattern maxima are not in the jammer directions have larger weights, causing them to appear as high 'sidelobes' in the adapted pattern.

At this point it is worth noting the differences between the canceller configurations presented in this section and those discussed previously. The SLC configurations of Section 6.3 consist of a system of auxiliaries that use a relatively small number of array elements. The individual auxiliary beams are slightly directive, and their combiner weights satisfy an orthogonality condition that allows good SLL performance for a wide range of possible jammer arrival angles. No a-priori informa-

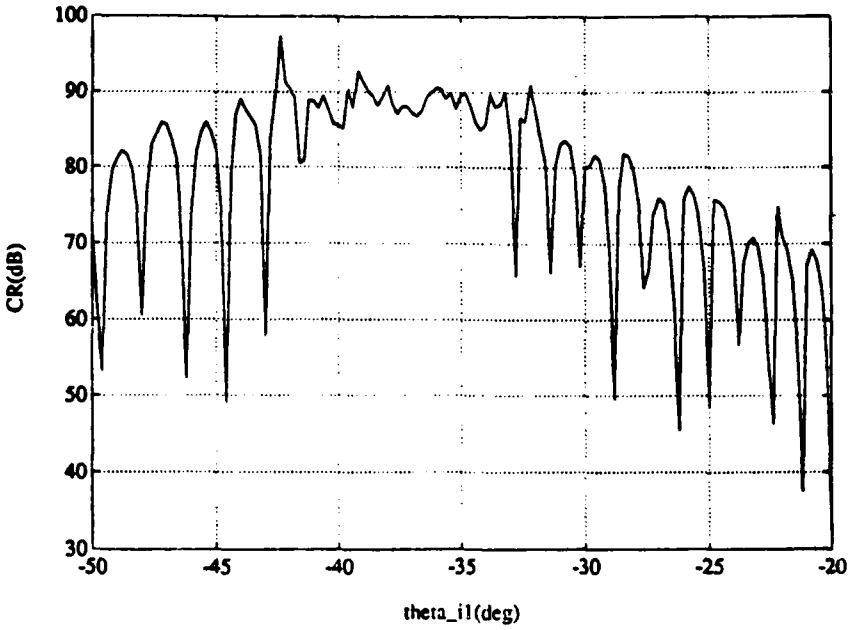

(a)

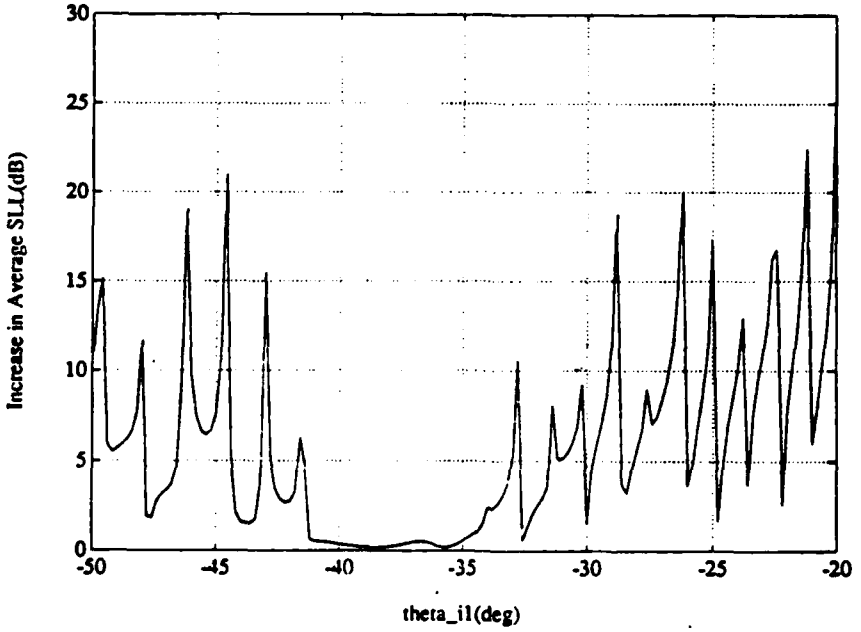

(b)

Figure 6.12: Performance of a SLC with multiple uniformly weighted steered beam auxiliaries. Three 40 dB CW jammers present. $\theta_{i2} = -39.25°$, $\theta_{i3} = -37.75°$ (a) Cancellation Ratio (b) Increase in ASLL

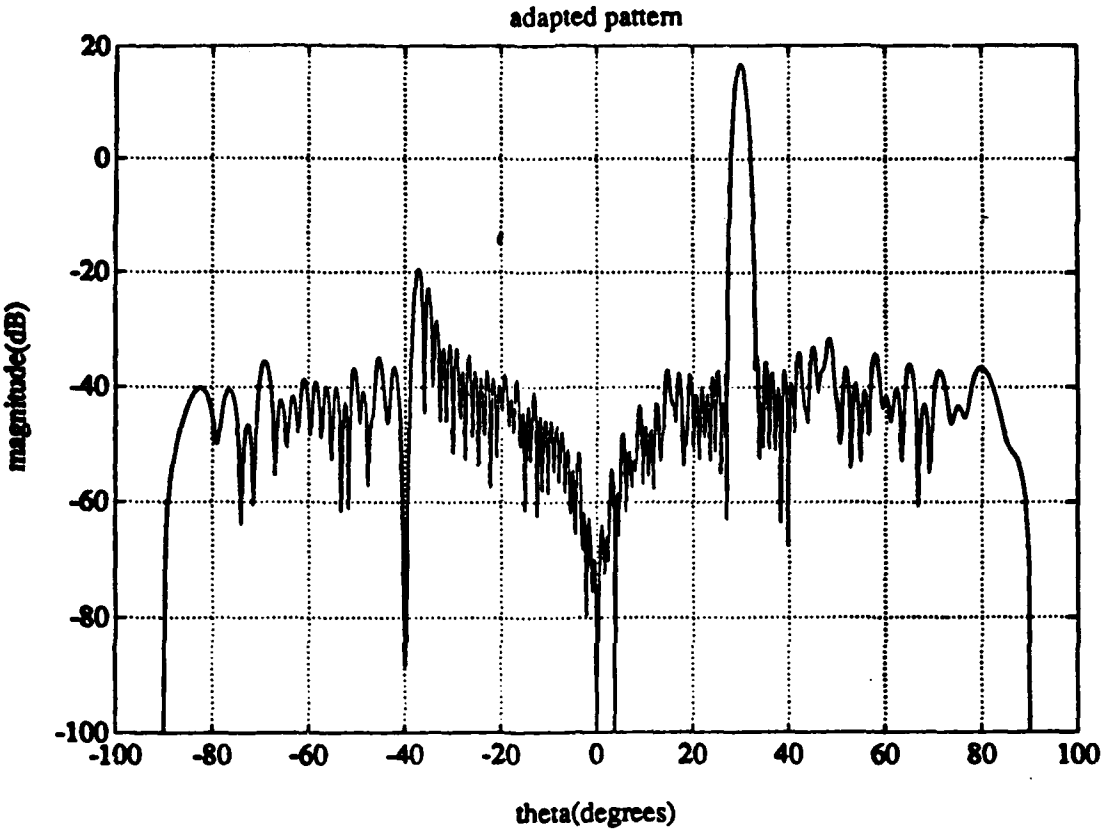

Figure 6.13: Adapted pattern resulting from 3 jammers within one auxiliary beamwidth. $\theta_{i1} = -40.0°$, $\theta_{i2} = -39.8°$, $\theta_{i3} = -40.2°$

tion on the number of jammers or their locations is necessary for good cancellation and SLL performance. The primary disadvantage to these configurations is that to maintain the orthogonality condition, the auxiliary scan angles need to be reconfigured as the mainbeam is scanned. On the other hand, the SLC configurations discussed briefly in this section consist of highly directive steered beams. Each auxiliary uses all the elements of the array. For such a system to provide both good cancellation and good SLL performance, the jammer arrival angles must either be known a-priori or estimated, for example, using modern spectral estimation techniques as in Gabriel[20]. In this case such an estimation procedure also adds to the complexity of the system. If for some reason the angle estimates are wrong, an

increase in SLL is likely. Each of these two approaches has its advantages and disadvantages, but our focus in this report has been to assume that jammer information is not known a-priori and to seek configurations that provide good performance for all possible jammer arrival angles.

In this chapter we have shown ways to choose auxiliaries that result in much better adapted pattern sidelobe behavior. The sidelobe degradation due to element reuse is eliminated if each auxiliary is formed from a combination of array elements, such that the auxiliary combiner is orthogonal to the mainbeam combiner in the sense of Equation (6.3). Because this orthogonality condition depends on the mainbeam scan angle (θ_d), the auxiliary combiners must be reconfigured as the mainbeam is scanned in order to maintain orthogonality to the mainbeam and avoid SLL degradation. We have shown how the auxiliary combiners should be chosen so that this reconfiguration only requires steering the auxiliary beams to the directions orthogonal to the mainbeam scan angle. We then showed several examples illustrating the performance of such steered beam auxiliaries. We found that to avoid resolution problems, each auxiliary should be formed from a different non-overlapping subarray, and the different subarrays should be equally spaced across the full array. To combat non-zero bandwidth jammers and retain low sidelobes, one should use a tapped delay line on the output of each auxiliary beams rather than relying on the TDL formed by the spatial separation between the different subarrays. These results are applied to the more general case of a planar array sidelobe canceller in the next chapter.

7. Auxiliary Selection for Planar Sidelobe Cancellers

7.1 Introduction

In this chapter we shall apply the results obtained with the linear array to sidelobe cancellers using a rectangular planar array of elements. Since the planar array has a 3-dimensional pattern and can discriminate against jammers based on both their θ and ϕ arrival angles, the number of possible combinations of jammer arrival angles that can be studied is limitless. Moreover, computational speed requirements do not permit evaluation of a particular configuration for all possible jammer scenarios, as was done for many of the linear array cases[1]. Instead, we shall examine the performance of various configurations for selected signal scenarios, relying on examination of the array patterns to provide information on the sidelobe level performance of these configurations. We find that in most cases the conclusions reached regarding auxiliary selection and element location for the linear array SLC also apply to the planar case.

We first examine planar array SLC performance with single-element auxiliaries. To adequately cancel multiple jammers requires auxiliary elements unequally spaced in both dimensions of the array. As with the linear array, the noise correlation between mainbeam and auxiliaries results in SLL degradation when the number of adaptive DOF exceeds the number of jammers. Auxiliary elements around the periphery of the planar array cause the least amount of SLL degradation.

[1]The calculations shown in this chapter were produced on a Cray X-MP/28 supercomputer. To take full advantage of the speed afforded by the Cray architecture, the FORTRAN code was written in such a way that operations on array elements may be replaced by operations on vectors of array elements. This process is called vectorization, and the FORTRAN code included in the Appendix is written in vectorized Cray FORTRAN. The results and 3-D patterns were plotted using MATLAB on a Sun 3/60 workstation.

Finally, we then show how this SLL degradation can be avoided by forming the auxiliary signals from rectangular subarrays of the main array, such that the orthogonality condition of Eq. (6.1) is satisfied.

7.2 Single-element Auxiliaries

We consider rectangular planar arrays of size $N_x \times N_y$ elements, where N_x and N_y are the number of elements in the x and y dimensions of the array, respectively (see Figure 2.1). The mainbeam signal is formed by weighting each row and each column with a Dolph-Chebyshev amplitude taper corresponding to a specified SLL.[4] Thus the magnitude of the mainbeam combiner weight on the $(i,j)^{th}$ element is the product of the corresponding weights of N_x and N_y element linear arrays. The mainbeam pattern, given in Eq. (2.44), is

$$F_M(\theta,\phi) = f(\theta,\phi)\sum_{l=1}^{N_x}\sum_{m=1}^{N_y} M_{lm}G_{lm}e^{j\pi[(l-1)\sin\theta\cos\phi+(m-1)\sin\theta\sin\phi]}\,, \qquad (7.1)$$

where

$$M_{lm} = M_l^x M_m^y\,. \qquad (7.2)$$

The M_l^x and M_m^y are the Chebyshev coefficients for N_x and N_y element linear arrays, each containing the appropriate beam steering factors. If there is no randomness present in the element combiner weights(i.e. $G_{lm} = 1$), the mainbeam pattern can be separated into the product of two linear array patterns as

$$F_M(\theta,\phi) = f(\theta,\phi)\left(\sum_{l=1}^{N_x} M_l^x e^{j\pi(l-1)\sin\theta\cos\phi}\right)\left(\sum_{m=1}^{N_y} M_m^y e^{j\pi(m-1)\sin\theta\sin\phi}\right)\,. \qquad (7.3)$$

A linear array, because of symmetry about its axis, has a pattern that can be plotted against a single spatial angle. Two angular dimensions are required to display the

radiation pattern of a planar array.

We can make use of FFT routines to compute 3-dimensional planar array patterns if we first make the spherical to rectangular transformation

$$u = \sin\theta\cos\phi\ ,\ v = \sin\theta\sin\phi\ , \tag{7.4}$$

so that Eq. (7.1) becomes

$$F_M(u,v) = f(u,v)\sum_{l=1}^{N_x}\sum_{m=1}^{N_y} M_{lm}G_{lm}e^{j\pi[(l-1)u+(m-1)v]}\ . \tag{7.5}$$

The transformation Eq. (7.4) was described in Section 3.4. The visible region $0° \leq \theta \leq 90°, 0° \leq \phi \leq 360°$ transforms via Eq. (7.4) to the area enclosed by the unit circle in the uv plane. We shall alternate between specifying desired and interfering signal arrival angles as (θ,ϕ) or (u,v).

Figure 7.1 shows the mainbeam pattern magnitude, $|F_M(u,v)|$, for an 80×50 array of elements with 50 dB Dolph-Chebyshev weighting on each row and column. The main lobe is steered to $(\theta_0,\phi_0) = (30°, 0°)$, or to $(u_0,v_0) = (0.5, 0.)$. No random errors are present in the array weights. The base of the surface is at -80 dBi, and the mainbeam peak is 35.5 dBi. The nulls at the origin($\theta = 0°$) and on the unit circle($\theta = 90°$) are due to the element pattern. Along the $u = u_0, v = v_0$ axes there are two ridges of sidelobes at the design SLL. Off of these axes, the product effect produces equal amplitude sidelobes in both the u and v directions at twice the design SLL, or -100 dB, relative to the mainbeam peak. We call this portion of the sidelobe region the off-axis region. If such a pattern were practically realizable, it would appear that jammers arriving in the off-axis region would be suppressed sufficiently by the mainbeam pattern itself and would not require any adaptive protection. In practice, the mainbeam SLL in the off-axis regions will be

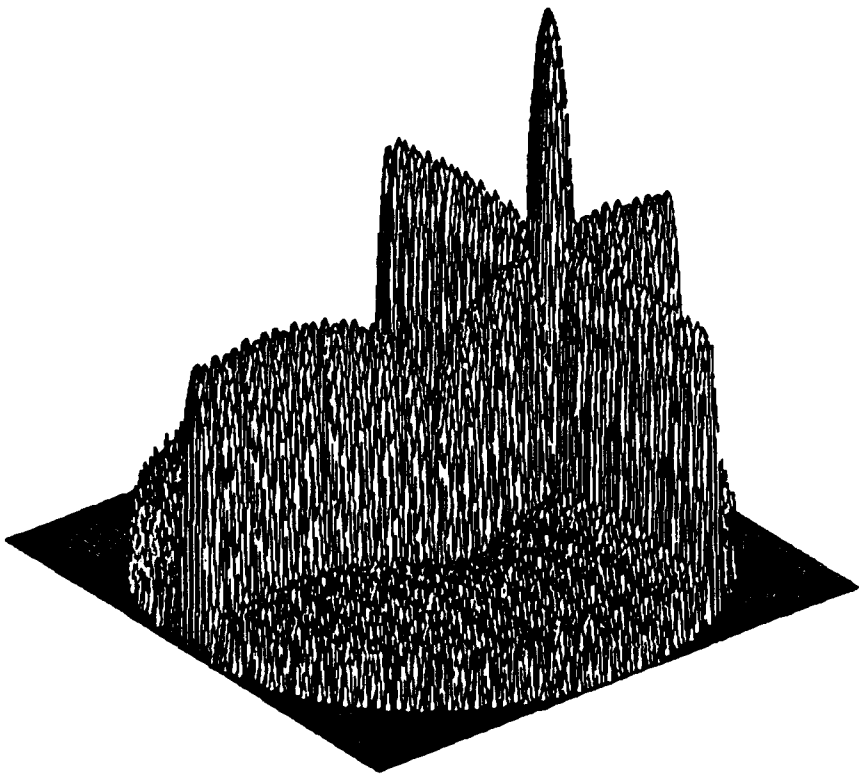

Figure 7.1: Mainbeam pattern magnitude resulting from an 80×50 array with 50 dB Dolph-Chebyshev weighting.

dominated by the random component of the pattern, but for now let us consider a simple planar sidelobe canceler using the ideal mainbeam of Figure 7.1.

Let the signal environment consist of a desired signal at $\theta_d = 30°, \phi_d = 0°$, and a single CW jammer at $\theta_{i1} = 48.5904°, \phi_{i1} = 180°$ ($u_{i1} = -0.75, v_{i1} = 0$). Suppose element (1,1) is used as a single auxiliary element. Cancellation of the jammer results in the adapted pattern shown in Figure 7.2. A contour plot of this 3-D pattern and some 2-D pattern cuts are shown in Figure 7.3. The pattern cut for $v = 0$ shows that the jammer (at $u_{i1} = -0.75, v_{i1} = 0$) is indeed suppressed. However, we see that the weighted element pattern dominates the adapted pattern in the off-axis regions, destroying the ultra-low sidelobe structure of the mainbeam in this region and rendering the system susceptible to jammers arriving in this region. This example illustrates how the auxiliary pattern (the element pattern in this case) may affect the adapted pattern sidelobe structure at angles other than near the interfering signals.

For the rest of the performance curves to be examined, we use the same 80×50 array but add randomness to the mainbeam combiner. A 55 dB Dolph-Chebyshev amplitude taper is applied to each row and column of elements. The random error levels are chosen so that the peak SLL is less than 50 dB. From the methods of Chapter 3 we choose element errors of ± 0.2711 dB and $\pm 0.6325°$. The resulting mainbeam pattern is shown in Figure 7.4. Although the off-axis region of this pattern is dominated by the randomness present in the array weights, the SLL in this region is still less than the SLL along the $u = u_0$, $v = v_0$ axes.

The performance of a planar array SLC with a single auxiliary element, as a function of the auxiliary location, is similar to that of the linear array SLC. As

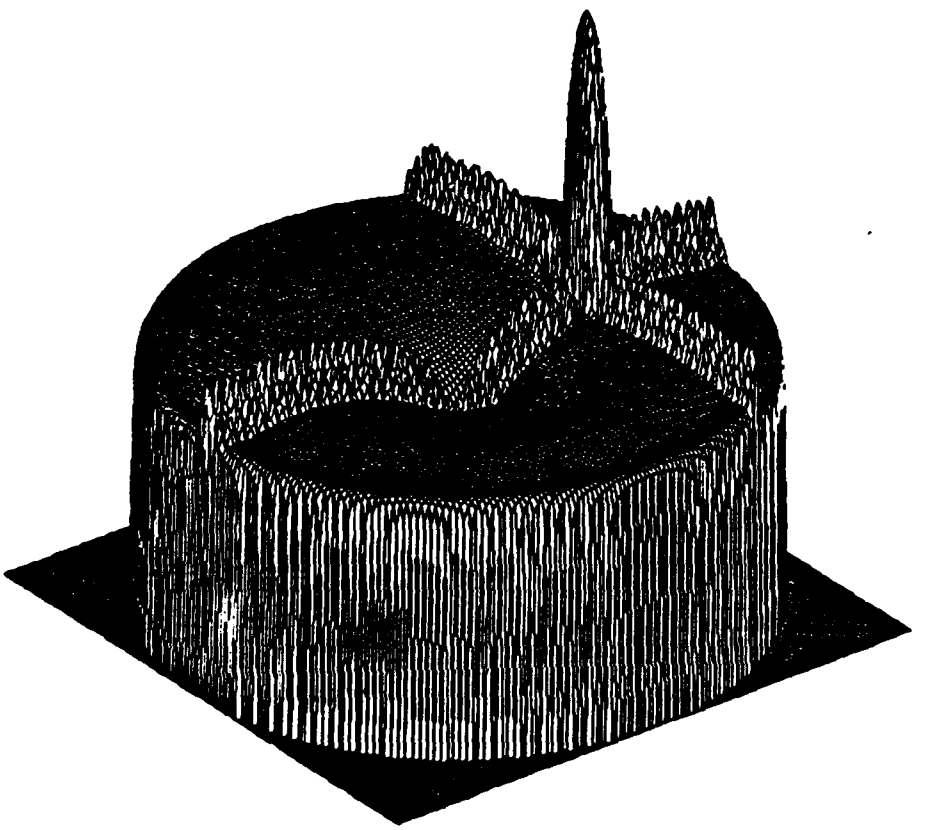

Figure 7.2: Adapted pattern resulting from the mainbeam pattern of Figure 7.1 using element (1,1) as the auxiliary element.

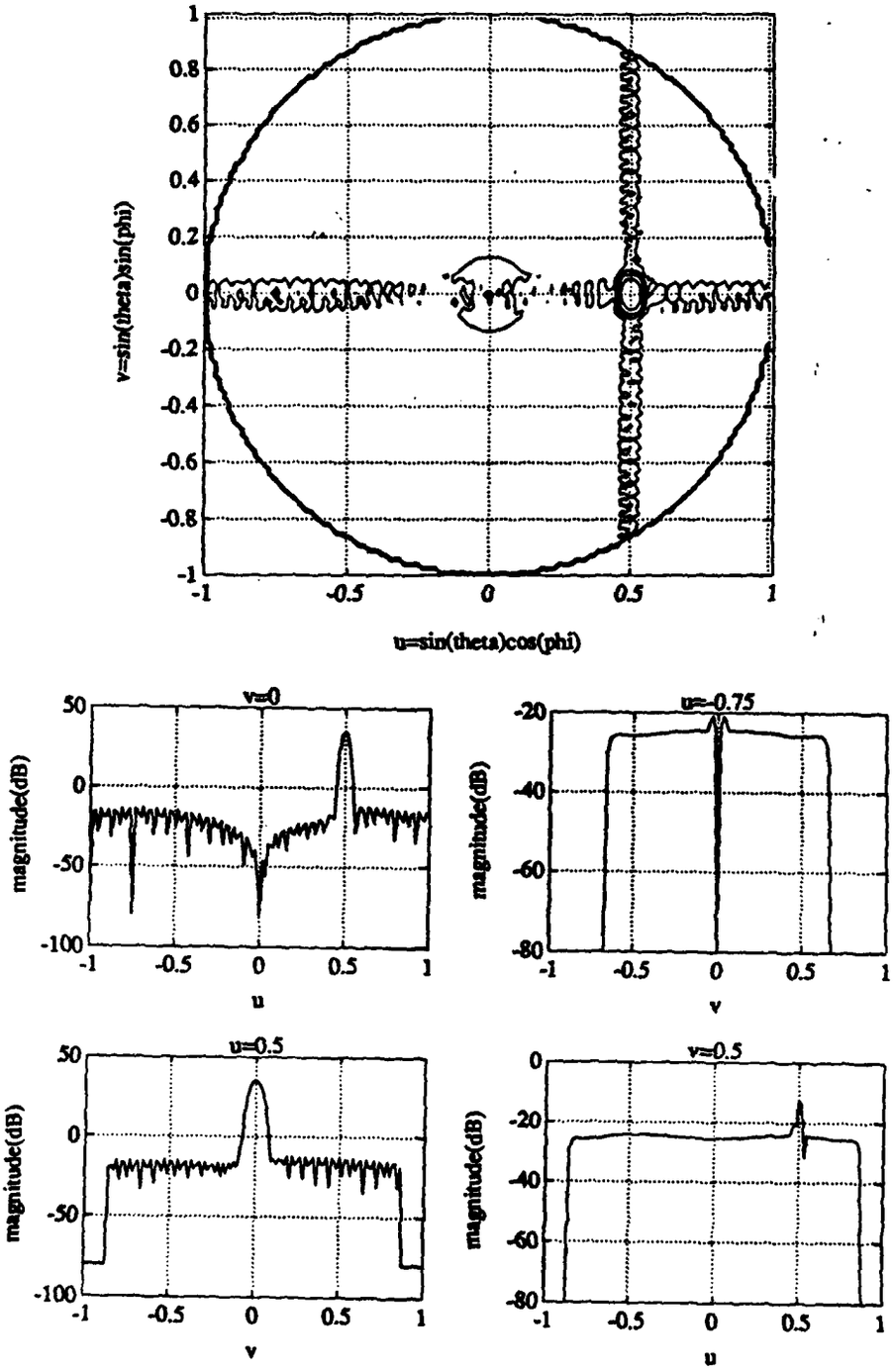

Figure 7.3: Contour plot and pattern cuts of the adapted pattern shown in Figure 7.2.

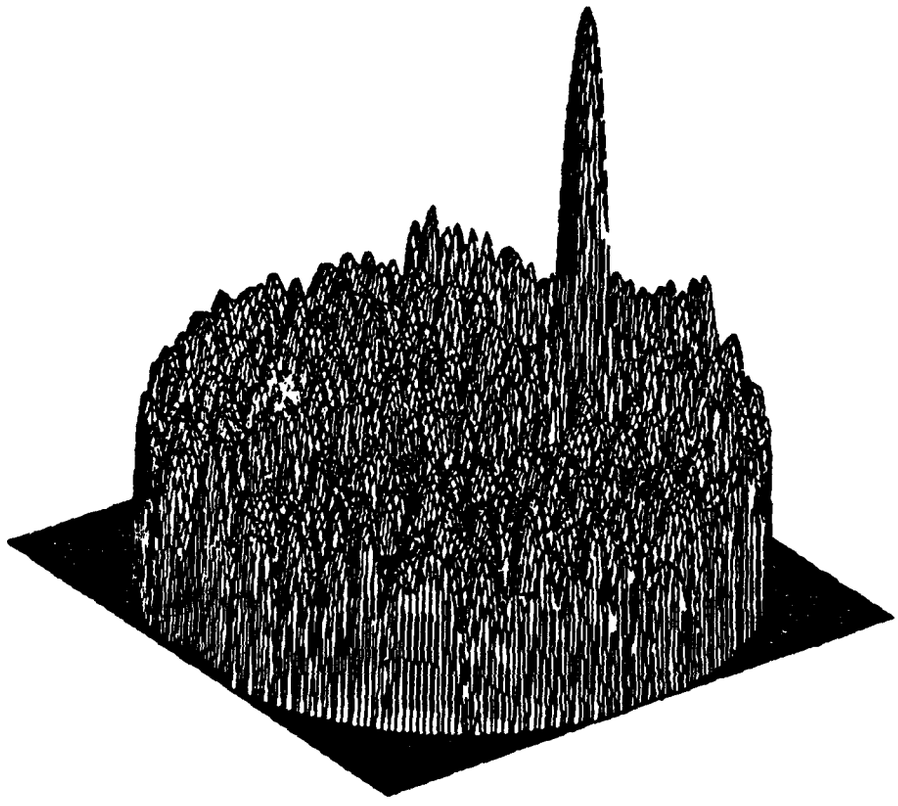

Figure 7.4: Mainbeam pattern of an 80 × 50 array with 55 dB Dolph-Chebyshev weighting. The element errors are ±0.2711 dB and ±0.6325°.

with the linear array, SLL degradation occurs when no jamming is present because of the non-zero noise correlation between the mainbeam and auxiliary signals, and this degradation is worse for center element auxiliaries than for auxiliaries located around the periphery of the array. With a center element auxiliary, however, the SLL degradation evident with the 80 × 50 array is not as severe as for the 100 element linear array shown in Figure 4.9. The increase in ASLL with no jammers for a center element auxiliary using the array of Figure 7.4 is 11 dB , while for the linear array of Figure 4.9 it was 25 dB. The reason for this difference is that the planar array has many more elements than the linear array used in the examples, its pattern is disrupted less by the weight on one element. Nevertheless, 11 dB is a significant increase in ASLL and can be avoided, as in the linear case, by forming the auxiliary signals from combinations of more than one element.

The SLL performance of the planar canceller with a single auxiliary depends on the location of the jammer. For example, Figure 7.5 shows two adapted patterns resulting from a single 40 dB CW jammer. In (a), the jammer is located at $(u_{i1}, v_{i1}) = (-0.5, 0.5)$, which is in the off-axis sidelobe region of the mainbeam pattern. The adapted pattern shows negligible change in SLL relative to the mainbeam pattern. (The increase in ASLL is 0.5 dB) In (b), the jammer is located at (0.5,0.5), at the peak of one of the sidelobes along the $v = v_0$ ridge of the mainbeam pattern. The adapted pattern magnitude is noticeably higher throughout the sidelobe region. To cancel the jammer, the weighted auxiliary pattern matches the mainbeam pattern magnitude in the jammer direction. Because the auxiliary pattern is nearly constant over most of visible space (The auxiliary pattern is just the element pattern.) and the mainbeam pattern magnitude over most of visible space

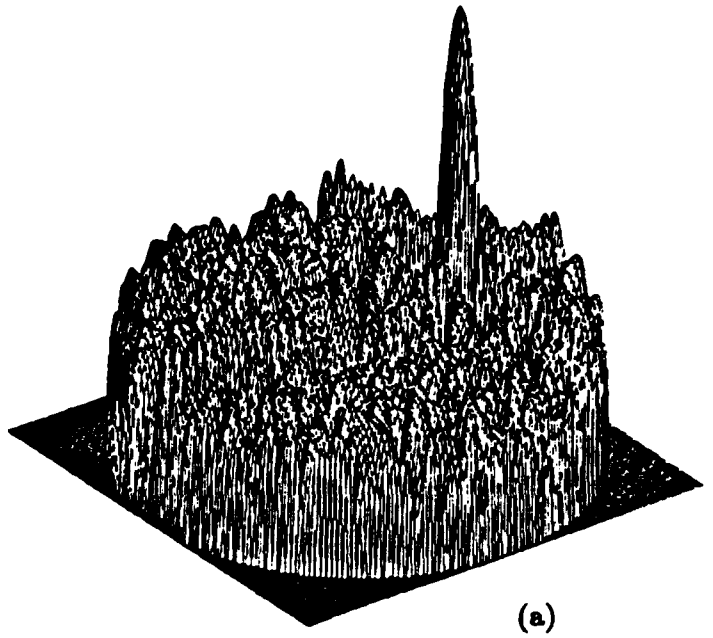

(a)

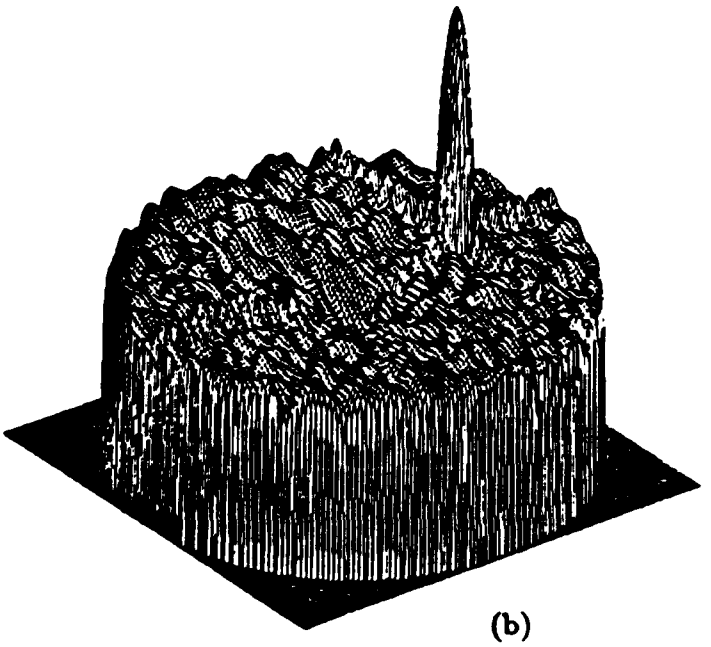

(b)

Figure 7.5: Adapted patterns from an SLC with element (40,25) as the auxiliary. A single 40 dB CW jammer is present. (a) $(u_{i1}, v_{i1}) = (-0.5, 0.5)$. (b) $(u_{i1}, v_{i1}) = (0.5, 0.5)$.

is less than its value along the $v = v_0$ ridge, the addition of the weighted auxiliary pattern increases the SLL most everywhere in the sidelobe region.

In a planar SLC with multiple auxiliary elements, the grating lobe and resolution problems are more complicated than for the linear case. Consider a canceller with two auxiliary elements. If these auxiliaries are chosen from the same row of the array, the weighted auxiliary pattern will depend only on the u coordinate (if we ignore the variation with v due to the element pattern). These auxiliaries will be unable to cancel two jammers arriving from different directions with the same u coordinate. In general, the weighted auxiliary pattern for any two auxiliary elements will vary in only one direction in uv space. Such auxiliaries are unable to cancel two jammers separated along the perpendicular direction. At least three non-collinear auxiliary elements are required to cancel any combination of 2 jammers. To completely avoid grating lobe and resolution problems in both the u and v dimensions will require additional auxiliary elements, located so that the auxiliaries are irregularly spaced in both dimensions of the array.

For linear array SLCs, we found that suitably chosen multiple auxiliary configurations provide excellent cancellation performance for a wide range of multiple jammer scenarios, but their SLL performance is poor. This problem also exists occurs for planar array cancellers. As an example, consider a canceller with five auxiliary elements, using elements (64,3),(13,32),(20,12),(51,8), and (5,40) of the array. The adapted pattern resulting from two 40 dB CW jammers, one arriving at $(u_{i1}, v_{i1}) = (-0.7071, 0.)$ and the other at $(u_{i2}, v_{i2}) = (0., 0.5)$, is shown in Figure 7.6. In this case the jammers are widely separated and do not require all the adaptive degrees of freedom. The cancellation is excellent(81 dB), but the SLL

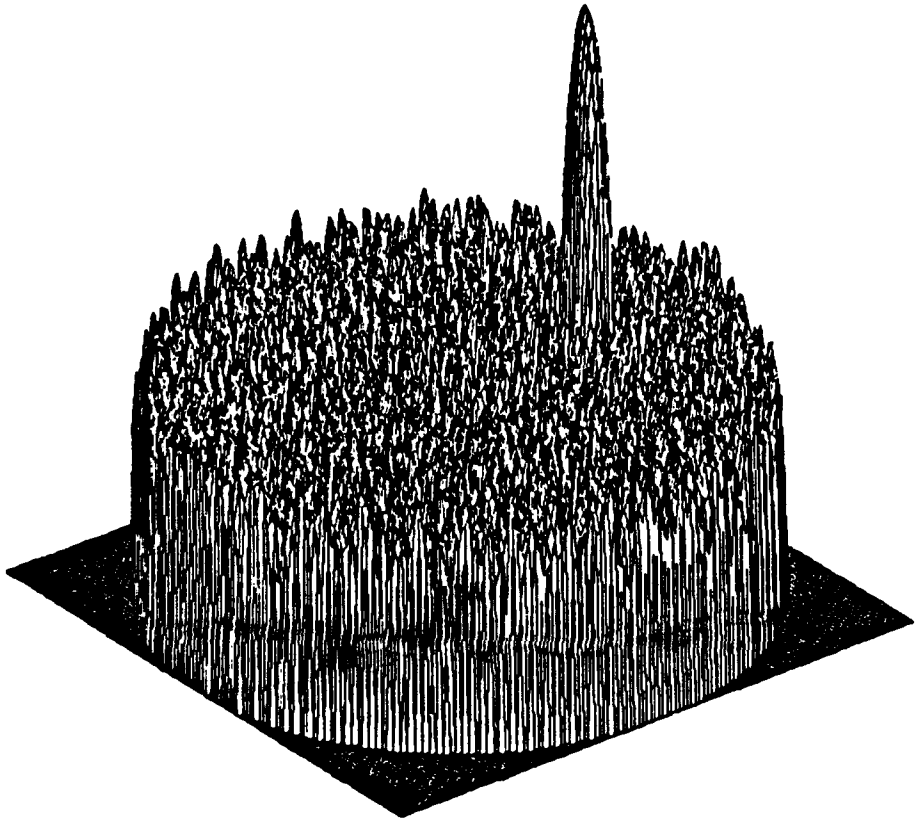

Figure 7.6: Adapted pattern from an SLC with 5 auxiliary elements. Two 40 dB CW jammers, $(u_{i1}, v_{i1}) = (-0.7071, 0.)$ and $(u_{i2}, v_{i2}) = (0., 0.5)$ are incident.

has increased noticeably over that of the mainbeam pattern. The sidelobes of the adapted pattern in Figure 7.6 are due to the large separation between auxiliary elements, and they swamp out the random component of the mainbeam pattern. Again, this increase in SLL occurs because the unused degrees of freedom respond to the noise correlation due to element reuse. This type of behavior is seen in the adapted patterns resulting from other jammer arrival angles as well. As the number of unused degrees of freedom increases, the SLL degradation also increases.

7.3 Auxiliaries meeting the orthogonality condition

To prevent the array weights from responding to the noise correlation between the mainbeam and auxiliary signals, we must form the auxiliary signals from combinations of multiple elements, or subarrays, so that Equation (6.1) is satisfied. In Chapter 6 we described how this condition can be met by steering the auxiliary patterns to the directions orthogonal to the desired signal direction, which we defined for a linear array and a specified subarray size. The same principles apply to the planar array, so we first extend the formulation of the last chapter to define the orthogonal directions for a planar array and rectangular subarrays.

Suppose we choose an $M = M_x \times M_y$ element rectangular subarray of adjacent elements to form an auxiliary signal. Denote the lower left corner of this subarray as element (k, l). Let the desired signal arrival angles be (θ_d, ϕ_d) or (u_d, v_d), where $u_d = \sin\theta_d \cos\phi_d$ and $v_d = \sin\theta_d \sin\phi_d$. The orthogonality condition then reduces to an M dimensional inner product,

$$\mathbf{M}_s^H \mathbf{A}_s^o = 0\,, \tag{7.6}$$

where $\mathbf{M_s}$ and $\mathbf{A_s^\alpha}$ are the mainbeam and auxiliary *subarray* combiner vectors. $\mathbf{M_s}$ is given by

$$\mathbf{M_s} = e^{-j\pi[(k-1)u_d+(l-1)v_d]}\left[m_{k,l},\ m_{k+1,l}e^{-j\pi u_d},\ \ldots,\ m_{k+M_x-1,l}e^{-j\pi(M_x-1)u_d},\right.$$
$$\left.\ldots,\ m_{k+M_x-1,l+M_y-1}e^{-j\pi[(M_x-1)u_d+(M_y-1)v_d]}\right]^T \tag{7.7}$$

and we wish to find $\mathbf{A_s^\alpha}$ such that Eq. (7.6) is satisfied.

We define the direction vector $\mathbf{X}$ as the vector of signals received on an $M_x \times M_y$ subarray of isotropic elements, due only to a single unit amplitude signal incident from the directions (u, v). $\mathbf{X}$ is given by

$$\mathbf{X} = \left[1,\ e^{j\pi u},\ \ldots,\ e^{j\pi(M_x-1)u},\ e^{j\pi v},\ e^{j\pi(u+v)},\ \ldots,\ e^{j\pi[(M_x-1)u+(M_y-1)v]}\right]^T . \tag{7.8}$$

The desired signal direction vector $\mathbf{X}_d$ is given by Eq. (7.8) evaluated at (u_d, v_d). The orthogonal directions (u_α, v_α) for $\alpha = 1, 2, \ldots, N$ are defined to be those directions producing direction vectors $\mathbf{X}_\alpha$ orthogonal to $\mathbf{X}_d$, satisfying

$$\mathbf{X}_d^H \mathbf{X}_\alpha = 0 . \tag{7.9}$$

These directions correspond to the null directions for a uniformly weighted subarray pattern steered to (u_d, v_d). Eq. (7.9) can be simplified to

$$\frac{\sin\left[\frac{\pi M_x}{2}(u_\alpha - u_d)\right]}{\sin\left[\frac{\pi}{2}(u_\alpha - u_d)\right]} \cdot \frac{\sin\left[\frac{\pi M_y}{2}(v_\alpha - v_d)\right]}{\sin\left[\frac{\pi}{2}(v_\alpha - v_d)\right]} = 0 . \tag{7.10}$$

The solutions to Eq. (7.10) are given by

$$\begin{aligned} u_\alpha &= u_d + \frac{2p_\alpha}{M_x} \\ v_\alpha &= v_d + \frac{2q_\alpha}{M_y} , \end{aligned} \tag{7.11}$$

where p_α and q_α are integers not both equal to zero (for a particular α), (u_α, v_α) is in the visible region and $\alpha = 1, 2, \ldots, N$. N is the number of solutions to Eq. (7.11) which lie in the visible region, and $N < M_x M_y$.

An auxiliary combiner $\mathbf{A}_s^\alpha$ steered to the orthogonal directions (u_α, v_α) will be given by

$$\begin{aligned}\mathbf{A}_s^\alpha \;=\; & \Big[a_{k,l},\; a_{k+1,l}e^{-j\pi u_\alpha},\; \ldots,\; a_{k+M_x-1,l}e^{-j\pi(M_x-1)u_\alpha}, \\ & \ldots,\; a_{k+M_x-1,l+M_y-1}e^{-j\pi[(M_x-1)u_\alpha+(M_y-1)v_\alpha]}\Big]^T \end{aligned} \tag{7.12}$$

If the $a_{r,s}^\alpha$ weights are chosen so that

$$a_{r,s}^\alpha = \frac{\kappa}{m_{r,s}}, \quad \begin{matrix} k \le r \le k + M_x - 1 \\ l \le s \le l + M_y - 1 \end{matrix}, \tag{7.13}$$

where κ is an arbitrary constant, Eq. (6.1) will be satisfied.

As with the linear array, auxiliary beams steered to the orthogonal directions will have their pattern maxima regularly distributed across visible space. These auxiliary patterns will also have pattern minima near the desired signal direction and in the other orthogonal directions.

In Chapter 6 we observed that for the linear array, the configuration yielding best overall performance was one that used steered beam auxiliaries from subarrays equally spaced across the whole array. Extending this result to the planar case, we consider a canceller configuration with subarrays equally spaced in both the x and y dimensions of the array. Specifically, we consider a SLC with nine auxiliaries using nine 4×4 element subarrays. These subarrays are equally spaced throughout the array as shown in Figure 7.7. The orthogonal directions are calculated from Eq. (7.11) with $M_x = M_y = 4$ and $(u_d, v_d) = (0.5, 0.)$. Each auxiliary beam is

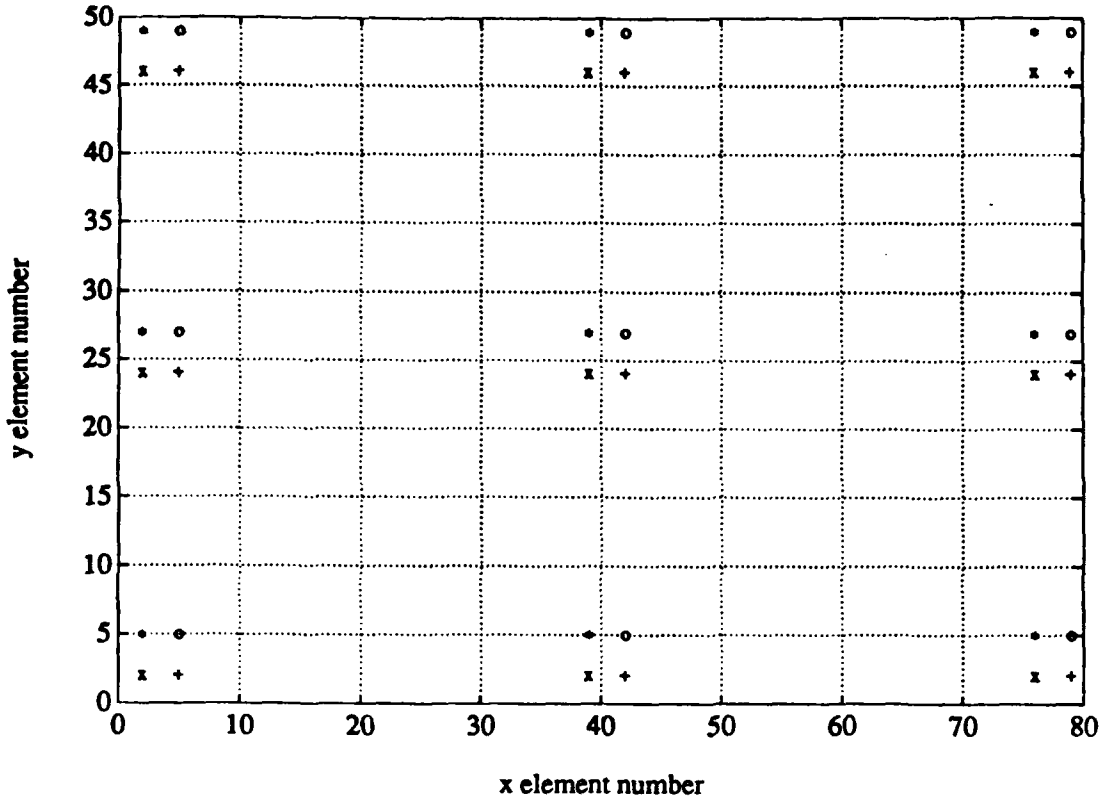

Figure 7.7: Subarrays used for planar SLC example with steered beam auxiliary signals.

steered to a different orthogonal direction. The auxiliary combiner weights are for each subarray are then obtained from Eqs. (7.12) and (7.13). The individual subarrays and the orthogonal directions to which they are steered are indicated in the Table 7.1.

We show in Figure 7.8 the adapted pattern resulting when two jammers are incident from directions $(u_{i1}, v_{i1}) = (-0.7071, 0.)$ and $(u_{i2}, v_{i2}) = (0., 0.5)$. Both jammers are cancelled (CR=87 dB) and the pattern exhibits little, if any, increase in SLL over that of the mainbeam pattern, even though only two of the nine available degrees of freedom are needed to cancel the jammers. The same jammer scenario resulted in a noticeable increase in SLL in Figure 7.6 for a configuration of only five

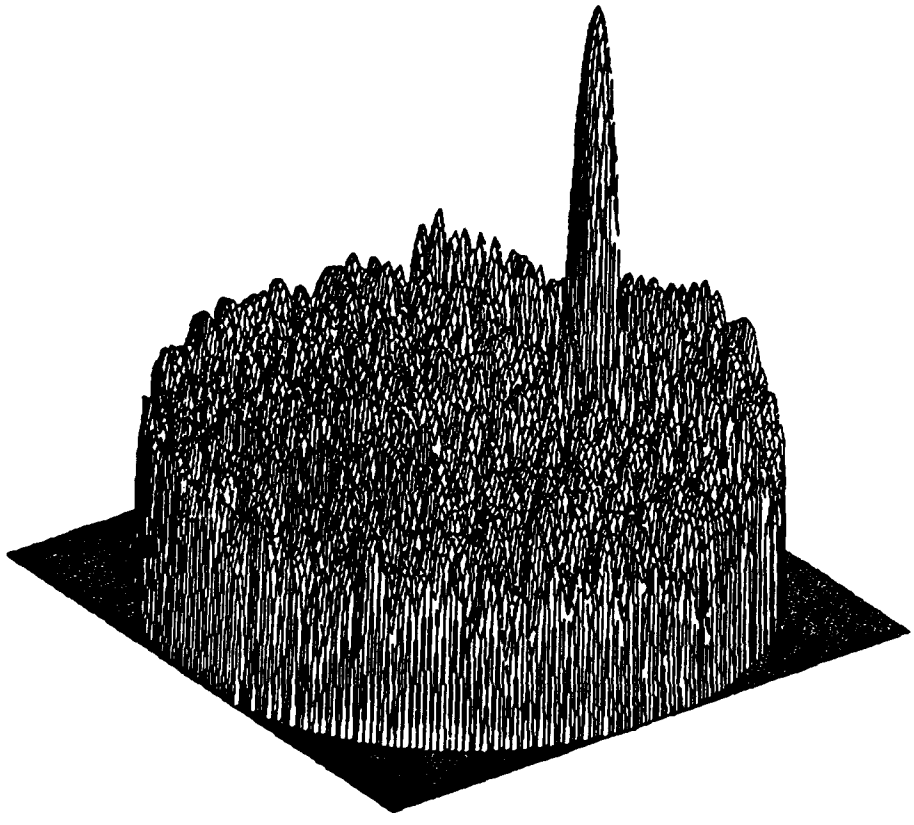

Figure 7.8: Adapted pattern from an SLC using nine steered beam auxiliaries from equally spaced subarrays. $(u_{i1}, v_{i1}) = (-0.7071, 0.)$ and $(u_{i2}, v_{i2}) = (0., 0.5)$.

Auxiliary	Subarray	$(\theta_\alpha, \phi_\alpha)$	(u_α, v_α)
1	(2,2)-(5,5)	$(45°, -135°)$	(-0.5,-0.5)
2	(39,2)-(42,5)	$(30°, -90°)$	(0.,-0.5)
3	(76,2)-(79,5)	$(45°, -45°)$	(0.5,-0.5)
4	(2,24)-(5,27)	$(30°, 180°)$	(-0.5,0.)
5	(39,24)-(42,27)	$(0°, 0°)$	(0.,0.)
6	(76,24)-(79,27)	$(90°, 0°)$	(1.0,0.)
7	(2,46)-(5,49)	$(45°, 135°)$	(-0.5,0.5)
8	(39,46)-(42,49)	$(30°, 90°)$	(0.,0.5)
9	(76,46)-(79,49)	$(45°, 45°)$	(0.5,0.5)

Table 7.1: Subarrays and orthogonal directions for a planar array SLC with multiple steered beam auxiliaries from equally spaced subarrays..

single-element auxiliaries.

The configuration of Figure 7.8 was examined for many other jammer scenarios, with the results paralleling our findings for the linear array. Scenarios of two CW jammers are effectively nulled without any noticable SLL increase, for all combinations of jammer arrival angles. This configuration has a sufficient number of degrees of freedom to cancel more than two jammers, but SLL degradation becomes evident when clusters of more than two jammers, all closely spaced, are cancelled. Also, some SLL degradation becomes evident for two jammers when the bandwidth is increased to $B = 0.001$. Thus, as we found for the linear array, it is best to use tapped delay lines behind the individual auxiliary beams to combat non-zero bandwidth, in order to preserve the good SLL performance attained by using auxiliaries

that satisfy the orthogonality condition.

For most jammer scenarios, auxiliary signals formed such that Eq. (6.1) is satisfied will result in better SLL performance than configurations of multiple auxiliary elements. The one situation where performance is worse for the steered beam auxiliaries is when the jammers are near the main lobe of the mainbeam pattern. In this region the steered beam auxiliaries have pattern minima, and thus large weight magnitudes are required to suppress the jammers. In this case the auxiliary patterns cause the adapted pattern SLL to increase, rather than the noise correlation.

We emphasize that other multiple subarray configurations, both equally and unequally spaced, have been examined, but they are simply too numerous to be presented here. The array configuration of Table 7.1 whose results are presented here has the best overall performance of the cases considered. There are several reasons why this configuration has excellent performance. First, the individual subarrays are spaced evenly in both dimensions of the array, and utilize the full aperture. Thus the auxiliary array has maximum resolution in all directions. Second, the auxiliary subarrays are large enough so that differences in the individual auxiliary patterns are enough to prevent any grating lobe problems from appearing. Finally, because we have used square subarrays, the system of auxiliary beams steered to the orthogonal directions provides essentially uniform coverage over all of visible space. In other words, the auxiliary beams have their maxima equally spaced in uv space. As a practical matter, we have only used $9 \times 16 = 144$ elements out of the 4000 total array elements.

In this chapter we have considered planar array sidelobe cancellers. Performance was illustrated for particular signal scenarios by examination of the 3-dimensional

array patterns. We found that SLL degradation due to element reuse is still a serious problem in canceller configurations with multiple single-element auxiliary signals. We then showed how auxiliary signals can be formed from rectangular subarrays such that Equation (7.6) is satisfied and the SLL degradation due to element reuse is eliminated. Best overall performance was obtained with a configuration of equally spaced subarrays, where each subarray is used to form an auxiliary beam steered to a different direction orthogonal to the mainbeam scan angle. Thus, in general, the conclusions obtained from the linear array regarding auxiliary selection also apply to the planar array.

8. Conclusions

This report has described the performance of adaptive sidelobe canceller arrays that use the same elements for both mainbeam and auxiliary signals. We first reviewed the mathematical formulation of the problem. We then discussed how random amplitude and phase errors affect the sidelobe level of the mainbeam pattern. We defined a new quantity, the integrated average SLL, which allowed the comparison of different canceller configurations on the basis of adapted pattern SLL performance.

The performance of a 100×1 linear array was calculated for numerous auxiliary configurations. We showed that for a single CW jammer, an end element auxiliary yields best performance, both with regards to cancellation and adapted pattern SLL. To cancel multiple jammers while avoiding resolution and grating lobe problems requires that the auxiliary elements be irregularly spaced throughout the array. The major consequence of element reuse is noise correlation between the mainbeam and auxiliary signals. Whenever the number of adaptive degrees of freedom exceed the number required to cancel the jammers, this noise correlation results in larger weight magnitudes and higher sidelobes. We also found that when combating non-zero bandwidth jammers, SLL degradation is less likely to occur if tapped delay lines are used on the outputs of each auxiliary, rather than relying on the tapped delay line formed by the spatial separation between auxiliary elements. (or auxiliary subarrays)

We showed how auxiliaries can be chosen from subarrays so that the noise correlation between the mainbeam and the auxiliary signals is zero. Doing this eliminates the SLL degradation caused by element reuse. One way to satisfy the orthogonality

condition (Equation (6.3)) is to choose auxiliaries whose patterns are steered to the directions orthogonal to the desired signal direction. The best overall performance was obtained for SLC configurations using equally spaced subarrays with the auxiliary pattern of each subarray steered to a different direction and satisfying the orthogonality relation in Equation (6.1). The improvement in sidelobe performance is attained at the cost of increased auxiliary complexity. A second drawback to this approach is that the the orthogonality condition will have to be maintained as the mainbeam pattern changes (i.e. as the radar beam is scanned). We noted how this may be accomplished by continuously scanning the auxiliary beams to the directions orthogonal to the mainbeam scan angle.

For an 80×50 planar array SLC, the same conclusions apply. However, because the planar array has many more elements than the linear array, the SLL degradation due to element reuse is not as severe as for the linear array. The SLL degradation is still significant, and can also be overcome using auxiliaries formed from subarrays steered to the directions orthogonal to the desired signal direction.

9. References

[1] S.P. Applebaum, "Adaptive Arrays", IEEE Transactions on Antennas and Propagation, Vol. AP-26, No. 5, pp. 585-598, Sept. 1976.

[2] R. T. Compton, Jr., *Adaptive Arrays–Concepts and Performance*, Prentice-Hall, Englewood Cliffs, NJ, 1988.

[3] I. J. Gupta, "Subarray Utilization in Adaptive Suppression of Weak Interfering Signals", Report 716111-4, The Ohio State University ElectroScience Laboratory, Columbus, OH, April 1986.

[4] M. W. Ganz and R. T. Compton, Jr., "Element Re-use in Adaptive Sidelobe Canceler Arrays", Report 717671-1, The Ohio State University ElectroScience Laboratory, Columbus, OH, December 1986.

[5] W. D. White, "Wideband Interference Cancellation in Adaptive Sidelobe Cancellers", IEEE Transactions on Aerospace and Electronic Systems", Vol. AES-19, No. 6, pp. 915-925, Nov. 1983.

[6] R. M. Davis and J. L. Gleich, "Element Placement in Adaptive Arrays and Sidelobe Cancellers", Syracuse Research Corporation.

[7] C. L. Dolph, "A Current Distribution for Broadside Arrays which Optimizes the Relationship between Beamwidth and Sidelobe Level", Proceedings of the IRE, Vol. 34, pp. 335-348, June 1946.

[8] A. D. Bresler, "A New Algorithm for Calculating the Current Distributions of Dolph-Chebyshev Arrays", IEEE Transactions on Antennas and Propagation, Vol. AP-28, No. 6, pp. 951-952, November 1976.

[9] R. E. Collin and F. J. Zucker, *Antenna Theory Part II*, McGraw-Hill, Inc., 1969.

[10] J. Ruze, "Physical Limitations on Antennas", Technical Report 248, Massachusetts Institute of Technology Research Laboratory of Electronics, October 1952.

[11] J. K. Hsiao, "Normalized relationship among errors and sidelobe levels", Radio Science, Vol.19, No. 1, pp. 292-302, Jan.-Feb. 1984.

[12] A. H. Quazi, "Array Beam Response in the Presence of Amplitude and Phase Fluctuations", Journal of the Acoustical Society of America, Vol. 72, No. 1, pp. 171-180, July 1982.

[13] J. Marcum, "A Statistical Theory of Target Detection by Pulsed Radar", IEEE Transactions on Information Theory, Vol. IT-6, No. 2, pp. 59-267, April 1960.

[14] S. Parl, "A New Method of Calculating the Generalized Q Function", IEEE Transactions on Information Theory, Vol. IT-26, No. 1., pp. 121-124, Jan. 1980.

[15] B. D. Steinberg, *Principles of Aperture and Array System Design-Including Random and Adaptive Arrays*, John Wiley and Sons, Inc. , 1976, pp. 154-156.

[16] R. T. Compton, Jr., "The Bandwidth Performance of a Two Element Adaptive Array with Tapped Delay Line Processing", IEEE Transactions on Antennas and Propagation, Vol. AP-36, No. 1, pp. 5-14, Jan. 1988.

[17] I. S. Reed, J. D. Mallett, and L. E. Brennan, "Rapid Convergence Rate in Adaptive Arrays", IEEE Transactions on Aerospace and Electronic Systems, Vol. AES-10, No. 6, pp. 853-863, Nov. 1974.

[18] J. T. Mayhan, A. J. Simmons, and W. C. Cummings, "Wideband Adaptive Antenna Nulling using Tapped Delay Lines", IEEE Transactions on Antennas and Propagation, Vol. AP-29, No. 6, pp. 923-936, Nov. 1981.

[19] J. P. Shelton and K. S. Kelleher, "Multiple Beams from Linear Arrays", IRE Transactions on Antennas and Propagation, AP-9, No. 1, p.154, March, 1961.

[20] W. F. Gabriel, "Using Spectral Estimation Techniques in Adaptive Processing Antenna Systems", IEEE Transactions on Antennas and Propagation, Vol. AP-34, No. 3, pp. 291-300, Mar. 1986.

A. Adaptive SLC Program Documentation

This appendix provides a brief description of the use of the computer programs that were used to produce the results of adaptive SLC performance contained in this report. These programs are called: 1)FILEGEN, 2)OPTFILEGEN, 3)MASTER, 4)CHINFILE, 5)INFILERD, 6)OUTFILERD1, 7)OUTFILERD2, and 7)PATTPLOT.

FILEGEN is a program that prompts the user for a description of the array, the auxiliary signal configuration, and the signal scenario, and creates an INPUT file containing this data.

OPTFILEGEN is a program that prompts the user to select the calculations to be done by program MASTER. These selections determine the form of the OUTPUT file produced by MASTER. First, the user specifies the names of the INPUT file and the OUTPUT file. Next the user selects the element pattern, and whether average SLL integration is to be done. If yes, program MASTER will also create another file, called the INTEG file, that contains the values of the subintegrals used in computing average SLLs. The INTEG file is then specified on all subsequent runs with the same array configuration (same INPUT file), thus avoiding the repetition of time consuming numerical integrations. Finally, the user is presented with the following menu:

::COMPUTATION MENU::
1–To CALC. performance at a single point and save PATTERN
2–To SCAN on THETA_D or PHI_D
3–To SCAN on THETA_I or PHI_I
4–To SCAN on SNR
5–To SCAN on INR
6–To END execution-no further computations
Enter code for desired option:

If option 1 is selected, MASTER calculates the system performance for the array and signal scenarios specified in the INPUT file. We call this a 'single point' calculation. The OUTPUT file in this case contains the description of the array and signal scenario, the various output power levels after adaptation, and the auxiliary channel weights. Typically this information is then read by subroutine OUTFILERD1 and used by program PATTPLOT to plot the various array antenna patterns. If one of options 2-5 is selected, one of the input variables (θ_d, ϕ_d, θ_i, ϕ_i, SNR, or INR) is varied (scanned) over a range specified by the user and performance is calculated for each value in the specified range. All other input parameters assume the values as specified in the INPUT file. We call the results of one of these options a 'scan'. The OUTPUT file in this case contains the values of the varying parameter and the output power levels, SINR, CR, etc. for each point calculated. These OUTPUT

files are typically read by OUTFILERD2 and used to produce plots of the various array performance measures as a function of the varying parameter.

Program MASTER reads the OPTION file and the INPUT file and performs the selected calculations of SLC performance. MASTER creates an OUTPUT file containing the results of these calculations, which may then be processed by a plotting program. The possibilities were described above. The functions of selecting the array, selecting the computations to be done, and actually performing the computations have been separated to allow for batch processing.

CHINFILE is a utility program that reads an INPUT file and allows a user to change parameters of the signal scenario without having to reenter the whole array configuration. Thus CHINFILE is useful when examining a particular array under a multitude of signal/jammer scenarios.

INFILERD is a utility subroutine that reads the INPUT file. It is used by MASTER and CHINFILE. Similarly, OUTFILERD1 and OUTFILERD2 are utility subroutines that read the OUTPUT files created by a 'single point' and a 'scan' calculation, respectively, from MASTER.

PATTPLOT reads an OUTPUT file from a 'single point' calculation and computes the following array patterns of interest:

Mainbeam Pattern
Mainbeam Array Factor
Individual Auxiliary Patterns
Weighted Auxiliary Pattern
Adapted Pattern .

PATTPLOT creates an 'x' array of angular data and 'y' arrays of the various pattern magnitudes as a function of angle. We use this data with the MATLAB software to get the plots shown in this report, but other plotting routines should be easy to incorporate into PATTPLOT.

Since the data from a 'scan' calculation is already in 'x-y' format, we use these OUTPUT files directly with MATLAB to get the plots contained in this report. But again, little modification should be required to use OUTFILERD2 in a different graphics environment.

```
C  Program FILEGEN creates the input file consisting of the array and
C   signal scenario data. The input file is read by MASTER which does
C   the computations.

      PROGRAM FILEGEN
      REAL SNR,INR(5),SIG2
      REAL AD,AI(5),PSIDL(12),BWD,BWI(5),TH_D,TH_I(5),PH_D,PH_I(5)
      REAL BEAM_TH,BEAM_PH,AUXTHETA(12),AUXPHI(12),PSI_IJ
      REAL OTHETA(24),OPHI(24),UD,VD
      REAL AUXGAIN,OFACT,SUM,MM0(100,50)
      INTEGER NUM_JAM,ILLCX(12),ILLCY(12),IURCX(12),IURCY(12)
      INTEGER N_X,N_Y,MX,MY,NUM_COMB(12),AUX_TYPE(12)
      COMPLEX G(100,50),MM(100,50),A(12,100,50),W(12)
      CHARACTER*20 FILENAME,OUTFILE
      COMMON/NAME/FILENAME,OUTFILE
      COMMON/SIGVARS/TH_D,TH_I,PH_D,PH_I,BWD,BWI,SNR,INR,AD,AI,SIG2,
     &               NUM_JAM
      COMMON/ARRVARS/N_X,N_Y,SPACING,BEAM_TH,BEAM_PH,G,MM,NUM_AUX,
     &                A,PSIDL,W,AMPVAR,PHVAR,ISEED
      COMMON/AUXVARS/AUX_TYPE,NUM_COMB,AUXTHETA,AUXPHI,ILLCX,ILLCY,
     &               IURCX,IURCY,DB


      PY=3.141592653589793E+00
      DTR=PY/180.0E+00
      RTD=1./DTR

      WRITE (6,10)
10    FORMAT (' ENTER # OF ELEMENTS IN X DIRECTION: ',$)
      READ (5,*) N_X
      WRITE (6,20)
20    FORMAT (' ENTER # OF ELEMENTS IN Y DIRECTION: ',$)
      READ (5,*) N_Y
      WRITE (6,21)
21    FORMAT (' ENTER THE INTERELEMENT SPACING IN WAVELENGTHS: ',$)
      READ (5,*) SPACING
      WRITE (6,25)
25    FORMAT (' ENTER MAIN BEAM THETA DIRECTION: ',$)
      READ (5,*) BEAM_TH
      WRITE (6,28)
28    FORMAT (' ENTER MAIN BEAM PHI DIRECTION: ',$)
      READ (5,*) BEAM_PH
      UD=SIN(BEAM_TH*DTR)*COS(BEAM_PH*DTR)
      VD=SIN(BEAM_TH*DTR)*SIN(BEAM_PH*DTR)
      WRITE (6,60)
60    FORMAT (' ENTER THE DESIRED SIGNAL THETA ANGLE: ',$)
      READ (5,*) TH_D
      WRITE (6,70)
70    FORMAT (' ENTER THE DESIRED SIGNAL PHI ANGLE: ',$)
      READ (5,*) PH_D
      WRITE (6,50)
50    FORMAT (' ENTER THE SNR: ',$)
      READ (5,*) SNR
      WRITE (6,51)
51    FORMAT (' ENTER THE DESIRED SIGNAL RELATIVE BANDWIDTH: '$)
      READ (5,*) BWD
      WRITE (6,80)
80    FORMAT (' ENTER THE NUMBER OF JAMMERS (0-5): ',$)
      READ (5,*) NUM_JAM
      DO 170 I=1,NUM_JAM
         WRITE (6,130) I
130      FORMAT ( ' ENTER INR FOR JAMMER #',I1,': ',$)
         READ (5,*) INR(I)
         WRITE (6,140) I
140      FORMAT (' ENTER BANDWIDTH FOR JAMMER #',I1,': ',$)
         READ (5,*) BWI(I)
```

```
            WRITE (6,150) I
150         FORMAT ( ' ENTER THETA FOR JAMMER #',I1,': ',$)
            READ (5,*) TH_I(I)
            WRITE (6,160) I
160         FORMAT (' ENTER PHI FOR JAMMER #',I1,': ',$)
            READ (5,*) PH_I(I)
170       CONTINUE
175       WRITE (6,185)
185       FORMAT(' Enter 1 for ideal G or enter 2 for random G:',$)
          READ (5,*) IGCODE
          IF (IGCODE.EQ.2) THEN
            WRITE (6,190)
            READ (5,*) ISEED
            ISEED0=ISEED          !  INITIAL VALUE OF SEED
            WRITE (6,*)
            WRITE (6,191)
            READ (5,*) AMPVAR
            WRITE (6,192)
            READ (5,*) PHVAR
          ELSE IF (IGCODE.NE.1) THEN
            GO TO 175
          END IF
190       FORMAT(' Enter seed for RAN routine(a large odd integer):',$)
191       FORMAT(' Specify maximum amplitude variation(dB):',$)
192       FORMAT(' Specify maximum phase unbalance(in degrees):',$)
          CALL G_SETUP(G,N_X,N_Y,IGCODE,AMPVAR,PHVAR,ISEED)
          CALL MM_SETUP(MM,MM0,SPACING,BEAM_TH,BEAM_PH,N_X,N_Y,DB)

C  Initialization and Re-initialization of A array
          A=(0.0,0.0)

          WRITE (6,240)
240       FORMAT (' ENTER THE NUMBER OF AUXILIARY SIGNALS (0-10): ',$)
          READ (5,*) NUM_AUX
          IF (NUM_AUX.NE.0) THEN

241       WRITE (6,*)
          WRITE (6,*) ' AUXILIARY SIGNAL OPTIONS:'
          WRITE (6,*) '   1--Specify individual elements,combiner weights'
          WRITE (6,*) '      for each auxiliary signal.'
          WRITE (6,*) '   2--Specify corner elements of a rectangular'

          WRITE (6,*) '      subarray to form an auxiliary beam in a '
          WRITE (6,*) '      specified direction--UNIFORM.'
          WRITE (6,*) '   3--Specify corner elements of a rectangular'
          WRITE (6,*) '      subarray to form an aux beam in a specified'
          WRITE (6,*) '      orthogonal direction, also meeting MB-AUX'
          WRITE (6,*) '      orthogonality.'
          WRITE (6,*)
          WRITE (6,245)
245       FORMAT (' Enter desired auxiliary signal option:',$)
          READ (5,*) IAUXOPT
          IF (IAUXOPT.EQ.1) THEN
            DO 306 I=1,NUM_AUX
              AUX_TYPE(I)=1
              WRITE (6,280) I
280           FORMAT (' ENTER THE # OF ELEMENTS COMBINED FOR AUX #',I1,
     &': ',$)
              READ (5,*) NUM_COMB(I)
              DO 305 J=1,NUM_COMB(I)
                WRITE (6,290) J
290             FORMAT (' ENTER <X,Y> COORDS OF ELEMENT #',I1,': ',$)
                READ (5,*) II,JJ
                WRITE (6,300)
300             FORMAT (' ENTER <MAG,PHASE (IN DEG)> OF COMBINER WEIGHT:
     & ',$)
```

```
              READ (5,*) AMAG,PHASE
              PHASE=PHASE*DTR
              A(I,II,JJ)=CMPLX(AMAG*COS(PHASE),AMAG*SIN(PHASE))
305         CONTINUE
306       CONTINUE
        ELSE IF (IAUXOPT.EQ.2) THEN
          DO 327 I=1,NUM_AUX
            AUX_TYPE(I)=IAUXOPT
            WRITE (6,335) I
            READ (5,*) AUXTHETA(I),AUXPHI(I)
            WRITE (6,*) 'ENTER <X,Y> COORDINATES OF ELEMENT FORMING'
            WRITE (6,355) I
            READ (5,*) ILLCX(I),ILLCY(I)
            WRITE (6,*) 'ENTER <X,Y> COORDINATES OF ELEMENT FORMING'
            WRITE (6,365) I
            READ (5,*) IURCX(I),IURCY(I)
            MX=IURCX(I)-ILLCX(I)+1
            MY=IURCY(I)-ILLCY(I)+1
            AUXGAIN=SQRT(FLOAT(MX*MY))
            DO 326 J=ILLCX(I),IURCX(I)
              DO 325 K=ILLCY(I),IURCY(I)
                CALL CALC_PSI(SPACING,AUXTHETA(I),AUXPHI(I),J,K,
     &                        PSI_IJ)
                A(I,J,K)=CEXP(CMPLX(0.,-1.*PSI_IJ))/AUXGAIN
325           CONTINUE
326         CONTINUE
327       CONTINUE
        ELSE IF (IAUXOPT.EQ.3) THEN
          DO 427 I=1,NUM_AUX
            AUX_TYPE(I)=IAUXOPT
            WRITE (6,*) 'ENTER <X,Y> COORDINATES OF ELEMENT FORMING'
            WRITE (6,355) I
            READ (5,*) ILLCX(I),ILLCY(I)
            WRITE (6,*) 'ENTER <X,Y> COORDINATES OF ELEMENT FORMING'
            WRITE (6,365) I
            READ (5,*) IURCX(I),IURCY(I)
            MX=IURCX(I)-ILLCX(I)+1
            MY=IURCY(I)-ILLCY(I)+1
            ICT=0
            DO 605 IP=AINT(-0.5*MX*(1+UD)),AINT(0.5*MX*(1-UD))
               DO 604 IQ=AINT(-0.5*MY*(1+VD)),AINT(0.5*MY*(1-VD))
                  IF (IP.EQ.0 .AND. IQ.EQ.0) GOTO 604
                  U=UD+2.*FLOAT(IP)/FLOAT(MX)
                  V=VD+2.*FLOAT(IQ)/FLOAT(MY)
                  R=SQRT(U**2+V**2)
                  IF (R.LE.1) THEN
                     ICT=ICT+1
                     OTHETA(ICT)=ASIN(R)*RTD
                     IF (U.EQ.0) THEN
                        OPHI(ICT)=SIGN(PI,V)*0.5*RTD
                     ELSE
                        OPHI(ICT)=ATAN2(V,U)*RTD
                     END IF
                  END IF
604           CONTINUE
605         CONTINUE
            WRITE (6,*) 'POSSIBLE ORTHOGONAL DIRECTIONS:'
            WRITE (6,610)
610         FORMAT(3X,'I',5X,'Theta',6X,'Phi',7X,'U',8X,'V',1X)
611         FORMAT(2X,I3,4X,F6.2,3X,F7.2,3X,F6.3,3X,F6.3,1X)
            DO 615 J=1,ICT
               WRITE (6,611) J,OTHETA(J),OPHI(J),SIN(OTHETA(J)*DTR)
     &                       *COS(OPHI(J)*DTR),SIN(OTHETA(J)*DTR)
     &                       *SIN(OPHI(J)*DTR)
615         CONTINUE
            WRITE (6,620) I
```

```
620         FORMAT('Enter no. for orth. direction for auxiliary #',
     &              I3,':',$)
            READ (5,*) JJ
            AUXTHETA(I)=OTHETA(JJ)
            AUXPHI(I)=OPHI(JJ)
            SUM=0.
            DO 426 J=ILLCX(I),IURCX(I)
              DO 425 K=ILLCY(I),IURCY(I)
                CALL CALC_PSI(SPACING,AUXTHETA(I),AUXPHI(I),J,K,
     &                        PSI_IJ)
                OFACT=MM0(ILLCX(I),ILLCY(I))/MM0(J,K)
                A(I,J,K)=OFACT*CEXP(CMPLX(0.,-1.*PSI_IJ))
                SUM=SUM+OFACT
425           CONTINUE
426         CONTINUE
            XNORM=SQRT(FLOAT(MX*MY))/ABS(SUM)
            DO 526 J=ILLCX(I),IURCX(I)
              DO 525 K=ILLCY(I),IURCY(I)
                A(I,J,K)=A(I,J,K)*XNORM
525           CONTINUE
526         CONTINUE
427       CONTINUE
          ELSE
            GO TO 241
          END IF

335       FORMAT(' ENTER AUXILIARY #',I1,' BEAM THETA,PHI DIRECTIONS (',
     &           'in degrees):',$)
355       FORMAT('  LOWER LEFT CORNER OF SUBARRAY FOR AUXILIARY #',
     &           I1,':',$)
365       FORMAT('  UPPER RIGHT CORNER OF SUBARRAY FOR AUXILIARY #',
     &           I1,':',$)

          END IF

          DO 405 I=1,NUM_AUX
            WRITE (6,400) I
400         FORMAT (' ENTER DELAY FOR AUX #',I1,'(WAVELENGTH FRACTION):
     & ',$)
            READ (5,*) PSI
            PSIDL(I)=-2.*PY*PSI
405       CONTINUE
          WRITE (6,410)
410       FORMAT (' ENTER FILENAME (<30 CHARACTERS): ',$)
          READ (5,420) FILENAME
420       FORMAT (A)
          OPEN (UNIT=1, FILE=FILENAME,
     &      STATUS='NEW')
          WRITE (1,*) N_X
          WRITE (1,*) N_Y
          WRITE (1,*) SPACING
          WRITE (1,*) BEAM_TH
          WRITE (1,*) BEAM_PH
          WRITE (1,*) NUM_AUX
          WRITE (1,*) SNR
          WRITE (1,*) TH_D
          WRITE (1,*) PH_D
          WRITE (1,*) BWD
          WRITE (1,*) NUM_JAM
          DO 430 I=1,NUM_JAM
             WRITE (1,*) INR(I)
             WRITE (1,*) TH_I(I)
             WRITE (1,*) PH_I(I)
             WRITE (1,*) BWI(I)
430       CONTINUE
          DO 450 I=1,N_X
```

```
            DO 440 J=1,N_Y
              WRITE (1,*) MM(I,J)
              WRITE (1,*) G(I,J)
              DO 439 K=1,NUM_AUX
                WRITE (1,*) A(K,I,J)
439           CONTINUE
440         CONTINUE
450       CONTINUE
          DO 460 I=1,NUM_AUX
            WRITE (1,*) PSIDL(I)
            WRITE (1,*) AUX_TYPE(I)
            IF (AUX_TYPE(I).EQ.1) THEN
              WRITE (1,*) NUM_COMB(I)
            ELSE
              WRITE (1,*) AUXTHETA(I),AUXPHI(I)
              WRITE (1,*) ILLCX(I),ILLCY(I),IURCX(I),IURCY(I)
            END IF
460       CONTINUE
          WRITE (1,*) ISEED0
          WRITE (1,*) AMPVAR
          WRITE (1,*) PHVAR
          WRITE (1,*) DB
          CLOSE (UNIT=1)

          STOP
          END

          SUBROUTINE MM_SETUP(MM,MM0,SPACING,BEAM_TH,BEAM_PH,
     &                        N_X,N_Y,DB)
C
C         This program calculates the weights
C         of a Dolph-Chebychev array.
C         The program uses Bresler's nested product algorithm.
C         For details see:
C                 'A New Algorithm for Calculating the Current Distribution
C                  of Dolph-Chebychev Arrays', A.D. Bresler, IEEE
C                  Trans. Antennas & Prop., Nov. 1980. p 951.
C
C
          REAL IK(0:50),XNP,SIG,ALPHA,Q,BETA,PY,MM0(100,50)
          REAL CHEBX(100),CHEBY(50),F,GAIN,D0,D0X,D0Y,XNORM
          COMPLEX MM(100,50),SUM
          INTEGER N_X,N_Y
          REAL BEAM_TH,BEAM_PH,PSI_IJ
          PY=3.14159265358979E+00
          DTR=PY/180.0E+0
          WRITE (6,9)
          WRITE (6,10)
          WRITE (6,11)
          WRITE (6,12)
9         FORMAT(' MAIN BEAM COMBINER OPTIONS:')
10        FORMAT('    1 -- FOR UNIFORM WEIGHTS')
11        FORMAT('    2-- FOR DOLPH-CHEBYSHEV WEIGHTS')
12        FORMAT(' Enter code for desired option:',$)
          READ (5,*) UC
          IF (UC.EQ.1) THEN

            GAIN=SQRT(FLOAT(N_X*N_Y))
            DO 51 I=1,N_X
              DO 50 J=1,N_Y
                CALL CALC_PSI(SPACING,BEAM_TH,BEAM_PH,I,J,PSI_IJ)
                MM(I,J)=CONJG(CEXP(CMPLX(0.,PSI_IJ)))/GAIN
50            CONTINUE
51          CONTINUE

          ELSE
```

```
      WRITE (6,1)
      READ (5,*) DB
1     FORMAT(' ENTER THE SIDELOBE RATIO IN DB (>0): ',$)
      IEVEN=0
      M=N_X
      IF (M.EQ.1) THEN
        CHEBX(1)=1
        GO TO 30
      END IF
      N=M/2
      IF (N.EQ.M/2.)THEN
        U=N-1
        IEVEN=1
      ELSE
        U=N
      END IF
      SIG=10**(DB/20.)
      Q=LOG(SIG+SQRT(SIG**2-1))
      BETA=(COSH(Q/(M-1.)))**2
      ALPHA=1.-1./BETA

      DO 14 NN=1,U
       IK(N-NN)=(M-1)*ALPHA*XNP(M,NN,ALPHA)
14    CONTINUE

      IK(N)=1.
      IF (IEVEN.EQ.1) THEN
        DO 17 I=1,N
          CHEBX(I)=IK(N+1-I)
          CHEBX(N+I)=IK(I)
17      CONTINUE
      ELSE
        CHEBX(N+1)=2*IK(0)
        DO 25 I=1,N
          CHEBX(I)=IK(N+1-I)
          CHEBX(N+I+1)=IK(I)
25      CONTINUE
      END IF

30    M=N_Y
      IEVEN=0
      IF (M.EQ.1) THEN
        CHEBY(1)=1
        GO TO 40
      END IF
      N=M/2
      IF (N.EQ.M/2.)THEN
        U=N-1
        IEVEN=1
      ELSE
        U=N
      END IF
      BETA=(COSH(Q/(M-1.)))**2
      ALPHA=1.-1./BETA

      DO 35 NN=1,U
        IK(N-NN)=(M-1)*ALPHA*XNP(M,NN,ALPHA)
35    CONTINUE

      IK(N)=1.

      IF (IEVEN.EQ.1) THEN
       DO 36 I=1,N
         CHEBY(I)=IK(N+1-I)
         CHEBY(N+I)=IK(I)
```

```
36        CONTINUE
         ELSE
          CHEBY(N+1)=2*IK(0)
          DO 37 I=1,N
            CHEBY(I)=IK(N+1-I)
            CHEBY(N+I+1)=IK(I)
37        CONTINUE
         END IF

C  Normalization: Formulas for directivity of D/C arrays from Balanis

40         F=1.+0.636*(2.*COSH(SQRT(Q**2.-PY**2.))/SIG)**2
           IF (N_X.EQ.1) THEN
             D0=2.*(SIG**2)/(1.+(SIG**2.-1.)*F*(2./N_Y))
           ELSE IF (N_Y.EQ.1) THEN
             D0=2.*(SIG**2)/(1.+(SIG**2.-1.)*F*(2./N_X))
           ELSE
             D0X=2.*(SIG**2)/(1.+(SIG**2.-1.)*F*(2./N_X))
             D0Y=2.*(SIG**2)/(1.+(SIG**2.-1.)*F*(2./N_Y))
             D0=PY*COS(DTR*BEAM_TH)*D0X*D0Y
           END IF
           SUM=0.
           DO 61 I=1,N_X
             DO 60 J=1,N_Y
               MM0(I,J)=CMPLX(CHEBX(I)*CHEBY(J))
               SUM=SUM+MM0(I,J)
60           CONTINUE
61         CONTINUE
           XNORM=SQRT(D0)/CABS(SUM)
           WRITE (6,*) ' Balanis gain=',D0
           DO 71 I=1,N_X
             DO 70 J=1,N_Y
               CALL CALC_PSI(SPACING,BEAM_TH,BEAM_PH,I,J,PSI_IJ)
               MM(I,J)=XNORM*MM0(I,J)*CONJG(CEXP(CMPLX(0.,PSI_IJ)))
70           CONTINUE
71         CONTINUE

         END IF

20       RETURN
         END

         FUNCTION XNP(M,N,ALPHA)
         REAL ALPHA,F

         XNP=1.0
         DO 10 I=1,N-1
           F=I*FLOAT(M-1-2*N+I)/FLOAT((N-I)*(N+1-I))
           XNP=XNP*ALPHA*F+1.0
10       CONTINUE

         RETURN
         END

         SUBROUTINE G_SETUP(G,N_X,N_Y,IGCODE,AMPVAR,PHVAR,ISEED)
         COMPLEX G(100,50)
         REAL YPH,PIJ,GIJ,EPS
         INTEGER N_X,N_Y

         CALL RANSET(ISEED)

         PI=4.*ATAN(1.)
         IF (IGCODE.EQ.1) THEN
           DO 11 I=1,N_X
             DO 10 J=1,N_Y
               G(I,J)=(1.,0.)
```

```
10          CONTINUE
11        CONTINUE
        ELSE IF (IGCODE.EQ.2) THEN
          DO 21 I=1,N_X
            DO 20 J=1,N_Y
              YPH=2.*RANF(`-1
              PIJ=PI*PHVAR*YPH/180.
              EPS=1.-10.**(-0.05*AMPVAR)
              GIJ=1+EPS*(2.*RANF()-1)
              G(I,J)=GIJ*CEXP(CMPIX(0.,PIJ))
20          CONTINUE
21        CONTINUE
        END IF

        RETURN
        END


        SUBROUTINE CALC_PSI(SPACING,THETA,PHI,I,J,PSI)
        REAL THETA,PHI,PSI,DTR
        PY=3.141592653589793E+00
        DTR=PY/180.0E+00
        PSI=((I-1)*COS(PHI*DTR)+(J-1)*SIN(PHI*DTR))
     &      *SIN(THETA*DTR)*2.*PY*SPACING
        RETURN
        END
```

```
C   This program creates the option file containing the information needed
C    by MASTER to do a specified set of calculations. This data is stored in
C    the file 'fort.2' which is read by program MASTER.

      PROGRAM OPTFILEGEN
      REAL ULO,UUP,THMAX,AERR,RERR
      CHARACTER*20 OPTFILE,FILENAME,OUTFILE,INTEGFILE

      PI=3.141592653589793E+00
      DTR=PI/180.

      WRITE (6,5)
      READ (5,6) OPTFILE
      WRITE (6,10)
      READ (5,6) FILENAME
      WRITE (6,11)
      READ (5,6) OUTFILE

5     FORMAT(' Enter name for option datafile:',$)
6     FORMAT(A)
10    FORMAT(' Enter name of input file containing array data:',$)
11    FORMAT(' Enter name of output datafile(results):',$)

      WRITE (6,3)
 3    FORMAT(//'ELEMENT PATTERN OPTIONS:',/,5X,
     &          '0--isotropic',/,5X,
     &          '1--finite length monopole over a dielectric',/,5X,
     &          '2--ideal monopole',/,3X,
     &         'Enter code for desired option:',$)
      READ (5,*) IELCODE

      WRITE (6,*)
      WRITE (6,12)
12    FORMAT(///' ::AVERAGE SLL INTEGRATION?:',/,5X,
     &        '1--YES',/,5X,
     &        '0--NO',/,3X,
     &        'Enter code for desired option:',$)
      READ (5,*) IAVCODE
      IF (IAVCODE.EQ.1) THEN
         WRITE (6,21)
         READ (5,*) IAVCODE2
         WRITE (6,22)
         READ (5,6) INTEGFILE
         IF (IAVCODE2.EQ.1) THEN
           WRITE (6,13)
           READ (5,*) THMAX
           UUP=SIN(THMAX*DTR)
           ULO=-1.0*UUP
           WRITE (6,15)
           READ (5,*) AERR,RERR
         END IF
      END IF
13    FORMAT(' Enter maximum theta value(deg.):',$)
15    FORMAT(' Enter absolute, relative errors for integration:',$)
21    FORMAT(/,' Enter 1 to compute subintegrals,'/
     &        ,'  else 0 to read from datafile:',$)
22    FORMAT(/,' Enter name of datafile for integration data:',$)

16     WRITE(6,20)
20     FORMAT(////
C*
     &   ,1X,'::COMPUTATION MENU:: ',//,3X
     & '1--To CALC. performance at a single point and save PATTERN',/,3X
     &   ,'2--To SCAN on THETA_D or PHI_D',/,3X
     &   ,'3--To SCAN on THETA_I or PHI_I',/,3X
     &   ,'4--To SCAN on SNR',/,3X
```

```
     &    ,'5--To SCAN on INR',/,3X
     &    ,'6--To END execution-no further computations',//,1X
     &    ,'Enter code for desired option:',$)

          READ(5,*) ICOMPCODE

          IF (ICOMPCODE.EQ.2) THEN
            WRITE (6,260)
            READ (5,*) I_TH_PH
            IF (I_TH_PH.EQ.1) THEN

            WRITE (6,210) 'D'
            READ (5,*) SCANMIN
            WRITE (6,220) 'D'
            READ (5,*) SCANMAX
            WRITE (6,230)
 40         READ (5,*) SIZE_INC
            NUM_PTS=INT((SCANMAX-SCANMIN)/SIZE_INC+1.5)
            IF (NUM_PTS.GT.400) THEN
               WRITE (6,250)
               GO TO 40
            END IF

            ELSE IF(I_TH_PH.EQ.2) THEN

            WRITE (6,270) 'D'
            READ (5,*) SCANMIN
            WRITE (6,280) 'D'
            READ (5,*) SCANMAX
            WRITE (6,230)
 60         READ (5,*) SIZE_INC
            NUM_PTS=INT((SCANMAX-SCANMIN)/SIZE_INC+1.5)
            IF (NUM_PTS.GT.400) THEN
               WRITE (6,250)
               GO TO 60
            END IF

            END IF

          ELSE IF (ICOMPCODE.EQ.3) THEN

            WRITE (6,255)
 77         READ (5,*) JAM_NUM
            IF (JAM_NUM.GT.5) THEN
              WRITE (6,256)
              GOTO 77
            END IF
            WRITE (6,260)
            READ (5,*) I_TH_PH
            IF (I_TH_PH.EQ.1) THEN

            WRITE (6,210) 'I'
            READ (5,*) SCANMIN
            WRITE (6,220) 'I'
            READ (5,*) SCANMAX
            WRITE (6,230)
 90         READ (5,*) SIZE_INC
            NUM_PTS=INT((SCANMAX-SCANMIN)/SIZE_INC+1.5)
            IF (NUM_PTS.GT.400) THEN
               WRITE (6,250)
               GO TO 90
            END IF

            ELSE IF(I_TH_PH.EQ.2) THEN

            WRITE (6,270) 'I'
```

```
            READ (5,*) SCANMIN
            WRITE (6,280) 'I'
            READ (5,*) SCANMAX
            WRITE (6,230)
101         READ (5,*) SIZE_INC
            NUM_PTS=INT((SCANMAX-SCANMIN)/SIZE_INC+1.5)
            IF (NUM_PTS.GT.400) THEN
               WRITE (6,250)
               GO TO 101
            END IF

            END IF

          ELSE IF (ICOMPCODE.EQ.4) THEN

            WRITE (6,310) 'SNR'
            READ (5,*) SCANMIN
            WRITE (6,320) 'SNR'
            READ (5,*) SCANMAX
            WRITE (6,230)
120         READ (5,*) SIZE_INC
            NUM_PTS=INT((SCANMAX-SCANMIN)/SIZE_INC+1.5)
            IF (NUM_PTS.GT.400) THEN
               WRITE (6,250)
               GO TO 120
            END IF

          ELSE IF (ICOMPCODE.EQ.5) THEN

            WRITE (6,255)
130         READ (5,*) JAM_NUM
            IF (JAM_NUM.GT.5) THEN
              WRITE (6,256)
              GOTO 130
            END IF
            WRITE (6,310) 'INR'
            READ (5,*) SCANMIN
            WRITE (6,320) 'INR'
            READ (5,*) SCANMAX
            WRITE (6,230)
145         READ (5,*) SIZE_INC
            NUM_PTS=INT((SCANMAX-SCANMIN)/SIZE_INC+1.5)
            IF (NUM_PTS.GT.400) THEN
               WRITE (6,250)
               GO TO 145
            END IF

          END IF

210       FORMAT(' ENTER THE MINIMUM THETA_',A1,' VALUE: ',$)
220       FORMAT(' ENTER THE MAXIMUM THETA_',A1,' VALUE: ',$)
230       FORMAT(' ENTER THE INCREMENT SIZE: ',$)
250       FORMAT(' ENTER A LARGER INCREMENT SIZE: ',$)
255       FORMAT(' ENTER NUMBER OF JAMMER: ',$)
256       FORMAT(' ENTER A SMALLER JAMMER NUMBER: ',$)
260       FORMAT(' ENTER 1 TO SCAN THETA AND 2 TO SCAN PHI: ',$)
270       FORMAT(' ENTER THE MINIMUM PHI_','A1,' VALUE: ',$)
280       FORMAT(' ENTER THE MAXIMUM PHI_','A1,' VALUE: ',$)
310       FORMAT(' ENTER THE MINIMUM ',A3,' VALUE: ',$)
320       FORMAT(' ENTER THE MAXIMUM ',A3,' VALUE: ',$)

          OPEN (UNIT=1,FILE=OPTFILE,STATUS='NEW')

          WRITE (1,6) FILENAME
          WRITE (1,6) OUTFILE
          WRITE (1,*) IELCODE
```

```
WRITE (1,*) IAVCODE
IF (IAVCODE.EQ.1) THEN
  WRITE (1,*) IAVCODE2
  WRITE (1,6) INTEGFILE
  IF (IAVCODE2.EQ.1) THEN
    WRITE (1,*) ULO,UUP
    WRITE (1,*) AERR,RERR
  END IF
END IF
WRITE (1,*) ICOMPCODE
IF (ICOMPCODE.NE.1) THEN
  IF (ICOMPCODE.EQ.2) WRITE (1,*) I_TH_PH
  IF (ICOMPCODE.EQ.3) THEN
    WRITE (1,*) JAM_NUM
    WRITE (1,*) I_TH_PH
  END IF
  IF (ICOMPCODE.EQ.5) WRITE (1,*) JAM_NUM
  WRITE (1,*) SCANMIN
  WRITE (1,*) SCANMAX
  WRITE (1,*) SIZE_INC
END IF

CLOSE (UNIT=1)


STOP
END
```

```
C   Program MASTER reads the OPTION file from OPTFILEGEN, then
C    the INPUT file from FILEGEN, and computes array performance.
C    Results are sent to an OUTPUT file whose name was specified in
C    the OPTION file. By default it is assumed that the OPTION file
C    resides on FORTRAN logical unit 2: fort.2 in UNICOS.

        PROGRAM MASTER
        REAL BEAM_TH,BEAM_PH,PDMAIN,PIMAIN,PNMAIN
        REAL SIG2,AVSLMAIN,SNR,INR(5)
        REAL YMAIN1,YMAIN2,YAUX1(12),YAUX2(12),ULO,UUP,U1,U2
        REAL AD,AI(5),BWD,BWI(5),TH_D,TH_I(5),PH_D,PH_I(5),PSIDL(12)
        INTEGER NUM_JAM,NUM_PTS,IAVCODE,ICOMPCODE
        INTEGER N_X,N_Y,NUM_AUX
        COMPLEX MM(100,50),G(100,50),A(12,100,50),W(12)
        COMPLEX YAM1(12),YAM2(12),YAA1(12,12),YAA2(12,12)
        CHARACTER*20 FILENAME,OUTFILE,INTEGFILE
        COMMON/SIGVARS/TH_D,TH_I,PH_D,PH_I,BWD,BWI,SNR,INR,AD,AI,SIG2,
     &                 NUM_JAM
        COMMON/ARRVARS/N_X,N_Y,SPACING,BEAM_TH,BEAM_PH,G,MM,NUM_AUX,
     &                  A,PSIDL,W,AMPVAR,PHVAR,ISEED0,DB,IELCODE
        COMMON/NAME/FILENAME,OUTFILE,INTEGFILE
        COMMON/INTVARS/IAVCODE,AVSLMAIN,YMAIN1,YMAIN2,YAUX1,YAUX2,
     &                  YAM1,YAM2,YAA1,YAA2,ULO,UUP,U1,U2
        COMMON/INT2D/V1,V2


C   Open option file--contains input, output file info, and data
C     regarding computations to be done

        READ (2,10) FILENAME
        READ (2,10) OUTFILE

10      FORMAT(A)

        WRITE (6,11) FILENAME
        WRITE (6,12) OUTFILE
11      FORMAT (/' INPUT FILENAME=',A20)
12      FORMAT (' OUTPUT FILENAME=',A20,/)

C   Initialize noise power to unity

        SIG2=1.0

        CALL INFILERD
C
        READ (2,*) IELCODE
        READ (2,*) IAVCODE

C  Compute the sub-integrals to enable quick calculation of Average SLL.
C   Also compute the average SLL of the main beam via integration

        IF (IAVCODE.EQ.1) THEN
          READ (2,*) IAVCODE2
          READ (2,10) INTEGFILE
          IF (IAVCODE2.EQ.1) THEN
            CALL INTEGSL
          ELSE
            OPEN (UNIT=3,FILE=INTEGFILE,STATUS='OLD')
            READ (3,*) ULO,UUP
            READ (3,*) U1,U2
            IF (N_Y.NE.1) READ (3,*) V1,V2
            READ (3,*) YMAIN1,YMAIN2
            DO 50 I=1,NUM_AUX
             READ (3,*) YAUX1(I),YAUX2(I)
             READ (3,*) YAM1(I),YAM2(I)
             DO 49 J=1,I-1
```

```
            READ (3,*) YAA1(I,J),YAA2(I,J)
49          CONTINUE
50        CONTINUE
          CLOSE (UNIT=3,STATUS='KEEP')
        END IF
        CALL AVSLCOMP(AVSLMAIN)
        IF (N_Y.EQ.1) THEN
          WRITE (6,13) U1,U2
        ELSE
          WRITE (6,15) U1,V1,U2,V2
        END IF
        WRITE (6,14) AVSLMAIN
      END IF
13    FORMAT(//' Mainbeam region(in u):[',F7.5,',',F7.5,']')
14    FORMAT(' Mainbeam Average SLL=',F9.4,' dB',/)
15    FORMAT(' Mainbeam region (in u,v):[(',F7.5,',',F7.5,') , ('
     &          ,F7.5,',',F7.5,')]')


      READ (2,*) ICOMPCODE

      IF (ICOMPCODE.EQ.1)  CALL SINGLEPT
C
      IF (ICOMPCODE.EQ.2)  CALL SCAN_D
C
      IF (ICOMPCODE.EQ.3)  CALL SCAN_I
C
      IF (ICOMPCODE.EQ.4)  CALL SCAN_SNR
C
      IF (ICOMPCODE.EQ.5)  CALL SCAN_INR
C
      IF (ICOMPCODE.EQ.6)  GO TO 99
C

99    STOP
      END


C     Subroutine CALC_PSI
C
C     This subroutine calculates the phase shift at the carrier center
C     frequency seen between element (I,J) and element (1,1) under
C     the assumption that the elements are arranged in a square
C     grid in the XY plane with half-wavelength element spacing.
C
C
      SUBROUTINE CALC_PSI(SPACING,THETA,PHI,I,J,PSI_IJ)
      REAL THETA,PHI,PSI_IJ
      PI=3.141592653589793E+00
      DTR=PI/180.0E+00
      PSI_IJ=((I-1)*COS(PHI*DTR)+(J-1)*SIN(PHI*DTR))
     &        *SIN(THETA*DTR)*2.*PI*SPACING

      RETURN
      END




C
C     SUBROUTINE ELEMENT_PATTERN multiplies a signal amplitude by
C     the selected element pattern. The element pattern is selected in
C     the option file:
C          IELCODE=1: an isotropic element
C          IELCODE=2: an isolated monopole on a dielectric coated
C                     ground plane.
```

```
C               IELCODE=3: an ideal infinitesimal monopole (a sin(theta)
C                          pattern)
C
      SUBROUTINE ELPATT(A,THETA,PHI,IELCODE)
      INTEGER IELCODE
      REAL A,THETA,PHI,PI,DTR,F1,RG,K0H,COSTH,SINTH
      REAL PNORM,HNORM,EPSR
      COMPLEX F2

      PI=3.141592653589793E+00
      DTR=PI/180.0E+00

      IF (IELCODE.EQ.0) THEN
       A=1.0
      ELSE IF (IELCODE.EQ.1) THEN
       EPSR=5.        !  Relative permittivity of dielectric layer
       HNORM=0.75     !  Height in wavelengths
       PNORM=1.828085343639275 !  Normalizing the element pattern

       K0H=2.*PI*HNORM
       COSTH=COS(THETA*DTR)
       SINTH=SIN(THETA*DTR)

       F1=SQRT(EPSR-SINTH**2)
       RG=(EPSR*COSTH-F1)/(EPSR*COSTH+F1)
       F2=CEXP(CMPLX(0.,K0H*COSTH))-CMPLX(COS(K0H),SIN(K0H)*COSTH)

       IF (THETA.EQ.0.) THEN
         A=0.
       ELSE
         A=CABS((F2+RG*CONJG(F2))/SINTH)/PNORM
       END IF
      ELSE IF (IELCODE.EQ.2) THEN
       A=ABS(SIN(THETA*DTR))
      END IF

      RETURN
      END


C     Subroutine MAIN
C     This subroutine calculates the performance of a phased array
C     with a coherent sidelobe canceller.  The auxilliary channels
C     for the canceller are each created by combining a weighted
C     sum of a few array elements.
C     This version contains E_*IJLM,  and other such routines, in
C     line. It should run faster and will enable the vectorization
C     of the major loops when put on the CRAY.
C
      SUBROUTINE MAIN(PD,PI,PN,PDMAIN,PIMAIN,PNMAIN)
      REAL SPACING,BEAM_TH,BEAM_PH,PATT,PI2
      REAL SNR,INR(5),SIG2,AMPVAR,PHVAR
      REAL AD,AI(5),BWD,BWI(5),TH_D,TH_I(5),PH_D,PH_I(5),PSIDL(12)
      REAL PD,PI,PN,PDMAIN,PIMAIN,PNMAIN
      REAL DSINC,X,PSI_IJ,PSI_LM,PSI,PSID,PSII(5),ATEMP
      REAL CTD,STD,CPD,SPD,CTI(5),STI(5),CPI(5),SPI(5),LNORM
      INTEGER N_X,N_Y,NUM_AUX,MAX_AUX,NUM_JAM,ISEED0,IND(12),NDD
      COMPLEX G(100,50)
      COMPLEX PTEMP1,PTEMP2,PTEMP3,R,E1,XG
      COMPLEX MM(100,50),A(12,100,50),V(12),TEMP,TEMP1,TEMP2
      COMPLEX VDES(12),VINT(12),VNSE(12),PHIDES(12,12)
      COMPLEX W(12),PHI(12,12),PHINSE(12,12),PHIINT(12,12),SV(12)
      COMMON/SIGVARS/TH_D,TH_I,PH_D,PH_I,BWD,BWI,SNR,INR,AD,AI,SIG2,
     &               NUM_JAM
      COMMON/ARRVARS/N_X,N_Y,SPACING,BEAM_TH,BEAM_PH,G,MM,NUM_AUX,
     &               A,PSIDL,W,AMPVAR,PHVAR,ISEED0
```

```
      COMMON/AOAVARS/CTD,STD,CPD,SPD,CTI,STI,CPI,SPI
      PARAMETER(PY=3.141592653589793E+00,MAX_AUX=12)

      LNORM=2*PY*SPACING
      PD=0.
      PI=0.
      PN=0.
      PIMAIN=0.
      PDMAIN=0.
      PNMAIN=0.
      V=(0.,0.)
      VDES=(0.,0.)
      VINT=(0.,0.)
      VNSE=(0.,0.)
      PHI=(0.,0.)
      PHIDES=(0.,0.)
      PHIINT=(0.,0.)
      PHINSE=(0.,0.)

C
C     The element pattern in the (theta,phi) directions are added
C        here as multiplicative gains on AD and AI.
C
      ATEMP=SQRT(10**(0.1*SNR))
      CALL ELPATT(PATT,TH_D,PH_D)
      AD=ATEMP*PATT

      DO 15 I=1,NUM_JAM
        ATEMP=SQRT(10.**(0.1*INR(I)))
        CALL ELPATT(PATT,TH_I(I),PH_I(I))
        AI(I)=ATEMP*PATT
15    CONTINUE

C
C     CALCULATE THE STEERING VECTOR, V; AND THE COVARIANCE MATRIX PHI
C
      DO 145 I=1,N_X
        DO 140 J=1,N_Y
          DO 135 K=1,NUM_AUX
           IF (CABS(A(K,I,J)).NE.0.) THEN
            DO 130 M=1,N_Y
              DO 125 L=1,N_X
               PSI_IJ=((I-1)*CPD+(J-1)*SPD)*STD*LNORM
               PSI_LM=((L-1)*CPD+(M-1)*SPD)*STD*LNORM
               PSI=PSI_LM-PSI_IJ-PSIDL(K)
               X=BWD*PSI*0.5
               IF (X.EQ.0.) THEN
                 DSINC=1.
               ELSE
                 DSINC=SIN(X)/X
               END IF
               R=AD*AD*DSINC*CEXP(CMPLX(0.,PSI))
               VDES(K)=VDES(K)+CONJG(A(K,I,J)*G(I,J))*MM(L,M)
     &                        *G(L,M)*R
125           CONTINUE
130         CONTINUE
           END IF
135       CONTINUE
140     CONTINUE
145   CONTINUE

      DO 250 KK=1,NUM_JAM

      DO 245 I=1,N_X
        DO 240 J=1,N_Y
          DO 235 K=1,NUM_AUX
```

```
              IF (CABS(A(K,I,J)).NE.0.) THEN
               DO 230 M=1,N_Y
                 DO 225 L=1,N_X
                   PSI_IJ=((I-1)*CPI(KK)+(J-1)*SPI(KK))*STI(KK)*LNORM
                   PSI_LM=((L-1)*CPI(KK)+(M-1)*SPI(KK))*STI(KK)*LNORM
                   PSI=PSI_LM-PSI_IJ-PSIDL(K)
                   X=BWI(KK)*PSI*0.5
                   IF (X.EQ.0.) THEN
                     DSINC=1.
                   ELSE
                     DSINC=SIN(X)/X
                   END IF
                   R=AI(KK)*AI(KK)*DSINC*CEXP(CMPLX(0.,PSI))
                   VINT(K)=VINT(K)+CONJG(A(K,I,J)*G(I,J))*MM(L,M)
     &                     *G(L,M)*R
225              CONTINUE
230            CONTINUE
              END IF
235         CONTINUE
240       CONTINUE
245     CONTINUE

250       CONTINUE

        DO 35 K=1,NUM_AUX
         PSI=-PSIDL(K)
         X=BWD*PSI*0.5
         IF (X.EQ.0) THEN
           DSINC=1.
         ELSE
           DSINC=SIN(X)/X
         END IF
         R=SIG2*DSINC*CEXP(CMPLX(0.,PSI))
         DO 45 J=1,N_Y
          DO 40 I=1,N_X
           VNSE(K)=VNSE(K)+CONJG(A(K,I,J))*MM(I,J)*R
40        CONTINUE
45       CONTINUE
35      CONTINUE

C  Computing the covariance matrix elements:

          DO 335 K=1,NUM_AUX
           DO 345 I=1,N_X
            DO 340 J=1,N_Y
             IF (CABS(A(K,I,J)).NE.0.) THEN
              DO 320 II=1,K
               DO 330 M=1,N_Y
                DO 325 L=1,N_X
                  IF (CABS(A(II,L,M)).NE.0.) THEN
                   PSI_IJ=((I-1)*CPD+(J-1)*SPD)*STD*LNORM
                   PSI_LM=((L-1)*CPD+(M-1)*SPD)*STD*LNORM
                   PSI=PSI_LM+PSIDL(II)-PSI_IJ-PSIDL(K)
                   X=BWD*PSI*0.5
                   IF (X.EQ.0.) THEN
                     DSINC=1.
                   ELSE
                     DSINC=SIN(X)/X
                   END IF
                   R=AD*AD*DSINC*CEXP(CMPLX(0.,PSI))
                  ELSE
                   R=0.
                  END IF
                  PHIDES(K,II)=PHIDES(K,II)+CONJG(A(K,I,J)*G(I,J))
     &                        *A(II,L,M)*G(L,M)*R
325             CONTINUE
```

```
330             CONTINUE
320            CONTINUE
              END IF
340           CONTINUE
345          CONTINUE
335         CONTINUE

            DO 490 KK=1,NUM_JAM

            DO 435 K=1,NUM_AUX
             DO 445 I=1,N_X
              DO 440 J=1,N_Y
               IF (CABS(A(K,I,J)).NE.0.) THEN
                DO 420 II=1,K
                 DO 430 M=1,N_Y
                  DO 425 L=1,N_X
                   IF (CABS(A(II,L,M)).NE.0.) THEN
                     PSI_IJ=((I-1)*CPI(KK)+(J-1)*SPI(KK))*STI(KK)*LNORM
                     PSI_LM=((L-1)*CPI(KK)+(M-1)*SPI(KK))*STI(KK)*LNORM
                     PSI=PSI_LM+PSIDL(II)-PSI_IJ-PSIDL(K)
                     X=BWI(KK)*PSI*0.5
                     IF (X.EQ.0.) THEN
                       DSINC=1.
                     ELSE
                       DSINC=SIN(X)/X
                     END IF
                     R=AI(KK)*AI(KK)*DSINC*CEXP(CMPLX(0.,PSI))
                   ELSE
                     R=0.
                   END IF
                   PHIINT(K,II)=PHIINT(K,II)+CONJG(A(K,I,J)*G(I,J))
     &                              *A(II,L,M)*G(L,M)*R
425                CONTINUE
430               CONTINUE
420              CONTINUE
                END IF
440            CONTINUE
445           CONTINUE
435         CONTINUE

490         CONTINUE

            DO 835 K=1,NUM_AUX
             DO 820 II=1,K
              PSI=-PSIDL(K)+PSIDL(II)
              X=BWD*PSI*0.5
              IF (X.EQ.0) THEN
                DSINC=1.
              ELSE
                DSINC=SIN(X)/X
              END IF
              R=SIG2*DSINC*CEXP(CMPLX(0.,PSI))
              DO 845 J=1,N_Y
               DO 840 I=1,N_X
                PHINSE(K,II)=PHINSE(K,II)+CONJG(A(K,I,J))*A(II,I,J)
     &                          *R
840             CONTINUE
845            CONTINUE
820           CONTINUE
835         CONTINUE


C
C
C
          DO 160 II=1,NUM_AUX
```

```
            V(II)=VDES(II)+VINT(II)+VNSE(II)
            SV(II)=-1.*V(II)
            DO 159 JJ=1,II
              PHI(II,JJ)=PHIDES(II,JJ)+PHIINT(II,JJ)+PHINSE(II,JJ)
              IF (JJ.NE.II) PHI(JJ,II)=CONJG(PHI(II,JJ))
159         CONTINUE
160       CONTINUE

c          write (6,*)
c         DO 93 I=1,NUM_AUX
c            WRITE (6,101) I,V(I)
c            WRITE (6,102) I,VDES(I)
c            WRITE (6,103) I,VINT(I)
c            WRITE (6,104) I,VNSE(I)
c93       CONTINUE
c         DO 92 I=1,NUM_AUX
c            DO 91 J=1,NUM_AUX
c               WRITE (6,105) I,J,PHI(I,J)
c               WRITE (6,106) I,J,PHIDES(I,J)
c               WRITE (6,107) I,J,PHIINT(I,J)
c               WRITE (6,108) I,J,PHINSE(I,J)
c91         CONTINUE
c92       CONTINUE
c101      FORMAT(' V(',I1,')=',E23.16,'+j',E23.16)
c102      FORMAT(' VDES(',I1,')=',E23.16,'+j',E23.16)
c103      FORMAT(' VINT(',I1,')=',E23.16,'+j',E23.16)
c104      FORMAT(' VNSE(',I1,')=',E23.16,'+j',E23.16)
c105      FORMAT(' PHI(',I1,',',I1,')=',E23.16,'+j',E23.16)
c106      FORMAT(' PHIDES(',I1,',',I1,')=',E23.16,'+j',E23.16)
c107      FORMAT(' PHIINT(',I1,',',I1,')=',E23.16,'+j',E23.16)
c108      FORMAT(' PHINSE(',I1,',',I1,')=',E23.16,'+j',E23.16)

C
C         Solve the system [PHI][W]=-[V]
C
          IF (NUM_AUX.GT.1) THEN
            CALL LUDCMP(PHI,NUM_AUX,MAX_AUX,IND,NDD)
            CALL LUBKSB(PHI,NUM_AUX,MAX_AUX,IND,SV)
            DO 170 I=1,NUM_AUX
              W(I)=SV(I)
170         CONTINUE
          ELSE IF (NUM_AUX.EQ.1) THEN
            W(1)=SV(1)/PHI(1,1)
          ELSE
            W=(0.0,0.0)
          END IF

C
C         Calculate the interference,desired, and noise signal power without auxiliar
C           elements; i.e. the interference,desired, and thermal noise power present
C           the main beam
C
          PTEMP1=(0.,0.)
          PTEMP2=(0.,0.)
          PTEMP3=(0.,0.)

          DO 550 I=1,N_X
           DO 549 J=1,N_Y
            DO 548 M=1,N_Y
             DO 547 L=1,N_X
              PSI_IJ=((I-1)*CPD+(J-1)*SPD)*STD*LNORM
              PSI_LM=((L-1)*CPD+(M-1)*SPD)*STD*LNORM
              PSI=PSI_LM-PSI_IJ
              X=BWD*PSI*0.5
              IF (X.EQ.0.) THEN
                DSINC=1.
```

```
            ELSE
              DSINC=SIN(X)/X
            END IF
            R=AD*AD*DSINC*CEXP(CMPLX(0.,PSI))
            PTEMP1=PTEMP1+CONJG(MM(I,J)*G(I,J))*MM(L,M)*G(L,M)*R
547         CONTINUE
548        CONTINUE
549       CONTINUE
550      CONTINUE

         DO 700 JAM_NUM=1,NUM_JAM

         DO 650 I=1,N_X
          DO 649 J=1,N_Y
           DO 648 M=1,N_Y
            DO 647 L=1,N_X
              PSI_IJ=((I-1)*CPI(JAM_NUM)+(J-1)*SPI(JAM_NUM))
     &              *STI(JAM_NUM)*LNORM
              PSI_LM=((L-1)*CPI(JAM_NUM)+(M-1)*SPI(JAM_NUM))
     &              *STI(JAM_NUM)*LNORM
              PSI=PSI_LM-PSI_IJ
              X=BWI(JAM_NUM)*PSI*0.5
              IF (X.EQ.0.) THEN
                DSINC=1.
              ELSE
                DSINC=SIN(X)/X
              END IF
              R=AI(JAM_NUM)*AI(JAM_NUM)*DSINC*CEXP(CMPLX(0.,PSI))
              PTEMP2=PTEMP2+CONJG(MM(I,J)*G(I,J))*MM(L,M)*G(L,M)*R
647         CONTINUE
648        CONTINUE
649       CONTINUE
650      CONTINUE

700      CONTINUE

         DO 750 J=1,N_Y
          DO 749 I=1,N_X
           PTEMP3=PTEMP3+CONJG(MM(I,J))*MM(I,J)*SIG2
749       CONTINUE
750      CONTINUE


         PDMAIN=0.5*REAL(PTEMP1)
         PIMAIN=0.5*REAL(PTEMP2)
         PNMAIN=0.5*REAL(PTEMP3)

C        Calculate the desired, interfering, and noise signal power at the
C          array output.
C
         PD=PDMAIN
         PI=PIMAIN
         PN=PNMAIN
         DO 300 I=1,NUM_AUX
           PTEMP1=(0.,0.)
           PTEMP2=(0.,0.)
           PTEMP3=(0.,0.)
           DO 299 J=1,I-1
             PTEMP1=PTEMP1+W(J)*PHIDES(I,J)
             PTEMP2=PTEMP2+W(J)*PHIINT(I,J)
             PTEMP3=PTEMP3+W(J)*PHINSE(I,J)
299        CONTINUE
           PD=PD+0.5*CABS(W(I))**2.*PHIDES(I,I)+REAL(CONJG(W(I))*
     &       (VDES(I)+PTEMP1))
           PI=PI+0.5*CABS(W(I))**2.*PHIINT(I,I)+REAL(CONJG(W(I))*
     &       (VINT(I)+PTEMP2))
```

```
          PN=PN+0.5*CABS(W(I))**2.*PHINSE(I,I)+REAL(CONJG(W(I))*
     &       (VNSE(I)+PTEMP3))
300     CONTINUE


        RETURN
        END

C  Subroutine LUDCMP is a general linear equation solver for
C   systems with complex coeffiecients. It is used by subroutine
C   MAIN to solve [PHI][W]=-[V] for the weights.

        SUBROUTINE LUDCMP(A,N,NP,INDX,D)
        PARAMETER (NMAX=12,TINY=1.0E-20)
        COMPLEX A(NP,NP),SUM,DUM1
        REAL VV(NMAX),AAMAX,DUM
        INTEGER INDX(NP),D,IMAX
        D=1
        DO 12 I=1,N
          AAMAX=0.
          DO 11 J=1,N
            IF (ABS(A(I,J)).GT.AAMAX) AAMAX=ABS(A(I,J))
11        CONTINUE
          IF (AAMAX.EQ.0.) PAUSE 'Singular matrix'
          VV(I)=1./AAMAX
12      CONTINUE
        DO 19 J=1,N
          IF (J.GT.1) THEN
            DO 14 I=1,J-1
              SUM=A(I,J)
              IF (I.GT.1) THEN
                DO 13 K=1,I-1
                  SUM=SUM-A(I,K)*A(K,J)
13              CONTINUE
                A(I,J)=SUM
              END IF
14          CONTINUE
          END IF
          AAMAX=0.
          DO 16 I=J,N
            SUM=A(I,J)
            IF (J.GT.1) THEN
              DO 15 K=1,J-1
                SUM=SUM-A(I,K)*A(K,J)
15            CONTINUE
              A(I,J)=SUM
            END IF
            DUM=VV(I)*ABS(SUM)
            IF (DUM.GT.AAMAX) THEN
              IMAX=I
              AAMAX=DUM
            END IF
16        CONTINUE
          IF (J.NE.IMAX) THEN
            DO 17 K=1,N
              DUM1=A(IMAX,K)
              A(IMAX,K)=A(J,K)
              A(J,K)=DUM1
17          CONTINUE
            D=-1*D
            VV(IMAX)=VV(J)
          END IF
          INDX(J)=IMAX
          IF (J.NE.N) THEN
            IF (A(J,J).EQ.(0.,0.)) A(J,J)=TINY
            DUM1=1./A(J,J)
```

```
            DO 18 I=J+1,N
              A(I,J)=A(I,J)*DUM1
18          CONTINUE
          END IF
19        CONTINUE
          IF (A(N,N).EQ.0.) A(N,N)=TINY
          RETURN
          END


          SUBROUTINE LUBKSB(A,N,NP,INDX,B)
          COMPLEX A(NP,NP),B(NP),SUM
          INTEGER INDX(NP),II,LL,I,J
          II=0
          DO 12 I=1,N
            LL=INDX(I)
            SUM=B(LL)
            B(LL)=B(I)
            IF (II.NE.0) THEN
              DO 11 J=II,I-1
                SUM=SUM-A(I,J)*B(J)
11            CONTINUE
            ELSE IF (SUM.NE.(0.,0.)) THEN
              II=I
            END IF
            B(I)=SUM
12        CONTINUE
          DO 14 I=N,1,-1
            SUM=B(I)
            IF (I.LT.N) THEN
              DO 13 J=I+1,N
                SUM=SUM-A(I,J)*B(J)
13            CONTINUE
            END IF
            B(I)=SUM/A(I,I)
14        CONTINUE
          RETURN
          END

C
C         SUBROUTINE SINGLE_PT calculates the array performance for
C         the values specified in the input file.  The performance values,
C         the adapted weights, and the main beam steering matrix (MM) are
C         sent to a data file for later processing by the output program
C

          SUBROUTINE SINGLEPT
          REAL BEAM_TH,BEAM_PH,SPACING,AMPVAR,PHVAR
          REAL PD,PI,PN,PDMAIN,PIMAIN,PNMAIN
          REAL SNR,INR(5),SIG2,AVSLMAIN,AVSL,AVSLCH
          REAL PY,DTR,RDES,RNSE,SINRMAIN,SINR_IR,CR,CRDB,PII
          REAL AD,AI(5),BWD,BWI(5),TH_D,TH_I(5),PH_D,PH_I(5),PSIDL(12)
          REAL CTD,STD,CPD,SPD,CTI(5),STI(5),CPI(5),SPI(5)
          INTEGER N_X,N_Y,NUM_JAM,NUM_AUX,ISEED0,IAVCODE,I_TYPE
          COMPLEX MM(100,50),G(100,50),A(12,100,50),W(12)
          CHARACTER*20 FILENAME,OUTFILE
          COMMON/SIGVARS/TH_D,TH_I,PH_D,PH_I,BWD,BWI,SNR,INR,AD,AI,SIG2,
         &               NUM_JAM
          COMMON/ARRVARS/N_X,N_Y,SPACING,BEAM_TH,BEAM_PH,G,MM,NUM_AUX,
         &                A,PSIDL,W,AMPVAR,PHVAR,ISEED0,DB,IELCODE
          COMMON/NAME/FILENAME,OUTFILE
          COMMON/AOAVARS/CTD,STD,CPD,SPD,CTI,STI,CPI,SPI
          COMMON/INTVARS/IAVCODE,AVSLMAIN

C     Compute sines, cosines of angles of arrival of des., inter. signals
```

```
      PY=3.141592653589793E+00
      DTR=PY/180.
      CTD=COS(TH_D*DTR)
      STD=SIN(TH_D*DTR)
      CPD=COS(PH_D*DTR)
      SPD=SIN(PH_D*DTR)
15    FORMAT(' TH_I(',I1,')=',F9.4,' degrees',3X,' PH_I(',I1,')=',
     &       F9.4,' degrees')
16    FORMAT(' U(',I1,')=',F9.4,'   V(',I1,')=',F9.4)
      DO 20 I=1,NUM_JAM
        CTI(I)=COS(TH_I(I)*DTR)
        STI(I)=SIN(TH_I(I)*DTR)
        CPI(I)=COS(PH_I(I)*DTR)
        SPI(I)=SIN(PH_I(I)*DTR)
20    CONTINUE
      WRITE (6,*)
      DO 21 I=1,NUM_JAM
        WRITE (6,15) I,TH_I(I),I,PH_I(I)
        WRITE (6,16) I,STI(I)*CPI(I),I,STI(I)*SPI(I)
21    CONTINUE
      CALL MAIN(PD,PI,PN,PDMAIN,PIMAIN,PNMAIN)
      RDES=10*LOG10(MAX(PD,1E-10)/MAX(PDMAIN,1E-10))
      RNSE=10*LOG10(PN/PNMAIN)
      SINRMAIN=10.*LOG10(MAX(PDMAIN,1E-10)/(PIMAIN+PNMAIN))
      SINR = 10*LOG10(MAX(PD,1E-10)/(PI+PN))
      SINR_IR=SINR-SINRMAIN
      IF (IAVCODE.EQ.1) THEN
        CALL AVSLCOMP(AVSL)
        AVSLCH=AVSL-AVSLMAIN
      END IF
      WRITE (6,*)
      WRITE (6,90) PD,10*LOG10(MAX(PD,1E-10))
      WRITE (6,91) PI,10*LOG10(MAX(PI,1E-10))
      WRITE (6,92) PN,10*LOG10(PN)
      WRITE (6,93) PDMAIN,10*LOG10(MAX(PDMAIN,1E-10))
      WRITE (6,94) PIMAIN,10*LOG10(MAX(PIMAIN,1E-10))
      WRITE (6,95) PNMAIN,10*LOG10(PNMAIN)
      WRITE (6,110) RDES
      WRITE (6,112) RNSE
      WRITE (6,113) SINR
      WRITE (6,114) SINR_IR
      IF (PIMAIN.EQ.0.) THEN
        CR=0.                          ! TO AVOID DIV/ZERO AT TH_I
        WRITE (6,111) CR,PIMAIN        !  AT NULLS OF THE ELEMENT PATTERN
      ELSE
        IF (PI.LT.1E-10) THEN
          PII=1.E-10
        ELSE
          PII=PI
        END IF
        CRDB=10.*LOG10(PIMAIN/PII)
        WRITE (6,115) CRDB
      END IF
      IF (IAVCODE.EQ.1) THEN
        WRITE (6,116) AVSL
        WRITE (6,117) AVSLCH
      END IF

      DO 100 I=1,NUM_AUX
        XMAG=CABS(W(I))
        XPHASE=ATAN2(AIMAG(W(I)),REAL(W(I)))/DTR
        WRITE (6,118) I,W(I),XMAG,XPHASE
100   CONTINUE
      WRITE (6,*)
 90   FORMAT (' PD=',E23.16,'=',F10.5,' dB')
 91   FORMAT (' PI=',E23.16,'=',F10.5,' dB')
```

```
 92     FORMAT (' PN=',E23.16,'=',F10.5,' dB')
 93     FORMAT (' PDMAIN=',E23.16,'=',F10.5,' dB')
 94     FORMAT (' PIMAIN=',E23.16,'=',F10.5,' dB')
 95     FORMAT (' PNMAIN=',E23.16,'=',F10.5,' dB')
110     FORMAT (' PD/PD0=',F10.5,' dB')
111     FORMAT (' CAN_RATIO=',F10.5,'  because PIMAIN=',F10.5)
112     FORMAT (' PN/PN0=',F10.5,' dB')
113     FORMAT (' SINR=',F10.5,' dB')
114     FORMAT (' SINR_IR=',F10.5,' dB')
115     FORMAT (' CAN_RATIO=',F10.5,' dB')
116     FORMAT (' AVERAGE SLL=',F10.5,' dB')
117     FORMAT (' CHANGE IN AVSL=',F10.5,' dB')
118     FORMAT (' W(',I1,')=',E23.16,'+j',E23.16,/,5X,
     &          '=',E23.16,'<',F10.5,' degrees')

        I_TYPE=0

        OPEN (UNIT=1, FILE=OUTFILE,
     &     STATUS='NEW')
        WRITE (1,120) FILENAME
120     FORMAT(A20)
        NUM_PTS=1
C       Write file type to file
        WRITE (1,*) I_TYPE
        WRITE (1,*) IELCODE
        WRITE (1,*) IAVCODE
        WRITE (1,*) NUM_PTS
        WRITE (1,*) NUM_AUX
        WRITE (1,*) N_X
        WRITE (1,*) N_Y
        WRITE (1,*) SPACING
        WRITE (1,*) BEAM_TH
        WRITE (1,*) BEAM_PH
        WRITE (1,*) PD
        WRITE (1,*) PI
        WRITE (1,*) PN
        WRITE (1,*) PDMAIN
        WRITE (1,*) PIMAIN
        WRITE (1,*) PNMAIN
        IF (IAVCODE.EQ.1) WRITE (1,*) AVSL
        DO 150 I=1,NUM_AUX
          WRITE (1,*) W(I)
150     CONTINUE
        DO 160 I=1,N_X
          DO 159 J=1,N_Y
             WRITE (1,*) MM(I,J)
             WRITE (1,*) G(I,J)
             DO 158 K=1,NUM_AUX
               WRITE (1,*) A(K,I,J)
158          CONTINUE
159       CONTINUE
160     CONTINUE
        DO 170 I=1,NUM_AUX
          WRITE (1,*) PSIDL(I)
170     CONTINUE

        CLOSE (UNIT=1)

        RETURN
        END


C       Subroutine SCAN_D calls subroutine MAIN repeatedly from within a
C       loop where the desired signal arrival angle varies.
C
        SUBROUTINE SCAN_D
```

```
      REAL BEAM_TH,BEAM_PH,SPACING,AMPVAR,PHVAR
      REAL TH_SAVE,PH_SAVE,ANG_MIN,ANG_MAX,SIZE_INC
      REAL PD,PI,PN,PDMAIN,PIMAIN,PNMAIN
      REAL SNR,INR(5),SIG2,AVSLMAIN,AVSL,AVSLCH
      REAL PY,DTR,RDES,RNSE,SINRMAIN,SINR_IR,CR,CRDB,PII
      REAL AD,AI(5),BWD,BWI(5),TH_D,TH_I(5),PH_D,PH_I(5),PSIDL(12)
      REAL CTD,STD,CPD,SPD,CTI(5),STI(5),CPI(5),SPI(5)
      INTEGER N_X,N_Y,NUM_JAM,NUM_AUX,ISEED0,IAVCODE,I_TYPE
      INTEGER NUM_PTS,INORM,I_TH_PH
      COMPLEX MM(100,50),G(100,50),A(12,100,50),W(12)
      CHARACTER*20 FILENAMF,OUTFILE
      COMMON/SIGVARS/TH_D,TH_I,PH_D,PH_I,BWD,BWI,SNR,INR,AD,AI,SIG2,
     &               NUM_JAM
      COMMON/ARRVARS/N_X,N_Y,SPACING,BEAM_TH,BEAM_PH,G,MM,NUM_AUX,
     &               A,PSIDL,W,AMPVAR,PHVAR,ISEED0,DB,IELCODE
      COMMON/NAME/FILENAME,OUTFILE
      COMMON/AOAVARS/CTD,STD,CPD,SPD,CTI,STI,CPI,SPI
      COMMON/INTVARS/IAVCODE,AVSLMAIN

C     Save theta, phi, and AD values before modifying them
      TH_SAVE=TH_D
      PH_SAVE=PH_D

C     Compute sines, cosines of angles of arrival of des., inter. signals

      PY=3.141592653589793E+00
      DTR=PY/180.0E+00
      DO 20 I=1,NUM_JAM
        CTI(I)=COS(TH_I(I)*DTR)
        STI(I)=SIN(TH_I(I)*DTR)
        CPI(I)=COS(PH_I(I)*DTR)
        SPI(I)=SIN(PH_I(I)*DTR)
20    CONTINUE

C  Read info on scan

      READ (2,*) I_TH_PH
      READ (2,*) ANG_MIN
      READ (2,*) ANG_MAX
      READ (2,*) SIZE_INC
      NUM_PTS=INT((ANG_MAX-ANG_MIN)/SIZE_INC+1.5)

      I_TYPE=I_TH_PH
      OPEN (UNIT=1, FILE=OUTFILE,STATUS='NEW')
      WRITE (1,*) FILENAME
C     Write file type to file
      WRITE (1,*) I_TYPE
      WRITE (1,*) IAVCODE
      IF (IAVCODE.EQ.1) WRITE (1,*) AVSLMAIN
      WRITE (1,*) NUM_PTS

      IF (I_TH_PH.EQ.1) THEN

        CPD=COS(PH_D*DTR)
        SPD=SIN(PH_D*DTR)

        DO 60 I=1,NUM_PTS
          TH_D=ANG_MIN+(I-1)*SIZE_INC
          CTD=COS(TH_D*DTR)
          STD=SIN(TH_D*DTR)
          CALL MAIN(PD,PI,PN,PDMAIN,PIMAIN,PNMAIN)
          WRITE (1,*) TH_D
          WRITE (1,*) PD
          WRITE (1,*) PI
          WRITE (1,*) PN
          WRITE (1,*) PDMAIN
```

```
            IF (IAVCODE.EQ.1) THEN
              CALL AVSLCOMP(AVSL)
              WRITE (1,*) AVSL
            END IF
60        CONTINUE

        ELSE IF(I_TH_PH.EQ.2) THEN

          CTD=COS(TH_D*DTR)
          STD=SIN(TH_D*DTR)
          DO 90 I=1,NUM_PTS
            PH_D=ANG_MIN+(I-1)*SIZE_INC
            CPD=COS(PH_D*DTR)
            SPD=SIN(PH_D*DTR)
            CALL MAIN(PD,PI,PN,PDMAIN,PIMAIN,PNMAIN)
            WRITE (1,*) PH_D
            WRITE (1,*) PD
            WRITE (1,*) PI
            WRITE (1,*) PN
            WRITE (1,*) PDMAIN
            IF (IAVCODE.EQ.1) THEN
              CALL AVSLCOMP(AVSL)
              WRITE (1,*) AVSL
            END IF
90        CONTINUE
        END IF

        WRITE (1,*) PIMAIN
        WRITE (1,*) PNMAIN

        CLOSE (UNIT=1)

C       Restore theta, phi, and AD values
        TH_D=TH_SAVE
        PH_D=PH_SAVE
        INORM=0
        RETURN
        END


C       Subroutine SCAN_I       calls subroutine MAIN repeatedly from within a
C       loop where an interference arrival angle varies.
C
        SUBROUTINE SCAN_I
        REAL BEAM_TH,BEAM_PH,SPACING,AMPVAR,PHVAR
        REAL TH_SAVE,PH_SAVE,ANG_MIN,ANG_MAX,SIZE_INC
        REAL PD,PI,PN,PDMAIN,PIMAIN,PNMAIN
        REAL SNR,INR(5),SIG2,AVSLMAIN,AVSL,AVSLCH
        REAL PY,DTR,RDES,RNSE,SINRMAIN,SINR_IR,CR,CRDB,PII
        REAL AD,AI(5),BWD,BWI(5),TH_D,TH_I(5),PH_D,PH_I(5),PSIDL(12)
        REAL CTD,STD,CPD,SPD,CTI(5),STI(5),CPI(5),SPI(5)
        INTEGER N_X,N_Y,NUM_JAM,NUM_AUX,ISEED0,IAVCODE,I_TYPE
        INTEGER NUM_PTS,INORM,I_TH_PH,JAM_NUM
        COMPLEX MM(100,50),G(100,50),A(12,100,50),W(12)
        CHARACTER*20 FILENAME,OUTFILE
        COMMON/SIGVARS/TH_D,TH_I,PH_D,PH_I,BWD,BWI,SNR,INR,AD,AI,SIG2,
     &                 NUM_JAM
        COMMON/ARRVARS/N_X,N_Y,SPACING,BEAM_TH,BEAM_PH,G,MM,NUM_AUX,
     &                 A,PSIDL,AMPVAR,PHVAR,ISEED0,DB,IELCODE
        COMMON/NAME/FILENAME,OUTFILE
        COMMON/AOAVARS/CTD,STD,CPD,SPD,CTI,STI,CPI,SPI
        COMMON/INTVARS/IAVCODE,AVSLMAIN

        READ (2,*) JAM_NUM

C     Save theta, phi and AI values so they won't be destroyed
```

```
        TH_SAVE=TH_I(JAM_NUM)
        PH_SAVE=PH_I(JAM_NUM)

C     Compute sines, cosines of angles of arrival of des., inter. signals

        PY=3.141592653589793E+00
        DTR=PY/180.0E+00
        CTD=COS(TH_D*DTR)
        STD=SIN(TH_D*DTR)
        CPD=COS(PH_D*DTR)
        SPD=SIN(PH_D*DTR)
        DO 20 I=1,NUM_JAM
          CTI(I)=COS(TH_I(I)*DTR)
          STI(I)=SIN(TH_I(I)*DTR)
          CPI(I)=COS(PH_I(I)*DTR)
          SPI(I)=SIN(PH_I(I)*DTR)
20      CONTINUE

C     Read rest of scan information

        READ (2,*) I_TH_PH
        READ (2,*) ANG_MIN
        READ (2,*) ANG_MAX
        READ (2,*) SIZE_INC
        NUM_PTS=INT((ANG_MAX-ANG_MIN)/SIZE_INC+1.5)
        I_TYPE=I_TH_PH+2

        OPEN (UNIT=1, FILE=OUTFILE,
     &     STATUS='NEW')
        WRITE (1,*) FILENAME
C       Write file type to file
        WRITE (1,*) I_TYPE
        WRITE (1,*) IAVCODE
        IF (IAVCODE.EQ.1) WRITE (1,*) AVSLMAIN
        WRITE (1,*) NUM_PTS
        WRITE (1,*) JAM_NUM


        IF (I_TH_PH.EQ.1) THEN

          DO 60 I=1,NUM_PTS
            TH_I(JAM_NUM)=ANG_MIN+(I-1)*SIZE_INC
            CTI(JAM_NUM)=COS(TH_I(JAM_NUM)*DTR)
            STI(JAM_NUM)=SIN(TH_I(JAM_NUM)*DTR)
            CALL MAIN(PD,PI,PN,PDMAIN,PIMAIN,PNMAIN)
            WRITE (1,*) TH_I(JAM_NUM)
            WRITE (1,*) PD
            WRITE (1,*) PI
            WRITE (1,*) PN
            WRITE (1,*) PIMAIN
            IF (IAVCODE.EQ.1) THEN
              CALL AVSLCOMP(AVSL)
              WRITE (1,*) AVSL
            END IF
60        CONTINUE

        ELSE IF(I_TH_PH.EQ.2) THEN

          DO 90 I=1,NUM_PTS
            PH_I(JAM_NUM)=ANG_MIN+(I-1)*SIZE_INC
            CPI(JAM_NUM)=COS(PH_I(JAM_NUM)*DTR)
            SPI(JAM_NUM)=SIN(PH_I(JAM_NUM)*DTR)
            CALL MAIN(PD,PI,PN,PDMAIN,PIMAIN,PNMAIN)
            WRITE (1,*) PH_I(JAM_NUM)
            WRITE (1,*) PD
            WRITE (1,*) PI
```

```
            WRITE (1,*) PN
            WRITE (1,*) PIMAIN
            IF (IAVCODE.EQ.1) THEN
              CALL AVSLCOMP(AVSL)
              WRITE (1,*) AVSL
            END IF
90        CONTINUE

        END IF

        WRITE (1,*) PDMAIN
        WRITE (1,*) PNMAIN

        CLOSE (UNIT=1)

C       Restore theta, phi, and AI
        TH_I(JAM_NUM)=TH_SAVE
        PH_I(JAM_NUM)=PH_SAVE
        INORM=1
        RETURN
        END


C       Subroutine SCAN_SNR calls subroutine MAIN repeatedly from within a
C       loop where the SNR varies.
C
        SUBROUTINE SCAN_SNR
        REAL BEAM_TH,BEAM_PH,SPACING,AMPVAR,PHVAR
        REAL RTEMP,SNR_MIN,SNR_MAX,SIZE_INC
        REAL PD,PI,PN,PDMAIN,PIMAIN,PNMAIN
        REAL SNR,INR(5),SIG2,AVSLMAIN,AVSL,AVSLCH
        REAL PY,DTR,RDES,RNSE,SINRMAIN,SINR_IR,CR,CRDB,PII
        REAL AD,AI(5),BWD,BWI(5),TH_D,TH_I(5),PH_D,PH_I(5),PSIDL(12)
        REAL CTD,STD,CPD,SPD,CTI(5),STI(5),CPI(5),SPI(5)
        INTEGER N_X,N_Y,NUM_JAM,NUM_AUX,ISEED0,IAVCODE,I_TYPE
        INTEGER NUM_PTS,INORM,I_TH_PH
        COMPLEX MM(100,50),G(100,50),A(12,100,50),W(12)
        CHARACTER*20 FILENAME,OUTFILE
        COMMON/SIGVARS/TH_D,TH_I,PH_D,PH_I,BWD,BWI,SNR,INR,AD,AI,SIG2,
     &                 NUM_JAM
        COMMON/ARRVARS/N_X,N_Y,SPACING,BEAM_TH,BEAM_PH,G,MM,NUM_AUX,
     &                  A,PSIDL,W,AMPVAR,PHVAR,ISEED0,DB,IELCODE
        COMMON/NAME/FILENAME,OUTFILE
        COMMON/AOAVARS/CTD,STD,CPD,SPD,CTI,STI,CPI,SPI
        COMMON/INTVARS/IAVCODE,AVSLMAIN

C     Compute sines, cosines of angles of arrival of des., inter. signals

        PY=3.141592653589793E+00
        DTR=PY/180.0E+00
        CTD=COS(TH_D*DTR)
        STD=SIN(TH_D*DTR)
        CPD=COS(PH_D*DTR)
        SPD=SIN(PH_D*DTR)
        DO 20 I=1,NUM_JAM
          CTI(I)=COS(TH_I(I)*DTR)
          STI(I)=SIN(TH_I(I)*DTR)
          CPI(I)=COS(PH_I(I)*DTR)
          SPI(I)=SIN(PH_I(I)*DTR)
20      CONTINUE

C     Read Scan information

        RTEMP=SNR

        READ (2,*) SNR_MIN
```

```
      READ (2,*) SNR_MAX
      READ (2,*) SIZE_INC
      NUM_PTS=INT((SNR_MAX-SNR_MIN)/SIZE_INC+1.5)

      I_TYPE=5
      OPEN (UNIT=1, FILE=OUTFILE,
     &    STATUS='NEW')
      WRITE (1,*) FILENAME
C     Write file type to file
      WRITE (1,*) I_TYPE
      WRITE (1,*) IAVCODE
      IF (IAVCODE.EQ.1) WRITE (1,*) AVSLMAIN
      WRITE (1,*) NUM_PTS

      DO 60 I=1,NUM_PTS
        SNR=SNR_MIN+(I-1)*SIZE_INC
        CALL MAIN(PD,PI,PN,PDMAIN,PIMAIN,PNMAIN)
        WRITE (1,*) SNR
        WRITE (1,*) PD
        WRITE (1,*) PI
        WRITE (1,*) PN
        WRITE (1,*) PDMAIN
        IF (IAVCODE.EQ.1) THEN
          CALL AVSLCOMP(AVSL)
          WRITE (1,*) AVSL
        END IF
60    CONTINUE

      WRITE (1,*) PIMAIN
      WRITE (1,*) PNMAIN

      CLOSE (UNIT=1)

      SNR=RTEMP
      INORM=0
      RETURN
      END

C     Subroutine SCAN_INR calls subroutine MAIN repeatedly from within a
C     loop where an INR varies.
C
      SUBROUTINE SCAN_INR
      REAL BEAM_TH,BEAM_PH,SPACING,AMPVAR,PHVAR
      REAL RTEMP,INR_MIN,INR_MAX,SIZE_INC
      REAL PD,PI,PN,PDMAIN,PIMAIN,PNMAIN
      REAL SNR,INR(5),SIG2,AVSLMAIN,AVSL,AVSLCH
      REAL PY,DTR,RDES,RNSE,SINRMAIN,SINR_IR,CR,CRDB,PII
      REAL AD,AI(5),BWD,BWI(5),TH_D,TH_I(5),PH_D,PH_I(5),PSIDL(12)
      REAL CTD,STD,CPD,SPD,CTI(5),STI(5),CPI(5),SPI(5)
      INTEGER N_X,N_Y,NUM_JAM,NUM_AUX,ISEED0,IAVCODE,I_TYPE
      INTEGER NUM_PTS,INORM,I_TH_PH,JAM_NUM
      COMPLEX MM(100,50),G(100,50),A(12,100,50),W(12)
      CHARACTER*20 FILENAME,OUTFILE
      COMMON/SIGVARS/TH_D,TH_I,PH_D,PH_I,BWD,BWI,SNR,INR,AD,AI,SIG2,
     &               NUM_JAM
      COMMON/ARRVARS/N_X,N_Y,SPACING,BEAM_TH,BEAM_PH,G,MM,NUM_AUX,
     &               A,PSIDL,W,AMPVAR,PHVAR,ISEED0,DB,IELCODE
      COMMON/NAME/FILENAME,OUTFILE
      COMMON/AOAVARS/CTD,STD,CPD,SPD,CTI,STI,CPI,SPI
      COMMON/INTVARS/IAVCODE,AVSLMAIN

C     Compute sines, cosines of angles of arrival of des., inter. signals

      PY=3.141592653589793E+00
      DTR=PY/180.0E+00
      CTD=COS(TH_D*DTR)
```

```
          STD=SIN(TH_D*DTR)
          CPD=COS(PH_D*DTR)
          SPD=SIN(PH_D*DTR)
          DO 20 I=1,NUM_JAM
            CTI(I)=COS(TH_I(I)*DTR)
            STI(I)=SIN(TH_I(I)*DTR)
            CPI(I)=COS(PH_I(I)*DTR)
            SPI(I)=SIN(PH_I(I)*DTR)
20        CONTINUE

C     Read scan information

          READ (2,*) JAM_NUM

          RTEMP=INR(JAM_NUM)

          READ (2,*) INR_MIN
          READ (2,*) INR_MAX
          READ (2,*) SIZE_INC
          NUM_PTS=INT((INR_MAX-INR_MIN)/SIZE_INC+1.5)

          I_TYPE=6
          OPEN (UNIT=1, FILE=OUTFILE,
     &       STATUS='NEW')
          WRITE (1,*) FILENAME
C         Write file type to file
          WRITE (1,*) I_TYPE
          WRITE (1,*) IAVCODE
          IF (IAVCODE.EQ.1) WRITE (1,*) AVSLMAIN
          WRITE (1,*) NUM_PTS
          WRITE (1,*) JAM_NUM

          DO 60 I=1,NUM_PTS
            INR(JAM_NUM)=INR_MIN+(I-1)*SIZE_INC
            CALL MAIN(PD,PI,PN,PDMAIN,PIMAIN,PNMAIN)
            WRITE (1,*) INR(JAM_NUM)
            WRITE (1,*) PD
            WRITE (1,*) PI
            WRITE (1,*) PN
            WRITE (1,*) PIMAIN
            IF (IAVCODE.EQ.1) THEN
              CALL AVSLCOMP(AVSL)
              WRITE (1,*) AVSL
            END IF
60        CONTINUE

          WRITE (1,*) PDMAIN
          WRITE (1,*) PNMAIN

          CLOSE (UNIT=1)

          INR(JAM_NUM)=RTEMP
          INORM=1
          RETURN
          END


          SUBROUTINE DISP_SIG
          REAL AD,AI(5),BWD,BWI(5),TH_D,TH_I(5),PH_D,PH_I(5)
          REAL SIG2,SNR,INR(5)
          INTEGER NUM_JAM
          COMMON/SIGVARS/TH_D,TH_I,PH_D,PH_I,BWD,BWI,SNR,INR,AD,AI,SIG2,
     &                   NUM_JAM

          WRITE (6,*)
          WRITE (6,*) 'SIGNAL SCENARIO:'
```

```
      WRITE (6,*)
      WRITE (6,*) ' SNR = ',SNR
      WRITE (6,*) ' TH_D = ',TH_D
      WRITE (6,*) ' PH_D = ',PH_D
      WRITE (6,*) ' BWD = ',BWD
      WRITE (6,*) ' NUM_JAM = ',NUM_JAM
      DO 20 I=1,5
         WRITE (6,900) I,INR(I),I,BWI(I)
20    CONTINUE
      DO 30 I=1,5
         WRITE (6,901) I,TH_I(I),I,PH_I(I)
30    CONTINUE

900   FORMAT ('  INR(',I1,')=',E12.5,'   BWI(',I1,')=',E12.5)
901   FORMAT ('  TH_I(',I1,')=',E12.5,'  PH_I(',I1,')=',E12.5)
      RETURN
      END


C  This subroutine uses the IMSL routines QDAGS(1-D) and TWODQ(2-D)
C    to compute
C    the integrated average SLL of the mainbeam and adapted power
C    patterns.  It is computed by first doing the integrations of
C    the mainbeam and auxiliary patterns, and then mainbeam-aux and
C    auxiliary-auxiliary cross product terms.  These subintegrals
C    are then weighted to give the integral of the adapted pattern.
C    The range of integration excludes the mainbeam region.

      SUBROUTINE INTEGSL
      REAL YMAIN1,YMAIN2,YAUX1(12),YAUX2(12),YR,YI
      COMPLEX YAM1(12),YAM2(12),YAA1(12,12),YAA2(12,12)
      COMPLEX F,TEMP,FMAX
      COMPLEX G(100,50),MM(100,50),A(12,100,50),W(12)
      REAL PSIDL(12),BEAM_TH,BEAM_PH
      REAL ULO,UUP,U1,U2,V1,V2
      INTEGER N_X,N_Y,NUM_AUX
      CHARACTER*20 FILENAME,OUTFILE,INTEGFILE
      COMMON/ARRVARS/N_X,N_Y,SPACING,BEAM_TH,BEAM_PH,G,MM,NUM_AUX,
     &                  A,PSIDL,W,AMPVAR,PHVAR,ISEED0,DB,IELCODE
      COMMON/INTVARS/IAVCODE,AVSLMAIN,YMAIN1,YMAIN2,YAUX1,YAUX2,
     &                  YAM1,YAM2,YAA1,YAA2,ULO,UUP,U1,U2
      COMMON/INT2D/V1,V2
      COMMON/AUXVARS/IAUX,JAUX
      COMMON/NAME/FILENAME,OUTFILE,INTEGFILE
      EXTERNAL MAINSQ,AUXSQ,REAA,IMAA,REAM,IMAM
      EXTERNAL MAINSQ2,AUXSQ2,REAA2,IMAA2,REAM2,IMAM2,VL,VU,VLF,VUF

      READ (2,*) ULO,UUP
      READ (2,*) AERR,RERR

      PI=3.141592653589793E+00
      DTR=PI/180.

      U0=SIN(BEAM_TH*DTR)*COS(BEAM_PH*DTR)
      V0=SIN(BEAM_TH*DTR)*SIN(BEAM_PH*DTR)

C  Computing the null to null mainlobe beamwidths (in u ) for
C  D/C linear array

      R=10.**(0.05*DB)
      XOU=COSH(LOG(R+SQRT(R**2.-1))/(N_X-1))
      UB=2./PI*ACOS(COS(0.5*PI/(N_X-1))/XOU)
      U1=U0-UB
      U2=U0+UB
```

```
C  Computing the sub-integrals of the mainbeam pattern, the auxiliary
C   beam patterns, and the cross-product terms.

      IF (N_Y.EQ.1) THEN

      CALL QDAGS(MAINSQ,ULO,U1,AERR,RERR,YMAIN1,ERRB)
      CALL QDAGS(MAINSQ,U2,UUP,AERR,RERR,YMAIN2,ERRB)
      DO 40 IAUX=1,NUM_AUX
        CALL QDAGS(AUXSQ,ULO,U1,AERR,RERR,YAUX1(IAUX),ERRB)
        CALL QDAGS(AUXSQ,U2,UUP,AERR,RERR,YAUX2(IAUX),ERRB)
        CALL QDAGS(REAM,ULO,U1,AERR,RERR,YR,ERRB)
        CALL QDAGS(IMAM,ULO,U1,AERR,RERR,YI,ERRB)
        YAM1(IAUX)=CMPLX(YR,YI)
        CALL QDAGS(REAM,U2,UUP,AERR,RERR,YR,ERRB)
        CALL QDAGS(IMAM,U2,UUP,AERR,RERR,YI,ERRB)
        YAM2(IAUX)=CMPLX(YR,YI)
        IF (IAUX.GT.1) THEN
          DO 38 JAUX=1,IAUX-1
            CALL QDAGS(REAA,ULO,U1,AERR,RERR,YR,ERRB)
            CALL QDAGS(IMAA,ULO,U1,AERR,RERR,YI,ERRB)
            YAA1(IAUX,JAUX)=CMPLX(YR,YI)
            CALL QDAGS(REAA,U2,UUP,AERR,RERR,YR,ERRB)
            CALL QDAGS(IMAA,U2,UUP,AERR,RERR,YI,ERRB)
            YAA2(IAUX,JAUX)=CMPLX(YR,YI)
38        CONTINUE
        END IF
40    CONTINUE

      ELSE

      XOV=COSH(LOG(R+SQRT(R**2.-1))/(N_Y-1))
      VB=2./PI*ACOS(COS(0.5*PI/(N_Y-1))/XOV)
      V1=V0-VB
      V2=V0+VB

      IRULE=5
      IRLE2=5

      CALL TWODQ(MAINSQ2,ULO,UUP,VL,VU,AERR,RERR,IRULE,YMAIN1,ERRB)
      CALL TWODQ(MAINSQ2,U1,U2,VLF,VUF,AERR,RERR,IRULE,YMAIN2,ERRB)
      DO 140 IAUX=1,NUM_AUX
        CALL TWODQ(AUXSQ2,ULO,UUP,VL,VU,AERR,RERR,IRLE2,YAUX1(IAUX)
     &             ,ERRB)
        CALL TWODQ(AUXSQ2,U1,U2,VLF,VUF,AERR,RERR,IRLE2,YAUX2(IAUX)
     &             ,ERRB)
        CALL TWODQ(REAM2,ULO,UUP,VL,VU,AERR,RERR,IRLE2,YR,ERRB)
        CALL TWODQ(IMAM2,ULO,UUP,VL,VU,AERR,RERR,IRLE2,YI,ERRB)
        YAM1(IAUX)=CMPLX(YR,YI)
        write (6,*) 'past yam1'
        CALL TWODQ(REAM2,U1,U2,VLF,VUF,AERR,RERR,IRLE2,YR,ERRB)
        CALL TWODQ(IMAM2,U1,U2,VLF,VUF,AERR,RERR,IRLE2,YI,ERRB)
        YAM2(IAUX)=CMPLX(YR,YI)
        IF (IAUX.GT.1) THEN
          DO 138 JAUX=1,IAUX-1
            CALL TWODQ(REAA2,ULO,UUP,VL,VU,AERR,RERR,IRLE2,YR,ERRB)
            CALL TWODQ(IMAA2,ULO,UUP,VL,VU,AERR,RERR,IRLE2,YI,ERRB)
            YAA1(IAUX,JAUX)=CMPLX(YR,YI)
            CALL TWODQ(REAA2,U1,U2,VLF,VUF,AERR,RERR,IRLE2,YR,ERRB)
            CALL TWODQ(IMAA2,U1,U2,VLF,VUF,AERR,RERR,IRLE2,YI,ERRB)
            YAA2(IAUX,JAUX)=CMPLX(YR,YI)
138       CONTINUE
        END IF
140   CONTINUE

      END IF
```

```
C    Store results in INTEGFILE for use with subsequent tests with
C      same array
       OPEN (UNIT=3,FILE=INTEGFILE,STATUS='NEW')
       WRITE (3,*) ULO,UUP
       WRITE (3,*) U1,U2
       IF (N_Y.NE.1) WRITE (3,*) V1,V2
       WRITE (3,*) YMAIN1,YMAIN2
       DO 50 I=1,NUM_AUX
        WRITE (3,*) YAUX1(I),YAUX2(I)
        WRITE (3,*) YAM1(I),YAM2(I)
        DO 49 J=1,I-1
         WRITE (3,*) YAA1(I,J),YAA2(I,J)
49      CONTINUE
50     CONTINUE
       CLOSE (UNIT=3,STATUS='KEEP')

       RETURN
       END

C  Combining these results to get the average SLL of the adapted pattern
C    over the specified limits

       SUBROUTINE AVSLCOMP(AVSLDB)
       REAL YMAIN1,YMAIN2,YAUX1(12),YAUX2(12)
       COMPLEX YAM1(12),YAM2(12),YAA1(12,12),YAA2(12,12)
       COMPLEX F,TEMP,FMAX
       COMPLEX G(100,50),MM(100,50),A(12,100,50),W(12),WE(12)
       REAL PSIDL(12),BEAM_TH,BEAM_PH,GAIN
       REAL T1,T2,AVSL,AVSLDB,ULO,UUP,U1,U2
       INTEGER N_X,N_Y,NUM_AUX
       COMMON/ARRVARS/N_X,N_Y,SPACING,BEAM_TH,BEAM_PH,G,MM,NUM_AUX,
     &                  A,PSIDL,W,AMPVAR,PHVAR,ISEED0,DB,IELCODE
       COMMON/INTVARS/IAVCODE,AVSLMAIN,YMAIN1,YMAIN2,YAUX1,YAUX2,
     &                 YAM1,YAM2,YAA1,YAA2,ULO,UUP,U1,U2
       COMMON/INT2D/V1,V2

       PI=3.141592653589793E+00

       DO 10 I=1,NUM_AUX
         WE(I)=W(I)*CEXP(CMPLX(0.,PSIDL(I)))
10     CONTINUE

       T1=0.
       T2=0.
       DO 20 I=1,NUM_AUX
         T1=T1+(CABS(WE(I))**2)*YAUX1(I)+2.*REAL(WE(I)*YAM1(I))
         T2=T2+(CABS(WE(I))**2)*YAUX2(I)+2.*REAL(WE(I)*YAM2(I))
         IF (I.GT.1) THEN
           DO 19 J=1,I-1
             T1=T1+2.*REAL(WE(I)*CONJG(WE(J))*YAA1(I,J))
             T2=T2+2.*REAL(WE(I)*CONJG(WE(J))*YAA2(I,J))
19         CONTINUE
         END IF
20     CONTINUE
       T1=T1+YMAIN1
       T2=T2+YMAIN2

       IF (N_Y.EQ.1) THEN
         AVSL=(T1+T2)/(U1-ULO+UUP-U2)
       ELSE
         AREASL=PI-(U2-U1)*(V2-V1)
         AVSL=(T1-T2)/AREASL
       END IF

       AVSLDB=10.*ALOG10(AVSL)
```

```
      RETURN
      END


      SUBROUTINE MAINPATT(U,V,F)
      COMPLEX MM(100,50),A(12,100,50),W(12)
      COMPLEX G(100,50),F,TEMP
      INTEGER N_X,N_Y,NUM_AUX
      REAL PSIDL(12),THETA,PHI,PSI,BEAM_TH,BEAM_PH,PATT,PI
      COMMON/ARRVARS/N_X,N_Y,SPACING,BEAM_TH,BEAM_PH,G,MM,NUM_AUX,
     &                A,PSIDL,W,AMPVAR,PHVAR,ISEED0,DB,IELCODE

c      write (6,*) U,V

      PI=3.141592653589793E+00
      DTR=PI/180.E+00
      TEMP=(0.0,0.0)
      DO 20 J=1,N_Y
        DO 19 I=1,N_X
          PSI=((I-1)*U+(J-1)*V)*2.*PI*SPACING
          TEMP=TEMP+MM(I,J)*G(I,J)*CEXP(CMPLX(0.,PSI))
19      CONTINUE
20    CONTINUE
      THETA=ASIN(SQRT(U**2+V**2))/DTR
      IF (THETA.NE.0) PHI=ATAN2(V,U)/DTR
      CALL ELPATT(PATT,THETA,PHI,IELCODE)
      F=TEMP*PATT
      RETURN
      END


      SUBROUTINE AUXPATT(U,V,IAUX,F)
      COMPLEX MM(100,50),A(12,100,50),W(12)
      COMPLEX G(100,50),F,TEMP
      INTEGER N_X,N_Y,NUM_AUX
      REAL PSIDL(12),BEAM_TH,BEAM_PH,U,V,PSI,PATT,PI
      COMMON/ARRVARS/N_X,N_Y,SPACING,BEAM_TH,BEAM_PH,G,MM,NUM_AUX,
     &                A,PSIDL,W,AMPVAR,PHVAR,ISEED0,DB,IELCODE


      PI=3.141592653589793E+00
      DTR=PI/180.
      TEMP=(0.0,0.0)
      DO 20 J=1,N_Y
        DO 19 I=1,N_X
          PSI=((I-1)*U+(J-1)*V)*2.*PI*SPACING
          TEMP=TEMP+A(IAUX,I,J)*G(I,J)*CEXP(CMPLX(0.,PSI))
19      CONTINUE
20    CONTINUE
      THETA=ASIN(SQRT(U**2+V**2))/DTR
      IF (THETA.NE.0) PHI=ATAN2(V,U)/DTR
      CALL ELPATT(PATT,THETA,PHI,IELCODE)
      F=TEMP*PATT

      RETURN
      END

C The following subroutines are called when doing the integrations
C  for the average SLL computations.

      REAL FUNCTION MAINSQ(U)
      REAL U,V
      COMPLEX F1
      CALL MAINPATT(U,V,F1)
      MAINSQ=REAL(F1*CONJG(F1))
      RETURN
```

```
      END

      REAL FUNCTION MAINSQ2(U,V)
      REAL U,V
      COMPLEX F1
      CALL MAINPATT(U,V,F1)
      MAINSQ2=REAL(F1*CONJG(F1))
      RETURN
      END

      REAL FUNCTION AUXSQ(U)
      REAL U,V
      COMPLEX F1
      COMMON/AUXVARS/IAUX,JAUX
      CALL AUXPATT(U,V,IAUX,F1)
      AUXSQ=REAL(F1*CONJG(F1))
      RETURN
      END

      REAL FUNCTION AUXSQ2(U,V)
      REAL U,V
      COMPLEX F1
      COMMON/AUXVARS/IAUX,JAUX
      CALL AUXPATT(U,V,IAUX,F1)
      AUXSQ2=REAL(F1*CONJG(F1))
      RETURN
      END

      REAL FUNCTION REAM(U)
      REAL U,V
      COMPLEX FM,FA
      COMMON/AUXVARS/IAUX,JAUX
      CALL MAINPATT(U,V,FM)
      CALL AUXPATT(U,V,IAUX,FA)
      REAM=REAL(FA*CONJG(FM))
      RETURN
      END

      REAL FUNCTION REAM2(U,V)
      REAL U,V
      COMPLEX FM,FA
      COMMON/AUXVARS/IAUX,JAUX
      CALL MAINPATT(U,V,FM)
      CALL AUXPATT(U,V,IAUX,FA)
      REAM2=REAL(FA*CONJG(FM))
      RETURN
      END

      REAL FUNCTION IMAM(U)
      REAL U,V
      COMPLEX FM,FA
      COMMON/AUXVARS/IAUX,JAUX
      CALL MAINPATT(U,V,FM)
      CALL AUXPATT(U,V,IAUX,FA)
      IMAM=AIMAG(FA*CONJG(FM))
      RETURN
      END

      REAL FUNCTION IMAM2(U,V)
      REAL U,V
      COMPLEX FM,FA
      COMMON/AUXVARS/IAUX,JAUX
      CALL MAINPATT(U,V,FM)
      CALL AUXPATT(U,V,IAUX,FA)
      IMAM2=AIMAG(FA*CONJG(FM))
      RETURN
```

```
END

REAL FUNCTION REAA(U)
REAL U,V
COMPLEX FI,FJ
COMMON/AUXVARS/IAUX,JAUX
CALL AUXPATT(U,V,IAUX,FI)
CALL AUXPATT(U,V,JAUX,FJ)
REAA=REAL(FI*CONJG(FJ))
RETURN
END

REAL FUNCTION REAA2(U,V)
REAL U,V
COMPLEX FI,FJ
COMMON/AUXVARS/IAUX,JAUX
CALL AUXPATT(U,V,IAUX,FI)
CALL AUXPATT(U,V,JAUX,FJ)
REAA2=REAL(FI*CONJG(FJ))
RETURN
END

REAL FUNCTION IMAA(U)
REAL U,V
COMPLEX FI,FJ
COMMON/AUXVARS/IAUX,JAUX
CALL AUXPATT(U,V,IAUX,FI)
CALL AUXPATT(U,V,JAUX,FJ)
IMAA=AIMAG(FI*CONJG(FJ))
RETURN
END

REAL FUNCTION IMAA2(U,V)
REAL U,V
COMPLEX FI,FJ
COMMON/AUXVARS/IAUX,JAUX
CALL AUXPATT(U,V,IAUX,FI)
CALL AUXPATT(U,V,JAUX,FJ)
IMAA2=AIMAG(FI*CONJG(FJ))
RETURN
END

REAL FUNCTION VL(U)
REAL U
VL=-1.*SQRT(1-U**2)
RETURN
END

REAL FUNCTION VLF(U)
REAL U,V1,V2
COMMON/INT2D/V1,V2
VLF=V1
RETURN
END

REAL FUNCTION VU(U)
REAL U
VU=SQRT(1-U**2)
RETURN
END

REAL FUNCTION VUF(U)
REAL U,V1,V2
COMMON/INT2D/V1,V2
VUF=V2
RETURN
```

END

```
C
C     Subroutine INFILERD reads the input file containing the array and
C      signal scenario data.
C

      SUBROUTINE INFILERD
      REAL BEAM_TH,BEAM_PH
      REAL SNR,INR(5),SIG2,AUXTHETA(12),AUXPHI(12)
      REAL AD,AI(5),BWD,BWI(5),TH_D,TH_I(5),PH_D,PH_I(5),PSIDL(12)
      INTEGER ILLCX(12),ILLCY(12),IURCX(12),IURCY(12),NUM_JAM
      INTEGER N_X,N_Y,NUM_AUX,NUM_COMB(12),AUX_TYPE(12)
      COMPLEX MM(100,50),A(12,100,50),W(12),G(100,50)
      CHARACTER*20 FILENAME,OUTFILE
      COMMON/NAME/FILENAME,OUTFILE
      COMMON/SIGVARS/TH_D,TH_I,PH_D,PH_I,BWD,BWI,SNR,INR,AD,AI,SIG2,
     &               NUM_JAM
      COMMON/ARRVARS/N_X,N_Y,SPACING,BEAM_TH,BEAM_PH,G,MM,NUM_AUX,
     &                A,PSIDL,W,AMPVAR,PHVAR,ISEED0,DB

      OPEN (UNIT=3, FILE=FILENAME,STATUS='OLD')
      READ (3,*) N_X
      READ (3,*) N_Y
      READ (3,*) SPACING
      READ (3,*) BEAM_TH
      READ (3,*) BEAM_PH
      READ (3,*) NUM_AUX
      READ (3,*) SNR
      READ (3,*) TH_D
      READ (3,*) PH_D
      READ (3,*) BWD
      READ (3,*) NUM_JAM
      DO 20 I=1,NUM_JAM
         READ (3,*) INR(I)
         READ (3,*) TH_I(I)
         READ (3,*) PH_I(I)
         READ (3,*) BWI(I)
20    CONTINUE
      DO 30 I=1,N_X
        DO 29 J=1,N_Y
          READ (3,*) MM(I,J)
          READ (3,*) G(I,J)
          DO 28 K=1,NUM_AUX
            READ (3,*) A(K,I,J)
28        CONTINUE
29      CONTINUE
30    CONTINUE
      DO 40 I=1,NUM_AUX
        READ (3,*) PSIDL(I)
        READ (3,*) AUX_TYPE(I)
        IF (AUX_TYPE(I).EQ.1) THEN
          READ (3,*) NUM_COMB(I)
        ELSE
          READ (3,*) AUXTHETA(I),AUXPHI(I)
          READ (3,*) ILLCY(I),ILLCY(I),IURCX(I),IURCY(I)
        END IF
40    CONTINUE
      READ (3,*) ISEED0
      READ (3,*) AMPVAR
      READ (3,*) PHVAR
      READ (3,*) DB
      CLOSE (UNIT=3)

      RETURN
      END
```

```
C
C     Program CHINFILE reads an INPUT file and echoes the data
C      to the screen.  It also provides an option to change a
C      parameter of the signal scenario and stores the data in
C      a new data file.
C

        PROGRAM CHINFILE
        REAL BEAM_TH,BEAM_PH
        REAL SNR,INR(5),SIG2,AUXTHETA(12),AUXPHI(12)
        REAL AD,AI(5),BWD,BWI(5),TH_D,TH_I(5),PH_D,PH_I(5),PSIDL(12)
        INTEGER ILLCX(12),ILLCY(12),IURCX(12),IURCY(12),NUM_JAM
        INTEGER N_X,N_Y,NUM_AUX,NUM_COMB(12),AUX_TYPE(12)
        COMPLEX G(100,50)
        COMPLEX MM(100,50),A(12,100,50),W(12)
        CHARACTER*20 FILENAME,OUTFILE,PRFNAME
        COMMON/NAME/FILENAME,OUTFILE
        COMMON/SIGVARS/TH_D,TH_I,PH_D,PH_I,BWD,BWI,SNR,INR,AD,AI,SIG2,
     &                 NUM_JAM
        COMMON/ARRVARS/N_X,N_Y,SPACING,BEAM_TH,BEAM_PH,G,MM,NUM_AUX,
     &                  A,PSIDL,W,AMPVAR,PHVAR,ISEED0
        COMMON/AUXVARS/AUX_TYPE,NUM_COMB,AUXTHETA,AUXPHI,ILLCX,ILLCY,
     &                 IURCX,IURCY,DB

        write (6,10)
10      format('Enter input datafile name:',$)
        read (5,11) FILENAME
11      FORMAT(A)

        CALL INFILERD

C  options to change parameters of the signal scenario:

      CALL DISP_SIG
490   WRITE (6,*)
      WRITE (6,500)
500   FORMAT(' ENTER 1 FOR SIGNAL SCENARIO CHANGES ELSE ENTER 0:',$)
      READ (5,*) ICHCODE
505   IF (ICHCODE.EQ.1) THEN
        WRITE (6,*)
        WRITE (6,*) 'CHANGE CODES:'
        WRITE (6,*) '  1--SNR              5--TH_I(I),PH_I(I)'
        WRITE (6,*) '  2--TH_D,PH_D        6--BWI(I)'
        WRITE (6,*) '  3--BWD              7--NUM_JAM'
        WRITE (6,*) '  4--INR(I)           8--NO FURTHER',
     &' CHANGES--STORE NEW INPUT DATA'
        WRITE (6,*)
        WRITE (6,510)
510     FORMAT(' ENTER DESIRED CHANGE CODE:',$)
        READ (5,*) ICHCODE2
        IF (ICHCODE2.EQ.1) THEN
          WRITE (6,512)
512       FORMAT(' ENTER NEW SNR(DB):',$)
          READ (5,*) SNR
        ELSE IF (ICHCODE2.EQ.2) THEN
          WRITE (6,515)
515       FORMAT(' ENTER NEW TH_D,PH_D (DEGREES):',$)
          READ (5,*) TH_D,PH_D
        ELSE IF (ICHCODE2.EQ.3) THEN
          WRITE (6,518)
518       FORMAT('ENTER NEW BWD:',$)
          READ (5,*) BWD
        ELSE IF (ICHCODE2.LT.7) THEN
520       WRITE (6,521)
521       FORMAT(' ENTER NUMBER OF JAMMER:',$)
          READ (5,*) JAM_NUM
```

```
          IF (JAM_NUM.GT.NUM_JAM) THEN
            GO TO 520
          ELSE IF (ICHCODE2.EQ.4) THEN
            WRITE (6,525) JAM_NUM
525         FORMAT(' ENTER NEW INR FOR JAMMER#',I1,':',$)
            READ (5,*) INR(JAM_NUM)
          ELSE IF (ICHCODE2.EQ.5) THEN
            WRITE (6,530) JAM_NUM
530         FORMAT(' ENTER NEW THETA,PHI (DEGREES) FOR JAMMER#',I1,
     &':',$)
            READ (5,*) TH_I(JAM_NUM),PH_I(JAM_NUM)
          ELSE IF (ICHCODE2.EQ.6) THEN
            WRITE (6,535) JAM_NUM
535         FORMAT(' ENTER NEW BANDWIDTH FOR JAMMER#',I1,':',$)
            READ (5,*) BWI(JAM_NUM)
          END IF
        ELSE IF (ICHCODE2.EQ.7) THEN
          ITEMP=NUM_JAM
          WRITE (6,540)
540       FORMAT(' ENTER NEW NUMBER OF JAMMERS(0-5):',$)
          READ (5,*) NUM_JAM
          IF (NUM_JAM.GT.ITEMP) THEN
            DO 1006 I=ITEMP+1,NUM_JAM
              WRITE (6,525) I
              READ (5,*) INR(I)
              WRITE (6,530) I
              READ (5,*) TH_I(I),PH_I(I)
              WRITE (6,535) I
              READ (5,*) BWI(I)
1006        CONTINUE
          ELSE IF (ITEMP.GT.NUM_JAM) THEN
            DO 1007 I=NUM_JAM+1,ITEMP
              INR(I)=0.
              TH_I(I)=0.
              PH_I(I)=0.
              BWI(I)=0.
1007        CONTINUE
          END IF
        END IF

        IF (ICHCODE2.NE.8) THEN
         CALL DISP_SIG
         GOTO 505
        END IF
      END IF

899   CALL DISP_SLC
      WRITE (6,900)
900   FORMAT(' ENTER 1 TO CHANGE DELAYS ELSE ENTER 0:',$)
      READ (5,*) ICHCODE3
      IF (ICHCODE3.EQ.1) THEN
         ICHCODE4=1
         DO 905 I=1,NUM_AUX
            WRITE (6,920) I
            READ (5,*) WVFR
            PSIDL(I)=-2.*3.141592653589793E+00*WVFR
905      CONTINUE
      END IF
920   FORMAT(' ENTER NEW DELAY FOR AUXILIARY #',I1,':',$)
      IF (ICHCODE3.NE.0) GOTO 899

C   REWRITING FILE WITH CHANGES TO SIGNAL SCENARIO

      IF (ICHCODE.NE.0.OR.ICHCODE4.EQ.1) THEN

890     FORMAT (' ENTER NEW INPUT DATA FILENAME: ',$)
```

```
891     FORMAT(A)
        WRITE (6,890)
        READ (5,891) FILENAME
        OPEN (UNIT=1,FILE=FILENAME,STATUS='NEW')
        WRITE (1,*) N_X
        WRITE (1,*) N_Y
        WRITE (1,*) SPACING
        WRITE (1,*) BEAM_TH
        WRITE (1,*) BEAM_PH
        WRITE (1,*) NUM_AUX
        WRITE (1,*) SNR
        WRITE (1,*) TH_D
        WRITE (1,*) PH_D
        WRITE (1,*) BWD
        WRITE (1,*) NUM_JAM
        DO 1008 I=1,NUM_JAM
          WRITE (1,*) INR(I)
          WRITE (1,*) TH_I(I)
          WRITE (1,*) PH_I(I)
          WRITE (1,*) BWI(I)
1008    CONTINUE
        DO 1011 I=1,N_X
          DO 1010 J=1,N_Y
            WRITE (1,*) MM(I,J)
            WRITE (1,*) G(I,J)
            DO 1009 K=1,NUM_AUX
              WRITE (1,*) A(K,I,J)
1009        CONTINUE
1010      CONTINUE
1011    CONTINUE
        DO 1012 I=1,NUM_AUX
          WRITE (1,*) PSIDL(I)
          WRITE (1,*) AUX_TYPE(I)
          IF (AUX_TYPE(I).EQ.1) THEN
            WRITE (1,*) NUM_COMB(I)
          ELSE
            WRITE (1,*) AUXTHETA(I),AUXPHI(I)
            WRITE (1,*) ILLCX(I),ILLCY(I),IURCX(I),IURCY(I)
          ENDIF
1012    CONTINUE
        WRITE (1,*) ISEED0
        WRITE (1,*) AMPVAR
        WRITE (1,*) PHVAR
        WRITE (1,*) DB

        CLOSE (UNIT=1,STATUS='KEEP')

      END IF

      STOP
      END

        SUBROUTINE DISP_SIG
        REAL AD,AI(5),BWD,BWI(5),TH_D,TH_I(5),PH_D,PH_I(5)
        REAL SIG2,SNR,INR(5)
        INTEGER NUM_JAM
        COMMON/SIGVARS/TH_D,TH_I,PH_D,PH_I,BWD,BWI,SNR,INR,AD,AI,SIG2,
     &                 NUM_JAM

        WRITE (6,*)
        WRITE (6,*) 'SIGNAL SCENARIO:'
        WRITE (6,*)
        WRITE (6,*) ' SNR = ',SNR
        WRITE (6,*) ' TH_D = ',TH_D
        WRITE (6,*) ' PH_D = ',PH_D
        WRITE (6,*) ' BWD = ',BWD
```

```
      WRITE (6,*) ' NUM_JAM = ',NUM_JAM
      DO 20 I=1,NUM_JAM
         WRITE (6,900) I,INR(I),I,BWI(I)
20    CONTINUE
      DO 30 I=1,NUM_JAM
         WRITE (6,901) I,TH_I(I),I,PH_I(I)
30    CONTINUE

900   FORMAT ('  INR(',I1,')=',E12.5,'   BWI(',I1,')=',E12.5)
901   FORMAT ('  TH_I(',I1,')=',E12.5,'  PH_I(',I1,')=',E12.5)
      RETURN
      END

      SUBROUTINE DISP_SLC
      REAL BEAM_TH,BEAM_PH,PSIDL(12)
      INTEGER N_X,N_Y,NUM_AUX
      COMPLEX G(100,50),MM(100,50),A(12,100,50),W(12)
      COMMON/ARRVARS/N_X,N_Y,SPACING,BEAM_TH,BEAM_PH,G,MM,NUM_AUX,
     &               A,PSIDL,W,AMPVAR,PHVAR,ISEED0


      WRITE (6,*)
      WRITE (6,*) 'SLC ARRAY CONFIGURATION:'
      WRITE (6,*)
      WRITE (6,*) ' N_X = ',N_X
      WRITE (6,*) ' N_Y = ',N_Y
      WRITE (6,*) ' ELEMENT SPACING = ',SPACING
      WRITE (6,*) ' BEAM_TH = ',BEAM_TH
      WRITE (6,*) ' BEAM_PH = ',BEAM_PH
      WRITE (6,*) ' NUM_AUX = ',NUM_AUX
      DO 900 I=1,NUM_AUX
         WVFR=PSIDL(I)/(-2.*3.141592653589793E+00)
         WRITE (6,910) I,WVFR
900   CONTINUE
910   FORMAT ('  PSIDL(',I2,')=',F12.5,' wavelengths')
      RETURN
      END
```

```
      SUBROUTINE OUTFILERD1
      REAL PSIDL(12),BEAMTH,BEAMPH
      COMPLEX W(12),MM(100,50),A(12,100,50),G(100,50)
      INTEGER NUMPTS,NUMAUX,IAVCODE
      CHARACTER*20 FILENAME,OUTFILE
      COMMON/NAME/FILENAME,OUTFILE
      COMMON/ARRVARS/NX,NY,SPACING,BEAMTH,BEAMPH,G,MM,NUMAUX,
     &                A,PSIDL,W,IELCODE
      COMMON/INTVARS/IAVCODE

      WRITE (6,10)
10    FORMAT(' Enter output datafile name:',$)
      READ (5,11) OUTFILE
11    FORMAT(A)

      OPEN (UNIT=1,FILE=OUTFILE,STATUS='OLD')

      READ (1,20) FILENAME
20    FORMAT(A)
      READ (1,*) ITYPE

      IF (ITYPE.NE.0) THEN
        WRITE (6,*) ' USE SCANPLOT'
        GO TO 999
      END IF

      READ (1,*) IELCODE
      READ (1,*) IAVCODE
      READ (1,*) NUMPTS
      READ (1,*) NUMAUX
      READ (1,*) NX
      READ (1,*) NY
      READ (1,*) SPACING
      READ (1,*) BEAMTH
      READ (1,*) BEAMPH
      READ (1,*) PD
      READ (1,*) PI
      READ (1,*) PN
      READ (1,*) PDMAIN
      READ (1,*) PIMAIN
      READ (1,*) PNMAIN
      IF (IAVCODE.EQ.1) READ (1,*) AVSL
      DO 40 I=1,NUMAUX
        READ (1,*) W(I)
40    CONTINUE
      DO 50 I=1,NX
        DO 49 J=1,NY
          READ (1,*) MM(I,J)
          READ (1,*) G(I,J)
          DO 48 K=1,NUMAUX
            READ (1,*) A(K,I,J)
48        CONTINUE
49      CONTINUE
50    CONTINUE
      DO 55 I=1,NUMAUX
        READ (1,*) PSIDL(I)
55    CONTINUE

      CLOSE (UNIT=1,STATUS='KEEP')

      RETURN
      END
```

```
C   PROGRAM PATTPLOT creates the datafile for pattern plotting using
C    MATLAB

      PROGRAM PATTPLOT
      REAL PSIDL(12),BEAMTH,BEAMPH
      COMPLEX W(12),MM(100,50),A(12,100,50),G(100,50)
      INTEGER NUMPTS,NUMAUX,IAVCODE
      CHARACTER*20 FILENAME,OUTFILE
      COMMON/NAME/FILENAME,OUTFILE
      COMMON/ARRVARS/NX,NY,SPACING,BEAMTH,BEAMPH,G,MM,NUMAUX,
     &                    A,PSIDL,W,IELCODE
      COMMON/INTVARS/IAVCODE

      RTD=57.2957795130823208768

      CALL OUTFILERD1

      RDES=10*LOG10(PD/PDMAIN)
      RNSE=10*LOG10(PN/PNMAIN)
      SINRMAIN=10.*LOG10(PDMAIN/(PIMAIN+PNMAIN))
      SINR = 10*LOG10(PD/(PI+PN))
      SINR_IR=SINR-SINRMAIN
c      IF (IAVCODE.EQ.1) THEN
c        CALL AVSLCOMP(AVSL)
c        AVSLCH=AVSL-AVSLMAIN
c      END IF

      CALL PLOTPATT

999   STOP
      END

      SUBROUTINE PLOTPATT
      REAL PLOTX(1000),PLOTY(1000)
      REAL PSIDL(12),BEAMTH,BEAMPH,PHI
      COMPLEX MM(100,50),A(12,100,50),G(100,50),W(12)
      CHARACTER*20 FILENAME,OUTFILE,PLOTFILE
      COMMON/ARRVARS/NX,NY,SPACING,BEAMTH,BEAMPH,G,MM,NUMAUX,
     &                    A,PSIDL,W,IELCODE
      COMMON/NAME/FILENAME,OUTFILE
      COMMON/PLOTVARS/PHI,PLOTX,PLOTY,NPTS

      WRITE (6,10)
10    FORMAT(' Enter name for plotfile:',$)
      READ (5,11) PLOTFILE
11    FORMAT(A)

      OPEN (UNIT=3,FILE=PLOTFILE,STATUS='NEW')

      IF (NY.NE.1) THEN
        WRITE (6,225)
        READ (5,*) PHI
225     FORMAT(' Enter phi angle(degrees) for desired pattern cut:',$)
      ELSE
        PHI=0.
      END IF

      WRITE (6,230)
230   FORMAT(' Enter number of points for pattern plot:',$)
      READ (5,*) NPTS

      WRITE (3,*) NPTS
      WRITE (3,*) NUMAUX

      IEL=1
      CALL PLOTMAIN(IEL)
```

```
      WRITE (3,*) (PLOTX(I), I=1,NPTS)
      WRITE (3,*) (PLOTY(I), I=1,NPTS)
      IEL=0
      CALL PLOTMAIN(IEL)
      WRITE (3,*) (PLOTY(I), I=1,NPTS)
      DO 240 IAUX=1,NUMAUX
        CALL PLOTAUX(IAUX)
        WRITE (3,*) (PLOTY(I), I=1,NPTS)
240   CONTINUE
      MMCODE=0
      CALL PLOTADAP(MMCODE)
      WRITE (3,*) (PLOTY(I), I=1,NPTS)
      MMCODE=1
      CALL PLOTADAP(MMCODE)
      WRITE (3,*) (PLOTY(I), I=1,NPTS)

999   CLOSE (UNIT=3,STATUS='KEEP')

      RETURN
      END

      SUBROUTINE PLOTADAP(MMCODE)
      REAL PLOTX(1000),PLOTY(1000)
      REAL PSIDL(12),BEAMTH,BEAMPH,PD
      COMPLEX MM(100,50),A(12,100,50),W(12),G(100,50)
      COMPLEX TEMP,PDTEMP,DLF
      REAL THETA,PHI,PATT,PSIIJ
      COMMON/ARRVARS/NX,NY,SPACING,BEAMTH,BEAMPH,G,MM,NUMAUX,
     &                    A,PSIDL,W,IELCODE
      COMMON/PLOTVARS/PHI,PLOTX,PLOTY,NPTS

C     WRITE (6,*) 'W(1)=',W(1),'  PHI=',PHI

      THINC=180./(NPTS-1)

      DO 10 ITH=1,NPTS
        THETA=-90.+(ITH-1)*THINC
        PDTEMP=(0.,0.)
        DO 9 I=1,NX
         DO 8 J=1,NY
          TEMP=(0.,0.)
          DO 6 K=1,NUMAUX
           TEMP=TEMP+W(K)*A(K,I,J)*CEXP(CMPLX(0.,PSIDL(K)))
6         CONTINUE
          IF (MMCODE.EQ.1) TEMP=MM(I,J)+TEMP
          CALL CALCPSI(SPACING,THETA,PHI,I,J,PSIIJ)
          PDTEMP=PDTEMP+TEMP*G(I,J)*CEXP(CMPLX(0.,PSIIJ))
8        CONTINUE
9       CONTINUE
        CALL ELPATT(PATT,THETA,PHI,IELCODE)
        PDTEMP=PDTEMP*PATT
        PD=CABS(PDTEMP)**2.
        PLOTX(ITH)=THETA
        PLOTY(ITH)=PD
10    CONTINUE

C   Pattern Normalization
      DO 20 J=1,NPTS
        IF (PLOTY(J).LT.1E-10) PLOTY(J)=1E-10
        PLOTY(J)=10*ALOG10(PLOTY(J))
20    CONTINUE

      RETURN
      END

      SUBROUTINE PLOTMAIN(IEL)
```

```
      REAL PLOTX(1000),PLOTY(1000)
      REAL PSIDL(12),BEAMTH,BEAMPH
      COMPLEX MM(100,50),A(12,100,50),W(12)
      COMPLEX TEMP,G(100,50)
      REAL THETA,PHI,PATT,PSIIJ
      COMMON/ARRVARS/NX,NY,SPACING,BEAMTH,BEAMPH,G,MM,NUMAUX,
     &                    A,PSIDL,W,IELCODE
      COMMON/PLOTVARS/PHI,PLOTX,PLOTY,NPTS

      THINC=180./(NPTS-1)

      DO 20 ITH=1,NPTS
        THETA=-90.+(ITH-1)*THINC
        TEMP=(0.,0.)
        DO 15 I=1,NX
          DO 14 J=1,NY
            CALL CALCPSI(SPACING,THETA,PHI,I,J,PSIIJ)
            TEMP=TEMP+MM(I,J)*G(I,J)*CEXP(CMPLX(0.,PSIIJ))
14        CONTINUE
15      CONTINUE
        IF (IEL.EQ.1) THEN
          CALL ELPATT(PATT,THETA,PHI,IELCODE)
          TEMP=TEMP*PATT
        END IF
        PD=CABS(TEMP)**2.
        PLOTX(ITH)=THETA
        PLOTY(ITH)=PD
20    CONTINUE

C   Pattern Normalization
      DO 25 J=1,NPTS
        IF (PLOTY(J).LT.1E-10) PLOTY(J)=1E-10
        PLOTY(J)=10*ALOG10(PLOTY(J))
25    CONTINUE

      RETURN
      END

      SUBROUTINE PLOTAUX(IAUX)
      REAL PLOTX(1000),PLOTY(1000)
      REAL PSIDL(12),BEAMTH,BEAMPH
      COMPLEX MM(100,50),A(12,100,50),W(12)
      COMPLEX TEMP,G(100,50)
      REAL THETA,PHI,PATT,PSIIJ
      COMMON/ARRVARS/NX,NY,SPACING,BEAMTH,BEAMPH,G,MM,NUMAUX,
     &                    A,PSIDL,W,IELCODE
      COMMON/PLOTVARS/PHI,PLOTX,PLOTY,NPTS

      THINC=180./(NPTS-1)

      DO 20 ITH=1,NPTS
        THETA=-90.+(ITH-1)*THINC
        TEMP=(0.0,0.0)
        DO 15 I=1,NX
          DO 14 J=1,NY
            CALL CALCPSI(SPACING,THETA,PHI,I,J,PSIIJ)
            TEMP=TEMP+A(IAUX,I,J)*G(I,J)*CEXP(CMPLX(0.,PSIIJ))
14        CONTINUE
15      CONTINUE
        CALL ELPATT(PATT,THETA,PHI,IELCODE)
        TEMP=TEMP*PATT
        PD=CABS(TEMP)**2.
        PLOTX(ITH)=THETA
        PLOTY(ITH)=PD
20    CONTINUE
```

```
C   Pattern Normalization
        DO 25 J=1,NPTS
          IF (PLOTY(J).LT.1E-10) PLOTY(J)=1E-10
          PLOTY(J)=10*ALOG10(PLOTY(J))
25      CONTINUE

        RETURN
        END


C       Subroutine CALCPSI
C
C       This subroutine calculates the phase shift at the carrier center
C       frequency seen between element (I,J) and element (1,1) under
C       the assumption that the elements are arranged in a square
C       grid in the XY plane with half-wavelength element spacing.
C
C
        SUBROUTINE CALCPSI(SPACING,THETA,PHI,I,J,PSIIJ)
        REAL THETA,PHI,PSIIJ,DTR,THETAR,PHIR
        PI=4.*ATAN(1.)
        DTR=PI/180.
        PHIR=PHI*DTR
        THETAR=THETA*DTR
        PSIIJ=((I-1)*COS(PHIR)+(J-1)*SIN(PHIR))*SIN(THETAR)
     &          *2.*PI*SPACING
        RETURN
        END

C
C       SUBROUTINE ELEMENT_PATTERN multiplies a signal amplitude by
C       the element pattern of an isolated monopole on a dielectric coated
C       ground plane.
C
C
        SUBROUTINE ELPATT(A,THETA,PHI,IELCODE)
        INTEGER IELCODE
        REAL A,THETA,PHI,PI,DTR,F1,RG,K0H,COSTH,SINTH
        REAL PNORM,HNORM,EPSR
        COMPLEX F2

        PI=3.141592653589793E+00
        DTR=PI/180.0E+00

        IF (IELCODE.EQ.0) THEN
         A=1.0
        ELSE IF (IELCODE.EQ.1) THEN
         EPSR=5.        !  Relative permittivity of dielectric layer
         HNORM=0.75     !  Height in wavelengths
         PNORM=1.828085343639275 !  Normalizing the element pattern

         K0H=2.*PI*HNORM
         COSTH=COS(THETA*DTR)
         SINTH=SIN(THETA*DTR)

         F1=SQRT(EPSR-SINTH**2)
         RG=(EPSR*COSTH-F1)/(EPSR*COSTH+F1)
         F2=CEXP(CMPLX(0.,K0H*COSTH))-CMPLX(COS(K0H),SIN(K0H)*COSTH)

         IF (THETA.EQ.0.) THEN
           A=0.
         ELSE
           A=CABS((F2+RG*CONJG(F2))/SINTH)/PNORM
         END IF
        ELSE IF (IELCODE.EQ.2) THEN
         A=ABS(SIN(THETA*DTR))
```

```
END IF

RETURN
END
```

```
      SUBROUTINE OUTFILERD2
      REAL DATAYMN(400),DATAX(400),DATAYD(400),
     &     DATAYI(400),DATAYN(400),DATAAV(400)
      REAL PDMAIN,PIMAIN,PNMAIN,AVSLMAIN
      INTEGER NUMPTS,JAMNUM,IAVCODE,ITYPE
      CHARACTER*20 FILENAME,OUTFILE

      OPEN (UNIT=1,FILE=OUTFILE,STATUS='OLD')

      READ (1,20) FILENAME
20    FORMAT(A)
      READ (1,*) ITYPE

      IF (ITYPE.EQ.0) THEN
        WRITE (6,*) ' USE PATTPLOT INSTEAD'
        GO TO 999
      END IF
      IF (ITYPE.EQ.1.OR.ITYPE.EQ.2.OR.ITYPE.EQ.5) THEN
        INORM=0
      ELSE
        INORM=1
      END IF
      READ (1,*) IAVCODE
      IF (IAVCODE.EQ.1) READ (1,*) AVSLMAIN
      READ (1,*) NUMPTS
      IF (INORM.EQ.1) READ (1,*) JAMNUM

      DO 60 I=1,NUMPTS
        READ (1,*) DATAX(I)
        READ (1,*) DATAYD(I)
        READ (1,*) DATAYI(I)
        READ (1,*) DATAYN(I)
        READ (1,*) DATAYMN(I)
        IF (IAVCODE.EQ.1) READ (1,*) DATAAV(I)
60    CONTINUE

      IF (INORM.EQ.1) THEN
        READ (1,*) PDMAIN
      ELSE
        READ (1,*) PIMAIN
      END IF
      READ (1,*) PNMAIN

      CLOSE (UNIT=1,STATUS='KEEP')

      RETURN
      END
```